Investigating perturbations in energy metabolism to identify targetable metabolic vulnerabilities in cancer

Oro Uchenunu

Department of Experimental Medicine McGill University

Montreal, Quebec, Canada

June 2022

A thesis submitted to McGill University in partial fulfillment of the requirements of the degree of Doctor of Philosophy

© Oro Uchenunu, 2022

TABLE OF CONTENTS

ABSTRACT	9-10
ABRÉGÉ	11-12
ACKNOWLEDGEMENTS	13-14
PUBLICATIONS	15-16
CONTRIBUTIONS TO ORIGINAL KNOWLEDGE	17-18
CONTRIBUTIONS OF AUTHORS	19-20
LIST OF FIGURES.	21-24
LIST OF ABBREVIATIONS	25-35
CHAPTER 1: Introduction.	36-193
1.1 Cancer burden and biology	36-38
1.2 Cancer metabolism	38-87
1.2.1 Warburg effect	38-39
1.2.2 Glucose metabolism	39-45
1.2.2.1 Glucose uptake	40-41
1.2.2.2 Glycolysis	41-45
1.2.3 Pyruvate metabolism: Crossroads between glycolysis and citric acid cycle	45-48
1.2.3.1 Cytosolic reduction of pyruvate	45-47
1.2.3.2 Mitochondrial oxidative decarboxylation of pyruvate into acetyl-CoA	47-48
1.2.4 Citric acid cycle (CAC)	48-66
1.2.4.1 Aberrant activity of CAC enzymes produces "oncometabolites"	56-66
1.2.4.1.1 2-Hydroxyglutarate (2-HG)	56-58
1.2.4.1.2 Succinate.	58-59

1.2.4.1.3 Fumarate	59-60
1.2.4.2 CAC anaplerosis and cataplerosis	60-66
1.2.4.2.1 CAC anaplerosis and glutamine metabolism	62-66
1.2.5 ETC and OXPHOS.	66-74
1.2.5.1 Mammalian Complex I	67-68
1.2.5.2 Mammalian Complex II	68-69
1.2.5.3 Mammalian Complex III	69-70
1.2.5.4 Mammalian Complex IV	70-71
1.2.5.5 Mammalian Complex V (F ₁ F ₀ ATP synthase)	71-72
1.2.5.6 Reactive oxygen species (ROS)	72-74
1.2.6 Amino acids metabolism in cancer	74-80
1.2.6.1 Aspartate	74-75
1.2.6.2 Asparagine	75-76
1.2.6.3 Serine and glycine.	76-78
1.2.6.4 Folate and methionine cycle	78-80
1.2.7 Lipid metabolism	80-84
1.2.7.1 <i>De novo</i> lipogenesis	81-82
1.2.7.2 Fatty acid uptake	82-83
1.2.7.3 Fatty acid oxidation	83-84
1.2.8 Pentose Phosphate Pathway (PPP)	84-85
1.2.9 Nucleotide metabolism	85-87
1.2.9.1 Purine biosynthesis	86
1.2.9.2 Pyrimidine biosynthesis	86-87

1.3 Dysregulation of metabolism in cancer	88-112
1.3.1 Transcriptional regulation of cancer metabolism	88-91
1.3.1.1 Hypoxia Inducible Factor (HIF)	88-89
1.3.1.2 MYC	89-90
1.3.1.3 p53	91
1.3.2 Metabolic regulation via cellular signaling pathways	92-112
1.3.2.1 RAS-RAF-MEK-ERK signaling pathway	92-94
1.3.2.1.1 RAS	92-93
1.3.2.1.2 RAF	93-94
1.3.2.2 AMPK: Regulator of intracellular energy homeostasis	94-98
1.3.2.3 PI3K-AKT-mTOR signaling	98-113
1.3.2.3.1 Upstream activators of mTOR signaling	99-104
1.3.2.3.2 Systemic effects of mTOR signaling	104-112
1.4 Central hypothesis and overarching goals	113
1.5 References.	113-193
CHAPTER 2: Mitochondrial complex IV defects induce metabolic and signal	ling perturbations
that expose potential vulnerabilities in HCT116 cells	194-272
2.1 Abstract.	195
2.2 Introduction.	195-197
2.3 Results	197- 208
2.3.1 SCO2 loss results in metabolic rewiring of HCT116 cells that is character	rized by increased
NAD+ regeneration	197- 200

2.3.2 Abrogation of SCO2 in HCT116 cells leads to alterations in acetyl-CoA and lipid	
metabolism	
2.3.3 Complex IV dysfunction in HCT116 cells results in increased succinate and 2-	
hydroxyglutarate levels	
2.3.4 SCO2 loss in HCT116 cells affects amino-acid metabolism	
2.3.5 Loss of mitochondrial complex IV function leads to induction of IGF1R/AKT axis with	
paradoxical reduction in mTOR signaling	
2.3.6 SCO2 loss leads to increased cell migration and altered expression of EMT markers in	
HCT116 cells	
2.3.7 SCO2-deficient HCT116 cells exhibit increased susceptibility to IGF1R and AKT	
inhibitors	
2.4 Figures	
2.5 Supplemental Figures	
2.6 Discussion	
2.7 Methods	
2.7.1 Cell lines and culture conditions	
2.7.2 Lentiviral infection of <i>SCO2</i> shRNA and expression constructs	
2.7.3 Flow cytometry analysis of cell cycle	
2.7.4 Flow cytometry analysis of apoptosis	
2.7.5 GC-MS for Stable Isotope Tracer Analysis (SITA)254-255	
2.7.6 GC-MS for Steady State metabolite analysis	
2.7.7 Glucose and lactate release assays	
2.7.8 Cell proliferation assays	

2.7.9 Western blotting and antibodies
2.7.10 Transwell migration assay
2.7.11 Generation of mRNA-seq libraries and <i>IDH1</i> and 2 mRNA sequencing analysis25
2.7.12 Isolation of RNA and RT-PCR Analysis
2.7.13 Live cell staining and confocal microscopy
2.7.14 IGF1 ELISA
2.7.15 Statistical analysis
2.7.16 Data Accessibility
2.8 Acknowledgements
2.9 Author contributions
2.10 References
2.11 Bridging text
CHAPTER 3: Energy stress induces metabolic reprogramming in colorectal cancer273-313
3.1 Abstract
3.2 Introduction
3.3 Results
3.3.1 Metabolic stress reduces proliferation of transformed colorectal cell lines more strongly than
non-transformed colon epithelial cells
3.3.2 Phenformin and glutamine depletion downregulate mTORC1 activity and inhibit protein
synthesis in CRC cell lines
3.3.3 Phenformin induces metabolic perturbations in CRC cells
3.3.4 Glutamine deprivation depletes CAC intermediates while simultaneously increasing the
levels of most amino acids in transformed colorectal cell lines

3.4 Figures	284-291
3.5 Discussion	291-296
3.6 Methods	296
3.6.1 Cell lines and culture conditions	296
3.6.2 Glutamine deprivation	296
3.6.3 Phenformin treatment	297
3.6.4 Metabolomics analysis	297-298
3.6.5 Cell proliferation assays	298
3.6.6 Western blotting and antibodies	298-299
3.6.7 Polysome Profiling.	299-300
3.6.8 Statistical analysis	300
3.7 References.	300-315
CHAPTER 4: Discussion.	316-349
4.1 Rewiring of signaling and metabolic networks underpins metabolic plasticity	and adaptation
of cancer cells to energy stress	316-321
4.2 Pharmacological strategies to target metabolic vulnerabilities in cancer	321-322
4.2.1 Pharmacological inhibition of glutamine uptake	322-323
4.2.2 Pharmacological inhibition of glutaminolysis	324-325
4.2.3 Drug combinations with glutamine metabolism inhibitors	325-326
4.2.4 Therapeutics targeting OXPHOS in cancer	327-330
4.2.5 Drug combinations with biguanides	330-332
4.3 Conclusion	332
4.4 Limitations and future perspectives	333

4.5 References
APPENDIX: Other works
A.1 Contributions to understanding of the molecular mechanisms of metabolic dysregulation in
cancer
A.1.1 Identification of hydride ion transfer complex that allows cells to overcome senescence and
drives tumorigenesis
A.1.2 Elucidating the mechanisms of the anti-neoplastic action of the sodium-glucose
cotransporter-2 (SGLT2) inhibitors
A.1.3 Establishing the role of PR/SET Domain 15 (PRDM15) in metabolic rewiring of B-cell
lymphomas
A.1.4 The role of mTORC1/4E-BP/eIF4E axis and HIF1 α in metabolic plasticity of cancer cells
and responses to the combinations of inhibitors of oncogenic kinases and biguanides377-389
A.2 Conclusion
A.3 References

ABSTRACT

Although metabolic differences between tumors and normal tissues were first observed over a century ago, the field of oncometabolism remained dormant in the subsequent years. It has only been until recently that dysregulation of cellular energetics was recognized as a hallmark of cancer. The advent of high throughput metabolomics technologies, computational systems biology and biochemical tools have aided in elucidating the various metabolic pathways exploited by cancer cells. Neoplastic cells strategically alter their metabolism to meet their bioenergetic and biosynthetic demands, which is particularly challenging in unfavorable microenvironments. However, emerging data indicate that cancer cells develop metabolic plasticity that allows them to rapidly remodel their metabolomes to survive and thrive in harsh tumor environments with limited nutrients and/or oxygen. The master regulators of cell growth and metabolism, AKT/mTOR (mechanistic/mammalian target of rapamycin) signaling axis plays a major role in governing metabolic processes essential to cancer cell survival and proliferation. This thesis highlights the crosstalk between the AKT/mTOR signaling and cancer metabolism. Specifically, my work elucidates plausible adaptive mechanisms that cancer cells turn on to survive energetic stress due to glutamine deprivation or inhibition of mitochondrial complexes I or IV. Specifically, the work in the thesis describes the changes in the glycolysis and citric acid cycle (CAC) resulting from the abrogation of the mitochondrial complex IV assembly protein, SCO2. These alterations in the metabolome were accompanied by rewiring of the AKT/mTOR signaling. The thesis also focuses on comparing energy production and utilization in colorectal cancer (CRC) cells and describes metabolic adaptations of CRC cells. To this end, we catalogued different energetic stressors and associated metabolic response networks that underpin adaptations of CRC cells to energy stress thus revealing potential targetable metabolic vulnerabilities. Altogether, this work provides previously unrecognized insights into metabolic adaptation and plasticity of cancer cells.

ABRÉGÉ

Bien que des différences métaboliques entre les tumeurs et les tissus normaux aient été observées pour la première fois il y a plus d'un siècle, le domaine de l'oncométabolisme est resté relativement méconnu jusqu'à récemment. L'avènement des technologies de métabolomique à haut debit et de la biologie intégrative a contribué à élucider les différentes voies métaboliques exploitées par les cellules cancéreuses pour répondre à leurs demandes bioénergétiques et biosynthétiques. Répondre à de telles demandes est particulièrement difficile pour les cellules tumorales dans des microenvironnements défavorables. Cependant, de nouvelles données indiquent que les cellules cancéreuses développent une plasticité métabolique qui leur permet de remodeler rapidement leurs métabolomes pour survivre et proliférer dans des environnements tumoraux difficiles avec des nutriments et/ou de l'oxygène limités. Le régulateur principal de la croissance et du métabolisme cellulaire, AKT/mTOR (Mechanistic/Mammalian Target of Rapamycin), joue un rôle majeur dans la régulation des processus métaboliques essentiels à la survie et à la prolifération des cellules cancéreuses. Cette thèse met en évidence les interactions entre la signalisation AKT/mTOR et le métabolisme du cancer. En particulier, mon travail élucide les mécanismes adaptatifs que les cellules cancéreuses activent pour survivre au stress énergétique dû à la privation de glutamine ou à l'inhibition des complexes mitochondriaux I ou IV. Les travaux de cette thèse décrivent les changements dans le cycle de la glycolyse et de l'acide citrique (CAC) résultant de l'abrogation de la protéine du complexe mitochondrial IV, SCO2. Ces altérations du métabolome sont accompagnées d'une adaptation de la voie de signalisation AKT/mTOR. Cette thèse se concentre également sur la comparaison de la production et de l'utilisation d'énergie dans les cellules du cancer colorectal (CCR) et décrit les adaptations métaboliques des cellules du CCR. À cette fin, nous avons répertorié différents facteurs de stress énergétique et les réseaux de réponse métabolique associés qui sous-tendent les adaptations des cellules CCR, révélant ainsi des vulnérabilités métaboliques potentielles ciblables. Dans l'ensemble, ces travaux fournissent des nouvelles connaissances sur l'adaptation métabolique et la plasticité des cellules cancéreuses.

ACKNOWLEDGEMENTS

Pursing a doctoral degree has been the most difficult challenge that I have had to face to date. It took an entire support system comprising of mentors, friends and family to see me through the completion of this degree and no number of words can express my gratitude. Nevertheless, I would still like to try.

First and foremost, I would like to thank my parents and siblings for always encouraging me during my studies. You provided me with support in every form required. I am especially grateful to you, dad for advising me to pursue scientific research up to the graduate level. In some ways, I feel this degree is partly yours because I know you sacrificed your own goals of attaining an advanced degree to raise the family.

I would like to express my appreciation to my wonderful friends that also encouraged me along the way. It has been a journey that you have all seen me through from the beginning to the end. This would definitely not have been possible without your support. You brought me joy and comfort in times when I especially needed it. I especially want to thank Genevieve Laniel Legaré for facilitating the process of finding an amazing lab for my Ph.D. studies. This experience all started with you and I am grateful to have you as a friend.

I sincerely want to express my gratitude to the past and current members of Drs. Ivan Topisirovic's and Michael Pollak's lab: Shannon, Marie-José, Elena, Hayley, Pedja, Kris, Aakshi, Nabila, Sophie, Matthew, Ranveer, Marie, Ye, David and Laura. All of you were instrumental in creating a convivial lab environment for me to work in during my studies. I appreciate your immense help with lab experiments and editing manuscripts. I look forward to fostering these relationships beyond the lab.

Finally, I would like to thank the members of my thesis committee, Drs. Ivan Topisirovic, Michael Pollak, Josie Ursini-Siegel, Koren Mann, Marc Fabian and Frederick Mallette for their invaluable insights during my committee meetings and one-on-one meetings when I needed guidance. I am especially grateful to you Ivan, for training me in scientific rigor, for supporting me and providing me with opportunities and, for being extremely patient with me in times when I needed it the most.

PUBLICATIONS

Chapter 2 was published as an original research article:

Uchenunu O*, Zhdanov AV*, Hutton P, Jovanovic P, Wang Y, Andreev DE, Hulea L, Papadopoli DJ, Avizonis D, Baranov PV, Pollak MN, Papkovsky DB and Topisirovic I. (2022). Mitochondrial complex IV defects induce metabolic and signaling perturbations that expose targetable vulnerabilities in HCT116 cells. FEBS Open Bio. 12(5):959-982. *co-first authors.

The following were published during my doctoral studies, but were not part of my principal projects:

Lo L, **Uchenunu O**, Botelho RJ, Antonescu CN, Karshafian R. (2022). AMP-activated protein kinase (AMPK) is required for recovery from metabolic stress induced by ultrasound microbubble treatment. bioRxiv 2022.03.02.482704 doi: https://doi.org/10.1101/2022.03.02.482704.

Igelmann S, Lessard F*, **Uchenunu O***, Bouchard J, Fernandez-Ruiz A, Rowell MC, Lopes-Paciencia S, Papadopoli D, Fouillen A, Ponce KJ, Huot G, Mignacca L, Benfdil M, Kalegari P, Wahba HM, Pencik J, Vuong N, Quenneville J, Guillon J, Bourdeau V, Hulea L, Gagnon E, Kenner L, Moriggl R, Nanci A, Pollak MN, Omichinski JG, Topisirovic I, Ferbeyre G. (2021). A hydride transfer complex reprograms NAD metabolism and bypasses senescence. Molecular Cell. 81(18):3848-3865. *co-second authors.

Papadopoli D, **Uchenunu O**, Palia R, Chekkal N, Hulea L, Topisirovic I, Pollak M, St-Pierre J. (2021). Perturbations of cancer cell metabolism by the antidiabetic drug canagliflozin. Neoplasia. 23(4):391-399.

Mzoughi S, Fong JY*, Papadopoli D*, Koh CM*, Hulea L*, Pigini P, Di Tullio F, Andreacchio G, Hoppe MM, Wollmann H, Low D, Caldez MJ, Peng Y, Torre D, Zhao JN, **Uchenunu O**, Varano G, Motofeanu CM, Lakshmanan M, Teo SX, Wun CM, Perini G, Tan SY, Ong CB, Al-

Haddawi M, Rajarethinam R, Hue SS, Lim ST, Ong CK, Huang D, Ng SB, Bernstein E, Hasson D, Wee KB, Kaldis P, Jeyasekharan A, Dominguez-Sola D, Topisirovic I, Guccione E. (2020). PRDM15 is a key regulator of metabolism critical to sustain B-cell lymphomagenesis. Nature Communications. 11(1):3520. *co-second authors.

Uchenunu O, Pollak M, Topisirovic I & Hulea L. (2019). Oncogenic kinases and perturbations in protein synthesis machinery and energetics in neoplasia. Journal of Molecular Endocrinology. 62(2):R83-R103.

Hulea L*, Gravel SP*, Morita M*, Cargnello M, **Uchenunu O**, Im YK, Lehhuédé C, Ma EH, Leibovitch M, McLaughlan S, Blouin MJ, Parisotto M, Papavasilou V, Lavoie C, Larsson O, Ohh M, Ferreira T, Greenwood C, Bridon G, Avizonis D, Ferbeyre G, Siegel P, Jones RG, Muller W, Ursini-Siegel J, St-Pierre J, Pollak M, Topisirovic I. (2018). Translational and HIF-1α-Dependent Metabolic Reprogramming Underpin Metabolic Plasticity and Responses to Kinase Inhibitors and Biguanides. Cell Metabolism. 28(6):817-832. *co-first authors

CONTRIBUTION TO ORIGINAL KNOWLEDGE

- 1) I deciphered the mechanisms underpinning metabolic adaptations of cancer cells to energy stress caused by dysfunction of mitochondrial complex IV. Specifically, I showed that the loss of SCO2 leads to a decrease in citric acid cycle (CAC) intermediates and compensatory increase in lactate production and other NAD+ regenerating reactions. Consistent with mitochondrial dysfunction due SCO2 deletion, I observed increase in pyruvate carboxylation and accumulation of lipid depots. In addition, the abrogation of SCO2 decreases the intracellular levels of most amino acids. Of note, SCO2 is thought to be a pivotal mediator of metabolic effects of tumor suppressor p53 (please see below). These results are therefore likely to be broadly applicable across the spectrum of neoplasia that are characterized by p53 dysfunction.
- 2) I provide evidence that SCO2 deletion leads to compensatory activation of AMPK and the IGF1R/AKT signaling axis, with paradoxical downregulation of mTORC1 signaling. These data implies that AMPK activation following the loss of SCO2 is essential to cell survival. We demonstrate similar rewiring of signaling in cells treated with mitochondrial complex III inhibitors. Furthermore, I demonstrated that SCO2 loss-induced signaling rewiring increases sensitivity of cells to IGF1R and AKT inhibitors, while decreasing the anti-proliferative effects of mTOR inhibitors. In long-term, these findings may inform strategies aiming to target cancer metabolism.
- 3) My data suggest that in addition to rendering HCT116 cells resilient to hypoxia, abrogation of SCO2 and accompanying signaling and metabolic reprogramming may increase the metastatic potential of colorectal cancer cells.

- 4) I showed that genetically distinct transformed colon cell lines are more sensitive to the drug(i.e., phenformin) or nutrient depletion-induced (i.e., glutamine depletion) energy stress
 compared to normal colon epithelial cells.
- 5) I catalogued a compendium of similarities and differences in the metabolic profiles of colorectal cancer and normal colon epithelial cells under drug-induced (e.g., phenformin) or nutrient-deprivation (glutamine)-induced energy stress. These data imply that α-ketoglutarate carboxylation may be a potentially targetable common metabolic vulnerability across genetically distinct colorectal cancer cell lines.

These contributions, in combination with those that I made in collaboration (please see the appendix) provide hitherto unappreciated insights into metabolic rewiring of cancer cells thus contributing to better understanding of metabolic reprogramming of neoplasia. I hope that in long-term, my findings in concert with other similar efforts will help establish molecular bases for exploiting metabolic perturbations of cancer cells in the clinic.

CONTRIBUTIONS OF AUTHORS

The thesis titled: "Investigating perturbations in energy metabolism to identify targetable metabolic vulnerabilities in cancer" is based on five chapters.

The contributions of the authors who participated in this project are as follows:

Chapter 1: I wrote the manuscript including the creation of the figures. The chapter was reviewed and edited by Dr. Michael Pollak and Dr. Ivan Topisirovic.

Chapter 2: The study was conceived by Dr. Alexandre V. Zhdanov, Dr. Michael Pollak, Dr. Ivan Topisirovic, Dr. Dmitri Papkovsy and me. Dr. Alexandre V. Zhdanov and I designed and conducted experiments on gene expression, cell functioning, migration, signaling and metabolism. Dr. Dmitry Andreev and Dr. Pavel Baranov carried out RNA-sequence analysis. Dr. Laura Hulea Dr. Daina Avizonis and Dr. David Papadopoli assisted with metabolic experiments. Predrag Jovanovic carried out the transwell migration assay and analysis. Ye Wang and Phillipe Hutton carried out ELISA and Western blotting experiments. Dr. Alexandre V. Zhdanov and I wrote the initial draft of the manuscript. Dr. Michael Pollak, Dr. Ivan Topisirovic, Dr. Dmitri Papkovsy provided funding. All authors contributed to the interpretation of the data and editing the final version of the manuscript.

Chapter 3: Dr. Michael Pollak, Dr. Ivan Topisirovic and I conceived the study. I designed and conducted all the experiments. I wrote the initial draft of the manuscript. Dr. Michael Pollak and Dr. Ivan Topisirovic provided the necessary funding. Dr. Ivan Topisirovic edited the final version of the manuscript.

Chapter 4: I wrote the text. Reviews and edits were done by Dr. Ivan Topisirovic.

Appendix: The chapter highlights the different publications I was involved in, which delineated the mechanisms of metabolic rewiring in both normal and tumor cells. I provided critical

experimental and intellectual inputs in these studies. Specifically, with Igelmann et al., I was involved in conceptualizing and designing metabolic experiments. I also analyzed and interpreted the data which led to Fig. 4.1.1A-J. In the publication with Papadopoli et al., I designed and performed cell proliferation assay (Fig. 4.1.2A). I was also partly responsible for acquiring and analyzing the metabolic data for Mzoughi et al. This was done for Fig. 4.1.3A, Fig. 4.1.3C and Fig. 4.1.3D. Additionally, I designed, experimented, analyzed and created figures on cell proliferation assay for Hulea et al. This is illustrated as Fig. 4.1.4A. I also analyzed and interpreted the metabolic data used to produce Fig. 4.1.4C. Dr. Michael Pollak, Dr. Ivan Topisirovic and I conceived the structure of the chapter. Dr. Ivan Topisirovic edited the final version of the chapter.

LIST OF FIGURES

Fig. 1.1 Cancer-related statistics in Canada, 2019
Fig. 1.2 Glucose uptake and glycolysis
Fig. 1.3 Schematic diagram of the citric acid cycle (CAC)
Fig. 1.4 mTOR signaling pathway
Fig. 2.1 SCO2 loss in HCT116 cells rewires glucose metabolism while decreasing PDHE1-α1
phosphorylation
Fig. 2.2 SCO2 loss in HCT116 cells reduces pyruvate oxidation while increasing pyruvate
reduction and carboxylation
Fig. 2.3 Complex IV deficiency alters fatty acid metabolism in HCT116 cells213-214
Fig. 2.4 SCO2 abrogation in HCT116 cells results in asymmetry in CAC intermediates and
decrease in the levels of the most amino acids
Fig. 2.5 SCO2 loss in HCT116 cells leads to activation of AKT and AMPK, suppression of
mTORC1, reduction in cell proliferation and increased cell migration217-219
Fig. 2.6 Complex IV deficiency increases sensitivity of HCT116 cells to IGF1R and AKT, but not
mTOR inhibitors
Fig. S2.1 SCO2 regulates glucose metabolism
Fig. S2.2 Inhibition of complex III or IV of the electron transport chain results in lipid droplet
accumulation in HCT116 cells
Fig. S2.3 HCT116 cells are devoid of mutations in <i>IDH1</i> and <i>IDH2</i> genes while the loss of <i>SCO2</i>
does not affect intracellular pH
Fig. S2.4 SCO2 deletion in HCT116 cells increases expression of SOD2226
Fig. S2.5 SCO2 loss rewires signaling, reduces proliferation and bolsters migration227-229

Fig. S2.6 Reduced complex IV activity increases sensitivity cancer cells to AKT
inhibitor
Fig. S2.7 Inhibition of AKT dampens the compensatory increase in glycolysis caused by the
deletion of SCO2 in HCT116 cells
Fig. S2.8 Depletion of mitochondrial complex IV activity reduces sensitivity of cancer cells to
mTOR inhibitors
Fig. S2.9 Densitometry analysis of Western blots
Fig. S2.10 Images and scans of Western blot films that are incorporated in the
manuscript
Fig. 3.1 Antiproliferative effects of nutrient deprivation and phenformin on epithelial colon
cells
Fig. 3.2 Suppression of global mRNA translation is associated with the time course inhibition of
mTORC1 signaling by phenformin and glutamine deprivation in CRC286-287
Fig. 3.3 Phenformin alters the metabolome of genetically heterogenous CRC cell lines288-289
Fig. 3.4 Glutamine deprivation reduces the levels of CAC intermediates but increases the levels of
most amino acids in genetically distinct CRC cell lines
Fig. A.1.1A Schematic of the multi-enzymatic complex (hydride transfer complex) underlying
metabolic reprogramming and senescence bypass
Fig. A.1.1B Model of NAD+ and NADPH regeneration by MDH1, ME1 and PC and schematic
of ¹³ C metabolite labeling patterns after incubating cells with ¹³ C ₆ -glucose357
Fig. A.1.1C Reduced expression of p53 reprograms metabolism in STAT3-depleted IMR90
cells

Fig. A.1.1D IMR90 cells depleted of STAT3 and p53 increases CAC anaplerosis via PC while
decreasing entry into the CAC through pyruvate dehydrogenase
Fig. A.1.1E Expression of the hydride transfer complex enzymes reprograms metabolism in
STAT3-depleted IMR90 cells
Fig. A.1.1F Expression of the hydride transfer complex enzymes increases CAC anaplerosis in
STAT3-depleted IMR90 cells
Fig. A.1.1G Schematic model of pyruvate carboxylase (PC) activity labeling pattern after 3-13C-
glucose flux. 3-13C-glucose is metabolized into 3-13C-pyruvate
Fig. A.1.1H Expression of the hydride transfer complex enzymes increases CAC anaplerosis via
PC in STAT3-depleted IMR90 cells
Fig. A.1.1I Schematic model of pyruvate carboxylase (PC) activity labeling pattern after 3,4-13C-
glucose flux. 3,4- ¹³ C-glucose is metabolized into 3- ¹³ C-pyruvate
Fig. A.1.1J PC mediates metabolic reprogramming in IMR90 cells depleted of p53 and
STAT3
Fig. A.1.2A Canagliflozin reduces the proliferation of NT2197 cells
Fig. A.1.3A PRDM15 transcriptionally reprograms metabolism in E μ -Myc tumor cells374-375
Fig. A.1.3B Schematic model of ¹³ C incorporation into CAC intermediates after incubating cells
in media containing ¹³ C-glutamine
Fig. A.1.3C Loss of PRDM15 in E μ -Myc tumor cells decreases the intracellular levels of CAC
intermediates derived from the oxidative decarboxylation of glutamine-derived α -
ketoglutarate
Fig. A.1.3D PRDM15 status has no effect on the activity of CAC
enzymes377

Fig. A.1.4A Lapatinib and phenformin work synergistically to inhibit the proliferation of HCT116
cells
Fig. A.1.4B Kinase inhibitors counters phenformin-induced changes in glucose
metabolism
Fig. A.1.4C Kinase inhibitors opposes phenformin-induced changes in reductive glutamine
metabolism
Fig. A.1.4D Schematic of ¹³ C metabolite labeling patterns after incubating cells with ¹³ C ₆ -
glucose
Fig. A.1.4E Deletion of 4E-BP in NT2197 cooperates with lapatinib and phenformin drug-induced
increases in the levels of aspartate and serine
Fig. A.1.4F Loss of 4E-BP increases the activity of PC in NT2197 cells
Fig. A.1.4G Schematic of the molecular mechanisms underlying the synergic efficacy of kinase
inhibitors (KI) and biguanides in treating cancer cells

LIST OF ABBREVIATIONS

1,3-BPG: 1,3-biphosphoglycerate

1C: one-carbon unit

2C: two-carbon unit

2-DG: 2-deoxyglucose

2-HG: 2-hydroxyglutarate

2-PG: 2-phosphoglycerate

3-PG: 3-phosphoglycerate

3-PP: 3-phosphopyruvate

3-PS: 3-phosphoserine

4E-BP: 4E-binding protein

5,10-methylene-THF: 5,10-methylenetetrahydrofolate

5hmC: 5-hydroxymethylcytosine

6PGDH: 6-phosphogluconate dehydrogenase

6PGL: 6-phosphogluconase

 α -KG: α -ketoglutarate

AABA: 2-amino-4-bis(aryloxybenzyl)aminobutanoic acid

ABAT: γ-aminobutyric acid transaminase

ACC: acetyl-CoA carboxylase

ACLY: ATP-citrate lyase

ACO: aconitase

ACS: acyl-CoA synthetase

ACSS2: acetyl-CoA synthetase 2

ADSL: adenylosuccinate lyase

ADSS: adenylosuccinate synthase

AGC: aspartate-glutamate carrier

ALDO: aldolase

ALKBH: AlkB homolog

ALL: acute lymphoblastic leukemia

ALT: alanine transaminase

AML: acute myeloid leukemia

AMP: adenosine monophosphate

AMPK: AMP-activated protein kinase

ARF: ADP ribosylation factor

ASNS: asparagine synthetase

AST: aspartate transaminase

ATP5O: ATP synthase subunit O

AU: arbitrary units

BCAA: branched chain amino acid

BPTES: bis-2-(5-phenylacetamido-1,2,4-thiadiazol-2-yl) ethyl sulfide

CAC: citric acid cycle

CAD: carbamoyl phosphate synthetase 2, aspartate transcarbamoylase, and dihydroorotase

CaMKK2: calcium/calmodulin-dependent protein kinase kinase β

CBS: cystathionine β -synthase

ChIP: chromatin immunoprecipitation

CLL: chronic lymphocytic leukemia

CML: chronic myeloid leukemia

COX: cytochrome c oxidase

CPT: carnitine palmitoyltransferase

CRC: colorectal cancer

CREB2: cAMP-responsive element binding 2

CRTC2: cyclic-AMP-regulated transcriptional co-activator 2

CS: citrate synthase

CSE: cystathionine γ-ligase

D-2-HGA: D-2-hydroxyglutaric aciduria

D2HGDH: D-2-hydroxyglutarate dehydrogenase

DHAP: dihydroxyacetone phosphate

DHFR: dihydrofolate reductase

DIC: differential interference contrast

DLBCL: diffuse large B-cell lymphoma

DMEM: Dulbecco's Modified Eagle's Medium

DMOG: dimethyloxallyl glycine

dNTP: deoxyribonucleotide

e3bp: e3 binding protein

EAA: essential amino acid

eEF2K: eukaryotic elongation factor 2 kinase

EGCG: epigallocatechin-3-gallate

EGF: epidermal growth factor

eIF2: eukaryotic translation initiation factor 2

eIF4E: eukaryotic translation initiation factor 4E

EMT: epithelial-mesenchymal transition

ETC: electron transport chain

ETF: electron-transferring flavoprotein

F-1,6-BP: fructose-1,6-biphosphate

F6P: fructose-6-phosphate

FA: fatty acid

FABP: fatty acid binding protein

FASN: fatty acid synthase

FATP: fatty acid transport protein

FBS: fetal bovine serum

FH: fumarate hydratase

FIH: factor inhibiting HIF

FLIM: fluorescence lifetime imaging

FNIP1/2: folliculin-folliculin interacting protein 1/2

FOXK1: forkhead/winged helix family k1

FTO: fat mass and obesity-associated

G6P: glucose-6-phosphate

G6PDH: glucose-6-phosphate dehydrogenase

GAAC: general amino acid control

GAB1: GRB2-associated binder 1

GABA: γ-aminobutyric acid

GAD: glutamate decarboxylase

GAP: glyceraldehyde-3-phosphate

GAP: GTPase-activating protein

GAPDH: glyceraldehyde-3-phosphate dehydrogenase

GCS: glycine cleavage system

GEF: guanine nucleotide exchange factor

GGT: γ-glutamyltransferase

GHB: γ-hydroxybutyrate

GLDC: glycine decarboxylase

GLUD: glutamate dehydrogenase

GLUL: glutamine synthetase

GLUT: glucose transporter

GMP: guanosine monophosphate

GMPS: guanosine monophosphate synthetase

GPD: glycerol-3-phosphate dehydrogenase

GPDH: glycerol-3-phosphate dehydrogenase

GPNA: γ-l-glutamyl-p-nitroanilide

GPx: glutathione peroxidase

GRB10: growth factor receptor-bound protein 10

GYS: glycogen synthase

HAT: histone acetyltransferase

HBV: hepatitis B virus

HCC: hepatocellular cancer

HCV: hepatitis C virus

HDAC: histone deacetylase

HIF: hypoxia inducible factor

HK: hexokinase

HLRCC: hereditary leiomyomatosis and renal cell cancer

HMT: histone methyl transferase

HOT: hydroxyacid-oxoacid transhydrogenase

HPV: human papillomavirus

HTC: hydride ion transfer complex

IDH: isocitrate dehydrogenase

IGF: insulin-like growth factors

IGF1R: insulin-like growth factor 1 receptor

IMP: inosine monophosphate

IMPDH: inosine monophosphate dehydrogenase

IR: insulin receptor

IRS-1: insulin receptor substrate-1

JmjC: Jumonji catalytic domain

KI: kinase inhibitor

L-2-HGA: L-2-hydroxyglutaric aciduria

L2HGDH: L-2-hydroxyglutarate dehydrogenase

LD: lipid droplet

LDH: lactate dehydrogenase

LDL: low-density lipoprotein

LHON: Leber hereditary optic neuropathy

LKB1: liver kinase B1

MAS: malate-aspartate shuttle

MAT: methionine adenosyl transferase

MCT: monocarboxylate transporter

MDH: malate dehydrogenase

ME: malic enzyme

MEF: mouse embryonic fibroblast

MPC1: mitochondrial pyruvate carrier complex 1

MPC2: mitochondrial pyruvate carrier complex 2

MS: methionine synthase

MTBSTFA: N-tert-butyldimethylsilyl-N-methyltrifluoroacetamide

MTHFD: methylenetetrahydrofolate dehydrogenase

MTHFR: methylenetetrahydrofolate reductase

mTORC1: mechanistic target of rapamycin complex 1

NBCL: non-Hodgkin's B-cell lymphoma

NDPK: nucleoside diphosphate kinase

NEAA: non-essential amino acid

NHL: non-Hodgkin's lymphoma

NMuMG: Normal Murine Mammary Gland

NSCLC: non-small-cell lung cancer

OGDD: 2-oxoglutarate/iron (II)-dependent dioxygenases

OGDH: 2-oxoglutarate dehydrogenase

OXPHOS: oxidative phosphorylation

P5CS: pyrroline-5-carboxylate synthase

PARP: poly (ADP-ribose) polymerase

PC: pyruvate carboxylase

PCa: prostate cancer

PCK: phosphoenolpyruvate carboxykinase

PDAC: pancreatic ductal adenocarcinoma

PDC: pyruvate dehydrogenase complex

PDH: pyruvate dehydrogenase

PDK: pyruvate dehydrogenase kinase

PDK1: 3-phosphoinositide-dependent protein kinase 1

PDP: pyruvate dehydrogenase phosphatase

PEP: phosphoenolpyruvate

PFK: phosphofructokinase

PFKFB: 6-phosphofructo-2-kinase/fructose-2,6-biphosphatase

PGI: phosphoglucose isomerase

PGK: phosphoglycerate kinase

PGM: phosphoglycerate mutase

PH: pleckstrin homology

PHD: prolyl hydroxylase

PHGDH: 3-phosphoglycerate dehydrogenase

PHGDH: phosphoglycerate dehydrogenase

PI: propidium iodide

PIP2: phosphatidyl inositol-4,5-biphosphate

PIP3: phosphatidyl inositol-3,4,5-triphosphate

PK: pyruvate kinase

PPAT: phosphoribosyl pyrophosphate amidotransferase

PPP: pentose phosphate pathway

PRA: 5-phosphoribosyl-1-amine

PRAS40: proline rich AKT1 substrate 40

PRDM15: PR/SET Domain 15

PRPP: phosphoribosyl pyrophosphate

PRPS: 5-phosphoribosylsynthetase

PRx: peroxiredoxin

PSAT1: phosphoserine aminotransferase 1

PSPH: phosphoserine phosphatase

PYCR: pyrroline-5-carboxylate reductase

R5P: ribose-5-phosphate

REDD1: regulated in development and DNA damage response 1

RHEB: ras homolog enriched in brain

RNR: ribonucleotide reductase

ROS: reactive oxygen species

RPI: ribose 5-phosphate isomerase

rpS6: ribosomal protein S6

RSK: p90 ribosomal protein S6 kinase

RTK: receptor tyrosine kinase

Ru5P: ribulose-5-phosphate

S6K: S6 kinase

SAH: S-adenosyl homocysteine

SAHH: S-adenosyl homocysteine hydrolase

SAICAR: succinylaminoimidazolecarboxamide ribose-5'-phosphate

SAM: S-adenosyl methionine

SCO2: synthesis of cytochrome c oxidase 2

SCS: succinyl-CoA synthetase

SDH: succinate dehydrogenase

SGLT: sodium-dependent glucose co-transporter

SGLT2: sodium-glucose cotransporter-2

SHMT: serine hydroxymethyltransferase

SITA: stable isotope tracer analysis

SITA: stable isotope tracer analysis

SLC25A: solute carrier family 25A

SLC2A: solute carrier 2A

SLC5A: solute carrier 5A

SOD2: superoxide dismutase 2

SSA: succinic semialdehyde

SSADH: succinic semialdehyde-dehydrogenase

SSP: serine synthesis pathway

STAT3: signal transducer and activation of transcription 3

STRAD: STE20-related kinase

TAG: triacylglycerol

TALDO: transaldolase

TBC1D7: TBC1 domain family member 7

TCSPC: time-correlated single photon counting

TET: ten-eleven translocation

TFAM: transcription factor a, mitochondrial

THF: tetrahydrofolate

TIGAR: TP53-induced glycolysis and apoptosis regulator

TISU: translation initiator of short 5' UTR

TKT: transketolase

TME: tumor microenvironment

TNBC: triple negative breast cancer

TPI: triose phosphate isomerase

TRx: thioredoxin

TSC: tuberous sclerosis complex

TSC2: tuberous sclerosis complex 2

UMP: uridine monophosphate

UMPS: uridine monophosphate synthetase

VHL: von-Hippel-Lindau

WT: wildtype

YY1: yin yang 1

CHAPTER 1: INTRODUCTION

1.1 Cancer burden and biology

Cancer imposes a significant burden on the Canadian healthcare system yearly as the population size grows and ages. Approximately 50 percent of Canadians are expected to be diagnosed with cancer in their lifetime (Canadian Cancer Statistics Advisory Committee, 2019) (Fig.1.1). In Canada, it was estimated that the number of new cancer cases will increase from 220,400 (1) to 225,800 cases (Canadian Cancer Statistics Advisory Committee, 2019) (Fig.1.1). This correlates with upsurge in cancer-related deaths (1) (Canadian Cancer Statistics Advisory Committee, 2019)



(Fig.1.1).

Fig. 1.1. Cancer-related statistics in Canada, 2019. (Canadian Cancer Statistics Advisory Committee, 2019).

Lung cancer was projected to be the leading cause of cancer-related deaths followed by colorectal, pancreatic and breast cancers (Canadian Cancer Statistics Advisory Committee, 2019). The steady rise in amount of cancer-associated mortality over the years is predominantly a reflection of poorly

understood biological underpinnings of the disease. Studying cancer etiology is particularly important in preventing and treating cancer, and thus reducing the cancer-related deaths. Cancer risk factors can be broadly classified into intrinsic and non-intrinsic risk factors. Unmodifiable intrinsic risks are spontaneous mutations that occur due to random errors in DNA replication (2). On the other hand, non-intrinsic risk factors include exogenous factors (carcinogens, viruses, physical activity, diet, smoking, UV radiation) and endogenous factors (metabolism, hormone levels, immunity, DNA damage response, genetic susceptibility) (2). Several studies link nonintrinsic factors to different types of cancers such as: smoking to lung cancer (3), Helicobacter pylori (H. pylori) to gastric cancer (Helicobacter & Cancer Collaborative (4), human papillomavirus (HPV) to cervical cancer (5) and head and neck cancer (6), hepatitis B virus (HBV), hepatitis C virus (HCV) to hepatocellular cancer (HCC) (7, 8) and UV radiation to melanoma (9). Overall, whether such risk factors are intrinsic or non-intrinsic, they may result in irreparable changes in the genome. Such lesions are frequently found in genes that regulate cellular processes including cell growth, proliferation, and cellular energetics (10, 11). This eventually leads to neoplasia.

There are over 200 different types of cancers (12). The diversity amongst the types of cancers makes them particularly challenging to diagnose and treat. Mutations in proto-oncogenes that generally regulate cell division, result in oncogenes that drive tumorigenesis (13). In addition, alterations in genes that act as tumor suppressors can trigger aberrant cell division (14). Molecular changes that are thought to underlie neoplasia are generally recognized as "hallmarks of cancer" that were originally published in 2000 (15). The hallmarks include: sustaining proliferative signaling, evading growth suppressors, resisting cell death, enabling replicative immortality, inducing angiogenesis, and activating invasion and metastasis (15). In 2011, "hallmarks of cancer"

were revised to include cancer cell abilities to reprogram energy metabolism, evade immune destruction, generate genome instability and tumor-promoting inflammation (10). Tumorigenesis is reliant on metabolic reprogramming which is often a direct and indirect consequence of oncogenic mutations. Inactivated tumor suppressor genes can also dysregulate cellular metabolism (16). Cancer cells rewire their metabolism to support the energetic demands of unchecked proliferation, fuel biosynthetic pathways and alleviate potentially deleterious effects of reactive oxygen species (ROS) (17).

1.2 Cancer metabolism

1.2.1 Warburg effect

Almost a century ago, Otto Warburg observed that tumors uptake more glucose compared to surrounding healthy tissues (18). He also observed that the cancer cells even in the presence of physiological oxygen tension metabolize glucose into lactate (18). This is termed as the "Warburg effect" or "aerobic glycolysis"(19). Warburg went on further to propose that this phenomenon is specific to cancer cells and is caused by dysfunctional mitochondria (20). To this end, Warburg postulated that proliferating cells adapt to abrogation of mitochondrial functions by upregulating glycolysis to meet ATP demands (20).

Subsequent studies have contradicted Warburg's hypotheses as aerobic glycolysis has been observed in normal proliferating thymocytes and lymphocytes (21, 22). Additionally, it was later found that defective mitochondria are not the cause of aerobic glycolysis in most cancer cells which is supported by data illustrating that the tumorigenic potential of cancer cells is markedly reduced by depleting mitochondrial DNA (23-25). In fact, most cancer cells not only retain their ability to carry out oxidative phosphorylation through fully functional mitochondria, but also reprogram their mitochondrial metabolism to circumvent the metabolic challenges associated with

their rapid proliferation (24, 26-29). Some cancer cells (e.g., HeLa, chronic lymphocytic leukemia (CLL) lymphocytes and melanoma) depend on oxidative phosphorylation (OXPHOS) and glycolysis to synthesize ATP (30-33). In particular, HeLa cells adapt their metabolism towards readily available substrates such as glucose and glutamine (which are catabolized in the mitochondria) (34). Exogenous lactate and acetate can also be oxidized by glioblastoma and breast cancer respectively to fuel neoplastic growth (35, 36). These and similar results illustrate the plasticity in cancer metabolism which is often needed to adapt to frequent changes in tumor microenvironment (TME). Other examples whereby cancer cells reprogram their cellular metabolism include increased glucose uptake (37), upregulated glycolysis (38), increased glutaminolysis (39), enhanced mitochondrial biogenesis (40) and perturbations in amino acid and lipid metabolism (41, 42).

Although the reduction of glucose into lactate produces fewer ATP molecules per glucose molecule when compared to its complete breakdown to produce carbon dioxide and water, ATP is synthesized faster and at comparable amounts via glycolysis (43-45). Equally important, glycolysis regenerates NAD+ and provides proliferating cells with the necessary intermediates for synthesizing amino acids, lipids and nucleotides (46). Aerobic glycolysis is advantageous for cancer cells as it enhances NADPH production through the oxidative branch of the closely associated pentose phosphate pathway (PPP) to detoxify ROS while meeting the bioenergetic and biosynthetic requirements of proliferation (47)

1.2.2 Glucose metabolism

Glucose is an essential macronutrient for mammalian cells (48). It is either obtained directly through the hydrolysis of ingested polysaccharides and disaccharides (48) or biosynthesized in the liver through gluconeogenesis (49). Glucose serves as a major source for

ATP which is used to drive cellular processes (48). In addition, glucose is a predominant carbon source used to biosynthesize building blocks such as amino acids, fatty acids and nucleotides (50).

1.2.2.1 Glucose uptake

Due to its hydrophilicity, glucose cannot move freely across the cell membrane (48). Glucose uptake into cells is facilitated by a family of membrane proteins called hexose or glucose transporters (GLUTs) (51) (Fig. 1.2.). Glucose is also transported by a family of sodium-dependent glucose co-transporters (SGLTs) which are structurally and functionally different from the GLUTs (52). SGLTs are encoded by solute carrier 5A (*SLC5A*) genes (52) while the GLUTs are expressed by a family of genes referred to as solute carrier 2A (*SLC2A*) (51).

To date, 14 GLUTs were described and they are divided into 3 classes (51) (53). The class I GLUTs include GLUT1-4, and represent the best characterized class of GLUTs (51). Their expression varies between different tissues and cell types (51). Furthermore, GLUTs 1-4 have different affinities for glucose (51). GLUT1 is primarily found in erythrocytes, brain and skeletal muscles (54). GLUT2 is expressed mostly in the liver, pancreas, intestines, and kidneys but absent in skeletal muscles (55, 56). GLUT3 and GLUT4 are both found predominantly in the neurons, whereby GLUT4 is also highly expressed in the heart and skeletal muscles and is sensitive to insulin (57-59). Importantly, certain cancers (e.g., breast and colorectal cancer) engage multiple glucose transporters such as GLUT2 and GLUT3 to support neoplastic growth (60).

In normal cells, glucose uptake is a tightly regulated process that responds to changes in the cellular energy demands (61, 62). External regulation of glucose transport involves response to hormones (insulin and glucagon) and growth factors [epidermal growth factor (EGF) and insulin-like growth factors (IGF)] (63). To fuel high energy demanding cellular processes (e.g., mRNA translation) and biosynthesize the macromolecules necessary for proliferation, cancer cells

often upregulate glucose uptake (64). Tumors are typically poorly vascularized which limits their access to nutrients and oxygen (65-67). Hence, neoplastic cells must adapt their metabolism (e.g., by enhancing the expression of glucose transporters) to survive conditions wherein nutrients and oxygen are limited (68). To this end, the expression of *SLC2A1* is elevated in various types of cancers (69-71) including colorectal adenocarcinomas (69). In hepatocellular carcinoma, high levels of *SLC2A2* were reported to correlate with poor overall survival (72). *SLC2A3* and *SLC2A4* are also overexpressed in bladder cancer (73) and alveolar rhabdomyosarcoma (74) respectively. Similar to GLUTs, SGLTs (SGLT1 and SGLT2) were suggested to enhance glucose uptake in tumors (75). It was demonstrated that in metastatic lung cancer, *SLC5A2* expression (*SLC5A2* encodes SGLT2) was higher in metastatic tumors relative to primary tumors (76) suggesting that glucose metabolism can be modulated to promote tumor progression. Overall, cancer cells appear to utilize different strategies to upregulate glucose uptake thus fueling neoplastic growth.

1.2.2.2 Glycolysis

Upon transport into the cell, glucose is partly catabolized in the cytosol and subsequently oxidized in the mitochondria (48). Glycolysis is catabolic process whereby glucose through a series of reactions is broken down into pyruvate in the cytosol (48) (Fig. 1.2). This process produces 2 moles of pyruvate, ATP and NADH per mole of glucose (48) (Fig. 1.2.). In the absence of oxygen, pyruvate gets reduced by lactate dehydrogenase (LDH) to produce NAD+ and lactate (48). As Warburg observed, neoplastic cells can convert pyruvate into lactate even in the presence of sufficient oxygen (18). In contrast, in most normal tissues, pyruvate is typically oxidized in mitochondria under normal oxygen tension (48).

Hexokinases (HKs) catalyze the first committed step in glycolysis by phosphorylating glucose to produce glucose-6-phosphate (G6P) using an ATP molecule (48) (Fig. 1.2.). This traps

the glucose molecules by preventing their efflux back to the extracellular space (48). In turn, G6P inhibits HKs as a part of a negative feed-back loop (77). There are four main isoforms of HK found in mammals which vary in their localization and kinetics with respect to different substrates [i.e., glucose and ATP; reviewed in (78)]. G6P is then converted into fructose-6-phosphate (F6P) by phosphoglucose isomerase (PGI) and subsequently phosphorylated to produce fructose-1,6-biphosphate (F-1,6-BP) which is catalyzed by phosphofructokinase 1 (PFK1) (48) (Fig. 1.2.). The phosphorylation of fructose-6-phosphate is another rate-limiting step of glycolysis which consumes one ATP (48). Moreover, PFK1 is allosterically inhibited by ATP and activated by AMP (79). This suggests that the activity of PFK1 is dependent on the bioenergetic state of the cell.

F-1,6-BP is split by aldolase (ALDO) into two 3-carbon glycolytic intermediates that are isomers of each other: dihydroxyacetone phosphate (DHAP) and glyceraldehyde-3-phosphate (GAP) (48) (Fig. 1.2). Since only GAP is further metabolized in glycolytic pathway, all DHAP molecules are isomerized into GAP by triose phosphate isomerase (TPI) (48) (Fig. 1.2). This signifies the end of the energy investment phase of glycolysis where two molecules of ATP are consumed to catabolize a molecule of glucose into three-carbon phosphate intermediates. The payoff phase of glycolysis begins when glyceraldehyde-3-phosphate dehydrogenase (GAPDH) oxidizes and phosphorylates GAP to produce 1,3-biphosphoglycerate (1,3-BPG) by utilizing one NAD+ molecule per molecule of GAP in the process (48) (Fig. 1.2). 1,3-BPG is then converted to 3-phosphoglycerate (3-PG) by phosphoglycerate kinase (PGK) (48) (Fig. 1.2). This reaction also yields one ATP molecule for each converted 1,3-BPG molecule (48) (Fig. 1.2). Afterwards, phosphoglycerate mutase (PGM) isomerizes 3-PG to 2-phosphoglycerate (2-PG) and subsequently enolase dehydrates 2-PG to produce phosphoenolpyruvate (PEP) (48) (Fig. 1.2). Pyruvate kinase

(PK) catalyzes the last reaction of the payoff phase whereby PEP is irreversibly converted to pyruvate while simultaneously producing ATP (48) (Fig. 1.2).

Glycolytic enzymes are essential for promoting the survival and proliferation of malignant cells (80). Elevated HK2 expression has been observed in many cancers (81) including brain metastasis of breast cancer which is significantly associated with poor patient survival post-craniotomy (82). In addition, HK2 appears to be essential for tumorigenesis in *in vivo* models of KRAS-driven lung cancer and HER2+ breast cancer (83). PGI overexpression is involved in tumor metastasis and epithelial-mesenchymal transition (EMT) in breast cancer (84). Elevated levels of PFK mRNA have been observed in lung and colon carcinomas (85, 86). Notwithstanding that *GAPDH* is widely regarded as a housekeeping gene, its overexpression was observed in colorectal carcinoma (87) and pancreatic cancer (88, 89). Accordingly, it has been suggested that GAPDH may exert antiapoptotic roles in drug-resistant chronic myeloid leukemia (CML) cancer (90). Likewise, some cancer types (e.g., lung, gastric and pancreatic cancers) upregulate PGK or ALDO expression which parallels with increased cell motility, angiogenesis and metastasis (91-93). Overall, these findings demonstrate that dysregulated glycolytic gene expression is likely to play a central role in cancer initiation and progression.

In mammals, there are 2 genes (*PKLR* and *PKM*) which encode 4 tissue-specific isoforms (PKL, PKR, PKM1 and PKM2) of PK (94, 95). Intriguingly, although PKL is expressed in the liver, kidneys, pancreas and intestine while PKR is expressed in erythrocytes, they are both encoded by the *PKLR* gene (95). Alternative splicing of the *PKM* gives rise to two proteoforms: PKM1 (expressed in in the brain, skeletal and cardiac muscles) and PKM2 (expressed in in embryonic tissue, leucocytes, intestine, and thymus) (95, 96). Despite having the same catalytic function, PKM1 is constitutively active and more efficient at converting PEP into pyruvate relative

to PKM2 (95). Serine can bind and activate PKM2, whereby PKM2 activity is diminished when serine is unavailable (97). This reduction in PKM2 activity turns cells to a fuel-efficient state whereby more pyruvate is redirected to the mitochondria (97). Prior to this discovery, PKM2 was observed to interact directly with phosphotyrosine peptides resulting in the release of its allosteric activator, F-1,6-BP (98). Abrogating the enzymatic activity of PKM2 diverts glycolytic intermediates from energy production to anabolic processes (e.g. lipid synthesis) when cancer cells are stimulated by growth factors such as IGF (98). Consequently, growth factors which initiate the phosphorylation of tyrosine residues on signaling proteins inhibit PKM2 and this is thought to allow transformed cells to transition between bioenergetic and biosynthetic modes (98). Similar to serine and F-1,6-BP, succinylaminoimidazolecarboxamide ribose-5'-phosphate (SAICAR), which is a metabolic intermediate of *de novo* purine nucleotide biosynthesis pathway was also shown to allosterically activate PKM2 and promote cancer cell survival in glucose-deprived conditions (99). Accordingly, high PKM2 levels have been associated with many cancers including lung, cervical, prostate and brain malignancies (100-102). When malignant cells were engineered to express PKM1 instead of PKM2, the cells switched from aerobic glycolysis to OXPHOS which correlated with reduced tumor formation following xenotransplantation (102). As such, the regulation of PKM2 can be commandeered by neoplasia to increase metabolic flexibility. However, there are conflicting reports demonstrating that the abrogation or inhibition of PKM2 promotes tumor growth (103-105). Interestingly, in one of these reports, low PKM2 activity which was observed in lung cancer cells subjected to hypoxia led to the activation of PPP to generate sufficient NADPH for ROS detoxification and thus survival of cancer cells (105). Collectively, these studies indicate that the role of PKM2 in tumorigenesis is likely to be context-dependent.

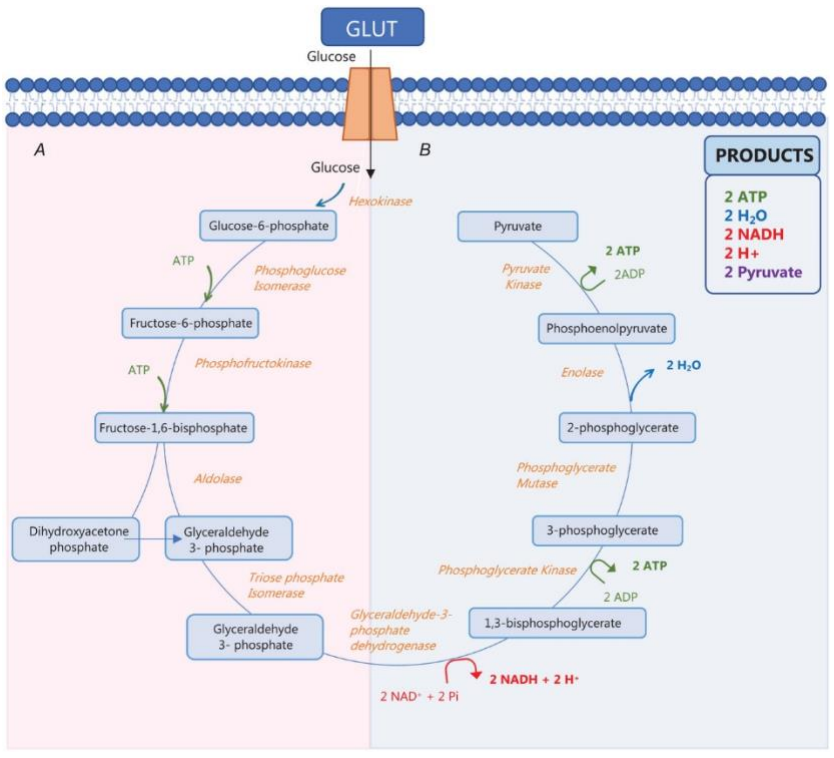


Fig. 1.2. Glucose uptake and glycolysis (106). Glucose is taken into the cell via specific glucose transporters (GLUTs). It is subsequently metabolized through a series of ten enzymatic reactions (orange) to produce pyruvate. Glycolysis is divided into an energy investment phase (A; pink box) which consumes ATP (green) and a payoff phase (B: blue box) which produces NADH, ATP and H₂O.

1.2.3 Pyruvate metabolism: Crossroads between glycolysis and citric acid cycle 1.2.3.1 Cytosolic reduction of pyruvate

Under anaerobic conditions, LDH catalyzes the reversible conversion of pyruvate to lactate with the concomitant oxidation of NADH in the cytosol of normal cells (48). Following its production, lactate is excreted into the extracellular space via monocarboxylate transporters (MCTs) (107). As mentioned above, it was observed that tumor cells metabolize glucose into lactate even in the presence of ample oxygen (20). Furthermore, the NAD+ pool generated by LDH is used to support successive rounds of glycolysis and increase the levels of anabolic intermediates

used by cancer cells (100, 108). Despite their high overall structural similarity, LDH exists as two distinct isoforms that exhibit significant differences in the charged residues surrounding the active sites. LDHA favors the conversion of pyruvate to lactate, while LDHB preferentially oxidizes lactate to pyruvate (109-111). Numerous studies demonstrate aberrant activation and abnormally high expression of LDHA in multiple cancers including colorectal cancer (CRC), liver cancer, non-small-cell lung cancer, pancreatic cancer and esophageal cancer (112-118). In addition to altering the metabolism to confer neoplastic growth advantage, the expression of LDHA promotes angiogenesis, cell invasion and metastasis (115, 119). While the upregulation of LDHB was shown to be essential to the proliferation of KRAS-driven lung cancer and triple negative breast cancer (120, 121), its low expression in hepatocellular carcinoma relative to noncancerous tissues correlated with unfavorable survival (122). This suggests that the role of LDHB in tumorigenesis seems to be context-dependent. Contrary to Warburg's findings, a recent hypothesis (i.e., "Reverse Warburg Effect") that supports oxidative mitochondrial metabolism in neoplasia proposes that stromal or transformed cells undergo aerobic glycolysis to produce lactate (123). Lactate is then released in the TME via MCT4 and is subsequently taken up through MCT1 transporter of surrounding cells as an energy source (123, 124). According to this model, LDHB catalyzes the oxidation of lactate to pyruvate which then enters the citric acid cycle (CAC). Metabolic cooperation of cancer cells within the TME is further substantiated in pancreatic and breast cancer models which revealed that lactate secreted by glycolytic hypoxic malignant cells can be taken up as fuel for aerobic tumor cells (36, 125). Moreover, secretion of lactate and subsequent acidification of TME is thought to induce angiogenesis while impairing tumor immunosurveillance (126). Of note, under physiological conditions, lactate released by brain, skeletal and muscle cells can be reconverted into glucose in the liver via the Cori cycle (127). Tumor cells extrude copious

amounts of lactate into the TME to maintain a high glycolytic flux which is thought to increase Cori cycle activity in the liver (128, 129). Overall, pyruvate-lactate metabolism impacts cancer fate in a cell-autonomous and systemic level.

1.2.3.2 Mitochondrial oxidative decarboxylation of pyruvate into acetyl-CoA

Under normoxia, pyruvate is chiefly imported into the mitochondrial matrix via the mitochondrial pyruvate carrier complex 1/2 (MPC1 and MPC2) to be irreversibly oxidatively decarboxylated to acetyl-CoA by pyruvate dehydrogenase (PDH) complex (PDC) which is accompanied by NAD+ reduction (48, 130, 131). Essentially, this reaction links glycolysis, fatty acid metabolism and CAC (132). PDC is assembled from an e3 binding protein (e3BP) and multiple copies of three enzymes: E1 (pyruvate dehydrogenase), E2 (dihydrolipoyl transacetylase), and E3 (dihydrolipoyl dehydrogenase) (126, 133). E1 is the rate-limiting enzyme of the complex (126). At high concentrations, the products from the reaction (i.e., acetyl-CoA and NADH) inhibit the activity of PDC (134). Instantaneous post-translational regulation is achieved via kinases and phosphatases (134). Tissue-specific pyruvate dehydrogenase kinase isozymes (PDK1-4) which differ in their enzymatic activities, inactivate PDC by phosphorylating specific serine residues located on the a subunit of the E1 enzyme in the complex (135, 136). In turn, pyruvate dehydrogenase phosphatases 1/2 (PDP1/2) restore PDC enzyme activity via dephosphorylating key regulatory residues (126, 134). Thus, PDKs and PDPs help in maintaining the mitochondrial acetyl-CoA pool to support CAC activity. Acetyl-CoA is a precursor used by histone acetyltransferases (HATs) to catalyze the addition of acetyl groups to the histone N-terminal tails (137). Based on this, HATs link epigenetic regulation to the metabolic status of the cells as they are dependent on glucose availability, lipid metabolism and mitochondrial function (138-140).

This makes acetyl-CoA a versatile and critical metabolic intermediate to fuel anabolic reactions and epigenetic remodeling processes.

Reduced expression levels of *MPC1* or *MPC2* in cancer have been shown to correlate with poor patient survival (141, 142). Increased expression of MPCs in CRC cells was found to not only increase mitochondrial pyruvate oxidation while suppressing aerobic glycolysis, but also to impair anchorage-independent growth (141). In addition, aberrant regulations of PDKs and PDPs which control the activity of PDC have been associated with different cancers (143-145). For instance, the enhanced PDK1 activity has been linked to increased invasiveness and tumor growth in head and neck squamous cancer cells (146) whereas the upregulation of PDK4 was reported to correlate with increased migration and invasion in CRC (147). Moreover, the activation of PDP1 was observed to increase OXPHOS, decrease cell proliferation and reduce tumor growth in a lung cancer cell line xenograft model (143). Collectively, these studies suggest that the PD(K/P):PDC axis acts as metabolic switch in cancer cells which increases metabolic flexibility by allowing adaptation to fluctuations in nutrient and oxygen availability as well as bioenergetic requirements.

1.2.4 Citric acid cycle (CAC)

Acetyl-CoA produced by PDC can enter the citric acid cycle (CAC; also referred to as Krebs cycle or tricarboxylic acid cycle), where the carbon atoms are converted to CO₂ while simultaneously producing reducing equivalents (i.e. NADH and FADH₂) (131) (Fig. 1.3). CAC starts with the irreversible condensation of acetyl-CoA, derived from oxidative decarboxylation of pyruvate, β-oxidation of fatty acids or catabolism of amino acids (e.g., leucine, isoleucine and tryptophan), with oxaloacetate to produce the six-carbon citrate which is catalyzed by citrate synthase (CS) in the mitochondrial matrix (148). Through feedback inhibition, citrate suppresses the activity of CS (149). NADH, ATP and succinyl-CoA are also inhibitors of CS (148, 150).

Importantly, citrate downregulates glycolysis by allosterically inactivating glycolytic enzymes PFK1 and PFK2 (148, 151). Furthermore, high levels of citrate suppress PDC and succinate dehydrogenase (SDH), thus repressing the CAC (152, 153). The role of CS in neoplasia remains poorly understood considering that the abrogation of its activity appears to result in contrasting phenotypes. While reduced CS expression led to marked increases in glycolysis and migration of cervical cancer cells, silencing CS expression inhibited invasion and migration of ovarian carcinoma cells (154, 155). In healthy prostate epithelial cells, citrate exits the CAC via the dicarboxylate antiporter solute carrier family 25 (SLC25A1) to be eventually secreted into the prostatic fluid to facilitate the maturation and motility of spermatozoa (156). A defining metabolic phenotype of normal prostate epithelial cells, which is elevated citrate production and secretion, is reversed during tumorigenesis (156). Thus, low concentrations of citrate serve as a useful biomarker of prostate cancer, wherein the citrate levels inversely correlate with the stage of prostate cancer (PCa) (157).

In most of the non-transformed cells, citrate is either transported to the cytosol through SLC25A1, to serve as a precursor molecule for fatty acid and cholesterol biosynthesis, or it is retained in the mitochondrial matrix where it is reversibly isomerized to isocitrate by aconitase (ACO) (148) (Fig. 1.3). ACO dehydrates citrate into cis-aconitate, an intermediate product, which is then rehydrated into isocitrate (158) (Fig. 1.3). Zinc acts as a competitive inhibitor of mitochondrial aconitase (ACO2), which prevents citrate oxidation in the CAC (159). This is particularly important for the physiological functions of prostate epithelial cells (159). Similar to citrate, intracellular zinc acts as a biomarker for PCa, whereby its levels are inversely correlated to the progression of the disease (159, 160). Indeed, previous studies have suggested decreased levels of zinc as a biomarker for the early diagnosis of PCa (161, 162). Consistent with this, the

downregulation of an important zinc transporter, ZIP1, is associated with reduced zinc levels in prostate cancer (160, 163). Thus, the metabolic reprogramming that underlies the transformation of prostate cells comprises a switch from physiological citrate-producing epithelial cells to neoplastic citrate-oxidizing cells. Collectively, these findings suggest that the intracellular zinc levels not only dictate the metabolic state of prostate cells but could be associated with the development of PCa.

In normal conditions, isocitrate is oxidatively decarboxylated into the five-carbon α ketoglutarate (α-KG) in a rate-limiting reaction catalyzed by NAD+-dependent isocitrate dehydrogenase (IDH) which concurrently produces the first NADH molecule of the CAC (148, 164) (Fig. 1.3). IDH is expressed in three isoforms: IDH1, IDH2, and IDH3 (151, 165). IDH1 is localized in the cytosol while IDH2 and IDH3 are found in the mitochondria (151, 165). Unlike mitochondrial IDH3 which depends on NAD(H), IDH1 and IDH2 prefer the use of NADP(H) as a cofactor (166). IDH1 and IDH2 have a high degree of sequence, structural and functional similarity between them (167, 168). Both isomers function as homodimers catalyzing the oxidative decarboxylation of isocitrate into α-KG while simultaneously producing NADPH necessary for protecting the cell against oxidative damage and fatty acid synthesis (169-172). Conversely, the reductive carboxylation of α-KG to isocitrate which is subsequently converted to citrate is important for regulating glycolysis and lipogenesis (173). The conversion of isocitrate to α-KG catalyzed by IDH3 is irreversible in contrast to the reversible processes of IDH1- and IDH2catalyzed reactions (174, 175). IDH3 is regulated through the concerted activities of ions and molecules as citrate, ADP and calcium ions are allosteric activators while ATP, α-KG, NADPH and NADH suppress IDH3 activity (176-178). Importantly, in tumors where biosynthetic processes are upregulated and often accompanied with reduced mitochondrial respiration either

due to hypoxia or defective ETC complexes, the elevated intramitochondrial NADH/NAD+ ratio impedes isocitrate oxidative decarboxylation in the CAC (179, 180). The high NADH/NAD+ ratio is often associated with the mitochondrial export of citrate depots for synthesizing fatty acids, phosphoglycerides and cholesterol (179, 180). IDH1 is also a major producer of NADPH which is required for lipid synthesis and ROS detoxification (173, 181-184). Overall, this suggests that the activities and the direction of reactions catalyzed via IDH isoenzymes are governed by the NAD(P)H/NAD(P)+ ratios which in turn affects fatty acid and energy metabolism in both normal and malignant cells. This metabolic flexibility allows cancer cells to sustain essential anabolic processes and NADH generation for OXPHOS.

It is worth mentioning that although the tumorigenic effects of IDH1 and IDH2 mutants have been well characterized (discussed in detail below), the role of IDH3 in neoplasia has not been well studied. Elevated levels of IDH3 α , the catalytic subunit of IDH3, have been observed in GBM tumor samples as compared to normal brain tissue whereby it was found that elevated IDH3 α promotes tumor progression in glioma mouse models (185). Accordingly, overexpression of IDH3 α reduced α -KG levels thus preventing hypoxia inducible factor (HIF) 1 α degradation and enhancing tumor growth in cervical cancer models (186). However, other studies provided contradictory data regarding the association between IDH3 α expression and intracellular α -KG concentrations (187), thus suggesting that the mechanism by which IDH3 drives oncogenesis may be context-dependent.

α-KG, also known as 2-oxoglutarate, is subjected to irreversible oxidative decarboxylation by 2-oxoglutarate dehydrogenase (OGDH) enzymatic complex in the mitochondrial matrix to generate the four-carbon succinyl-CoA and the second NADH molecule of the CAC [(148) Fig. 1.3]. The OGDH complex is not only functionally analogous to the PDC, but also structurally

similar as the OGDH complex also consists of multiple copies of a thiamine pyrophosphatedependent dehydrogenase (E1), dihydrolipoamide succinyltransferase (E2) and dihydrolipoamide dehydrogenase (E3) (188). The OGDH complex requires thiamine pyrophosphate as a cofactor and is activated by calcium ions and suppressed by NADH and succinyl-CoA; two of the end products of the reaction it catalyzes (188-190). α-KG is an important cofactor for 2oxoglutarate/iron (II)-dependent dioxygenases (OGDDs) including Jumonji catalytic (JmjC) domain containing N-methyl-lysine and N-methyl-arginine histone demethylases, which are known to epigenetically control gene expression (191). Aberrant regulation of these enzymes is implicated in many different types of cancers including breast and prostate cancer (191, 192). Hence, it is crucial for normal cells to maintain optimal intracellular concentrations of α-KG to preserve their epigenetic landscape. On the contrary, breast cancer cells appear to deplete their α-KG pool by upregulating OGDH levels and reduce α-KG into succinyl-CoA (193). This is congruent with reports demonstrating that the inhibition of OGDH results in the accumulation of α-KG which in turn increases levels of the α-KG-dependent chromatin modification 5hydroxymethylcytosine (5hmC) (194, 195). This is mirrored by attenuated malignant progression and metastasis in p53^{-/-} pancreatic ductal adenocarcinoma and breast cancer (194, 195). Overall, this illustrates that alterations in α-KG levels result in epigenetic perturbations that play a major role in determining the fate of malignant cells.

Next, succinyl-CoA is hydrolyzed into succinate via succinyl-CoA synthetase (SCS) by substrate-level phosphorylation producing GTP in the process which is converted into ATP by mitochondrial nucleoside diphosphate kinase (NDPK) (148, 196, 197) Fig. 1.3. Succinyl-CoA also serves as a precursor in important biosynthetic pathways. For example, the 5-aminolevulinic acid, which is a condensation product of succinyl-CoA with glycine, is exported to the cytosol

which marks the first step of heme biosynthesis in the liver and erythroid cells (198). In addition to succinyl-CoA, succinate can be produced via the γ-aminobutyric acid (GABA) shunt, whereby GABA which is synthesized from glutamate by glutamate decarboxylase (GAD), is subsequently transaminated into succinic semialdehyde (SSA) through GABA transaminase (ABAT) that finally gets oxidized into succinate via SSA-dehydrogenase (SSADH) (199, 200). Although, there are limited studies on the GABA shunt in tissues other than neurons, recent findings showed that decreased expression of GAD impeded branched chain amino acid (BCAA) uptake in non-small-cell lung cancer (NSCLC) (201, 202). Furthermore, low expression of GAD reduced the proliferation of both NSCLC and castration-resistant prostate cancer cells (201, 202). These observations further highlight metabolic pathways that appear to be hijacked by transformed cells to drive tumorigenesis.

SDH, a component of complex II of the electron transport chain (ETC) located on the inner mitochondrial membrane, oxidizes succinate into fumarate [(148) Fig. 1.3]. Unlike the other CAC dehydrogenases that reduce NAD+, SDH produces FADH2 (148) Fig. 1.3. The SDH complex consists of 6 subunits (SDHA, SDHB, SDHC, SDHD, SDHAF1 and SDHAF2) (203, 204). Increased levels of oxaloacetate inhibit SDH complex thereby downregulating the CAC (202). Fumarase, also referred to as fumarate hydratase (FH), catalyzes reversible hydration of fumarate into malate, while consuming water in the process [(148, 205) Fig. 1.3]. Loss-of-function mutations in the SDH complex and FH in the accumulation of succinate and fumarate, respectively (206). The accumulation of either succinate or fumarate has been associated with different cancers such as renal cell carcinoma, thus suggesting that SDH and FH exhibit tumor-suppressive properties (206).

Malate dehydrogenase (MDH) catalyzes the final enzymatic reaction which completes one turn of the CAC (148, 207). In this reaction, oxaloacetate is regenerated from malate with the concomitant reduction of NAD+ to NADH (148, 207) Fig. 1.3. The resulting oxaloacetate can then be used for the next round of CAC (148, 207). MDH exists as two isoforms (MDH1 and MDH2) that differ in their subcellular localization and preference for cofactors (208, 209). MDH1 is found in the cytosol while MDH2 is localized in the mitochondrial matrix (208, 209). Both MDH isoforms are part of the malate-aspartate shuttle (MAS) in which MDH1 reduces cytosolic oxaloacetate into malate with the concurrent oxidation of NADH into NAD+ while MDH2 predominantly catalyzes the reverse reaction, thus converting the mitochondrial malate pool into oxaloacetate and NADH (209). Hence, the mitochondrial malate reserves are composed of cytosolic-derived malate (imported to the mitochondria via the SLC25A11 transporter) and mitochondrial-based malate (produced by FH) (209). As such, MDH1 supports aerobic glycolysis by maintaining a high cytosolic NAD+/NADH ratio while indirectly reducing mitochondrial NAD+/NADH ratio. The MDH2 isoform is allosterically activated by elevated malate levels and inhibited by high concentrations of oxaloacetate (210). Elevated levels of MDH2 expression in prostate cancer have been associated with markedly shorter period of relapse-free survival postchemotherapy (Liu et al., 2013). This suggests that aberrant MDH2 activity may be implicated in the metabolic reprogramming required for cancer cell progression (211).

Considering that the CAC enzymes evolved before the presence of oxygen on earth, it was proposed that the fundamental role of the CAC is the biosynthesis of metabolites (e.g. hemes, amino acids, nucleic acids, fatty acids) (148). However, CAC has evolved to also play a bioenergetic role by producing ATP, NADH and FADH₂ (148) Fig. 1.3. The NADH and FADH₂ subsequently feed the ETC via complex I and II respectively to ultimately generate ATP via

OXPHOS (148). Hence, under physiological conditions the CAC is coupled to OXPHOS due to the oxidation of NADH and FADH₂ (148).

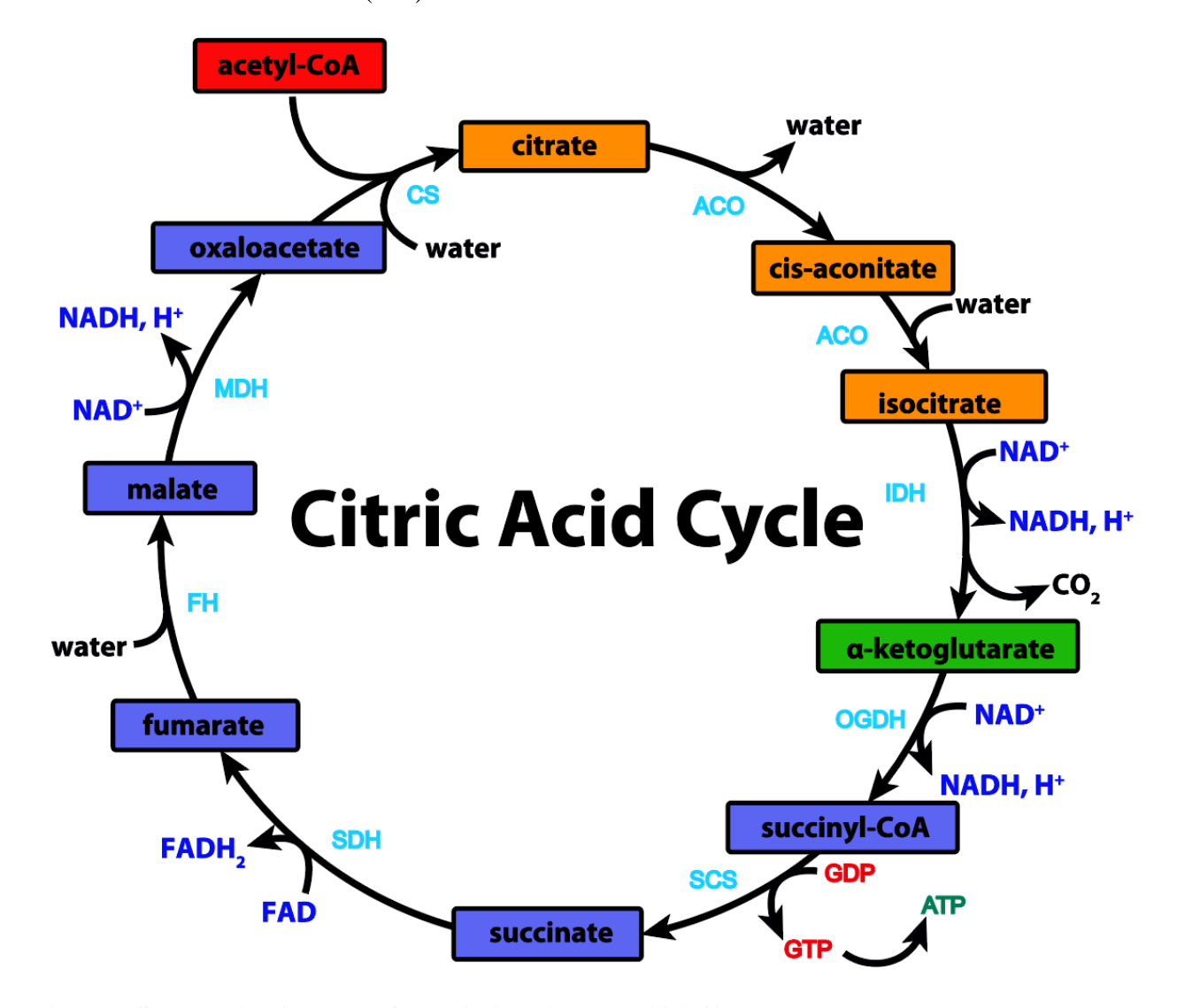


Fig. 1.3. Schematic diagram of the citric acid cycle (CAC). 2-carbon containing acetyl-CoA (shown in a red box) enters the CAC by condensing with 4-carbon oxaloacetate to produce 6-carbon citrate. Citrate is oxidatively decarboxylated through a series of enzymes to release CO₂ in the process while simultaneously producing 1 ATP molecule and reducing equivalents NADH (3) and FADH₂(1). 6-carbon containing CAC intermediates are denoted in orange boxes while 5-carbon and 4-carbon containing CAC intermediates are represented with green and indigo boxes. The enzymes catalyzing CAC reactions are in cyan (adapted figure: George-stock.adobe.com).

1.2.4.1 Aberrant activity of CAC enzymes produces "oncometabolites"

1.2.4.1.1 2-Hydroxyglutarate (2-HG)

The intracellular levels of α-KG directly affect the activities of OGDDs including teneleven translocation (TET) family of DNA methylases, JmjC family of histone demethylases, prolyl hydroxylases (PHDs), AlkB homolog (ALKBH) DNA repair enzymes and fat mass and obesity-associated protein (FTO) which demethylates mRNA (212-215). OGDDs couple the oxidation of substrate to the oxidative decarboxylation of α -KG to produce succinate and CO₂ (214). Heterozygous somatic mutations observed in *IDH1* and *IDH2* have been known to indirectly modulate the activities of OGDDs (212, 216, 217). It was shown that missense mutations in IDH1/2 genes (mostly affecting active site amino acid residues: R132 in IDH1, R140 and R172 in IDH2) result in the loss of normal enzymatic activity while attaining the ability to reduce α -KG into the D-enantiomer of 2-hydroxyglutarate (D-2-HG also known as R-2-HG) (212, 218-220). D-2-HG and L-2-HG (the L-enantiomer also referred to as S-2-HG) bind to the active sites of OGDDs as competitive inhibitors due to their structural similarities to α-KG (212, 216). Thus, these neomorphic mutations in *IDH1/2* lead to accumulation of D-2-HG which suppresses OGDDs thus leading to epigenetic alterations (via histone and DNA methylation). Considering that OGDDs play a role in regulating normal cellular differentiation, it is not surprising that *IDH1* and *IDH2* are frequently mutated genes in cancers such as glioma, acute myeloid leukemia (AML) and chondrosarcoma whereby IDH1 and IDH2 mutations are often associated with gene silencing and dedifferentiation of cells (221-223). This is consistent with findings that demonstrate either exogenously expressing mutant IDH1/2 or treating non-transformed cells with cell-permeable D-2-HG impedes cell differentiation and inhibits H3K9 demethylases (224, 225).

Interestingly, D-2-HG and L-2-HG can accumulate in cells with wildtype *IDH1/2* genes (179, 226, 227). Studies have revealed that α -KG can be converted to D-2-HG by hydroxyacid-oxoacid transhydrogenase (HOT) while simultaneously producing SSA from γ -hydroxybutyrate (GHB) in normal cells (228, 229). Furthermore, overexpression of 3-phosphoglycerate dehydrogenase (PHGDH) in breast cancer, which catalyzes the first reaction of serine biosynthesis to produce 3-phosphohydroxypyruvate by NAD⁺-coupled oxidation of 3-PG has been suggested to reduce α -KG to D-2-HG (230). Although both D-2-HG and L-2-HG can be produced from α -KG, L-2-HG can be formed by LDHA and MDH1/2 in acidic pH and/or when oxygen is limited (231-234). Taken together, the studies suggest that cancer cells utilize L-2-HG and D-2-HG to reprogram epigenome and facilitate tumor progression (227, 235).

Under physiological conditions, the harmful effects of D-2-HG and L-2-HG are prevented as they are converted to α-KG by D-2-hydroxyglutarate dehydrogenase (D2HGDH) and L-2-hydroxyglutarate dehydrogenase (L2HGDH) respectively (236-238). Although intracellular levels of 2-HGs are kept at micromolar range by 2HGDHs, the millimolar levels of D-2-HG observed in patients diagnosed with type II D-2-hydroxyglutaric aciduria (D-2-HGA), AML and glioblastoma due to mutations in *IDH1/2* genes exceeds the catalytic ability of D2HGDH which leads to accumulation of D-2-HG in the plasma, urine and cerebrospinal fluids (216, 236, 239-242). In addition, loss-of-function mutations in *D2HGDH* and *L2HGDH* are responsible for autosomal recessive neurometabolic disorders, type I D-2-HGA and L-2-hydroxyglutaric aciduria (L-2-HGA) respectively (237, 242). Intriguingly, patients diagnosed with L-2-HGA are predisposed to developing brain tumors while patients diagnosed with D-2-HGA appear not to exhibit increased cancer incidence (241, 243). Of note, type II D-2-HGA patients which are characterized by mutations in IDH1/2 typically present with more D-2-HG built-up in their plasma, urine and

cerebrospinal fluid as compared to type I D-2-HGA patients having inactivated D2HGDH (241, 242). Nonetheless, the mortality of patients with severe D-2-HGA is exceptionally high during infancy (241, 242). This significantly confounds potential comparisons of cancer susceptibility between different types of D-2-HGA (241, 242). Furthermore, considering that L-2-HG is five to ten times more potent than D-2-HG in suppressing OGDDs, this may potentially explain the discrepancy between L-2-HGA and D-2-HGA in cancer predisposition. Moreover, even in the absence of IDH1/2 mutations, elevated levels of D-2-HG and L-2-HG have been observed in different cancer types such as colorectal cancer, breast cancer, renal cell carcinoma and diffuse large B-cell lymphoma (235). Notwithstanding that the molecular underpinnings of 2-HG enantiomer function(s) in neoplasia remain incompletely understood, both enantiomers are likely to play a prominent role in tumorigenesis and tumor progression.

1.2.4.1.2 Succinate

Other than 2-HGs, OGDDs are susceptible to competitive inhibition by succinate due to its structural similarity to α -KG (191, 244). Inactivating mutations found in some of SDH complex subunits (SDHB, SDHC, SDHD and SDHAF2) lead to a buildup of succinate which is commonly observed in familial and sporadic paraganglioma and pheochromocytomas (245-248). Similarly to 2-HG, succinate acts as an oncometabolite by attenuating OGDD functions which includes abrogating the epigenetic remodeling by JmjC domain-containing histone demethylases and the TET family of DNA hydroxylases (244). Also, OGDDs like PHDs (i.e., PHD1-3) and factor inhibiting HIF (FIH) regulate HIF- α levels in response to alterations in intracellular oxygen tension. Namely, in normoxia specific proline (P402 and P564 in HIF- 1α ; P405 and P531 in HIF- 2α) and asparagine (N803 in HIF- 1α and N851 in HIF- 2α) residues in the HIF- α are hydroxylated by PHDs and FIH respectively to facilitate polyubiquitinylation and proteasomal degradation

mediated by the tumor suppressor von-Hippel-Lindau (VHL)-E3 ubiquitin ligase (249-254). As discussed in a greater detail below, HIF-1/2 regulates genes that are involved in both systemic responses to hypoxia, such as angiogenesis and erythropoiesis, and in cellular responses, such as alterations in glucose metabolism (255).

Mutations in *SDHD* and *SDHB* genes (which are commonly observed in hereditary paraganglioma and pheochromocytoma, respectively), activate hypoxic and angiogenic pathways, which is mediated by elevated succinate levels (255-257). These loss-of-function mutations in SDH subunits abolish the activity of the SDH complex leading to the accumulation of succinate in the mitochondrial matrix that consequently leaks into the cytosol to inhibit PHDs, ultimately stabilizing HIF-1/2α (256, 258). Moreover, reduced expression of SDHD has been observed in gastric and colorectal carcinoma while patients with mutations in *SDHB* and *SDHC* are susceptible to developing early-onset renal cell or papillary thyroid carcinoma (259-262). Thus, defects in the SDH complex which are often associated with succinate buildup, lead to a "pseudohypoxic" state wherein HIF is activated even under normoxia. Collectively, mutations in SDH subunits result in accumulation of succinate that favors tumorigenesis and tumor progression via epigenetic dysregulation, and aberrant activation of HIF.

1.2.4.1.3 Fumarate

Inactivating mutations in the homotetrametric enzyme FH leads to the accumulation of fumarate which is commonly observed in patients diagnosed with fumaric aciduria, an autosomal recessive metabolic disorder typically associated with severe encephalopathy, as well as hereditary leiomyomatosis and renal cell cancer (HLRCC) (263, 264). Similar to the *SDH* genes, *FH* mutations are often germline, and are associated with the loss of the wild-type allele and decreased FH activity in the tumors (263, 265). FH is therefore regarded as a tumor

suppressor because decrease in its activity causes the intracellular buildup of the oncometabolite, fumarate, which akin to 2-HG and succinate competitively inhibits OGDDs including PHDs, histone demethylases and TET proteins (244, 266). HLRCC tumors in patients with germline FH mutations have been reported to increase not only HIF- 1α and HIF- 2α but also their gene targets such as *VEGFA* and *SLC2A1* which suggests that fumarate-mediated inhibition of HIF- $1/2\alpha$ PHDs confers a survival advantage to HLRCC tumors (267). Additionally, recent findings show that the loss of FH and the subsequent accumulation of fumarate promotes EMT by inhibiting TET-mediated demethylation of the antimetastatic miRNA cluster miR-200, which results in the expression of EMT-related transcription factors (e.g., ZEB2) and markers (e.g., vimentin) (268). Overall, these studies demonstrate that accumulation of fumarate caused by mutations in *FH* promotes tumor growth and progression in the context of neoplasia of the kidney and potentially other malignancies.

1.2.4.2 CAC anaplerosis and cataplerosis

CAC intermediates serve as precursors for producing macromolecules such as succinyl-CoA for heme biosynthesis, citrate for fatty acid synthesis and oxaloacetate for aspartate and nucleic acid synthesis (269). The consumption of CAC intermediates is referred to as cataplerosis. In order to maintain CAC, which is necessary for generating the reducing equivalents (NADH and FADH₂) and energy required to sustain cell growth and proliferation, intermediates utilized in cataplerotic processes must be replenished (269). This process of replacing depleted pools of CAC intermediates is termed anaplerosis. Under normal physiological conditions, cataplerotic and anaplerotic reactions are coordinated to maintain the levels of CAC intermediates for biosynthetic and bioenergetic pathways in the cell (269, 270).

The anaplerotic and cataplerotic metabolic pathways are organ-specific and are dependent on the organismal metabolic state (270). GTP-dependent phosphoenolpyruvate carboxykinase (PCK) isozymes (PCK1 localized in the cytosol and PCK2 localized in the mitochondrial matrix) catalyze the decarboxylation of oxaloacetate to PEP used for de novo glucose synthesis (gluconeogenesis) in the liver and kidneys (269). In skeletal muscles, PEP can be converted back to pyruvate that subsequently enters the CAC via acetyl-CoA (270). During fasting, characterized by low levels of insulin and elevated levels of glucagon and glucocorticoids, PCK1 mRNA is upregulated to promote hepatic gluconeogenesis (271, 272). In addition, PCK1 activity is detected in nongluconeogenic tissues such as white and brown adipose tissues (273). It has been proposed that during glucose starvation, increased cAMP levels stimulate PCK1 transcription which indirectly mediates the synthesis of 3-glycerol phosphate (glyceroneogenesis) to form oxaloacetate needed for the re-esterification of free fatty acids in adipose and hepatic tissues released as very low-density lipoproteins (274, 275). An anaplerotic counterpart of PCK exists to prevent the extensive efflux of oxaloacetate from the CAC. Namely, the tetrametric ATP-dependent pyruvate carboxylase (PC) carboxylates pyruvate to form oxaloacetate which represents a key anaplerotic pathway whereby alanine and lactate are metabolized into pyruvate to replenish depleted oxaloacetate pools for gluconeogenesis, the urea cycle and lipogenesis (269, 276). PC is predominantly localized in the mitochondrial matrix and is highly catalytically active in many organs including liver, skeletal muscles, heart and pancreas (269). Considering that PC is allosterically activated by acetyl-CoA which is the key metabolite in fatty acid synthesis and β oxidation, it suggests that fatty acid metabolism is linked to the regulation of anaplerotic flux via oxaloacetate and energy availability for gluconeogenesis (269, 277). Overexpression and/or elevated PC activity have been demonstrated to contribute to metabolic reprogramming and tumor

progression in several cancer models including NSCLC, breast and papillary thyroid cancer (278-280). Curiously, PCK2, the cataplerotic partner of PC, is also overexpressed in lung and breast cancer (281, 282). Glucose deprivation was shown to bolster the expression of PCK2 and increase PC activity in lung cancer models while being associated with the increased conversion of lactate to pyruvate and subsequently into PEP via oxaloacetate (281, 283). Also, amino acid starvation augments PCK2 expression required for the survival breast cancer cells in the context of amino acid withdrawal (282). These findings suggest that cancer cells may activate gluconeogenic and/or glyceroneogenic pathways previously assumed to be restricted to specialized tissues (adipose, liver and kidney) in order to survive nutrient scarcity. Although, these pathways eventually result in the production of glucose (via gluconeogenesis) and glycerol (via glyceroneogenesis), it is worth underscoring the importance of metabolic intermediates along these pathways which serve as precursors for building biomass in cancer cells. Finally, these findings illustrate high metabolic flexibility of cancer cells that allows them to adapt to fluctuations in TME.

1.2.4.2.1 CAC anaplerosis and glutamine metabolism

After glucose, glutamine is the second most consumed nutrient and most abundant amino acid in the blood stream making up over 20-25% of the free amino acid pool found at concentrations of 0.5-0.8 mM (284-286). Although digested food can be absorbed through the small intestine and metabolized to produce glutamine, most of the glutamine is catabolized in the small intestine and liver (286). Since skeletal muscles, adipose tissues and lungs are capable of synthesizing glutamine, glutamine is considered a non-essential amino acid (NEAA) (286). In skeletal muscles, the cytosolic concentration of glutamine ranges from 10 mM to 30 mM and serves as an important glutamine reserve that is readily released into the plasma in response to stress (287). Under certain conditions including injury or sepsis, glutamine uptake by kidneys,

gastrointestinal tract and immune cells is markedly elevated which renders glutamine a conditionally essential amino acid (288). Intestinal cells are particularly dependent on glutamine as they quickly become necrotic when deprived of glutamine (288). Unlike other NEAA, glutamine has a broad range of functions which include donating the amide nitrogen needed for *de novo* synthesis of nitrogen-containing metabolites (e.g. asparagine, purines and pyrimidines), fueling OXPHOS through the oxidative decarboxylation of glutamine-derived α-KG via the CAC, and serving as a substrate for ureagenesis and ammoniagenesis in liver and kidney, respectively (286). In addition, glutamine is utilized for ROS detoxification, acid-base buffering and gluconeogenesis (286, 289, 290). Essentially, under physiological conditions, glutamine is a source of carbon and nitrogen atoms to support a variety of metabolic pathways while indirectly maintaining systemic acid-base pH homeostasis.

Glutamine is imported into cells through several amino acid transporters including SLC1A5 (ASCT2) as well as SLC38A1 (SNAT1) and SLC38A2 (SNAT2) (291, 292). Glutamine can then be transported across the mitochondrial membranes by lesser-known and inadequately characterized mitochondrial glutamine transporters into the matrix to be deamidated by glutaminase (which is encoded by 2 genes: kidney-type *GLS* and liver-type *GLS2*) into glutamate and ammonia (293-295). Subsequently, mitochondrial glutamate is either further deamidated and oxidized to α-KG by glutamate dehydrogenase (GLUD) or transaminated into α-KG via amino acid transaminases such as alanine transaminases (ALT2 or GPT2) and aspartate transaminases (AST2 or GOT2) (296, 297). Alternatively, mitochondrial glutamate can be exported through SLC25A18 and SLC25A22 transporters to the cytosol where it participates in several metabolic activities that include serving as an exchange factor for extracellular cystine import via SLC7A11 (xCT), and being a precursor for *de novo* synthesis of other amino acids [e.g., alanine, aspartate,

serine and proline catalyzed by cytosolic ALT1, AST1, phosphoserine aminotransferase 1 (PSAT1) and pyrroline-5-carboxylate synthase (P5CS), respectively] (289, 298, 299). Moreover, glutamine serves as a substrate for biosynthesis of glutathione, a tripeptide ROS scavenger composed of glutamate, cysteine and glycine (289, 298, 299). In addition, glutamine-derived α -KG is implicated in a variety of the bioenergetic and biosynthetic activities of the CAC (289). α -KG also serves as a cofactor for OGDDs and drives the malate-aspartate shuttle via its role as an exchange factor (289). Overall, glutamine regulates a wide range of cellular activities as a direct or indirect substrate (via the functions of glutamate and α -KG) of key metabolic pathways and/or by acting as a cofactor in pivotal enzymatic reactions.

Similar to glucose, glutamine is thought to be frequently exploited by cancer cells to support neoplastic growth (300). The excessive demand for glutamine by cancer cells was first described by Harry Eagle when he demonstrated that for optimal growth, HeLa cells require 10-100-fold molar excess of glutamine relative to other amino acids in culture medium (301). Some cancer cell lines including those derived from pancreatic cancer, acute myelogenous leukemia, and small cell lung cancer have been shown to be "addicted" to glutamine inasmuch as they are strongly dependent on exogenous glutamine despite the fact that they can synthesize it from glucose (302). Glutamine metabolism is also upregulated in glioblastoma but also in non-transformed activated proliferating T-lymphocytes (39, 303). Interestingly, glutamine was found to activate glucose metabolism in cancer cells in which CAC intermediates are used as precursors for synthesizing other amino acids, nucleotides and fatty acids (39). In the absence of glucose, glutamine metabolism can be elevated in association with increased malic enzyme 1 (ME1) and PCK2 activities in an attempt to compensate for the loss of glucose as a bioenergetic and biosynthetic source in B-cell lymphoma and lung cancer cell lines (283, 304). It was also observed

that α-KG produced from glutamine was oxidatively decarboxylated in the CAC to produce either oxaloacetate that is subsequently converted to PEP by PCK2 or malate by MDH2 (39, 283, 305). PEP and malate are then exported to the cytosol for pyruvate synthesis (39, 283, 305). Cytosolic malate is oxidatively decarboxylated by ME1 to yield NADPH needed for fatty acid synthesis and pyruvate which is reduced to lactate via LDHA (39). In addition, it was reported that in pancreatic ductal adenocarcinoma (PDAC) cells glutamine-derived aspartate is transported into the cytosol to be converted into oxaloacetate by AST1 that is then reduced into malate by MDH1 and finally decarboxylated into pyruvate via NADPH-producing ME1 (306). The production of NADPH through this metabolic route is used to reduce glutathione for detoxifying ROS, hence highlighting the role of glutamine metabolism in maintaining cellular redox homeostasis (306).

Inside the mitochondria, the metabolic fate of glutamine-derived α -KG is closely associated with CAC enzymes and ETC complex activities or lack thereof (180, 307-309). Brown adipocytes reductively carboxylate glutamine-derived α -KG into isocitrate which is then converted into citrate and exported to the cytosol for *de novo* lipid synthesis (310). This cataplerotic route accounted for 90% of the total flux of glutamine into lipids in brown adipocytes (310). In the context of mitochondrial dysfunctions (including mutations in either FH or mitochondrial DNA, genetic lesions or pharmacological inhibition of complexes I or III of the ETC), α -KG produced from glutamine has been shown to be reductively carboxylated to allow lipogenesis and aspartate synthesis in rapidly proliferating malignant cells (180, 307, 311, 312). Furthermore, hypoxia has been demonstrated to promote the reductive carboxylation of glutamine-generated α -KG into isocitrate via IDH1 (313) or IDH2 in melanoma (314), with the concomitant elevated synthesis of 2-HG in several cancer cell lines with wildtype IDH1 and IDH2 (179). Furthermore, glutamine is the primary source of α -KG catalyzed into 2-HG by mutant IDH1 in glioma cells (308). This

preferential use of glutamine-derived α -KG is thought to constitute a targetable metabolic vulnerability in mutant IDH1-expressing cells as they are more sensitive to GLS inhibition as compared to WT IDH1-expressing cells (308).

Although many tumor cell types profoundly depend on glutamine metabolism to refill their diminished pools of CAC intermediates, it has been reported that the inhibition of glutaminolysis in some glioblastoma cell lines can induce a compensatory CAC anaplerotic mechanisms in which PC carboxylates glucose-derived pyruvate into oxaloacetate (315). Hence, glucose-dependent CAC anaplerosis via PC allows cells to become "independent" of glutamine. Conceivably, this could be, at least in part, an underlying mechanism of resistance against drugs targeting glutaminolysis (315). Additionally, *de novo* glutamine synthesis via glutamine synthetase (GLUL) activity in which glutamine is produced from the co-substrates, glutamate and ammonia, may render cells glutamine independent. GLUL expression has been associated with enhanced metastatic potential of HCC, while induction of GLUL expression by glutamine starvation promotes nucleotide synthesis and amino acid transport thereby maintaining cell survival and proliferation of glioma and breast cancer cell lines (316-318). Overall, these findings imply that metabolic rewiring caused by glutamine deprivation may decrease sensitivity of certain cancer subtypes to the therapies targeting glutamine metabolism.

1.2.5 ETC and OXPHOS

NADH and FADH₂ reducing equivalents that are largely generated via CAC, are chiefly oxidized in the ETC through a series of redox reactions that create an electrochemical gradient which is harnessed to produce ATP by OXPHOS (48, 319, 320). The ETC comprises of free electron carriers (ubiquinone and cytochrome C) and 4 bound protein complexes (I-IV) that are embedded within the inner mitochondrial membrane in close proximity to the mitochondrial

matrix where the most of CAC reactions are catalyzed (48). The reaction sequence begins with NADH and FADH₂ donating electrons to complex I (NADH-ubiquinone oxidoreductase) and complex II (succinate:ubiquinone oxidoreducatase) respectively (48, 320). Electrons are subsequently transferred to ubiquinone (CoQ) followed by complex III and ultimately to complex IV via cytochrome C (48, 319, 320). Complex IV reduces oxygen (the final electron acceptor) to produce water in the process (48, 320). The movement of electrons along the ETC is coupled to protons being pumped into the intermembrane space by complexes I, III and IV (319, 320). The translocation of protons from the mitochondrial matrix to the intermembrane space creates a proton motive force, a proton gradient, used to drive the synthesis of ATP from ADP by complex V, ATP synthase (319, 321). Thus, the OXPHOS system includes the 4 complexes of the ETC which generates the proton motive force in addition to complex V which produces ATP.

1.2.5.1 Mammalian Complex I

Mammalian complex I, which is also referred to as NADH dehydrogenase, is the first and largest multicomponent enzyme complex of the ETC composed of 45 different subunits with a combined molecular mass of approximately 1 MDa (319, 322). As the name implies, complex I oxidizes NADH to NAD+, which involves the transfer of electrons from NADH to ubiquinone (CoQ) (323). Specifically, two electrons are transferred from NADH through a chain of cofactors including flavin mononucleotide and a series of eight iron-sulfur clusters arranged from low to high electron potentials, to CoQ consequently producing ubiquinol (QH₂) in the inner mitochondrial membrane (322, 323). This translocation of electrons, one at a time from NADH to CoQ, induces a conformational change in the complex that facilitates the pumping of four protons from the mitochondrial matrix to the intermembrane space (322, 324). It is thought that complex I generates approximately 40% of the proton flux (323). Defects in the complex I have been

associated with neurodegenerative diseases including Leigh's and Parkinson's disease (325-327). The role of complex I in tumorigenesis has been controversial whereby it was suggested that inactivation of complex I has both tumor-suppressive and tumor-promoting effects (328-330). Notably, these findings were obtained using models bearing different mutations in the various subunits of complex I. Thus, it is plausible that the discrepancy between the aforementioned studies stems from diverse genetic alterations that although impacting the function of complex I may not result in a common phenotype.

1.2.5.2 Mammalian Complex II

In parallel to complex I, electrons are fed into the ETC via complex II (SDH) which is also a component of the CAC (331). Structurally, SDHC and SDHD contain the CoQ binding site and are embedded in the inner mitochondrial membrane to anchor the entire complex (332, 333). The succinate binding pocket along with the iron-sulfur clusters and a flavoprotein are covalently attached to a FAD cofactor and are both found in SDHA and SDHB subunits which extend into the mitochondrial matrix (319, 334). Complex II converts FADH2 to FAD while simultaneously reducing CoQ into QH2 (331). Similar to complex I, electrons are transferred sequentially from FADH2 to CoQ via iron-sulfur clusters (335). Unlike complex I, electron transport from FADH2 to CoQ is not accompanied by proton translocation from the matrix to the intermembrane space (335). As a result of bypassing complex I, electrons transferred from complex II to CoQ forego the opportunity to be coupled to proton ejection by complex I.

Except for complex I and II, other lesser-known enzymes donate electrons to the CoQ pool (336). They include the electron-transferring flavoprotein (ETF)-ubiquinone oxidoreductase, the mitochondrial glycerol-3-phosphate dehydrogenase and the dihydroorotate dehydrogenase (DHODH) enzyme (337). The ETF-ubiquinone oxidoreductase enzyme is located on the

mitochondrial matrix-facing side of the inner mitochondrial membrane (338). ETF transfers electrons generated during the oxidation of fatty acids, branched chain amino acids, lysine, tryptophan and choline (338, 339). The mitochondrial glycerol-3-phosphate dehydrogenase is a component of glycerophosphate shuttle with a prominent role in linking glycolysis, OXPHOS and fatty acid metabolism. Moreover, the DHODH catalyzes a rate-limiting of the *de novo* pyrimidine synthesis pathway whereby dihydroorotate is converted to orotate (336, 340-342).

1.2.5.3 Mammalian Complex III

The electrons from QH₂ are donated to the dimeric complex III (referred to as cytochrome bc₁ complex or CoQ-cytochrome c reductase) of the ETC which is localized in the inner membrane of the mitochondria (319, 320). The catalytic subunits of the complex are cytochrome b (b_L and b_H), cytochrome c₁ and a high electron potential iron-sulfur cluster in the Rieske center (319, 320). Cytochrome b has two CoQ binding sites: (i) a QH₂ oxidation site (Q₀) located on the cytosolic side which is associated with the low potential cytochrome b_L and (ii) a Q⁻ reduction site (Q_i) found on the mitochondrial matrix side and linked to the high potential cytochrome b_H (343). The oxidation of QH₂ into ubisemiquinone (QH⁻) after transferring an electron to the Rieske center is coupled with the release of two protons into the mitochondrial intermembrane space (344). The electron is subsequently transferred to cytochrome c₁, which then provides the electron to the mobile electron carrier, cytochrome c (344). Newly formed QH⁻ found at the Q₀ site donates the second electron to cytochrome b_H at the Q_i site via cytochrome b_L (319). Next, the electron is lost to CoQ of the Q_i site from the reduced cytochrome b_H to regenerate QH⁻ (319). A second QH₂ molecule is oxidized at the Q₀ site which leads to the ejection of two more protons into the intermembrane space (319). This is accompanied by one additional electron being transferred to the iron-sulfur cluster while the second electron is transferred by cytochrome b_H to QH⁻ of the Qi

site to yield QH₂ (319). Complex III deficiency underpins neurological disorders including Leigh syndrome and Leber hereditary optic neuropathy (LHON), whereby aberrant complex III function has also been observed in breast, colorectal cancer and lung cancer (345-348). This suggests that complex III may play a prominent role in neoplasia

1.2.5.4 Mammalian Complex IV

Functionally similar to CoQ, cytochrome c is loosely attached to the outer surface of the inner mitochondrial membrane by electrostatic interactions and shuttles electrons from complex III to complex IV (cytochrome c oxidase) where molecular oxygen is reduced to water (319-321). Complex IV is composed of 13 subunits with the 3 core components (COX1, COX2 and COX3) encoded by the mitochondrial DNA (347). Considering the complexity of Complex IV and the fact that its subunits are assembled on both sides of the membrane, the enzyme complex requires 18 assembly factors, many of which have not been well-characterized (347, 349). The complex IV also contains cofactors (heme and copper) embedded into the core proteins, COX1 and COX2 (349). COX1 has 2 heme molecules and a copper ion in the Cu_B site, while COX2 has a Cu_A site formed by 2 copper ions (349). After cytochrome c is reduced by complex III, it moves along the surface of the membrane to interact with the COX2 subunit of complex IV via electrostatic interaction while simultaneously transferring the electrons to the CuA site of the COX2 subunit (319). The electrons are subsequently transported from Fe_a to the active binuclear center (Fe_{a3} and Cu_B) of COX1 where oxygen is bound and converted to water (319). COX3 is located on both sides of COX1 along with COX2, stabilizes both COX1 and COX2 and is primarily involved in pumping protons into the intermembrane space (319, 335). Analogous to complex I and III, the donation of four electrons at a time to oxygen is coupled to the translocation of eight protons from the mitochondrial matrix (350). The four protons are used to form two water molecules while the

remaining protons enter the intermembrane space (350). As suspected, defects in mitochondrial complex IV resulting in decreased enzyme complex activity have been linked to neurodegenerative diseases such as LHON, Leigh-like syndrome and infantile-onset encephalopathy (347). Furthermore, mutations or aberrant expression of complex IV subunits, which either elevates or diminish the activity of the complex have been associated with shorter progression-free survival and increased invasiveness in different types of cancers including colorectal cancer, glioma, breast and esophageal cancer (351). The disruption of complex IV function was also demonstrated to induce Warburg Effect and enhance the metastatic potential of non-transformed skeletal myoblasts (351). This suggests that complex IV dysfunction may be crucial to metabolic reprogramming and tumor progression in a number of cancer subtypes.

1.2.5.5 Mammalian Complex V (F_1F_0 ATP synthase)

Altogether, complexes I, III and IV pump a total of ten protons into the intermembrane space generating an electrochemical proton gradient known as the mitochondrial membrane potential (335). The mitochondrial membrane potential together with the proton concentration creates a proton-motive force that is essential for energy production during OXPHOS because it couples the ETC complexes to the catalytic activity of complex V (335). Complex V comprises two functionally distinct multisubunit domains: an extra-membranous F₁ domain situated in the mitochondrial matrix and a transmembrane F₀ domain located in the inner mitochondrial membrane (319, 335). Protons are translocated into the mitochondrial matrix from the intermembrane space via the F₀ to F₁ domains (335). The movement of protons and the transfer of energy are coupled to a conformational change in the complex leading to the phosphorylation of ADP with inorganic phosphate to form ATP at the F₁ domain (335). Alternatively, complex V can hydrolyze ATP to drive the efflux of protons from the mitochondrial matrix into the

intermembrane space in order to sustain the proton-motive force (347, 352). This reverse-mode of complex V is typically observed in mitochondria with impaired respiration or leaky inner membranes (347, 352). Importantly, the persistent reverse-mode operation of complex V could deplete cellular ATP reserves, inevitably driving the cell into an energy crisis which could be exacerbated if there is an increased cellular demand for ATP (352, 353). Mutations in mtDNA genes encoding two of the F₀ subunits, ATP6 and ATP8 have been observed in patients with LHON, breast cancer and osteosarcoma (347, 354, 355). Surprisingly, the exogenous expression of mutant ATP6 T8993G in prostate cancer PC3 cell line through cybrid transfer was demonstrated to significantly impair mitochondrial ATP synthesis and result in bigger tumors in mice compared to wildtype ATP6 cybrids (356). Moreover, the decreased expression of the α subunit of complex V in colon cancer cells was associated with decreased sensitivity to chemotherapy (357). Altogether, these findings suggest that impaired OXPHOS due to the abrogation of complex V may play an important role in tumorigenesis and chemoresistance.

1.2.5.6 Reactive oxygen species (ROS)

Under physiological conditions, 0.2-2% of the electrons leak out from ETC complexes and interact with oxygen to produce ROS (319). Thus, low levels of ROS are inevitably generated as byproducts of cellular respiration (335). The main sites for ROS production in the ETC are complexes I and III where electrons leak to partially reduce oxygen to superoxide anion (335, 358). The rate at which superoxide anion is generated is dependent on the concentration of the one-electron donors and the rate at which these donors react with oxygen (335). When the iron-sulfur centers and flavin mononucleotide site of complex I accept electrons from NADH, they can react with oxygen to produce superoxide anion (335). Hence, the production of ROS is closely associated with the NAD+/NADH ratio, considering that a buildup of NADH which is usually

observed when the ETC is disrupted results in elevated levels of superoxide at complex I (335). The QH₂ oxidation site of complex III is another prominent location of superoxide anion production that creates an unstable QH⁻ intermediate that can react with oxygen to produce superoxide anion in both the mitochondrial intermembrane space and matrix (319, 335). Accordingly, inhibitors of complex I (e.g., rotenone and piercidin) and III (e.g., antimycin A) which block electron transfer in the ETC increase ROS production (319, 359).

ROS act as second-messengers in signaling pathways mediating various intracellular processes including autophagy and apoptosis (360, 361). Elevated ROS levels, however, are toxic to cells (319, 347). ROS damage DNA, lipids and proteins (323, 347). To counteract potentially deleterious effects of ROS, the cell utilizes antioxidant systems (335). To this end, the highly reactive and unstable super oxide anion is quickly converted to the more stable hydrogen peroxide by manganese SOD (Mn-SOD) localized in the mitochondrial matrix or copper/zinc SOD (Cu,Zn-SOD) located in the intermembrane space (335). The importance of Mn-SOD is underscored by the findings associating the loss of this enzyme with perinatal lethality (362, 363). The amount of hydrogen peroxide diffused out (or exported via aquaporins) of the mitochondria is dependent on the activities of catalase (commonly found in the mitochondria of heart and liver tissues), glutathione peroxidase/reductase (GPx) system and thioredoxin peroxidase/reductase system located in the mitochondrial matrix (335, 358). GPx uses hydrogen peroxide to oxidize glutathione (GSH) to glutathione disulfide (GSSG) (335, 364). Hydrogen peroxide also oxidizes the cysteine residue in the catalytic site of peroxiredoxin (PRx) that is subsequently reduced by thioredoxin (TRx) (335). Notably, both GPx and TRx antioxidant systems require NADPH for their reductive activities and thus, indirectly dependent on the various metabolic pathways that generate NADPH (335). Increased levels of ROS have been observed in the context of mitochondrial dysfunction

and suggested to drive bladder and prostate cancer progression (356, 365). Although heightened ROS levels promote DNA damage and genomic instability, the precise underlying mechanism of the role of ROS in tumorigenesis remains largely elusive.

1.2.6 Amino acids metabolism in cancer

In addition to glutamine, the levels of other NEAAs including serine, glycine, glutamate, alanine, aspartate and asparagine have been shown to have a major impact on cancer cell fate (298, 366). Although there are many well-characterized metabolic pathways to biosynthesize NEAAs, highly proliferative malignant cells occasionally require exogenous reserves of NEAAs to meet their high bioenergetic and biosynthetic demands. Consistent with this, emerging data indicate that production and availability of NEAAs play a central role in tumorigenesis, tumor progression and therapeutic responses across a broad range of cancers.

1.2.6.1 Aspartate

The CAC plays a prominent role in amino acid metabolism by providing metabolic precursors such as oxaloacetate and α -KG for the biosynthesis of various NEAAs (366). Aspartate is generated from oxaloacetate and glutamate-derived nitrogen by cytosolic (AST1) and mitochondrial (AST2) isoforms of glutamate oxaloacetate transaminase (366). Aspartate is involved in transferring electrons from the cytosol to the mitochondria via the malate-aspartate shuttle (MAS) which involves the exchange of mitochondrial aspartate for cytosolic glutamate and malate through the aspartate-glutamate carrier 1/2 (AGC1/2 or SLC25A12/SLC25A13 respectively) and malate- α -KG antiporters (OGC/SLC25A11) respectively (366, 367). Since the plasma concentration of aspartate is low and it is inefficiently imported into most cancer cells, *de novo* synthesis via ASTs is considered to be the primary source of aspartate in cancer cells (366). Recent reports have demonstrated that one of the major functions of mitochondrial respiration in

cancer cells is to support aspartate biosynthesis (311, 312). As aspartate is essential for nucleotide synthesis, it plays a key role in cellular proliferation (298). Therefore, aspartate availability is positively correlated with *in vivo* tumor growth whereas the inhibition of aspartate biosynthesis suppresses neoplastic growth in both breast and pancreatic cancers (306, 311, 312, 368, 369). In response to ETC inhibition, some cancer cell lines (e.g., ovarian cancer COLO-704, breast cancer MDA-MB-157 and acute monocytic leukemia NOMO-1) are able to maintain their intracellular aspartate levels by upregulating the expression of aspartate importers, SLC1A3 or SLC1A2 (370). Altogether, these findings indicate that aspartate biosynthesis plays a major role in metabolic reprograming of cancer, whereby increase in aspartate levels provides malignant cells with flexibility to adapt to the defects in mitochondrial functions.

1.2.6.2 Asparagine

Asparagine is another NEAA that is thought to be indispensable for malignant cell proliferation under certain conditions including glutamine deprivation (366). In cancer cells, asparagine was found to enhance the expression of GLUL, the rate limiting enzyme for *de novo* glutamine synthesis (371). Intriguingly, albeit asparagine supplementation did not restore the levels of other NEAAs or CAC intermediates, it increased glutamine synthesis and breakdown leading to the recovery of global protein synthesis (371). Through its role as an amino acid exchange factor, asparagine also mediates amino acid uptake wherein intracellular asparagine is exchanged for extracellular amino acids (serine, histidine and arginine) (372). Ubiquitously expressed ATP-dependent asparagine synthetase (ASNS) irreversibly converts aspartate into asparagine by utilizing the amide nitrogen from glutamine (373). ASNS expression is induced in response to metabolic stressors including glutamine and glucose deprivation and ER stress which is mediated by the GCN2-EIF2α-ATF4 and PERK-EIF2α-ATF4 axis (298, 373, 374). Acute

lymphoblastic leukemia (ALL) cells frequently do not express functional ASNS and are thus reliant on exogenous asparagine (375, 376). Based on this, L-asparaginase that degrades and thus, limits availability of the asparagine is used as a first line therapy in ALL (377-379). In addition, high expression of ASNS is observed in castration-resistant prostate cancer, glioma and neuroblastoma wherein it correlates rapid tumor progression and poor prognosis (380, 381).

Notably, human cells do not express asparaginase and are thus incapable of breaking down asparagine (382, 383). Although the exogenous expression of ASNS enhances glutamine and nucleotide synthesis while inducing CAC anaplerosis, it suppresses proliferation and survival of cancer cells in the absence of exogenous glutamine (371). This suggests that the lack of asparaginase activity in humans may be an evolutionary adaptive mechanism to survive abnormal fluctuations in plasma glutamine levels (371). Recent reports indicate that low intracellular asparagine level impedes breast cancer metastasis which was associated with decreased expression of asparagine-rich EMT-related proteins (384). In summary, these findings indicate that asparagine metabolism, particularly in the absence of glutamine, regulates amino acid homeostasis, protein and nucleotide synthesis and thereby play a critical role in tumor cell proliferation and metastatic progression.

1.2.6.3 Serine and glycine

Serine can be exogenously taken up by the cells via amino acid transporters SLC6A14, SLC38A2, SLC1A5 and SLC38A5 (291, 298, 385, 386). In addition, serine can be biosynthesized from glycolytic intermediate, 3-PG (298). The rate-limiting step in the serine synthesis pathway (SSP) involves the oxidation of 3-PG to 3-phosphopyruvate (3-PP) by phosphoglycerate dehydrogenase (PHGDH), which is then transaminated to 3-phosphoserine (3-PS) by PSAT1 (387, 388). In the third and final step of the pathway, 3-PS is dephosphorylated into serine by

phosphoserine phosphatase (PSPH) (387). Some of the transporters (i.e., SLC38A2, SLC38A5 and SLC6A14) that facilitate the import of serine also mediate the uptake of other amino acids including glycine (291, 298, 385, 386). In addition to utilizing identical amino acid transporters, both serine and glycine are biosynthetically linked as serine can be converted to glycine in the cytosol and mitochondria by serine hydroxymethyltransferase (SHMT1) and (SHMT2) respectively (387, 389). Taking into account that the carbon and nitrogen atoms in serine and glycine are derived from 3-PG and glutamate, respectively during de novo biosynthesis, serine and glycine metabolisms are closely associated with glucose and glutamine metabolism (390). Recent findings show that many cancer cell types are dependent on exogenous supply of serine whereby serine starvation markedly inhibits the growth of some neoplastic cells in cell culture and in vivo (391). In turn, breast cancer and melanoma cells upregulate serine biosynthesis by diverting glycolytic intermediates to the SSP or increasing the expression of SSP enzymes including PHGDH (391-393). Accordingly, suppressing PHGDH levels in breast cancer cell lines was associated with decreased proliferation while the overexpression of PSAT1 in colon carcinoma stimulated cell proliferation and facilitated chemoresistance (392, 394). Expression of SHMT2 was shown to be induced by MYC or hypoxia (395). Importantly, increased SHMT2 expression appeared to prevent hypoxia-induced cell death by maintaining NADPH production and thus, bolstering ROS protection capacity (395). In the context of cancer, serine is regarded as the more conditionally essential amino acid relative to glycine because the proliferation rates of CRC and lung cancer cell lines were found to be unaltered by the absence glycine in the media, whereas the removal of only serine decreased proliferation to the same extent as the deprivation of both amino acids (396). The role of glycine metabolism in tumor cells has been controversial as it was reported that rapidly, but not slowly proliferating cancer cells depend on exogenous glycine (397).

Furthermore, it was proposed that glycine is only imported and metabolized by cells when extracellular serine is depleted (398). These findings suggest that transformed cells promote survival and proliferation by rewiring serine and glycine metabolism as a possible adaptive response to nutrient deprivation and oxidative stress (298).

1.2.6.4 Folate and methionine cycle

The SHMT catalytic activity requires a folate carrier, tetrahydrofolate (THF), as a cofactor which accepts one-carbon (1C) unit from serine to produce 5,10-methylenetetrahydrofolate (5,10methylene-THF) in parallel to two-carbon (2C) unit glycine (366). The 5,10-methylene-THF subsequently undergoes a series of redox transformations by folate cycle enzymes to produce various 1C-THF species, including the regeneration of THF (399-401). The folate cycle begins with the reduction of folate (commonly known as vitamin B9) by dihydrofolate reductase (DHFR) into the biologically active THF. Folate cycle requires both mitochondrial and cytosolic isoforms of folate enzymes including the multifunctional NADP-dependent methylenetetrahydrofolate dehydrogenase (MTHFD1/2/1L) (399-401). Glycine contributes to the folate cycle by donating 1C unit to THF via the activity of glycine decarboxylase (GLDC) of the glycine cleavage system (GCS) to generate 5,10-methylene-THF (402). The folate cycle produces THF-containing intermediates that serve as precursors for thymidine synthesis and contribute to the production of purines, ATP, and NADPH (366, 391, 398). It is thought that serine is the more significant 1C unit contributor of the folate cycle relative to glycine (402). The preferential consumption of serine over glycine implies that a demand for 1C units might be driving serine-to-glycine conversion because this reaction donates 1C unit to the folate cycle while the reverse reaction consumes 1C unit from the folate cycle (398). This is consistent with existing data showing that glycine consumption inhibits angiogenesis and tumor growth in CRC, melanoma and liver cancer (403405). The conversion of glycine to serine depletes the 1C pool needed for nucleotide synthesis and cell proliferation (396). The folate cycle plays a prominent role in cancer cell metabolism. For instance, elevated MTHFD2 expression in breast cancer correlates with poor survival of patients (406). In addition, GLDC was found to be highly expressed in tumor-initiating cells of NSCLC wherein it induces glycolysis, intracellular serine level, and pyrimidine metabolism (394, 406). Although the GCS system supports tumorigenesis by generating 1C units for nucleotide synthesis, it is suggested that its primary role may be the detoxification/degradation of intracellular glycine (407, 408).

One of the 1C-THF species, 5-methyl-tetrahydrofolate (methyl-THF), which is generated by the folate cycle is used to drive the methionine cycle (366). In the methionine cycle, homocysteine is re-methylated to form methionine by methionine synthase (MS) using methyl-THF (366). Methyl-THF can be derived from the breakdown of 5,10-methylene-THF via cytosolic NADPH-dependent methylenetetrahydrofolate reductase (MTHFR) (366). Hence, the synthesis of methionine couples the methionine cycle to the folate cycle. Methionine can further be converted into S-adenosyl methionine (SAM) via the ATP-dependent methionine adenosyl transferase (MAT) (409). SAM acts as the principal donor of methyl groups for histone, DNA and RNA methylation reactions that underpin epigenetic and epitranscriptomic programs, (400). SAM is then demethylated by histone methyl transferase (HMT) to yield S-adenosyl homocysteine (SAH) which is ultimately converted to homocysteine via SAH hydrolase (SAHH) (366). This completes one turn of the methionine cycle. The homocysteine intermediate can leave the methionine cycle to enter a trans-sulfuration pathway consisting of the condensation of homocysteine with serine to produce cystathionine via cystathionine β-synthase (CBS), and the cleavage of cystathionine to cysteine by cystathionine γ-ligase (CSE) (410). Cysteine further participates in glutathione synthesis and thus, antioxidant protection against ROS (411). 1C metabolic cycles are closely connected to other metabolic pathways (400, 412). Thus, it is not surprising that aberrant regulation of 1C metabolism is observed across a broad range of cancer types including CRC and HCC (413, 414).

Although malignant cells can synthesize methionine, most cancer cells rely on extracellular supply of methionine (415, 416). This phenomenon is only observed in transformed cells and is referred to as the Hoffman effect or methionine stress sensitivity (415, 416). It describes the underlying inhibitory mechanism of tumor cell proliferation when exogenous methionine is substituted for its metabolic precursor, homocysteine, which reflects the increased demand for metabolites derived from methionine (417, 418). The Hoffman effect is supported by recent data reporting that defects in the methionine cycle of lung tumor initiating cells result in loss of tumorigenic potential (419). This was attributed to alterations in cellular methylation due to reduction in SAM (419). In addition, breast cancer cell lines were demonstrated to be oxidatively stressed when methionine was replaced with homocysteine (418). The cells responded by redirecting homocysteine out of the methionine cycle for glutathione synthesis thus reducing production of methionine and SAM (418). Therefore, certain cancer cell types such as breast cancer reprogram their methionine metabolism in order to meet the demands for tumorigenesis and tumor survival.

1.2.7 Lipid metabolism

Lipids are a complex group of macromolecules with varying structures and functions (420). The large vacuoles in adipocytes and lipid droplets are the primary storage sites for lipids (421, 422). They contain triglycerides that serve as important energy sources because they can be metabolized to produce ATP when nutrients are limited (420, 423). Although phospholipids are

the major component of biological membranes, other membrane lipids such as cholesterol, glycolipids and phosphatidylinositols facilitate membrane fluidity, cell recognition and function as secondary messengers, respectively (420, 424). Considering their versatile roles, lipids represent essential biomolecules in both normal and cancer cells (424).

1.2.7.1 *De novo* lipogenesis

The primary precursor of several lipid species are fatty acids (FAs), which are either derived from exogenous sources including diet or generated from lipids synthesized by lipogenic tissues (liver, breast and adipose tissues) (420, 423). The production of triglycerides and phospholipids involves the esterification of FAs with glycerol, which is generated from glycerol-3-phosphate (425). Glycerol synthesis is linked to glycolysis whereby glycerol-3-phosphate is produced from DHAP via glycerol-3-phosphate dehydrogenase (GPDH) (426). In turn, the main substrate for FA synthesis is cytosolic acetyl-CoA which is derived from acetate or citrate (423). The CAC produces mitochondrial citrate from either the reductive carboxylation of glutaminederived α-KG or through the oxidative decarboxylation of glucose-generated pyruvate, that is exported to the cytosol (423). In the cytosol, citrate is cleaved to produce acetyl-CoA by ATPcitrate lyase (ACLY). Acetyl-CoA is then used as the substrate for the rate-limiting acetyl-CoA carboxylases (ACCs) to irreversibly generate the two-carbon donor malonyl-CoA (423). Eventually, the serial condensation of malonyl-CoA molecules and one priming acetyl-CoA by the NADPH-dependent fatty acid synthase (FASN) yields palmitate, the initial product of FA synthesis (423). Palmitate can be desaturated and/or elongated to generate other FA species (423). Considering that most normal tissues prefer the use of circulating lipids instead of de novo biosynthesis as the primary source of FAs, the role of FASN in non-transformed cells is of minor importance in well-nourished individuals (42). Nonetheless, a wide variety of tumors and premalignant lesions upregulate FA synthesis through the coordinated expression of several lipogenic enzymes (42). The three main enzymes of FA biosynthesis- ACLY, ACC and FASN- are upregulated in several cancer types such as breast cancer and NSCLC (427-430). While it was demonstrated that silencing either ACC or FASN was associated with the induction of apoptosis and formation of ROS in breast and ovarian cancers, the inhibition of ACLY in human lung adenocarcinoma cell lines resulted in growth arrest in cell culture and *in vivo* (427, 429). When cancer cells are subjected to hypoxia or deprived of lipids, they increase acetate uptake via MCTs and by upregulating the expression of ATP-dependent acetyl-CoA synthetase 2 (ACSS2) which catalyzes the conversion of acetate to acetyl-CoA (35, 431, 432). Also, glioblastomas were shown to accumulate acetyl-CoA from glucose and acetate catabolism which was accompanied by elevated ACSS2 expression (35). Overall, the increase in lipogenesis even in the presence of exogenous lipid sources, allows tumor cells to meet their high metabolic demands and to adapt to exogenous lipid scarcity (424).

1.2.7.2 Fatty acid uptake

In addition to upregulating *de novo* FA synthesis, cancers have developed means to efficiently obtain lipids and FAs from the tumor microenvironment (433). Although lipids can be taken up by the cells through the endocytosis of low-density lipoprotein (LDL) via LDL receptor, free FAs are imported into the cells either via CD36 fatty acid translocase or the FA transport proteins (FATPs/SLC27A1-6) (434, 435). FA uptake can also be facilitated by FA binding proteins (FABPs) which are intracellular lipid chaperones (436). These different metabolic routes of obtaining FAs are often upregulated to meet the high metabolic needs of tumor cells (437-439). Consistently, the uptake of palmitate from the extracellular milieu has been demonstrated to promote migration and metastasis in squamous cell carcinoma (440). Thus, tumor cells develop

strategies to access FAs essential to neoplastic growth, whereby these mechanisms play a prominent role under conditions wherein *de novo* FA synthesis is suppressed (e.g., hypoxia) (441, 442).

1.2.7.3 Fatty acid oxidation

When nutrients are limiting, lipolysis disintegrates lipid droplets by cleaving acyl chains off triacylglycerides (423). The liberated FAs are coupled to CoA by acyl-CoA synthetase (ACS) (423). Subsequently, the FAs are converted to acylcarnitines by carnitine palmitoyltransferase 1 (CPT1) that are shuttled to the mitochondrial matrix via the carnitine-acylcarnitine translocase (SLC25A20) (423). Here, the FAs are transferred back to CoA by CPT2 (423). β-oxidation generates energy through the step-wise shortening of acyl-CoA molecules yielding one molecule of FADH₂ and NADH for every 2-carbon unit of acetyl-CoA removed from the acyl chain (423). The acetyl-CoA molecules produced can be oxidatively decarboxylated via the CAC to produce more NADH and FADH₂ (423). The reducing equivalents from both β-oxidation and CAC are finally oxidized via OXPHOS to produce ATP (423). Complete FA oxidation of palmitate produces approximately twice the amount of energy compared to the catabolism of glucose into carbon dioxide and water (423). Importantly, FA synthesis and oxidation are mutually exclusive and are regulated by negative feedback wherein CPT1 activity is inhibited by high levels of malonyl-CoA generated by ACC during FA synthesis (423). Considering that oxygen is required for FA oxidation, the catabolism of FAs is thought not to be a significant contributor to energy production in hypoxic tumor cells (443). In keeping with this, hypoxia increased the accumulation of lipid droplets, and suppressed β-oxidation by inhibiting the expression of acyl-CoA dehydrogenases (444). Paradoxically, it was reported that some neoplastic cells require βoxidation, especially when subjected to metabolic stress such as hypoxia or glucose deprivation

(445). For example, the brain isoform of CPT1 (i.e., CPT1C), is induced by hypoxia or glucose depletion in tumor cells to support ATP production (445). These contradictory findings illustrate that understanding of the role of FA oxidation in neoplasia is incomplete. Nonetheless, these findings suggest that targeting FA catabolism may limit the metabolic plasticity of tumor cells.

1.2.8 Pentose Phosphate Pathway (PPP)

The pentose phosphate pathway (PPP), which is also referred to as the hexose monophosphate shunt, branches from the glycolytic pathway (446). In PPP, after G6P is formed by HK, it is irreversibly oxidized by the rate-limiting NADP-dependent G6P dehydrogenase (G6PDH) to produce 6-phosphoglucono-δ-lactone in the oxidative branch of the PPP (447). 6phosphoglucono-δ-lactone is then hydrolyzed via 6-phosphogluconase (6PGL) to yield 6phosphogluconate (446, 447). 6-phosphogluconate is oxidatively decarboxylated via NADPdependent 6-phosphogluconate dehydrogenase (6PGDH) to generate ribulose-5-phosphate (Ru5P) (446, 447). Consequentially, the oxidative branch of the PPP produces 2 molecules of NADPH per molecule of G6P. The non-oxidative branch of the PPP involves the conversion of Ru5P by ribose 5-phosphate isomerase (RPI) to form ribose-5-phosphate (R5P) (447), which is followed by a series of reversible reactions catalyzed by transketolase (TKT) and transaldolase (TALDO). Both enzymes utilize glycolytic/gluconeogenic intermediates, such as F6P and G3P, to produce PPP intermediates and vice versa they can generate glycolytic/gluconeogenic intermediates from PPP intermediates (446). Hence, the PPP is coordinated with glycolysis and gluconeogenesis to control the production of NADPH and R5P (447, 448). Taken together, the PPP supports cell survival and proliferation by directly or indirectly providing NADPH needed to drive lipid biosynthesis and ROS scavenging, while simultaneously generating R5P molecules required for nucleotide synthesis (447).

Studies have suggested that cancer cells may reprogram their metabolism to redirect carbon units derived from glucose into both arms of the PPP (447). PPP reprogramming in tumor cells is facilitated due to the reversible nature of most of the reactions in the nonoxidative arm (446). PPP has also been thought to play a major role in metabolic plasticity of cancer cells (446). For example, when cells are under oxidative stress, the PPP is utilized to enhance NADPH production via the oxidative branch, and to simultaneously direct the nonoxidative branch towards resynthesizing more G6P molecules needed to support the oxidative branch (446). Since G6PDH is negatively regulated by NADPH, it is expected that the activity of this enzyme is elevated in cancer cells with high NADPH consumption (449). In line with this, increased activity of G6PDH was reported in cervical cancer (450). In addition, it was shown that pancreatic cancer cells primarily engage the nonoxidative branch of PPP to produce ribonucleotides for the synthesizing nucleic acids (451, 452). This is occasionally supported by elevated TKT expression (451, 452). In summary, the aberrant expression, and activities of the PPP enzymes in cancer cells allow them to adapt to oxidative stress while supporting their rapid proliferative rates.

1.2.9 Nucleotide metabolism

Nucleotides play several diverse roles in a cell including providing energy to coenzymes in the form of ATP, acting as cofactors (e.g., FAD, NAD and NADP) and regulators (e.g., AMP and ADP) of various metabolic enzymes, along with providing the essential building blocks for nucleic acid synthesis (453). The synthesis of DNA and RNA is enhanced to support cell growth and proliferation especially in rapidly proliferating lymphocytes and cancer cells (454). Activated lymphocytes and tumor cells greatly induce *de novo* nucleotide synthesis pathways plausibly due to the limiting concentrations of nucleosides and nitrogenous bases available in blood (455).

1.2.9.1 Purine biosynthesis

R5P molecules, which are predominantly derived from the PPP, are used to produce phosphoribosyl pyrophosphate (PRPP) via 5-phosphoribosylsynthetase (PRPS) (454). The purine biosynthetic pathway takes place in the cytosol and commences with the conversion of PRPP into 5-phosphoribosyl-1-amine (PRA) by the rate-limiting PRPP amidotransferase (PPAT) (453, 456). PRA undergoes a series of reactions to build the purine rings which involves the use of glutamine and aspartate as the primary nitrogen atom providers while THF, bicarbonate, and glycine donate the carbon atoms needed to generate inosine monophosphate (IMP) (453, 454). The resulting IMP is used to synthesize both guanosine monophosphate (GMP) [via inosine monophosphate dehydrogenase (IMPDH) and guanosine monophosphate synthetase (GMPS)] and adenosine monophosphate (AMP) [through the activities of adenylosuccinate synthase (ADSS) and adenylosuccinate lyase (ADSL)] (456). De novo purine synthesis is regulated by product inhibition as AMP and GMP repress PRPS and PRA through a negative feedback loop (453). Enzymes involved in the nucleotide biosynthesis pathway such as IMPDH and PRPS2 have been shown to be important for MYC-driven oncogenesis because their abrogation correlates with decreased proliferation of B-cell lymphoma and small cell lung cancer (457, 458).

1.2.9.2 Pyrimidine biosynthesis

Unlike purine biosynthesis which begins with PRPP as the main precursor metabolite, pyrimidines are synthesized as free rings to which R5P molecules are subsequently attached (453). The first three reactions of *de novo* pyrimidine synthesis occur in the cytosol and are catalyzed by a trifunctional enzyme called carbamoyl phosphate synthetase 2, aspartate transcarbamoylase, and dihydroorotase (CAD) (456). Specifically, CAD uses bicarbonate to convert glutamine into carbamoyl phosphate which represents the rate-limiting step of the pathway (456). Carbamoyl

phosphate co-reacts with aspartate to produce N-carbamoyl-L-aspartate that is ultimately dehydrated into dihydroorotate (453, 456). CAD catalyzes the assembly of the dihydroorotate ring by incorporating nitrogen atoms from glutamine and aspartate, while the carbon atoms of the ring are derived from aspartate and bicarbonate (454). As previously mentioned, dihydroorotate is oxidized into orotate by DHODH (453). The R5P molecules are linked to the orotate ring and subsequently decarboxylated into uridine monophosphate (UMP) via the catalytic activities of orotase phosphoribosyltransferase and orotidylic acid decarboxylase, respectively (453, 456, 459). Orotase phosphoribosyltransferase and orotidylic acid decarboxylase are components of the bifunctional uridine monophosphate synthetase (UMPS) (453, 456, 459). UMP acts as a negative regulator of pyrimidine biosynthesis through feedback inhibition of carbamoyl phosphate synthetase 2 domain of CAD (453). UMP is phosphorylated using 2 ATP molecules in sequential reactions catalyzed by UMP/CMP kinase and nucleoside-diphosphate kinase to produce UTP (459). UTP and glutamine serve as substrates of the ATP-dependent CTP synthase to generate CTP (459). Deoxyribonucleotides (dNTPs) such as dTTP are produced using dUMP as a precursor that can be methylated with 5,10-methylene-THF by thymidylate synthase to generate dTMP, which in turn is further phosphorylated to generate dTTP (460). dUMP is itself formed through the reduction and subsequent dephosphorylation of UTP by ribonucleotide reductase (RNR) or via the deamidation of dCMP derived from the hydrolysis of DNA (460, 461). De novo pyrimidine biosynthesis is upregulated in transformed breast cancer cells (462). The induction of de novo pyrimidine biosynthesis was accompanied by higher CAD expression and activity compared to non-transformed breast cells (462).

1.3 Dysregulation of metabolism in cancer

Perturbation in cellular energy metabolism and metabolic flexibility in cancer cells play a major role in tumor initiation, progression and therapeutic responses. Several transcription factors and signaling pathways that are frequently dysregulated in neoplasia are thought to orchestrate metabolic rewiring in cancer cells and underpin metabolic plasticity of neoplasia.

1.3.1 Transcriptional regulation of cancer metabolism

1.3.1.1 Hypoxia Inducible Factor (HIF)

It is proposed that one of the predominant mechanisms underlying the Warburg effect is the activation of the HIF complex, which functions as a transcription factor that is physiologically activated in response to hypoxia (463). Given that solid tumors rapidly outstrip their vascular supply because of their neoplastic growth, most cells in the tumor bed are thought to be exposed to low oxygen levels ranging between 1% - 2% (464, 465). The HIF complex is thought to upregulate the expression of genes to sustain cancer cell proliferation and survival under hypoxia (463). In some cancer subtypes, HIF is aberrantly activated even under normoxic conditions which is usually caused by genetic lesions such as the amplification of HER2 oncogene in breast cancer (466). HIF gene family comprises alpha and beta subunits that assemble into heterodimers to regulate transcription (467). Humans express 3 paralogues of HIF-α subunit (HIF-1α, HIF-2α/EPAS, HIF-3α) as well as 2 HIF-β paralogues (HIF-1β/ARNT, HIF-2β/ARNT2) (467). HIFs appears to function in non-redundant manner whereby HIF-1 upregulates glycolytic genes while HIF-2 stimulates expression of genes associated with lipoprotein metabolism (468). Notably, genetic inactivation of the VHL tumor suppressor gene, which is common in clear cell renal carcinoma, leads to constitutive stabilization of HIF-1α and HIF-2α (254). Intriguingly, during the progression of clear cell renal carcinoma, the expression of HIF-1α is occasionally abolished and HIF-2 (a heterodimer of HIF-2 α and HIF-1 β) takes over the transcriptional control of genes previously regulated by HIF-1 (469). Considering that HIF regulates the transcription of genes encoding 13 different glucose transporters (e.g., GLUT1 and GLUT3) and glycolytic enzymes (e.g., HK1, HK2, LDHA, ENO1, PKM, PGK1, GAPDH and TPI), it is thought that it plays a major role in regulation of aerobic glycolysis (470). Furthermore, as an adaptive response, HIF promotes the transcription of genes that induce mitochondrial breakdown via autophagy such as BNIP and BNIP3L, when cells are subjected to chronic hypoxia (471, 472). HIF also attenuates oxidative decarboxylation in the CAC and induces reductive metabolism of glutamine which at least in part is achieved via suppression of OGDH (41, 473, 474). Taken together, HIF plays a prominent role in orchestrating metabolic reprograming of neoplasia.

1.3.1.2 MYC

Similar to HIF, the MYC family of oncoproteins (CMYC, MYCL and MYCN) are transcription factors that are approximated to regulate the transcription of 15% of the whole human genome (472, 475). Although MYC expression is tightly regulated in non-transformed cells, MYC has been found to be overexpressed or aberrantly regulated in up to 70% of all types of cancers through diverse mechanisms, such as genetic copy-number gain (chromosome amplification or translocation), super-enhancer activation, and altered protein stability (476). For instance, aberrant expression of CMYC is observed in up to 70–80% of CRC (477). There is evidence demonstrating that enhanced MYC activation is a major promoter of malignant transformation, and that MYC-driven tumors and cancers driven by other oncogenes (e.g., *KRAS*) constitutively depend on elevated MYC levels for tumor progression (478, 479). Notably, aberrant MYC expression is postulated to play a major role in modulating global metabolic reprogramming, to enable the production of bioenergetic substrates and biomass needed to support neoplastic growth (480).

CMYC was reported to regulate the global metabolic rewiring of CRC by regulating 215 metabolic reactions (481). Similar to HIF, MYC acts as a promoter of glucose metabolism given that MYC directly upregulates the transcription of several glycolytic genes (e.g., *SLC2A1*, *HK2*, *ENO1*, *LDHA*) (37, 482). Interestingly, MYC cooperates with HIF-1 to upregulate the expression of key glycolytic genes in response to hypoxia, such as *HK2* and *PDK1* in MYC-driven Burkitt's lymphoma cells (38). This suggests that crosstalk between MYC and HIF-1 plays a prominent role in governing the glucose metabolism in lymphoma and potentially other cancer types (38).

In addition to regulating glucose metabolism, MYC also modulates amino acid metabolism (483, 484). MYC was reported to elevate the mRNA levels of large neutral essential amino acid transporters (SLC7A5 and SLC43A1) (485). MYC also upregulates glutamine metabolism by activating glutamine transporters (SLC1A5 and SLC38A5) and inducing the expression of glutamine-utilizing enzymes (GLS1, PRPS2 and CAD) which collectively results in increased glutamine uptake (483, 486-488). Interestingly, a recent study showed that glutamine deprivation in cancer cells altered CMYC expression, wherein the major CMYC isoform is downregulated while the CMYC 1 isoform was upregulated (316, 489). The alterations in CMYC and CMYC 1 expression levels were mirrored by increased expression of GLUL which catalyzes de novo glutamine synthesis (316, 489). Consistent with its central role in glutamine metabolism, overexpression of MYC was shown to induce "glutamine addiction" and increase sensitivity of colon cancer cells and MYC-transformed rat fibroblasts to mitochondrial inhibitors including metformin (490). Furthermore, ATP production and oxygen consumption were elevated when glutamine rather than glucose was the carbon source in MYC-overexpressing rat fibroblast (490). Altogether, these findings illustrate that MYC-driven metabolic perturbations play a prominent role in tumorigenesis and tumor progression across diverse types of neoplasia.

1.3.1.3 p53

It is generally thought that the tumor suppressor gene, *TP53* is the most commonly mutated gene in cancer; it is mutated in over 50% of all cancer types (491). For example, mutations in *TP53* gene occur in approximately 40%-50% of sporadic CRC (492). p53, the protein product of the *TP53* gene, is widely recognized as a transcription factor that plays a central role in responses to a variety of cellular stressors (DNA damage, hypoxia, nutrient fluctuation and mitogenic oncogenes) by modulating cell proliferation, senescence, DNA repair, and apoptosis (493). However, there is an accumulating evidence that suggests that the tumor suppressor function of p53 is also mediated by its metabolic regulatory activities (491).

p53 has been shown to regulate glucose metabolism through the downregulation of glucose transporters (i.e., SLC2A1, SLC2A3 and SLC2A4) (494, 495). Furthermore, activated p53 inhibits the expression of several glycolytic enzymes such as HK2 and PGM (496-498). Conversely, p53 induces TIGAR (TP53-induced glycolysis and apoptosis regulator) which depletes intracellular fructose-2,6-bisphosphate levels leading to the inhibition of glycolysis (496-498). Although p53 suppress glucose uptake and glycolysis, reports indicate that it stimulates mitochondrial functions and OXPHOS (499). For example, p53 induces expression of SCO2 (Synthesis of Cytochrome c Oxidase 2) in CRC cells whereby the abrogation of the *SCO2* gene in cells with wildtype p53 protein recapitulated the metabolic switch from OXPHOS to aerobic glycolysis that occurs in p53-deficient cells (499). Collectively, these studies suggest that p53 suppresses glucose metabolism while stimulating mitochondrial respiration. Moreover, these results provide mechanistic evidence that links loss of p53 function with Warburg effect in cancer cells.

1.3.2 Metabolic regulation via cellular signaling pathways

Activating mutations in oncogenes and loss-of-function mutations in tumor suppressor genes result in the dysregulation of several intracellular signaling pathways. Although aberrant signaling pathways are well established as facilitators of uncontrolled proliferation and enhanced survival of tumor cells, abnormal function of transduction pathways also underpin critical metabolic processes needed to drive tumorigenesis (500).

1.3.2.1 RAS-RAF-MEK-ERK signaling pathway

The RAS-RAF-MEK-ERK signaling cascade, one of the most extensively studied signaling pathways, couples stimuli from the cell surface receptors to transcription factors that regulate gene expression. This pathway is frequently hyperactivated by genetic alterations in upstream signaling molecules such as receptor tyrosine kinases (RTKs) or activating mutations in downstream transducers (i.e., RAS and RAF) (501). The aberrant activation of the RAS-RAF-MEK-ERK prevents apoptosis while stimulating cell cycle progression (502). Moreover, there is growing body of evidence that implicates the constitutive activation of the RAS-RAF-MEK-ERK signaling pathway in inducing metabolic perturbations in cancer cells which includes promoting aerobic glycolysis (503).

1.3.2.1.1 RAS

Collectively, the three *RAS* genes (*HRAS*, *NRAS* and *KRAS*) are one of the most frequently mutated oncogenes in cancer with *KRAS* being the most prevalent (86%) (504). RAS proteins are GTPases that transduce extracellular signals from cell surface RTKs in response to growth factors and other extracellular stimuli to downstream intracellular effector pathways (e.g. ERK1/2 signaling pathway) (505). Mutations in RAS proteins have been demonstrated to profoundly affect metabolism in a variety of malignancies (506). For instance, oncogenic RAS has been implicated

in several nodes of glucose metabolism. Transcriptomic and stable isotope tracer analysis indicated that KRAS-transformed mouse embryonic fibroblasts, PDAC and CRC cells have elevated glucose uptake and glycolysis (507-509). The abrogation of mutant KRAS has been associated the downregulation of glucose transporter (*SLC2A1*) and several glycolytic genes (*HK1*, *HK2*, *PFK1* and *LDHA*) in PDAC (508). KRAS mutants also promote the nonoxidative arm of the PPP as illustrated by the increased carbon flux into glycolytic intermediates (G3P, F6P) that are then fed into the PPP and non-oxidative PPP intermediate (sedohepulose-7-phosphate) (508). Moreover, recent reports suggest that KRAS and HK1 interact in GTP-dependent manner, whereby this interaction is required to stimulate the hexokinase (509). In spite of indications of a direct GTP-dependent interaction between KRAS and HK1, KRAS predominantly regulates most metabolic pathways through MAPK-dependent signaling cascades to ultimately provide biomass for neoplastic growth (509, 510).

1.3.2.1.2 RAF

The serine/threonine RAF family of kinases which include ARAF, BRAF and CRAF become activated by GTP-bound RAS proteins (511). In addition, activating RAF mutations result in the constitutive activation of ERK1/2 signaling pathway (512). Among the three isoforms of RAF, BRAF has the highest mutation rate, occurring in 30–70% of melanomas, 30–50% of thyroid cancers, and 5–20% of colorectal cancers (511, 513). The majority of these tumors harbor BRAF V600E point mutation which favors the active structural conformation of BRAF causing the constitutive activation of ERK1/2 pathway (514). This ultimately promotes Warburg Effect and cell proliferation (515). Accordingly, BRAF-mutated CRC cell lines upregulate the glucose transporter SLC2A1, to increase glucose uptake (516). In addition, the BRAF V600E point mutation sustains melanoma cells by upregulating glycolytic enzymes including GAPDH,

PGAM1 and LDHA (517). Interestingly, it was shown that BRAF-mutated melanomas have reduced levels of the mitochondrial master regulator PGC1α, and decreased OXPHOS (518). Collectively these findings provide insights in the role of RAF mutations in metabolic rewiring of neoplasia.

1.3.2.2 AMPK: Regulator of intracellular energy homeostasis

It is critical for cells to maintain energy homeostasis by coordinating energy consumption and production. Dysregulation of energy homeostasis is implicated in promoting various diseases such as type 2 diabetes, obesity, and cancer. AMP-activated protein kinase (AMPK) is considered to represent a major intracellular energy sensor, that is activated in response to alterations in energetic status of the cell caused by various stressors including nutrient deficiency, oxidative stress and hypoxia (519, 520). AMPK is a heterotrimeric serine/threonine kinase complex consisting of a catalytic α subunit (α 1 and α 2) and two regulatory β (β 1 and β 2) and γ (γ 1, γ 2 and γ 3) subunits (520-522). The expression of the different AMPK subunit isoforms is tissue-specific (523). Notably, AMPK $\alpha 1$, $\beta 1$, and $\gamma 1$ subunits are ubiquitously expressed while the other AMPK subunit isoforms exhibit a more restricted expression pattern (523). For example, α2 is highly expressed in skeletal and cardiac muscle, and it is the predominant α -subunit in these tissues (523). Cellular energy depletion typically results in the increase of AMP/ATP or ADP/ATP ratios, whereby AMP or ADP bind directly to the γ subunit of AMPK (523). This induces a conformational change in the α subunit and prevents dephosphorylation of the α subunit activation loop threonine residue (T172 in humans) by phosphatases (524-527). Threonine residue (T172 in humans) found in the activation loop of the α subunit is phosphorylated by upstream kinases including as the serine/threonine kinase liver kinase B1 (LKB1), and calcium/calmodulindependent protein kinase kinase β (CAMKK2) (528, 529). The phosphorylation of AMPK at T172 increases AMPK activity by up to 100-fold in cell-free assays (526).

LKB1 functions as a constitutive heterotrimer found in complex with the kinase-dead STE20-related kinase (STRAD) and the STE20 family scaffolding protein (MO25) (530, 531). LKB1 is primarily responsible for the activation of AMPK under energy stress in most mammalian tissues (532). Nonetheless, AMPK can also be phosphorylated and activated independently of LKB1, in response to increased intracellular calcium levels by CAMKK2 (533). In this way, CAMKK2 couples calcium signaling to AMPK-dependent metabolic programs (534). Of note, CAMKK2 has been demonstrated to also activate AMPK following metabolic stressors, such as amino acid deprivation and hypoxia (535-537). Taken together, the role of AMPK as a sensor of metabolic stress is facilitated by the catalytic activities of both LKB1 and CAMKK2.

Importantly, it has been reported that the lysosomal membrane surface facilitates the phosphorylation of AMPK by LKB1 (538, 539). These studies provide mechanistic insights into AMPK activation under conditions of glucose deprivation (538, 539). In glucose-starved cells, LKB1 is tethered to the scaffolding protein, AXIN (538, 539). The LKB1-AXIN-AMPK complex was shown to be localized to the late endosome/lysosomes by binding to the lysosomal protein, LAMTOR1 (also known as Ragulator1), a component of v-ATPase-Ragulator complex (538).

There is accumulating evidence indicating that AMPK plays a major role in detecting oxidative stress. For example, ROS modulates AMPK activity by direct posttranslational modifications of the α-subunit (540, 541). However, the resulting effects of such modifications seem to be context-dependent. Exposure of HEK293 cells to H₂O₂ induced the oxidation and S-glutathionylation of C299 and C304 in the α-subunit, which result in activation of AMPK (541). Conversely, treating cardiomyocytes with H₂O₂ causes the oxidation of the C130 and C174 in the

α-subunit that coincides with the inhibition of AMPK (540). Although further work is warranted to define the role of AMPK in sensing ROS levels, these studies suggest that AMPK acts as a critical node linking energy and redox status in the cell.

AMPK not only senses the cellular energy status but also ATP levels by suppressing ATPconsuming biosynthetic pathways (e.g., protein synthesis and fatty acid synthesis), while concurrently promoting pathways that regenerate ATP through the breakdown of macromolecules and organelles (e.g., glycolysis and fatty acid oxidation). Specifically, energy stress activates AMPK which can promote glucose uptake by phosphorylating and degrading TXNIP, a negative regulator of glucose metabolism, resulting in the upregulation and surface translocation of SLC2A1 glucose transporter (542). Once glucose is catabolized to restore ATP to ADP/AMP ratios, AMPK is subsequently dephosphorylated which ultimately induces TXNIP to suppress glucose uptake as energy homeostasis is re-established (542). Conversely, AMPK prevents the storage of glycogen by inhibitory phosphorylation of glycogen synthases (GYS1 and GYS2) (543). It also downregulates gluconeogenesis through the phosphorylation and nuclear exclusion of cyclic-AMP-regulated transcriptional co-activator 2 (CRTC2) and class II histone deacetylases (HDACs), which are key cofactors for the transcription of gluconeogenic genes (544). Additionally, AMPK suppresses lipid synthesis through the direct inhibitory phosphorylation of acetyl-CoA carboxylase 1/2 (ACC1/2) which catalyzes the rate-limiting step of fatty acid synthesis (523, 545). In parallel to inhibiting fatty acid synthesis, activated AMPK stimulates fatty acid oxidation by reducing the levels of ACC2-generated malonyl-CoA (523). This alleviates the repression of CPT1 thus promoting fatty acid oxidation (523). In summary, AMPK-dependent inhibition of gluconeogenesis and lipid synthesis limits ATP consumption while promoting ATPgenerating metabolic processes under energy stress.

Considering that protein synthesis is one of the most energetically demanding cellular process, AMPK inhibits this process when nutrients are limited. AMPK-dependent downregulation of protein synthesis is mostly mediated through the direct inhibition of mechanistic target of rapamycin complex 1 (mTORC1 complex) through two independent mechanisms: the activating phosphorylation of tuberous sclerosis complex 2 (TSC2), a negative mTORC1 regulator, and the inhibitory phosphorylation of RAPTOR (546, 547). AMPK also suppresses protein synthesis by phosphorylating eukaryotic elongation factor 2 kinase (eEF2K) which is a negative regulator of mRNA translation elongation (548). Notably, eEF2K can also be directly phosphorylated by mTOR (549), thus illustrating crosstalk between AMPK and mTOR signaling pathways.

Tumor-suppressive functions of AMPK have been described in prostate cancer wherein AMPK-mediated inhibition of lipogenesis was associated with tumor growth arrest (550). While the inhibition of AMPK due to a hypomorphic mutation decreases LKB1 expression and markedly accelerates tumor development in PTEN(+/-) mice, activating AMPK by administering well recognized mitochondrial inhibitors (such as metformin, phenformin or A-769662) to PTEN(+/-) mice significantly delayed tumor onset (551). Finally, it has been demonstrated that AMPK counteracts Warburg effect thus attenuating tumor growth in mouse models (552). Nevertheless, under certain contexts including nutrient and oxygen deprivation, AMPK activation engenders tumor cells with growth advantage by increasing metabolic plasticity and allowing cells to adapt to energy stress (553). This is for example illustrated by observations that under energy stress activated AMPK inhibits ACC1/2 in order to maintain NADPH levels by reducing NADPH-consuming fatty-acid synthesis while elevating NADPH-generating fatty-acid oxidation (554). This facilitated anchorage-independent growth and solid tumor formation in vivo mouse models

(554). These and other findings suggest that whereas AMPK plays a tumor suppressive role during tumor initiation, it attains a tumor promoting role once tumors outstrip their vasculature and are exposed to metabolic stress (555).

1.3.2.3 PI3K-AKT-mTOR signaling

The PI3K-AKT-mTOR signaling pathway underpins many essential cellular processes such as cell growth, protein synthesis, proliferation and energy metabolism (556). Similar to the RAS-RAF-MEK-ERK signaling cascade, the PI3K signaling pathway is activated when RTKs bind to growth factors, hormones or mitogens (557) (Fig. 1.4). This triggers the intracellular autophosphorylation of tyrosine residues on the RTKs which act as cell membrane anchors for PI3K (558-560). Subsequently, PI3K phosphorylates phosphatidyl inositol-4,5-biphosphate (PIP₂) to yield phosphatidyl inositol-3,4,5-triphosphate (PIP₃) (Fig. 1.4). PIP₃ translocates the serine/threonine kinase, AKT, to the cell membrane where it is phosphorylated within its activation loop (at T308) and activated by 3-phosphoinositide-dependent protein kinase 1 (PDK1) (561) (Fig. 1.4). A major negative regulator of the PI3K signaling pathway, is the tumor suppressor PTEN which dephosphorylates PIP₃ into PIP₂ (562) (Fig. 1.4). Although the PI3K/AKT pathway has been reported to promote glucose uptake and glycolysis through the translocation of glucose transporter, SLC2A4 and activation of 6-phosphofructo-2-kinase/fructose-2,6-biphosphatase (PFKFB) respectively, the signaling pathway predominantly regulates various metabolic processes via its downstream effector mTOR (563-565).

mTOR is a serine/threonine kinase which acts downstream of the PI3K signaling pathway (Fig. 1.4). mTOR is the catalytic subunit of two functionally and structurally distinct protein complexes. The mTORC1 complex is composed of mTOR, mLST8, proline rich AKT1 substrate 40 (PRAS40), DEPTOR and RAPTOR while mTORC2 is composed mTOR, mLST8, mSIN1,

DEPTOR, PROTOR 1/2 and RICTOR (566-570). Between the two complexes, the functions of mTORC1 complex are better defined whereby it has been shown that it promotes glycolysis, lipid synthesis, cell growth and protein synthesis while the activities of mTORC2 are mostly obscure (570, 571). Nonetheless, mTORC2 has been demonstrated to regulate proliferation, cell survival and cytoskeletal organization primarily via the phosphorylation of AGC kinases including AKT, SGK1 and PKC (572, 573). While mTORC2 modulates metabolism mainly through the activation of AKT, the complex also regulates cytoskeletal remodeling and cell migration through the phosphorylation of PKCα, PKCδ, PKCζ, PKCγ and PKCε (570, 574-578). Also, mTORC2-mediated phosphorylation and activation of SGK1 promotes epithelial sodium ion transport and cell survival (579, 580).

1.3.2.3.1 Upstream activators of mTOR signaling

AKT phosphorylate and inhibits TSC2 which together with TSC1 and TBC1 domain family member 7 (TBC1D7) comprises tuberous sclerosis complex (TSC) (581) (Fig. 1.4). The TSC complex is GTPase-activating protein (GAP) that inhibits the activator of mTORC1, ras homolog enriched in brain (RHEB) GTPase (582, 583) (Fig. 1.4). Thus, the inhibition of the TSC complex by AKT results in the activation of mTORC1. DNA damage and hypoxia induce regulated in development and DNA damage response 1 (REDD1) protein which facilitates the dissociation of inhibitory 14–3–3 protein from TSC2 leading to mTORC1 inhibition (584-586) (Fig. 1.4).

Interestingly, ERK1/2 from the RAS-RAF-MEK-ERK signaling pathway can phosphorylate TSC2 (at S540 and S664) and RAPTOR (at S8, S696 and S863) directly which activate mTORC1 (587-590). In addition, ERK1/2 indirectly leads to the phosphorylation of TSC2 (at S1798) and RAPTOR (at S719, S721 and S722) via p90 ribosomal protein S6 kinase (RSK),

thus promoting mTORC1 signaling (591-594) (Fig. 1.4). The interaction between the RAS-RAF-MEK-ERK and PI3K-AKT-mTORC1 pathways results in negative regulation of each other's activity via cross-inhibition (595). For instance, the activation of ERK induces the phosphorylation of GRB2-associated binder 1 (GAB1) at six serine/threonine residues (T312, S381, S454, T476, S581, S597) which hinders GAB1-mediated recruitment of PI3K to the EGF receptor and thus decrease the phosphorylation of AKT (596). The ERK phosphorylation sites on GAB1 recruit the protein tyrosine phosphatase, SHP2, which dephosphorylates and regulate RASGAP and PI3K (595, 597). Conversely, AKT inhibits the MAPK signaling pathway via the phosphorylation of RAF (598). This is demonstrated in a study which show that high concentrations of IGF1 markedly activate AKT resulting in the phosphorylation and repression of RAF activity in breast cancer and melanoma cell lines (598-600). Intriguingly, it was shown that although activating BRAF mutations initiate nevi development, AKT activation is required to bypass MAPK-mediated cell cycle arrest or senescence (600). AKT reduces RAS-RAF-MEK-ERK signaling to levels it can cooperate with to transform nevi into melanomas (600). Collectively, these illustrate crosstalk between the RAS-RAF-MEK-ERK and PI3K-AKT-mTORC1 signaling pathways and thus, indicate cooperation between the two pathways in regulating metabolic processes and tumor development.

Amino acids, glucose, energy stress and oxygen and growth factors activate mTORC1 (570). Specifically, mTORC1 indirectly responds to high AMP/ATP ratio, glucose deprivation and hypoxia partly through the activation of AMPK which in turn inhibits mTORC1 as previously discussed (547, 601, 602) (Fig. 1.4). However, glucose starvation also suppresses mTORC1 complex independent of AMPK (603, 604). Glucose depletion inhibits Rag GTPases (RagA/RagB) which prevents the localization and activation of mTORC1 at the lysosome (603,

604) (Fig. 1.4). Additionally, mTORC1 senses amino acid levels through Rag GTPases (605, 606) (Fig. 1.4). Rag GTPases function as heterodimeric complexes of RagA or RagB with RagC or RagD and are attached to the lysosome through their association with the Ragulator/LAMTOR complex (that is composed of MP1, p14, p18, HBXIP and c7ORF59) (607, 608). The Ragulator/LAMTOR complex which associates with a v-ATPase at the lysosomal surface, not only acts as a scaffold for Rag GTPases but also has a guanine nucleotide exchange factor (GEF) activity for RagA/B (608). The presence of amino acids stimulates the GEF activity of the Ragulator in a v-ATPase-dependent manner resulting in RagA/B-GTP loading and the subsequent recruitment of mTORC1 to the lysosome where it also interacts with RHEB (608) (Fig. 1.4). Interestingly, a few additional components involved in amino acid sensing by mTORC1 have been identified such as the folliculin-folliculin interacting protein 1/2 (FNIP1/2) complex which acts as a GAP for RagC/D GTPases (609, 610). However, glutamine and asparagine have been demonstrated to stimulate mTORC1 independently of Rag GTPases but through ADP ribosylation factor (ARF) family GTPases (611-613). Of note, specific amino acids (e.g., leucine and arginine) are amongst the most potent activators of mTORC1. Leucine and arginine activate mTORC1 via GATOR1 and GATOR2 complexes (614). GATOR1 complex (composed of DEPDC5, Nprl2 and Nprl3) is inhibited by the GATOR2 complex (consisting of Mios, WDR24, WDR59, Seh1L and Sec13)(614). GATOR1 which suppresses mTORC1 activity by acting as a GAP for RagA/B, is anchored to the lysosome by another complex, KICSTOR (comprised of KAPTIN, ITFG2, c12orf66, and SZT2) (614, 615). Cytosolic leucine and arginine activate mTORC1 by binding and inactivating Sestrin2 and CASTOR1 respectively which are inhibitors of GATOR2 (616-620). In addition to the extensive studies on the effects of glucose and amino acids on mTORC1 signaling,

recent findings indicate that mTORC1 senses intracellular levels of nucleotides and lipids (621, 622).

Compared to mTORC1, there are fewer known activators of the mTORC2 complex. mTORC2 appears to be to be predominantly activated by insulin and other growth factors via PI3K (623). PI3K-dependent regulation of mTORC2 is facilitated by the mSIN1 subunit of the complex which contains a phosphoinositide-binding pleckstrin homology (PH) domain that inhibits mTORC2 in the absence of insulin but activates mTORC2 when insulin is present by binding to PIP₃ generated at the plasma membrane (624) (Fig. 1.4). Interestingly, PI3K promotes the association of mTORC2 with ribosomes which results in mTORC2 activation (625). When AKT is partially activated due to phosphorylation of T308, it phosphorylates mSIN1 (at T86) which induces mTORC2 to phosphorylate (at S473) and fully activate AKT (626). Although the partial activation of AKT is sufficient to phosphorylate and thus activate mTORC1, fully activated AKT phosphorylates a more diverse set of effectors containing an RXXS/T motif (568). As such, mTORC2 promotes mTORC1 signaling via AKT-dependent phosphorylation of TSC2 and other effectors. However, mTORC2 is regulated by mTORC1 as a result of a negative feedback loop between mTORC1 and PI3K (627, 628). Specifically, elevated mTORC1 increases the activity of one of its downstream effectors, S6 kinase (S6K), resulting in the phosphorylation and degradation of insulin receptor substrate-1 (IRS-1) which in turn recruits PI3K (627-629). Furthermore, mTORC1 phosphorylates and activates growth factor receptor-bound protein 10 (GRB10), which negatively regulates insulin/IGF-1 receptor signaling upstream of AKT and mTORC2 (630, 631). More recently, AMPK has been revealed as a positive regulator of mTORC2 during periods of glucose deprivation (632, 633). AMPK activates mTORC2 by phosphorylating mTOR and RICTOR when PI3K signaling is downregulated (632). While the existence of positive and negative feedback loops between mTORC1 and mTORC2 signaling elucidate potential drug targets, the interconnectivity between the two complexes is indicative of cooperation between the mTOR complexes in mediating metabolic processes.

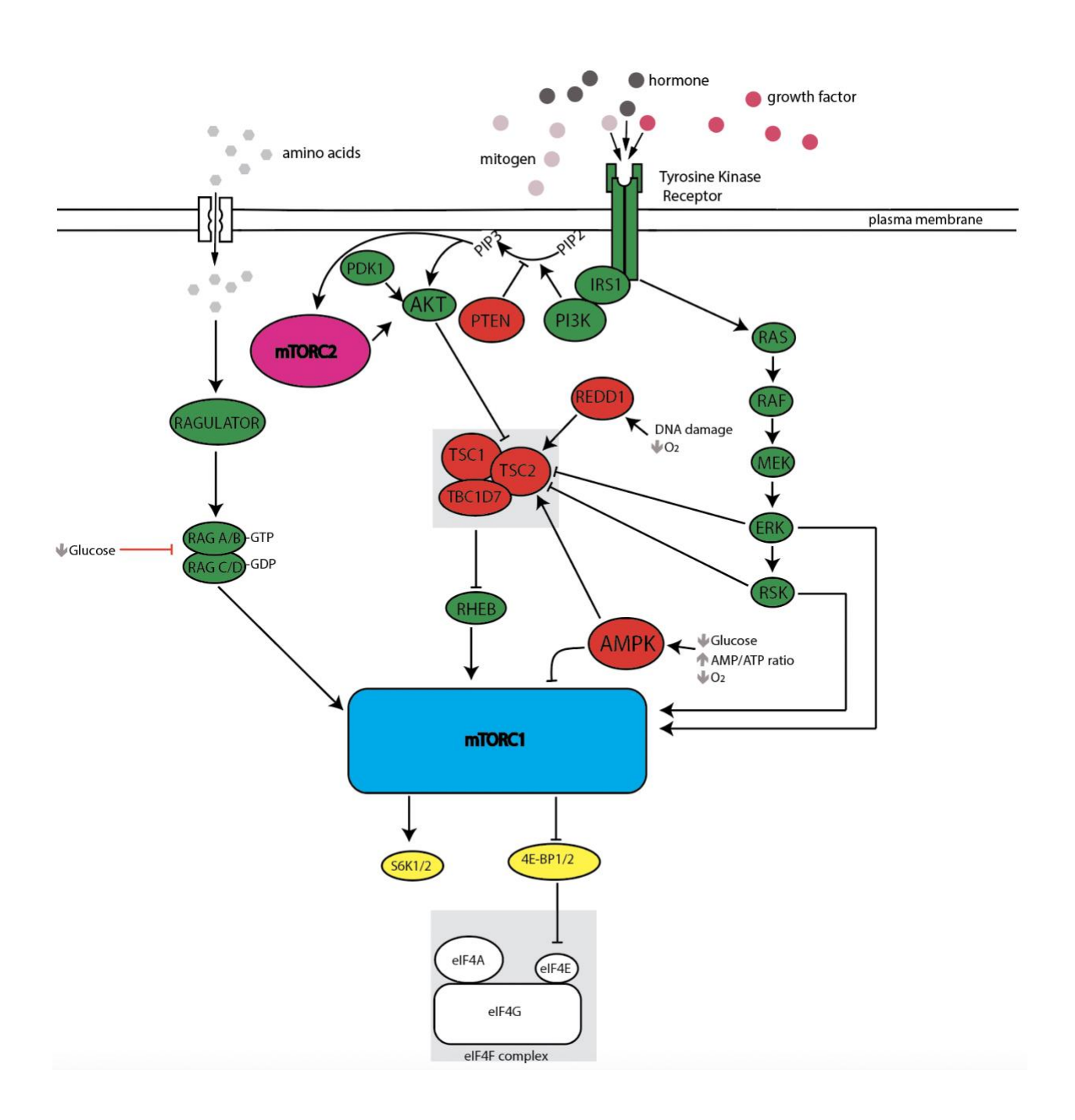


Fig. 1.4. mTOR signaling pathway. mTOR exists in two distinct complexes: mTORC1 (blue) and mTORC2 (magenta). mTOR is activated by hormones, growth factors via receptor tyrosine kinases as well as amino acids imported from the extracellular space. mTORC1 is also modulated by intracellular cues such as AMP/ATP ratio and levels of oxygen. Furthermore, mTORC1 signaling pathway interacts with the MAPK/RSK pathway. Upstream regulators of mTORC1 are shown in green (positive regulators) and red (negative regulators) while the downstream effectors are shown in yellow.

1.3.2.3.2 Systemic effects of mTOR signaling

mTOR signaling coordinates anabolic and catabolic processes to maintain energy homeostasis. In well-fed states, nutrient levels, and growth factors in the blood are increased which trigger anabolic processes while during starvation, catabolic processes are induced due to depleted growth factors and energy sources (570). The disruption of cellular energy homeostasis due to the upregulation or downregulation of mTOR result in tissue-specific abnormalities that are frequently lethal.

Under physiological conditions, when plasma glucose concentration is reduced, adaptive processes involving mTOR signaling such as gluconeogenesis are induced (570). Moreover, constitutive activation of mTORC1 signaling due to the abrogation of TSC1 in the liver diminishes the production of ketone bodies as compensatory energy sources during fasting (634). The importance of diminishing mTORC1 signaling when the levels of nutrient (such as amino acids and glucose) are low is further underscored by the findings that the whole-body knock-in mice expressing a constitutively active form of RagA die due to their inability to induce autophagy in the liver during the perinatal fasting period (603). In pancreatic β -cells, mTORC1 has a biphasic effect on their function. The hyperactivation of mTORC1 through the loss of TSC2 in β -cells

initially leads to increased pancreatic β-cell mass, elevated insulin production, and higher glucose tolerance in young mice which eventually leads to decreased β-cell mass, reduced insulin levels and hyperglycemia (635, 636). This is also consistent with prolonged mTORC1 hyperactivation induced by nutrient overload as commonly observed in type 2 diabetes and obesity (637, 638). Type 2 diabetes is often associated with diminished insulin production due to β-cell exhaustion caused by chronic exposure to excess of nutrients (i.e., glucose) (639). Furthermore, increased mTORC1 activity in insulin-responsive tissues results in insulin resistance because of enhanced negative feedback inhibition of insulin/PI3K/AKT signaling by S6K and via IRS-1 (638, 640). In addition, since mTORC2 fully activates AKT downstream of insulin-driven PI3K signaling, prolonged pharmacological or genetic inhibition of mTORC2 in the liver, muscle or adipocytes impedes response to insulin which is associated with glucose intolerance (641-645). In liverspecific RICTOR-knockout mice, AKT is inhibited which reduces glucokinase activity and glycolysis in the liver (641). Taken together, these findings provide evidence that both mTORC1 and mTORC2 regulate organismal glucose homeostasis.

In the presence of nutrients and insulin, mTORC1 promotes adipogenesis and lipogenesis (646). However, the inhibition of mTORC1 induces lipolysis and fatty acid oxidation (647). The hyperactivation of mTORC1 through the constitutive expression of activated RHEB in adipocytes upregulates lipogenesis while inhibiting lipolysis (648). Consistently, the abrogation of RAPTOR in the liver hinders mTORC1-driven *de novo* lipogenesis in the liver due to reduced expression of lipogenic genes including *Srebp1c* and *Fas* (649). Although the deletion of RAPTOR in adipocytes leads to hepatic steatosis, lipodystrophy and insulin resistance in mice, it also protects mice against diet-induced obesity and hypercholesterolemia because adipogenesis is downregulated (650, 651). Similar to mTORC1, mTORC2 regulates lipid homeostasis in the liver

and adipose tissue (646). The inhibition of mTORC2 through the loss of RICTOR in adipocytes markedly increases the overall lean mass of mice due to growth in the size of non-adipose organs such as heart, kidney, spleen, and bone (645, 652). Furthermore, the inactivation of RICTOR in adipocytes was associated with hyperinsulinemia, increased lipolysis in adipose tissue and insulin resistance in skeletal muscles and liver of mice (645, 652). Although hepatic insulin resistance is frequently linked to fatty liver due to the impaired ability of insulin to repress lipolysis, liverspecific deletion of RICTOR actually protects mice against high-fat diet-induced fatty liver (641, 642). Additionally, suppressing mTORC2 in the liver impairs insulin-driven hepatic lipogenesis which is accompanied by decreases in the expression of transcription factors (i.e., SREBP1c and PPAR γ) and lipogenic enzymes (e.g., ACC and FASN) (641). However, the expression of genes regulating fatty acid oxidation (e.g., *CPT1* and *PPARa*) are increased (641). In summary, both mTORC1 and mTORC2 play pivotal tissue-specific roles in regulating organismal lipid metabolism.

mTORC1 signaling promotes and maintains muscle mass. For instance, mTORC1 induces muscle hypertrophy and prevents muscle atrophy resulting from disuse (653). Conversely, when mTORC1 signaling is downregulated, hypertrophy is impeded (653). It is worth mentioning that these effects on muscle growth are only observed during acute activation of mTORC1 signaling. Chronic activation of mTORC1 due to abrogation of TSC1 leads to muscle atrophy and low body mass because the muscles lack the ability to trigger autophagy which is a critical cellular process for muscle growth (654). Collectively, this suggests that periods of mTORC1 activation and inhibition is required for optimal muscle growth and function.

The PI3K-AKT-mTORC1 axis is frequently hyperactivated in cancer (655, 656). Hyperactivation of this axis stem from activating mutations in positive regulators including

PIK3CA and AKT genes, and/or inactivation of tumor suppressors that suppress this signaling axis including PTEN and TSC genes (655-657). These mutations occur in diverse cancer types including breast cancer, CRC and glioblastoma (658). More recently, activating mutations in mTOR have also been described in endometrial carcinoma, CRC, melanoma, renal cell cancer and bladder cancer (655, 656, 659). This has garnered interest as targeting the PI3K-AKT-mTORC1 pathway presents a potential therapeutic opportunity in cancer (658). Notwithstanding the modest success of applying allosteric mTOR and PI3K inhibitors in the clinic, the outcomes of these approaches were lesser than initially expected (655). This was largely attributed to incomplete understanding of the complexity of the mechanisms underpinning pro-oncogenic activities of the PI3K-AKT-mTORC1 pathway, and in particular the precise role of downstream effectors of mTOR in oncogenesis and tumor progression (655).

Considering that the effectors of mTORC1 and their impacts on cancer-related processes have been extensively covered in previous reviews (556, 565, 570, 647, 660), herein I will focus on findings highlighting the impacts of mTOR effectors on cellular metabolism pertinent to this thesis.

To date, the best studied downstream effectors of mTORC1 signaling are S6Ks (S6K1 and S6K2 in humans), and eukaryotic translation initiation factor 4E (eIF4E) binding proteins (4E-BP1-3 in humans) (661-663) (Fig. 1.4). Specifically, mTORC1 phosphorylates 4E-BPs (at T37/T46, followed by T70 and finally S65 in human 4E-BP1) (661-663). When unphosphorylated, 4E-BPs sequester eIF4E (mRNA cap-binding subunit of the eIF4F complex) and impedes its association with the scaffolding protein eIF4G1 (664). When mTORC1 phosphorylates 4E-BPs, they dissociate from eIF4E, and thus allow the eIF4F complex assembly (665) (Fig. 1.4). eIF4F complex recruits mRNA to the ribosome during translation initiation and is composed of

eIF4E, eIF4G1 and eIF4A (DEAD box RNA helicase) (666-669) (Fig. 1.4). mTORC1 regulates mRNA translation initiation via the phosphorylation of 4E-BPs and S6Ks (664, 670). In addition, mTORC1 stimulates translation elongation by directly or indirectly (via S6Ks) phosphorylating and inactivating eEF2K, whereby eEF2K negatively regulates ribosome translocation by phosphorylating and inhibiting eEF2 (670, 671). Importantly, protein synthesis is one of the most energy consuming processes in the cell (672). By altering the rates of global protein synthesis, mTORC1 therefore modulates cellular energy consumption (673).

Although mTORC1 stimulates global protein synthesis, translation of a subset of mRNAs is particularly sensitive to changes in mTORC1 activity (41, 674-678) (676-678). For example, the mTORC1-4E-BP-eIF4E axis regulates mitochondrial activity and biogenesis by selectively promoting the translation of nucleus-encoded mitochondria-related mRNAs [(such as components of complex I and V, mitochondrial ribosomal proteins and transcription factor a, mitochondrial (TFAM)] (679). Importantly, the mRNA that encodes these proteins typically harbor 5'UTR/TISU elements (Translation Initiator of Short 5' UTR; SAASATGGCGGC, in which S is C or G) and their translation is eIF4E sensitive, but unaffected by eIF4A inhibition (594, 679-681). Consequently, by inducing the translation of nucleus-encoded mitochondria-related mRNAs, mTORC1 upregulates ATP generating capacity to support the protein synthesis and other energy demanding cellular processes. In addition, the mTORC1-4E-BP axis regulates translation of mRNAs encoding enzymes involved in NEAA synthesis including PC, PHGDH, PSAT1 and ASNS (41). To this end, mTORC1-driven upregulation in translation of the aforementioned mRNAs has been shown to underpin metabolic plasticity of breast cancer, CRC and melanoma cells and determine their responses to the drug combinations of oncogenic kinase inhibitors and

biguanides (41). Collectively, these findings demonstrate that mTORC1-dependent translational control plays a major role in regulating metabolic rewiring of neoplasia.

mTOR can modulate glutamine metabolism via post-transcriptional and post-translational regulation of glutaminolysis-related genes (647, 660). Specifically, mTORC1 promotes glutaminolysis by increasing GLS levels through the S6K1-dependent regulation of CMYC (682) and activating GLUD through the abrogation of mitochondrial-localized sirtuin (SIRT4) which inhibits GLUD activity through ADP-ribosylation (683). While it is proposed that CMYC downregulates the expression of post-transcriptional repressors of GLS (i.e., miR-23a/b), mTORC1 promotes the proteasome-mediated degradation of a transcription factor, cAMPresponsive element binding 2 (CREB2), which contains a recognition motif in the promoter region of SIRT4 (483). Thus, mTORC1 activates glutaminolysis via negative regulation of miR-23a/b and CREB2 which promotes GLS and GLUD activities respectively. mTORC2 may also regulate glutamine metabolism post-transcriptionally considering that it has been demonstrated to upregulate CMYC expression and a knockdown of RICTOR reduces the intracellular levels of α-KG that are probably derived from glutaminolysis (679, 684). Furthermore, mTORC2 may promote glutaminolysis, by inhibiting expression of GLUL via AKT-dependent cytoplasmic localization of GLUL transcription factors (FOXO3 and FOXO4) (685). Collectively, these reports firmly establish mTOR as a regulator of glutamine metabolism.

At the cellular level, mTOR regulates glucose metabolism chiefly through HIF-1 α and CMYC which increase the expression glucose transporters and glycolytic enzymes as previously discussed (647, 660). mTORC1 indirectly upregulates the transcription of HIF-1 α via the phosphorylation of signal transducer and activation of transcription 3 (STAT3) during hypoxia (686). Also, a recent study demonstrated that the transcription factor forkhead/winged helix family

k1 (FOXK1) is another mediator of mTORC1-regulated expression of HIF-1α (687). mTORC1 also promotes the translation of HIF-1α through the phosphorylation of its two downstream substrates: 4E-BP1 and S6K1 (686). This is consistent with reports illustrating that the deletion of TSC2, and thus activation of mTORC1 results in the accumulation of HIF-1α while the pharmacological inhibition of mTORC1 with rapamycin decreases the expression of HIF-1α (688, 689). Likewise, mTORC1 enhances the translation of CMYC mRNA in a 4E-BP1 and S6K1dependent manner (682, 690). Given that glucose metabolic reprogramming is frequently observed in many cancers including breast, lung, pancreatic and colorectal cancers, it is not surprising that these cancers are also associated with the hyperactivation of mTOR, amplification of CMYC and increased aerobic glycolysis facilitated by elevated expression of glucose transporters such as SLC2A1 (656, 691, 692). mTORC2 regulates glucose metabolism through AKT which phosphorylates HK2 to promote its association with mitochondria and directly couple intramitochondrial ATP synthesis to glucose metabolism (693, 694). AKT also promotes glycolysis through phosphorylation and activation of PFK2 (563) and upregulating the expression of SLC2A1 (62). In fact, oncogenic activation of AKT has been shown to mediate aerobic glycolysis for the sustained growth and survival of cancer cells (695). mTORC2 also modulates glucose metabolism independent of AKT. In glioblastoma, mTORC2 inactivates class IIa histone deacetylases, which leads to the acetylation of FOXO1 and FOXO3 and thus activates CMYC to upregulate glycolytic gene expression (684). Taken altogether, the findings support that both mTORC1 and mTORC2 complexing are implicated in the regulation of glucose metabolism and metabolic reprogramming in cancer cells.

As previously stated, mTORC1 regulates mitochondrial activity through a 4E-BP-dependent selective translational regulation of mitochondrial-related mRNAs (679). Other studies

have further corroborated the role of mTOR signaling in mitochondrial metabolism. For example, the inhibition of mTORC1 with rapamycin reduces the mitochondrial membrane potential, oxygen consumption, and ATP synthesis while altering the mitochondrial phosphoproteome (696). The suppression of mTORC1 via silencing of RAPTOR downregulates genes encoding proteins involved in OXPHOS and mitochondrial biogenesis, thus impairing mitochondrial respiration (679, 697, 698). mTORC1 modulates mitochondrial respiration through transcriptional regulators such as PGC-1α and yin yang 1 (YY1) (698, 699). In fact, mTOR and RAPTOR interact with YY1, and inhibition of mTOR disrupts the interaction and coactivation of YY1 by PGC-1α (699). Contrary to mTORC1, the role of mTORC2 remains poorly understood. The inhibition of mTORC2 through silencing RICTOR was demonstrated to have no effect on the expression of ETC complexes I-IV proteins or mitochondrial respiration (700). Although the knockdown of RICTOR does not alter the levels of mitochondrial proteins such as ATP5O (ATP synthase subunit O, mitochondrial) and TFAM, it decreases α -KG levels which is a key CAC intermediate (679). Also, genes implicated in mitochondrial transport and function were among a set of genes that was proposed to be translationally downregulated by mTOR catalytic inhibitors but not by rapamycin, would suggest that mTORC2 is involved in the translational regulation of these genes (675, 680). However, this can also be explained by the inability of rapamycin to inhibit the phosphorylation of 4E-BP as previously reported (701, 702). Furthermore, subsequent studies confirmed that the mTORC1/4E-BP1 rather than mTORC2 regulates the translation of nuclear-encoded mRNAs with mitochondrial functions such as ATP5O (679, 680). Nonetheless, when stimulated by growth factors, mTORC2 localizes to the mitochondria-associated endoplasmic reticulum membranes where it phosphorylates and activates AKT (693). In turn, AKT phosphorylates HK2 which stimulates glycolysis, decreases the mitochondrial membrane potential and thus, affects

mitochondrial physiology and metabolism (693). Specifically, mTORC2 deficiency via the loss of RICTOR disrupts mitochondria-associated endoplasmic reticulum membranes leading to increases in mitochondrial membrane potential, ATP production and calcium uptake (693). Overall, although extensive studies have provided evidence elucidating the functions of mTORC1 in mitochondrial metabolism, further research is warranted to fill the gaps in knowledge regarding the role of mTORC2 in mitochondrial metabolism.

In addition to the metabolic processes discussed above, mTOR signaling is implicated in the biosynthesis and transport of amino acids (e.g., serine, methionine and cysteine), fatty acid synthesis and lipid metabolism, pentose phosphate pathway and nucleotide synthesis at various levels of regulation ranging from transcriptional to post-translational mechanisms (647, 660). This underscores the pertinent role of mTOR in mediating metabolic reprogramming of cancer cells. It is worth noting that although mTOR regulates several biosynthetic processes, mTOR activity is often regulated by the products of such processes. For example, mTOR regulates glucose and glutamine metabolism while being simultaneously regulated by glucose and glutamine (570, 647). As such mTOR is required to sense the energetic state of cells which promotes the anabolism or catabolism of nutrients. Even though there is an abundance of research elucidating the regulatory activities of mTORC1 in cancer metabolism, much is still left to uncover with regards to mTORC2. This thesis aims to further study the extensive crosstalk between mTOR signaling and metabolic reprogramming in the context of various energetic stressors in order to highlight vulnerabilities that can be targeted in cancer.

1.4 CENTRAL HYPOTHESIS AND OVERARCHING GOALS

Tumor cells must overcome energy stress as they outgrow their vascular supply. To this end, neoplastic cells must constantly adjust their metabolism to fluctuations in nutrients and oxygen in their microenvironment. Based on this, it is hypothesized that impeding the mechanism that allow cancer cells to adapt to energy stress will result in their death. Therefore, the overarching objective of this thesis is to dissect the mechanisms that underpin the alterations in the metabolome of cancer cells subjected to energy stress with a goal to identify potentially targetable and clinically exploitable vulnerabilities. Specifically, we set out to address the mechanisms that allow cancer cells to adapt to dysfunction of mitochondrial complex IV (Chapter 2), pharmacological inhibition of mitochondrial complex I, and nutrient deprivation (Chapter 3).

1.5 REFERENCES

- 1. Brenner DR, Weir HK, Demers AA, Ellison LF, Louzado C, Shaw A, et al. Projected estimates of cancer in Canada in 2020. Cmaj. 2020;192(9):E199-e205.
- 2. Wu S, Zhu W, Thompson P, Hannun YA. Evaluating intrinsic and non-intrinsic cancer risk factors. Nat Commun. 2018;9(1):3490.
- 3. Doll R, Hill AB. The mortality of doctors in relation to their smoking habits; a preliminary report. Br Med J. 1954;1(4877):1451-5.
- 4. Gastric cancer and Helicobacter pylori: a combined analysis of 12 case control studies nested within prospective cohorts. Gut. 2001;49(3):347-53.
- 5. Arnheim Dahlström L, Andersson K, Luostarinen T, Thoresen S, Ögmundsdottír H, Tryggvadottír L, et al. Prospective seroepidemiologic study of human papillomavirus and other risk factors in cervical cancer. Cancer Epidemiol Biomarkers Prev. 2011;20(12):2541-50.

- 6. Agalliu I, Gapstur S, Chen Z, Wang T, Anderson RL, Teras L, et al. Associations of Oral α -, β -, and γ -Human Papillomavirus Types With Risk of Incident Head and Neck Cancer. JAMA Oncol. 2016;2(5):599-606.
- 7. Ringelhan M, O'Connor T, Protzer U, Heikenwalder M. The direct and indirect roles of HBV in liver cancer: prospective markers for HCC screening and potential therapeutic targets. J Pathol. 2015;235(2):355-67.
- 8. Sun CA, Wu DM, Lin CC, Lu SN, You SL, Wang LY, et al. Incidence and cofactors of hepatitis C virus-related hepatocellular carcinoma: a prospective study of 12,008 men in Taiwan. Am J Epidemiol. 2003;157(8):674-82.
- 9. Veierød MB, Weiderpass E, Thörn M, Hansson J, Lund E, Armstrong B, et al. A prospective study of pigmentation, sun exposure, and risk of cutaneous malignant melanoma in women. J Natl Cancer Inst. 2003;95(20):1530-8.
- 10. Hanahan D, Weinberg RA. Hallmarks of cancer: the next generation. Cell. 2011;144(5):646-74.
- 11. Bertram JS. The molecular biology of cancer. Mol Aspects Med. 2000;21(6):167-223.
- 12. Song Q, Merajver SD, Li JZ. Cancer classification in the genomic era: five contemporary problems. Hum Genomics. 2015;9:27.
- 13. Shtivelman E, Lifshitz B, Gale RP, Canaani E. Fused transcript of abl and bcr genes in chronic myelogenous leukaemia. Nature. 1985;315(6020):550-4.
- 14. Matlashewski G, Lamb P, Pim D, Peacock J, Crawford L, Benchimol S. Isolation and characterization of a human p53 cDNA clone: expression of the human p53 gene. EMBO J. 1984;3(13):3257-62.
- 15. Hanahan D, Weinberg RA. The hallmarks of cancer. Cell. 2000;100(1):57-70.

- 16. Jones RG, Thompson CB. Tumor suppressors and cell metabolism: a recipe for cancer growth. Genes Dev. 2009;23(5):537-48.
- 17. McGuirk S, Audet-Delage Y, St-Pierre J. Metabolic Fitness and Plasticity in Cancer Progression. Trends Cancer. 2020;6(1):49-61.
- 18. Warburg O. The Metabolism of Carcinoma Cells. The Journal of Cancer Research. 1925;9(1):148.
- 19. Racker E. Bioenergetics and the problem of tumor growth: an understanding of the mechanism of the generation and control of biological energy may shed light on the problem of tumor growth. American scientist. 1972;60(1):56-63.
- 20. Warburg O. On the origin of cancer cells. Science. 1956;123(3191):309-14.
- 21. Wang T, Marquardt C, Foker J. Aerobic glycolysis during lymphocyte proliferation. Nature. 1976;261(5562):702-5.
- 22. Brand K. Glutamine and glucose metabolism during thymocyte proliferation. Pathways of glutamine and glutamate metabolism. Biochem J. 1985;228(2):353-61.
- 23. Weinhouse S. The Warburg hypothesis fifty years later. Z Krebsforsch Klin Onkol Cancer Res Clin Oncol. 1976;87(2):115-26.
- 24. Magda D, Lecane P, Prescott J, Thiemann P, Ma X, Dranchak PK, et al. mtDNA depletion confers specific gene expression profiles in human cells grown in culture and in xenograft. BMC Genomics. 2008;9:521.
- 25. Cavalli LR, Varella-Garcia M, Liang BC. Diminished tumorigenic phenotype after depletion of mitochondrial DNA. Cell Growth Differ. 1997;8(11):1189-98.
- 26. Wallace DC. Mitochondria and cancer. Nat Rev Cancer. 2012;12(10):685-98.

- 27. Whitaker-Menezes D, Martinez-Outschoorn UE, Flomenberg N, Birbe RC, Witkiewicz AK, Howell A, et al. Hyperactivation of oxidative mitochondrial metabolism in epithelial cancer cells in situ: visualizing the therapeutic effects of metformin in tumor tissue. Cell Cycle. 2011;10(23):4047-64.
- 28. Villa AM, Doglia SM. Mitochondria in tumor cells studied by laser scanning confocal microscopy. J Biomed Opt. 2004;9(2):385-94.
- 29. Pollak M. Targeting oxidative phosphorylation: why, when, and how. Cancer Cell. 2013;23(3):263-4.
- 30. Reitzer LJ, Wice BM, Kennell D. Evidence that glutamine, not sugar, is the major energy source for cultured HeLa cells. J Biol Chem. 1979;254(8):2669-76.
- 31. Rodríguez-Enríquez S, Vital-González PA, Flores-Rodríguez FL, Marín-Hernández A, Ruiz-Azuara L, Moreno-Sánchez R. Control of cellular proliferation by modulation of oxidative phosphorylation in human and rodent fast-growing tumor cells. Toxicol Appl Pharmacol. 2006;215(2):208-17.
- 32. Kumar PR, Moore JA, Bowles KM, Rushworth SA, Moncrieff MD. Mitochondrial oxidative phosphorylation in cutaneous melanoma. British Journal of Cancer. 2021;124(1):115-23.
- 33. Jitschin R, Hofmann AD, Bruns H, Giessl A, Bricks J, Berger J, et al. Mitochondrial metabolism contributes to oxidative stress and reveals therapeutic targets in chronic lymphocytic leukemia. Blood. 2014;123(17):2663-72.
- 34. Rossignol R, Gilkerson R, Aggeler R, Yamagata K, Remington SJ, Capaldi RA. Energy substrate modulates mitochondrial structure and oxidative capacity in cancer cells. Cancer Res. 2004;64(3):985-93.

- 35. Mashimo T, Pichumani K, Vemireddy V, Hatanpaa KJ, Singh DK, Sirasanagandla S, et al. Acetate is a bioenergetic substrate for human glioblastoma and brain metastases. Cell. 2014;159(7):1603-14.
- 36. Kennedy KM, Scarbrough PM, Ribeiro A, Richardson R, Yuan H, Sonveaux P, et al. Catabolism of exogenous lactate reveals it as a legitimate metabolic substrate in breast cancer. PLoS One. 2013;8(9):e75154.
- 37. Osthus RC, Shim H, Kim S, Li Q, Reddy R, Mukherjee M, et al. Deregulation of glucose transporter 1 and glycolytic gene expression by c-Myc. J Biol Chem. 2000;275(29):21797-800.
- 38. Kim JW, Gao P, Liu YC, Semenza GL, Dang CV. Hypoxia-inducible factor 1 and dysregulated c-Myc cooperatively induce vascular endothelial growth factor and metabolic switches hexokinase 2 and pyruvate dehydrogenase kinase 1. Mol Cell Biol. 2007;27(21):7381-93.
- 39. DeBerardinis RJ, Mancuso A, Daikhin E, Nissim I, Yudkoff M, Wehrli S, et al. Beyond aerobic glycolysis: transformed cells can engage in glutamine metabolism that exceeds the requirement for protein and nucleotide synthesis. Proc Natl Acad Sci U S A. 2007;104(49):19345-50.
- 40. Li F, Wang Y, Zeller KI, Potter JJ, Wonsey DR, O'Donnell KA, et al. Myc stimulates nuclearly encoded mitochondrial genes and mitochondrial biogenesis. Molecular and cellular biology. 2005;25(14):6225-34.
- 41. Hulea L, Gravel SP, Morita M, Cargnello M, Uchenunu O, Im YK, et al. Translational and HIF-1α-Dependent Metabolic Reprogramming Underpin Metabolic Plasticity and Responses to Kinase Inhibitors and Biguanides. Cell Metab. 2018;28(6):817-32.e8.

- 42. Menendez JA, Lupu R. Fatty acid synthase and the lipogenic phenotype in cancer pathogenesis. Nat Rev Cancer. 2007;7(10):763-77.
- 43. Vander Heiden MG, Cantley LC, Thompson CB. Understanding the Warburg effect: the metabolic requirements of cell proliferation. Science. 2009;324(5930):1029-33.
- 44. Locasale JW, Cantley LC. Metabolic flux and the regulation of mammalian cell growth. Cell Metab. 2011;14(4):443-51.
- 45. Shestov AA, Liu X, Ser Z, Cluntun AA, Hung YP, Huang L, et al. Quantitative determinants of aerobic glycolysis identify flux through the enzyme GAPDH as a limiting step. Elife. 2014;3.
- 46. DeBerardinis RJ, Lum JJ, Hatzivassiliou G, Thompson CB. The biology of cancer: metabolic reprogramming fuels cell growth and proliferation. Cell Metab. 2008;7(1):11-20.
- 47. Jin L, Zhou Y. Crucial role of the pentose phosphate pathway in malignant tumors (Review). Oncol Lett. 2019;17(5):4213-21.
- 48. Lehninger AL, Nelson, D. L., & Cox, M. M. Lehninger principles of biochemistry. New York: Worth Publishers; 2000; 1-1158.
- 49. Rui L. Energy metabolism in the liver. Compr Physiol. 2014;4(1):177-97.
- 50. Palm W, Thompson CB. Nutrient acquisition strategies of mammalian cells. Nature. 2017;546(7657):234-42.
- 51. Joost HG, Thorens B. The extended GLUT-family of sugar/polyol transport facilitators: nomenclature, sequence characteristics, and potential function of its novel members (review). Mol Membr Biol. 2001;18(4):247-56.
- 52. Wright EM. Renal Na(+)-glucose cotransporters. Am J Physiol Renal Physiol. 2001;280(1):F10-8.

- 53. Mueckler M, Thorens B. The SLC2 (GLUT) family of membrane transporters. Molecular aspects of medicine. 2013;34(2-3):121-38.
- 54. Mueckler M, Caruso C, Baldwin SA, Panico M, Blench I, Morris HR, et al. Sequence and structure of a human glucose transporter. Science. 1985;229(4717):941-5.
- 55. Fukumoto H, Seino S, Imura H, Seino Y, Eddy RL, Fukushima Y, et al. Sequence, tissue distribution, and chromosomal localization of mRNA encoding a human glucose transporter-like protein. Proceedings of the National Academy of Sciences of the United States of America. 1988;85(15):5434-8.
- 56. Gould GW, Thomas HM, Jess TJ, Bell GI. Expression of human glucose transporters in Xenopus oocytes: kinetic characterization and substrate specificities of the erythrocyte, liver, and brain isoforms. Biochemistry. 1991;30(21):5139-45.
- 57. Fukumoto H, Kayano T, Buse JB, Edwards Y, Pilch PF, Bell GI, et al. Cloning and characterization of the major insulin-responsive glucose transporter expressed in human skeletal muscle and other insulin-responsive tissues. J Biol Chem. 1989;264(14):7776-9.
- 58. Koepsell H. Glucose transporters in brain in health and disease. Pflugers Arch. 2020;472(9):1299-343.
- 59. James DE, Strube M, Mueckler M. Molecular cloning and characterization of an insulinregulatable glucose transporter. Nature. 1989;338(6210):83-7.
- 60. Adekola K, Rosen ST, Shanmugam M. Glucose transporters in cancer metabolism. Curr Opin Oncol. 2012;24(6):650-4.
- 61. Leto D, Saltiel AR. Regulation of glucose transport by insulin: traffic control of GLUT4. Nature Reviews Molecular Cell Biology. 2012;13(6):383-96.

- 62. Barthel A, Okino ST, Liao J, Nakatani K, Li J, Whitlock JP, Jr., et al. Regulation of GLUT1 gene transcription by the serine/threonine kinase Akt1. J Biol Chem. 1999;274(29):20281-6.
- 63. Thompson CB. Rethinking the regulation of cellular metabolism. Cold Spring Harb Symp Quant Biol. 2011;76:23-9.
- 64. Liberti MV, Locasale JW. The Warburg Effect: How Does it Benefit Cancer Cells? Trends in Biochemical Sciences. 2016;41(3):211-8.
- 65. Vaupel P, Harrison L. Tumor hypoxia: causative factors, compensatory mechanisms, and cellular response. Oncologist. 2004;9 Suppl 5:4-9.
- 66. Vaupel P, Thews O, Hoeckel M. Treatment resistance of solid tumors: role of hypoxia and anemia. Med Oncol. 2001;18(4):243-59.
- 67. Siemann DW, Horsman MR. Modulation of the tumor vasculature and oxygenation to improve therapy. Pharmacol Ther. 2015;153:107-24.
- 68. Gouirand V, Guillaumond F, Vasseur S. Influence of the Tumor Microenvironment on Cancer Cells Metabolic Reprogramming. Front Oncol. 2018;8:117.
- 69. Jun YJ, Jang SM, Han HL, Lee KH, Jang KS, Paik SS. Clinicopathologic significance of GLUT1 expression and its correlation with Apaf-1 in colorectal adenocarcinomas. World J Gastroenterol. 2011;17(14):1866-73.
- 70. Luo XM, Zhou SH, Fan J. Glucose transporter-1 as a new therapeutic target in laryngeal carcinoma. J Int Med Res. 2010;38(6):1885-92.
- 71. Grabellus F, Nagarajah J, Bockisch A, Schmid KW, Sheu SY. Glucose transporter 1 expression, tumor proliferation, and iodine/glucose uptake in thyroid cancer with emphasis on poorly differentiated thyroid carcinoma. Clin Nucl Med. 2012;37(2):121-7.

- 72. Flavahan WA, Wu Q, Hitomi M, Rahim N, Kim Y, Sloan AE, et al. Brain tumor initiating cells adapt to restricted nutrition through preferential glucose uptake. Nat Neurosci. 2013;16(10):1373-82.
- 73. Han AL, Veeneman BA, El-Sawy L, Day KC, Day ML, Tomlins SA, et al. Fibulin-3 promotes muscle-invasive bladder cancer. Oncogene. 2017;36(37):5243-51.
- 74. Armoni M, Quon MJ, Maor G, Avigad S, Shapiro DN, Harel C, et al. PAX3/forkhead homolog in rhabdomyosarcoma oncoprotein activates glucose transporter 4 gene expression in vivo and in vitro. J Clin Endocrinol Metab. 2002;87(11):5312-24.
- 75. Ganapathy V, Thangaraju M, Prasad PD. Nutrient transporters in cancer: relevance to Warburg hypothesis and beyond. Pharmacol Ther. 2009;121(1):29-40.
- 76. Ishikawa N, Oguri T, Isobe T, Fujitaka K, Kohno N. SGLT gene expression in primary lung cancers and their metastatic lesions. Jpn J Cancer Res. 2001;92(8):874-9.
- 77. Aleshin AE, Zeng C, Bourenkov GP, Bartunik HD, Fromm HJ, Honzatko RB. The mechanism of regulation of hexokinase: new insights from the crystal structure of recombinant human brain hexokinase complexed with glucose and glucose-6-phosphate. Structure. 1998;6(1):39-50.
- 78. Wilson JE. Isozymes of mammalian hexokinase: structure, subcellular localization and metabolic function. Journal of Experimental Biology. 2003;206(12):2049-57.
- 79. Kemp RG, Foe LG. Allosteric regulatory properties of muscle phosphofructokinase. Mol Cell Biochem. 1983;57(2):147-54.
- 80. Lincet H, Icard P. How do glycolytic enzymes favour cancer cell proliferation by nonmetabolic functions? Oncogene. 2015;34(29):3751-9.

- 81. Pedersen PL, Mathupala S, Rempel A, Geschwind JF, Ko YH. Mitochondrial bound type II hexokinase: a key player in the growth and survival of many cancers and an ideal prospect for therapeutic intervention. Biochim Biophys Acta. 2002;1555(1-3):14-20.
- 82. Palmieri D, Fitzgerald D, Shreeve SM, Hua E, Bronder JL, Weil RJ, et al. Analyses of resected human brain metastases of breast cancer reveal the association between up-regulation of hexokinase 2 and poor prognosis. Mol Cancer Res. 2009;7(9):1438-45.
- 83. Patra KC, Wang Q, Bhaskar PT, Miller L, Wang Z, Wheaton W, et al. Hexokinase 2 is required for tumor initiation and maintenance and its systemic deletion is therapeutic in mouse models of cancer. Cancer Cell. 2013;24(2):213-28.
- 84. Ahmad A, Aboukameel A, Kong D, Wang Z, Sethi S, Chen W, et al. Phosphoglucose isomerase/autocrine motility factor mediates epithelial-mesenchymal transition regulated by miR-200 in breast cancer cells. Cancer Res. 2011;71(9):3400-9.
- 85. Bando H, Atsumi T, Nishio T, Niwa H, Mishima S, Shimizu C, et al. Phosphorylation of the 6-phosphofructo-2-kinase/fructose 2,6-bisphosphatase/PFKFB3 family of glycolytic regulators in human cancer. Clin Cancer Res. 2005;11(16):5784-92.
- 86. Minchenko OH, Ogura T, Opentanova IL, Minchenko DO, Ochiai A, Caro J, et al. 6-Phosphofructo-2-kinase/fructose-2,6-bisphosphatase gene family overexpression in human lung tumor. Ukr Biokhim Zh (1999). 2005;77(6):46-50.
- 87. Tang Z, Yuan S, Hu Y, Zhang H, Wu W, Zeng Z, et al. Over-expression of GAPDH in human colorectal carcinoma as a preferred target of 3-bromopyruvate propyl ester. J Bioenerg Biomembr. 2012;44(1):117-25.
- 88. Mikuriya K, Kuramitsu Y, Ryozawa S, Fujimoto M, Mori S, Oka M, et al. Expression of glycolytic enzymes is increased in pancreatic cancerous tissues as evidenced by proteomic

- profiling by two-dimensional electrophoresis and liquid chromatography-mass spectrometry/mass spectrometry. Int J Oncol. 2007;30(4):849-55.
- 89. Guo C, Liu S, Sun MZ. Novel insight into the role of GAPDH playing in tumor. Clin Transl Oncol. 2013;15(3):167-72.
- 90. Colell A, Green DR, Ricci JE. Novel roles for GAPDH in cell death and carcinogenesis. Cell Death Differ. 2009;16(12):1573-81.
- 91. Du S, Guan Z, Hao L, Song Y, Wang L, Gong L, et al. Fructose-bisphosphate aldolase a is a potential metastasis-associated marker of lung squamous cell carcinoma and promotes lung cell tumorigenesis and migration. PLoS One. 2014;9(1):e85804.
- 92. Hwang TL, Liang Y, Chien KY, Yu JS. Overexpression and elevated serum levels of phosphoglycerate kinase 1 in pancreatic ductal adenocarcinoma. Proteomics. 2006;6(7):2259-72.
- 93. Zieker D, Königsrainer I, Weinreich J, Beckert S, Glatzle J, Nieselt K, et al. Phosphoglycerate kinase 1 promoting tumor progression and metastasis in gastric cancer detected in a tumor mouse model using positron emission tomography/magnetic resonance imaging. Cell Physiol Biochem. 2010;26(2):147-54.
- 94. Takenaka M, Yamada K, Lu T, Kang R, Tanaka T, Noguchi T. Alternative splicing of the pyruvate kinase M gene in a minigene system. Eur J Biochem. 1996;235(1-2):366-71.
- 95. Dayton TL, Jacks T, Vander Heiden MG. PKM2, cancer metabolism, and the road ahead. EMBO Rep. 2016;17(12):1721-30.
- 96. Noguchi T, Inoue H, Tanaka T. The M1- and M2-type isozymes of rat pyruvate kinase are produced from the same gene by alternative RNA splicing. J Biol Chem. 1986;261(29):13807-12.

- 97. Chaneton B, Hillmann P, Zheng L, Martin ACL, Maddocks ODK, Chokkathukalam A, et al. Serine is a natural ligand and allosteric activator of pyruvate kinase M2. Nature. 2012;491(7424):458-62.
- 98. Christofk HR, Vander Heiden MG, Wu N, Asara JM, Cantley LC. Pyruvate kinase M2 is a phosphotyrosine-binding protein. Nature. 2008;452(7184):181-6.
- 99. Keller KE, Tan IS, Lee YS. SAICAR stimulates pyruvate kinase isoform M2 and promotes cancer cell survival in glucose-limited conditions. Science. 2012;338(6110):1069-72.
- 100. Tran Q, Lee H, Park J, Kim SH, Park J. Targeting Cancer Metabolism Revisiting the Warburg Effects. Toxicol Res. 2016;32(3):177-93.
- 101. Wiese EK, Hitosugi T. Tyrosine Kinase Signaling in Cancer Metabolism: PKM2 Paradox in the Warburg Effect. Front Cell Dev Biol. 2018;6:79.
- 102. Christofk HR, Vander Heiden MG, Harris MH, Ramanathan A, Gerszten RE, Wei R, et al. The M2 splice isoform of pyruvate kinase is important for cancer metabolism and tumour growth. Nature. 2008;452(7184):230-3.
- 103. Hitosugi T, Kang S, Vander Heiden MG, Chung TW, Elf S, Lythgoe K, et al. Tyrosine phosphorylation inhibits PKM2 to promote the Warburg effect and tumor growth. Sci Signal. 2009;2(97):ra73.
- 104. Lv L, Li D, Zhao D, Lin R, Chu Y, Zhang H, et al. Acetylation targets the M2 isoform of pyruvate kinase for degradation through chaperone-mediated autophagy and promotes tumor growth. Mol Cell. 2011;42(6):719-30.
- 105. Anastasiou D, Poulogiannis G, Asara JM, Boxer MB, Jiang JK, Shen M, et al. Inhibition of pyruvate kinase M2 by reactive oxygen species contributes to cellular antioxidant responses. Science. 2011;334(6060):1278-83.

- 106. Kierans SJ, Taylor CT. Regulation of glycolysis by the hypoxia-inducible factor (HIF): implications for cellular physiology. J Physiol. 2021;599(1):23-37.
- 107. Halestrap AP. Monocarboxylic acid transport. Compr Physiol. 2013;3(4):1611-43.
- 108. Feron O. Pyruvate into lactate and back: from the Warburg effect to symbiotic energy fuel exchange in cancer cells. Radiother Oncol. 2009;92(3):329-33.
- 109. Cahn RD, Zwilling E, Kaplan NO, Levine L. Nature and Development of Lactic Dehydrogenases: The two major types of this enzyme form molecular hybrids which change in makeup during development. Science. 1962;136(3520):962-9.
- 110. Dawson DM, Goodfriend TL, Kaplan NO. Lactic dehydrogenases: Functions of the two types rates of synthesis of the two major forms can be correlated with metabolic differentiation. Science. 1964;143(3609):929-33.
- 111. Read JA, Winter VJ, Eszes CM, Sessions RB, Brady RL. Structural basis for altered activity of M- and H-isozyme forms of human lactate dehydrogenase. Proteins. 2001;43(2):175-85.
- 112. Goldman RD, Kaplan NO, Hall TC. Lactic dehydrogenases in human neoplastic tissues. Cancer Res. 1964;24:389-99.
- 113. He TL, Zhang YJ, Jiang H, Li XH, Zhu H, Zheng KL. The c-Myc-LDHA axis positively regulates aerobic glycolysis and promotes tumor progression in pancreatic cancer. Med Oncol. 2015;32(7):187.
- 114. Koukourakis MI, Giatromanolaki A, Sivridis E, Bougioukas G, Didilis V, Gatter KC, et al. Lactate dehydrogenase-5 (LDH-5) overexpression in non-small-cell lung cancer tissues is linked to tumour hypoxia, angiogenic factor production and poor prognosis. British journal of cancer. 2003;89(5):877-85.

- 115. Feng Y, Xiong Y, Qiao T, Li X, Jia L, Han Y. Lactate dehydrogenase A: A key player in carcinogenesis and potential target in cancer therapy. Cancer Med. 2018;7(12):6124-36.
- 116. Sheng SL, Liu JJ, Dai YH, Sun XG, Xiong XP, Huang G. Knockdown of lactate dehydrogenase A suppresses tumor growth and metastasis of human hepatocellular carcinoma. Febs j. 2012;279(20):3898-910.
- 117. Koukourakis MI, Giatromanolaki A, Sivridis E, Gatter KC, Harris AL. Lactate dehydrogenase 5 expression in operable colorectal cancer: strong association with survival and activated vascular endothelial growth factor pathway--a report of the Tumour Angiogenesis Research Group. J Clin Oncol. 2006;24(26):4301-8.
- 118. Yao F, Zhao T, Zhong C, Zhu J, Zhao H. LDHA is necessary for the tumorigenicity of esophageal squamous cell carcinoma. Tumour Biol. 2013;34(1):25-31.
- 119. Miao P, Sheng S, Sun X, Liu J, Huang G. Lactate dehydrogenase A in cancer: a promising target for diagnosis and therapy. IUBMB Life. 2013;65(11):904-10.
- 120. McCleland ML, Adler AS, Shang Y, Hunsaker T, Truong T, Peterson D, et al. An integrated genomic screen identifies LDHB as an essential gene for triple-negative breast cancer. Cancer Res. 2012;72(22):5812-23.
- 121. McCleland ML, Adler AS, Deming L, Cosino E, Lee L, Blackwood EM, et al. Lactate dehydrogenase B is required for the growth of KRAS-dependent lung adenocarcinomas. Clin Cancer Res. 2013;19(4):773-84.
- 122. Chen R, Zhou X, Yu Z, Liu J, Huang G. Low Expression of LDHB Correlates With Unfavorable Survival in Hepatocellular Carcinoma: Strobe-Compliant Article. Medicine (Baltimore). 2015;94(39):e1583.

- 123. Bonuccelli G, Tsirigos A, Whitaker-Menezes D, Pavlides S, Pestell RG, Chiavarina B, et al. Ketones and lactate "fuel" tumor growth and metastasis: Evidence that epithelial cancer cells use oxidative mitochondrial metabolism. Cell Cycle. 2010;9(17):3506-14.
- 124. Pavlides S, Whitaker-Menezes D, Castello-Cros R, Flomenberg N, Witkiewicz AK, Frank PG, et al. The reverse Warburg effect: aerobic glycolysis in cancer associated fibroblasts and the tumor stroma. Cell Cycle. 2009;8(23):3984-4001.
- 125. Sonveaux P, Végran F, Schroeder T, Wergin MC, Verrax J, Rabbani ZN, et al. Targeting lactate-fueled respiration selectively kills hypoxic tumor cells in mice. J Clin Invest. 2008;118(12):3930-42.
- 126. Ruiz-Iglesias A, Mañes S. The Importance of Mitochondrial Pyruvate Carrier in Cancer Cell Metabolism and Tumorigenesis. Cancers (Basel). 2021;13(7):1488.
- 127. Waterhouse C, Keilson J. Cori cycle activity in man. The Journal of clinical investigation. 1969;48(12):2359-66.
- 128. Draoui N, Feron O. Lactate shuttles at a glance: from physiological paradigms to anticancer treatments. Dis Model Mech. 2011;4(6):727-32.
- 129. Holroyde CP, Gabuzda TG, Putnam RC, Paul P, Reichard GA. Altered Glucose Metabolism in Metastatic Carcinoma. Cancer Research. 1975;35(12):3710-4.
- 130. Prochownik EV, Wang H. The Metabolic Fates of Pyruvate in Normal and Neoplastic Cells. Cells. 2021;10(4):762.
- 131. McCommis KS, Finck BN. Mitochondrial pyruvate transport: a historical perspective and future research directions. The Biochemical journal. 2015;466(3):443-54.
- 132. Reed LJ, Hackert ML. Structure-function relationships in dihydrolipoamide acyltransferases. J Biol Chem. 1990;265(16):8971-4.

- 133. Koike M, Reed LJ, Carroll WR. alpha-Keto acid dehydrogenation complexes. IV. Resolution and reconstitution of the Escherichia coli pyruvate dehydrogenation complex. J Biol Chem. 1963;238:30-9.
- 134. Strumiło S. Short-term regulation of the mammalian pyruvate dehydrogenase complex. Acta Biochim Pol. 2005;52(4):759-64.
- 135. Sugden MC, Holness MJ. Interactive regulation of the pyruvate dehydrogenase complex and the carnitine palmitoyltransferase system. Faseb j. 1994;8(1):54-61.
- 136. Gudi R, Bowker-Kinley MM, Kedishvili NY, Zhao Y, Popov KM. Diversity of the pyruvate dehydrogenase kinase gene family in humans. J Biol Chem. 1995;270(48):28989-94.
- 137. Bradshaw PC. Acetyl-CoA Metabolism and Histone Acetylation in the Regulation of Aging and Lifespan. Antioxidants (Basel). 2021;10(4):572.
- 138. Lee JV, Carrer A, Shah S, Snyder NW, Wei S, Venneti S, et al. Akt-dependent metabolic reprogramming regulates tumor cell histone acetylation. Cell Metab. 2014;20(2):306-19.
- 139. McDonnell E, Crown SB, Fox DB, Kitir B, Ilkayeva OR, Olsen CA, et al. Lipids Reprogram Metabolism to Become a Major Carbon Source for Histone Acetylation. Cell Rep. 2016;17(6):1463-72.
- 140. Martínez-Reyes I, Diebold Lauren P, Kong H, Schieber M, Huang H, Hensley Christopher T, et al. TCA Cycle and Mitochondrial Membrane Potential Are Necessary for Diverse Biological Functions. Molecular Cell. 2016;61(2):199-209.
- 141. Schell JC, Olson KA, Jiang L, Hawkins AJ, Van Vranken JG, Xie J, et al. A role for the mitochondrial pyruvate carrier as a repressor of the Warburg effect and colon cancer cell growth. Molecular cell. 2014;56(3):400-13.

- 142. Cai H, Kumar N, Ai N, Gupta S, Rath P, Baudis M. Progenetix: 12 years of oncogenomic data curation. Nucleic Acids Res. 2014;42(Database issue):D1055-62.
- 143. Shan C, Kang H-B, Elf S, Xie J, Gu T-L, Aguiar M, et al. Tyr-94 phosphorylation inhibits pyruvate dehydrogenase phosphatase 1 and promotes tumor growth. The Journal of biological chemistry. 2014;289(31):21413-22.
- 144. Stacpoole PW. Therapeutic Targeting of the Pyruvate Dehydrogenase Complex/Pyruvate Dehydrogenase Kinase (PDC/PDK) Axis in Cancer. J Natl Cancer Inst. 2017;109(11).
- 145. Woolbright BL, Rajendran G, Harris RA, Taylor JA. Metabolic Flexibility in Cancer: Targeting the Pyruvate Dehydrogenase Kinase:Pyruvate Dehydrogenase Axis. Molecular Cancer Therapeutics. 2019;18(10):1673.
- 146. McFate T, Mohyeldin A, Lu H, Thakar J, Henriques J, Halim ND, et al. Pyruvate dehydrogenase complex activity controls metabolic and malignant phenotype in cancer cells. The Journal of biological chemistry. 2008;283(33):22700-8.
- 147. Leclerc D, Pham DNT, Lévesque N, Truongcao M, Foulkes WD, Sapienza C, et al. Oncogenic role of PDK4 in human colon cancer cells. British journal of cancer. 2017;116(7):930-6.
- 148. Martínez-Reyes I, Chandel NS. Mitochondrial TCA cycle metabolites control physiology and disease. Nature Communications. 2020;11(1):102.
- 149. Wiegand G, Remington SJ. Citrate synthase: structure, control, and mechanism. Annu Rev Biophys Biophys Chem. 1986;15:97-117.
- 150. Smith CM, Williamson JR. Inhibition of citrate synthase by succinyl-CoA and other metabolites. FEBS Lett. 1971;18(1):35-8.

- 151. Eniafe J, Jiang S. The functional roles of TCA cycle metabolites in cancer. Oncogene. 2021;40(19):3351-63.
- 152. Taylor WM, Halperin ML. Regulation of pyruvate dehydrogenase in muscle. Inhibition by citrate. J Biol Chem. 1973;248(17):6080-3.
- 153. Hillar M, Lott V, Lennox B. Correlation of the effects of citric acid cycle metabolites on succinate oxidation by rat liver mitochondria and submitochondrial particles. J Bioenerg. 1975;7(1):1-16.
- 154. Chen L, Liu T, Zhou J, Wang Y, Wang X, Di W, et al. Citrate synthase expression affects tumor phenotype and drug resistance in human ovarian carcinoma. PloS one. 2014;9(12):e115708-e.
- 155. Lin C-C, Cheng T-L, Tsai W-H, Tsai H-J, Hu K-H, Chang H-C, et al. Loss of the respiratory enzyme citrate synthase directly links the Warburg effect to tumor malignancy. Sci Rep. 2012;2:785-.
- 156. Haferkamp S, Drexler K, Federlin M, Schlitt HJ, Berneburg M, Adamski J, et al. Extracellular Citrate Fuels Cancer Cell Metabolism and Growth. Frontiers in Cell and Developmental Biology. 2020;8(1518).
- 157. Costello LC, Franklin RB, Narayan P. Citrate in the diagnosis of prostate cancer. Prostate. 1999;38(3):237-45.
- 158. Pechter KB, Meyer FM, Serio AW, Stülke J, Sonenshein AL. Two roles for aconitase in the regulation of tricarboxylic acid branch gene expression in Bacillus subtilis. J Bacteriol. 2013;195(7):1525-37.

- 159. Costello LC, Liu Y, Franklin RB, Kennedy MC. Zinc inhibition of mitochondrial aconitase and its importance in citrate metabolism of prostate epithelial cells. J Biol Chem. 1997;272(46):28875-81.
- 160. Franklin RB, Feng P, Milon B, Desouki MM, Singh KK, Kajdacsy-Balla A, et al. hZIP1 zinc uptake transporter down regulation and zinc depletion in prostate cancer. Mol Cancer. 2005;4:32.
- 161. Gonick P, Oberleas D, Knechtges T, Prasad AS. Atomic absorption spectrophotometric determination of zinc in the prostate. Invest Urol. 1969;6(4):345-7.
- 162. Habib FK, Mason MK, Smith PH, Stitch SR. Cancer of the prostate: early diagnosis by zinc and hormone analysis? Br J Cancer. 1979;39(6):700-4.
- 163. Singh KK, Desouki MM, Franklin RB, Costello LC. Mitochondrial aconitase and citrate metabolism in malignant and nonmalignant human prostate tissues. Molecular cancer. 2006;5:14-
- 164. Scagliola A, Mainini F, Cardaci S. The Tricarboxylic Acid Cycle at the Crossroad Between Cancer and Immunity. Antioxidants & Redox Signaling. 2019;32(12):834-52.
- 165. Bell JL, Baron DN. Subcellular distribution of the isoenzymes of NADP isocitrate dehydrogenase in rat liver and heart. Enzymol Biol Clin (Basel). 1968;9(5):393-9.
- 166. Dalziel K, Londesborough JC. The mechanisms of reductive carboxylation reactions. Carbon dioxide or bicarbonate as substrate of nicotinamide-adenine dinucleotide phosphate-linked isocitrate dehydrogenase and malic enzyme. Biochem J. 1968;110(2):223-30.
- 167. Narahara K, Kimura S, Kikkawa K, Takahashi Y, Wakita Y, Kasai R, et al. Probable assignment of soluble isocitrate dehydrogenase (IDH1) to 2q33.3. Hum Genet. 1985;71(1):37-40.

- 168. Xu X, Zhao J, Xu Z, Peng B, Huang Q, Arnold E, et al. Structures of human cytosolic NADP-dependent isocitrate dehydrogenase reveal a novel self-regulatory mechanism of activity. J Biol Chem. 2004;279(32):33946-57.
- 169. Jo SH, Lee SH, Chun HS, Lee SM, Koh HJ, Lee SE, et al. Cellular defense against UVB-induced phototoxicity by cytosolic NADP(+)-dependent isocitrate dehydrogenase. Biochem Biophys Res Commun. 2002;292(2):542-9.
- 170. Hausinger RP. FeII/alpha-ketoglutarate-dependent hydroxylases and related enzymes. Crit Rev Biochem Mol Biol. 2004;39(1):21-68.
- 171. Lee SH, Jo SH, Lee SM, Koh HJ, Song H, Park JW, et al. Role of NADP+-dependent isocitrate dehydrogenase (NADP+-ICDH) on cellular defence against oxidative injury by gammarays. Int J Radiat Biol. 2004;80(9):635-42.
- 172. Shechter I, Dai P, Huo L, Guan G. IDH1 gene transcription is sterol regulated and activated by SREBP-1a and SREBP-2 in human hepatoma HepG2 cells: evidence that IDH1 may regulate lipogenesis in hepatic cells. J Lipid Res. 2003;44(11):2169-80.
- 173. Koh HJ, Lee SM, Son BG, Lee SH, Ryoo ZY, Chang KT, et al. Cytosolic NADP+-dependent isocitrate dehydrogenase plays a key role in lipid metabolism. J Biol Chem. 2004;279(38):39968-74.
- 174. Ramachandran N, Colman RF. Chemical characterization of distinct subunits of pig heart DPN-specific isocitrate dehydrogenase. J Biol Chem. 1980;255(18):8859-64.
- 175. Stoddard BL, Dean A, Koshland DE, Jr. Structure of isocitrate dehydrogenase with isocitrate, nicotinamide adenine dinucleotide phosphate, and calcium at 2.5-A resolution: a pseudo-Michaelis ternary complex. Biochemistry. 1993;32(36):9310-6.

- 176. Gabriel JL, Zervos PR, Plaut GW. Activity of purified NAD-specific isocitrate dehydrogenase at modulator and substrate concentrations approximating conditions in mitochondria. Metabolism. 1986;35(7):661-7.
- 177. Aogaichi T, Evans J, Gabriel J, Plaut GW. The effects of calcium and lanthanide ions on the activity of bovine heart nicotinamide adenine dinucleotide-specific isocitrate dehydrogenase. Arch Biochem Biophys. 1980;204(1):350-6.
- 178. Kim YO, Koh HJ, Kim SH, Jo SH, Huh JW, Jeong KS, et al. Identification and functional characterization of a novel, tissue-specific NAD(+)-dependent isocitrate dehydrogenase beta subunit isoform. J Biol Chem. 1999;274(52):36866-75.
- 179. Wise DR, Ward PS, Shay JE, Cross JR, Gruber JJ, Sachdeva UM, et al. Hypoxia promotes isocitrate dehydrogenase-dependent carboxylation of α-ketoglutarate to citrate to support cell growth and viability. Proc Natl Acad Sci U S A. 2011;108(49):19611-6.
- 180. Mullen AR, Wheaton WW, Jin ES, Chen PH, Sullivan LB, Cheng T, et al. Reductive carboxylation supports growth in tumour cells with defective mitochondria. Nature. 2011;481(7381):385-8.
- 181. Tran AN, Lai A, Li S, Pope WB, Teixeira S, Harris RJ, et al. Increased sensitivity to radiochemotherapy in IDH1 mutant glioblastoma as demonstrated by serial quantitative MR volumetry. Neuro Oncol. 2014;16(3):414-20.
- 182. Itsumi M, Inoue S, Elia AJ, Murakami K, Sasaki M, Lind EF, et al. Idh1 protects murine hepatocytes from endotoxin-induced oxidative stress by regulating the intracellular NADP(+)/NADPH ratio. Cell Death Differ. 2015;22(11):1837-45.
- 183. Panieri E, Santoro MM. ROS homeostasis and metabolism: a dangerous liason in cancer cells. Cell Death & Disease. 2016;7(6):e2253-e.

- 184. Carracedo A, Cantley LC, Pandolfi PP. Cancer metabolism: fatty acid oxidation in the limelight. Nat Rev Cancer. 2013;13(4):227-32.
- 185. May JL, Kouri FM, Hurley LA, Liu J, Tommasini-Ghelfi S, Ji Y, et al. IDH3α regulates one-carbon metabolism in glioblastoma. Sci Adv. 2019;5(1):eaat0456.
- 186. Zeng L, Morinibu A, Kobayashi M, Zhu Y, Wang X, Goto Y, et al. Aberrant IDH3α expression promotes malignant tumor growth by inducing HIF-1-mediated metabolic reprogramming and angiogenesis. Oncogene. 2015;34(36):4758-66.
- 187. Zhang D, Wang Y, Shi Z, Liu J, Sun P, Hou X, et al. Metabolic Reprogramming of Cancer-Associated Fibroblasts by IDH3α Downregulation. Cell Reports. 2015;10(8):1335-48.
- 188. Tretter L, Adam-Vizi V. Alpha-ketoglutarate dehydrogenase: a target and generator of oxidative stress. Philos Trans R Soc Lond B Biol Sci. 2005;360(1464):2335-45.
- 189. Garland PB. Some kinetic properties of pig-heart oxoglutarate dehydrogenase that provide a basis for metabolic control of the enzyme activity and also a stoicheiometric assay for coenzyme A in tissue extracts. Biochem J. 1964;92(2):10c-2c.
- 190. Smith CM, Bryla J, Williamson JR. Regulation of mitochondrial alpha-ketoglutarate metabolism by product inhibition at alpha-ketoglutarate dehydrogenase. J Biol Chem. 1974;249(5):1497-505.
- 191. Tommasini-Ghelfi S, Murnan K, Kouri FM, Mahajan AS, May JL, Stegh AH. Cancer-associated mutation and beyond: The emerging biology of isocitrate dehydrogenases in human disease. Science Advances. 2019;5(5):eaaw4543.
- 192. Cloos PA, Christensen J, Agger K, Helin K. Erasing the methyl mark: histone demethylases at the center of cellular differentiation and disease. Genes Dev. 2008;22(9):1115-40.

- 193. Wei Q, Qian Y, Yu J, Wong CC. Metabolic rewiring in the promotion of cancer metastasis: mechanisms and therapeutic implications. Oncogene. 2020;39(39):6139-56.
- 194. Morris JPt, Yashinskie JJ, Koche R, Chandwani R, Tian S, Chen CC, et al. α-Ketoglutarate links p53 to cell fate during tumour suppression. Nature. 2019;573(7775):595-9.
- 195. Atlante S, Visintin A, Marini E, Savoia M, Dianzani C, Giorgis M, et al. α-ketoglutarate dehydrogenase inhibition counteracts breast cancer-associated lung metastasis. Cell Death Dis. 2018;9(7):756.
- 196. Lacombe M-L, Tokarska-Schlattner M, Boissan M, Schlattner U. The mitochondrial nucleoside diphosphate kinase (NDPK-D/NME4), a moonlighting protein for cell homeostasis. Laboratory Investigation. 2018;98(5):582-8.
- 197. Krebs HA, Wiggins D. Phosphorylation of adenosine monophosphate in the mitochondrial matrix. Biochem J. 1978;174(1):297-301.
- 198. Ponka P. Tissue-specific regulation of iron metabolism and heme synthesis: distinct control mechanisms in erythroid cells. Blood. 1997;89(1):1-25.
- 199. Jiang S, Yan W. Succinate in the cancer–immune cycle. Cancer Letters. 2017;390:45-7.
- 200. Yogeeswari P, Sriram D, Vaigundaragavendran J. The GABA shunt: an attractive and potential therapeutic target in the treatment of epileptic disorders. Curr Drug Metab. 2005;6(2):127-39.
- 201. Gao Y, Chen L, Du Z, Gao W, Wu Z, Liu X, et al. Glutamate Decarboxylase 65 Signals through the Androgen Receptor to Promote Castration Resistance in Prostate Cancer. Cancer Research. 2019;79(18):4638-49.

- 202. Samborska B, Griss T, Ma EH, Jones N, Williams KS, Sergushichev A, et al. A non-canonical role for glutamate decarboxylase 1 in cancer cell amino acid homeostasis, independent of the GABA shunt. bioRxiv. 2021:2021.02.17.431489.
- 203. Rutter J, Winge DR, Schiffman JD. Succinate dehydrogenase Assembly, regulation and role in human disease. Mitochondrion. 2010;10(4):393-401.
- 204. Dalla Pozza E, Dando I, Pacchiana R, Liboi E, Scupoli MT, Donadelli M, et al. Regulation of succinate dehydrogenase and role of succinate in cancer. Semin Cell Dev Biol. 2020;98:4-14.
- 205. Akiba T, Hiraga K, Tuboi S. Intracellular distribution of fumarase in various animals. J Biochem. 1984;96(1):189-95.
- 206. King A, Selak MA, Gottlieb E. Succinate dehydrogenase and fumarate hydratase: linking mitochondrial dysfunction and cancer. Oncogene. 2006;25(34):4675-82.
- 207. Srere PA. The enzymology of the formation and breakdown of citrate. Adv Enzymol Relat Areas Mol Biol. 1975;43:57-101.
- 208. Reyes Romero A, Lunev S, Popowicz GM, Calderone V, Gentili M, Sattler M, et al. A fragment-based approach identifies an allosteric pocket that impacts malate dehydrogenase activity. Communications Biology. 2021;4(1):949.
- 209. Musrati RA, Kollárová M, Mernik N, Mikulásová D. Malate dehydrogenase: distribution, function and properties. Gen Physiol Biophys. 1998;17(3):193-210.
- 210. Minárik P, Tomásková N, Kollárová M, Antalík M. Malate dehydrogenases--structure and function. Gen Physiol Biophys. 2002;21(3):257-65.
- 211. Liu Q, Harvey CT, Geng H, Xue C, Chen V, Beer TM, et al. Malate dehydrogenase 2 confers docetaxel resistance via regulations of JNK signaling and oxidative metabolism. Prostate. 2013;73(10):1028-37.

- 212. Xu W, Yang H, Liu Y, Yang Y, Wang P, Kim S-H, et al. Oncometabolite 2-hydroxyglutarate is a competitive inhibitor of α -ketoglutarate-dependent dioxygenases. Cancer cell. 2011;19(1):17-30.
- 213. Zhao S, Lin Y, Xu W, Jiang W, Zha Z, Wang P, et al. Glioma-derived mutations in IDH1 dominantly inhibit IDH1 catalytic activity and induce HIF-1alpha. Science (New York, NY). 2009;324(5924):261-5.
- 214. Loenarz C, Schofield CJ. Expanding chemical biology of 2-oxoglutarate oxygenases. Nature Chemical Biology. 2008;4(3):152-6.
- 215. Ye D, Guan K-L, Xiong Y. Metabolism, activity, and targeting of D-and L-2-hydroxyglutarates. Trends in cancer. 2018;4(2):151-65.
- 216. Chowdhury R, Yeoh KK, Tian YM, Hillringhaus L, Bagg EA, Rose NR, et al. The oncometabolite 2-hydroxyglutarate inhibits histone lysine demethylases. EMBO Rep. 2011;12(5):463-9.
- 217. Koivunen P, Lee S, Duncan CG, Lopez G, Lu G, Ramkissoon S, et al. Transformation by the (R)-enantiomer of 2-hydroxyglutarate linked to EGLN activation. Nature. 2012;483(7390):484-8.
- 218. Yan H, Parsons DW, Jin G, McLendon R, Rasheed BA, Yuan W, et al. IDH1 and IDH2 mutations in gliomas. N Engl J Med. 2009;360(8):765-73.
- 219. Ward PS, Patel J, Wise DR, Abdel-Wahab O, Bennett BD, Coller HA, et al. The common feature of leukemia-associated IDH1 and IDH2 mutations is a neomorphic enzyme activity converting alpha-ketoglutarate to 2-hydroxyglutarate. Cancer Cell. 2010;17(3):225-34.
- 220. Dang L, White DW, Gross S, Bennett BD, Bittinger MA, Driggers EM, et al. Cancer-associated IDH1 mutations produce 2-hydroxyglutarate. Nature. 2010;465(7300):966.

- 221. Dang L, Su SM. Isocitrate Dehydrogenase Mutation and (R)-2-Hydroxyglutarate: From Basic Discovery to Therapeutics Development. Annu Rev Biochem. 2017;86:305-31.
- 222. Yang H, Ye D, Guan K-L, Xiong Y. IDH1 and IDH2 mutations in tumorigenesis: mechanistic insights and clinical perspectives. Clinical cancer research: an official journal of the American Association for Cancer Research. 2012;18(20):5562-71.
- 223. Reiter-Brennan C, Semmler L, Klein A. The effects of 2-hydroxyglutarate on the tumorigenesis of gliomas. Contemp Oncol (Pozn). 2018;22(4):215-22.
- 224. Lu C, Ward PS, Kapoor GS, Rohle D, Turcan S, Abdel-Wahab O, et al. IDH mutation impairs histone demethylation and results in a block to cell differentiation. Nature. 2012;483(7390):474-8.
- 225. Bardella C, Al-Dalahmah O, Krell D, Brazauskas P, Al-Qahtani K, Tomkova M, et al. Expression of Idh1(R132H) in the Murine Subventricular Zone Stem Cell Niche Recapitulates Features of Early Gliomagenesis. Cancer Cell. 2016;30(4):578-94.
- 226. Terunuma A, Putluri N, Mishra P, Mathé EA, Dorsey TH, Yi M, et al. MYC-driven accumulation of 2-hydroxyglutarate is associated with breast cancer prognosis. The Journal of clinical investigation. 2014;124(1):398-412.
- 227. Shim EH, Livi CB, Rakheja D, Tan J, Benson D, Parekh V, et al. L-2-Hydroxyglutarate: an epigenetic modifier and putative oncometabolite in renal cancer. Cancer Discov. 2014;4(11):1290-8.
- 228. Struys EA, Verhoeven NM, Brunengraber H, Jakobs C. Investigations by mass isotopomer analysis of the formation of D-2-hydroxyglutarate by cultured lymphoblasts from two patients with D-2-hydroxyglutaric aciduria. FEBS Lett. 2004;557(1-3):115-20.

- 229. Struys EA, Korman SH, Salomons GS, Darmin PS, Achouri Y, van Schaftingen E, et al. Mutations in phenotypically mild D-2-hydroxyglutaric aciduria. Ann Neurol. 2005;58(4):626-30.
- 230. Fan J, Teng X, Liu L, Mattaini KR, Looper RE, Vander Heiden MG, et al. Human phosphoglycerate dehydrogenase produces the oncometabolite D-2-hydroxyglutarate. ACS Chem Biol. 2015;10(2):510-6.
- 231. Rzem R, Vincent MF, Van Schaftingen E, Veiga-da-Cunha M. L-2-hydroxyglutaric aciduria, a defect of metabolite repair. J Inherit Metab Dis. 2007;30(5):681-9.
- 232. Intlekofer AM, Wang B, Liu H, Shah H, Carmona-Fontaine C, Rustenburg AS, et al. L-2-Hydroxyglutarate production arises from noncanonical enzyme function at acidic pH. Nature chemical biology. 2017;13(5):494-500.
- 233. Oldham WM, Clish CB, Yang Y, Loscalzo J. Hypoxia-Mediated Increases in L-2-hydroxyglutarate Coordinate the Metabolic Response to Reductive Stress. Cell Metab. 2015;22(2):291-303.
- 234. Intlekofer AM, Dematteo RG, Venneti S, Finley LW, Lu C, Judkins AR, et al. Hypoxia Induces Production of L-2-Hydroxyglutarate. Cell Metab. 2015;22(2):304-11.
- 235. Colvin H, Nishida N, Konno M, Haraguchi N, Takahashi H, Nishimura J, et al. Oncometabolite D-2-Hydroxyglurate Directly Induces Epithelial-Mesenchymal Transition and is Associated with Distant Metastasis in Colorectal Cancer. Sci Rep. 2016;6:36289-.
- 236. Struys EA, Salomons GS, Achouri Y, Van Schaftingen E, Grosso S, Craigen WJ, et al. Mutations in the D-2-hydroxyglutarate dehydrogenase gene cause D-2-hydroxyglutaric aciduria. Am J Hum Genet. 2005;76(2):358-60.
- 237. Rzem R, Veiga-da-Cunha M, Noël G, Goffette S, Nassogne M-C, Tabarki B, et al. A gene encoding a putative FAD-dependent L-2-hydroxyglutarate dehydrogenase is mutated in L-2-

- hydroxyglutaric aciduria. Proceedings of the National Academy of Sciences of the United States of America. 2004;101(48):16849-54.
- 238. Struys EA. D-2-Hydroxyglutaric aciduria: unravelling the biochemical pathway and the genetic defect. J Inherit Metab Dis. 2006;29(1):21-9.
- 239. Linninger A, Hartung GA, Liu BP, Mirkov S, Tangen K, Lukas RV, et al. Modeling the diffusion of D-2-hydroxyglutarate from IDH1 mutant gliomas in the central nervous system. Neuro Oncol. 2018;20(9):1197-206.
- 240. Hariharan VA, Denton TT, Paraszcszak S, McEvoy K, Jeitner TM, Krasnikov BF, et al. The Enzymology of 2-Hydroxyglutarate, 2-Hydroxyglutaramate and 2-Hydroxysuccinamate and Their Relationship to Oncometabolites. Biology (Basel). 2017;6(2).
- 241. Losman J-A, Kaelin WG, Jr. What a difference a hydroxyl makes: mutant IDH, (R)-2-hydroxyglutarate, and cancer. Genes & development. 2013;27(8):836-52.
- 242. Kranendijk M, Struys EA, Salomons GS, Van der Knaap MS, Jakobs C. Progress in understanding 2-hydroxyglutaric acidurias. Journal of inherited metabolic disease. 2012;35(4):571-87.
- 243. Moroni I, Bugiani M, D'Incerti L, Maccagnano C, Rimoldi M, Bissola L, et al. L-2-hydroxyglutaric aciduria and brain malignant tumors: a predisposing condition? Neurology. 2004;62(10):1882-4.
- 244. Xiao M, Yang H, Xu W, Ma S, Lin H, Zhu H, et al. Inhibition of α-KG-dependent histone and DNA demethylases by fumarate and succinate that are accumulated in mutations of FH and SDH tumor suppressors. Genes & development. 2012;26(12):1326-38.

- 245. Astuti D, Latif F, Dallol A, Dahia PL, Douglas F, George E, et al. Gene mutations in the succinate dehydrogenase subunit SDHB cause susceptibility to familial pheochromocytoma and to familial paraganglioma. American journal of human genetics. 2001;69(1):49-54.
- 246. Baysal BE, Ferrell RE, Willett-Brozick JE, Lawrence EC, Myssiorek D, Bosch A, et al. Mutations in SDHD, a mitochondrial complex II gene, in hereditary paraganglioma. Science. 2000;287(5454):848-51.
- 247. Niemann S, Müller U. Mutations in SDHC cause autosomal dominant paraganglioma, type 3. Nat Genet. 2000;26(3):268-70.
- 248. Hao HX, Khalimonchuk O, Schraders M, Dephoure N, Bayley JP, Kunst H, et al. SDH5, a gene required for flavination of succinate dehydrogenase, is mutated in paraganglioma. Science. 2009;325(5944):1139-42.
- 249. Huang LE, Gu J, Schau M, Bunn HF. Regulation of hypoxia-inducible factor 1alpha is mediated by an O2-dependent degradation domain via the ubiquitin-proteasome pathway. Proceedings of the National Academy of Sciences of the United States of America. 1998;95(14):7987-92.
- 250. Ivan M, Kondo K, Yang H, Kim W, Valiando J, Ohh M, et al. HIFalpha targeted for VHL-mediated destruction by proline hydroxylation: implications for O2 sensing. Science. 2001;292(5516):464-8.
- 251. Jaakkola P, Mole DR, Tian YM, Wilson MI, Gielbert J, Gaskell SJ, et al. Targeting of HIF-alpha to the von Hippel-Lindau ubiquitylation complex by O2-regulated prolyl hydroxylation. Science. 2001;292(5516):468-72.

- 252. Epstein AC, Gleadle JM, McNeill LA, Hewitson KS, O'Rourke J, Mole DR, et al. C. elegans EGL-9 and mammalian homologs define a family of dioxygenases that regulate HIF by prolyl hydroxylation. Cell. 2001;107(1):43-54.
- 253. Semenza GL. HIF-1: mediator of physiological and pathophysiological responses to hypoxia. Journal of Applied Physiology. 2000;88(4):1474-80.
- 254. Schofield CJ, Ratcliffe PJ. Oxygen sensing by HIF hydroxylases. Nature Reviews Molecular Cell Biology. 2004;5(5):343-54.
- 255. Gimenez-Roqueplo AP, Favier J, Rustin P, Rieubland C, Kerlan V, Plouin PF, et al. Functional consequences of a SDHB gene mutation in an apparently sporadic pheochromocytoma. J Clin Endocrinol Metab. 2002;87(10):4771-4.
- 256. Selak MA, Armour SM, MacKenzie ED, Boulahbel H, Watson DG, Mansfield KD, et al. Succinate links TCA cycle dysfunction to oncogenesis by inhibiting HIF-alpha prolyl hydroxylase. Cancer Cell. 2005;7(1):77-85.
- 257. Gimenez-Roqueplo AP, Favier J, Rustin P, Mourad JJ, Plouin PF, Corvol P, et al. The R22X mutation of the SDHD gene in hereditary paraganglioma abolishes the enzymatic activity of complex II in the mitochondrial respiratory chain and activates the hypoxia pathway. American journal of human genetics. 2001;69(6):1186-97.
- 258. Tannahill GM, Curtis AM, Adamik J, Palsson-McDermott EM, McGettrick AF, Goel G, et al. Succinate is an inflammatory signal that induces IL-1β through HIF-1α. Nature. 2013;496(7444):238-42.
- 259. Vanharanta S, Buchta M, McWhinney SR, Virta SK, Peçzkowska M, Morrison CD, et al. Early-onset renal cell carcinoma as a novel extraparaganglial component of SDHB-associated heritable paraganglioma. Am J Hum Genet. 2004;74(1):153-9.

- 260. Oermann EK, Wu J, Guan K-L, Xiong Y. Alterations of metabolic genes and metabolites in cancer. Seminars in cell & developmental biology. 2012;23(4):370-80.
- 261. Killian JK, Kim SY, Miettinen M, Smith C, Merino M, Tsokos M, et al. Succinate dehydrogenase mutation underlies global epigenomic divergence in gastrointestinal stromal tumor. Cancer discovery. 2013;3(6):648-57.
- 262. Aggarwal RK, Luchtel RA, Machha V, Tischer A, Zou Y, Pradhan K, et al. Functional succinate dehydrogenase deficiency is a common adverse feature of clear cell renal cancer. Proceedings of the National Academy of Sciences. 2021;118(39):e2106947118.
- 263. Tomlinson IP, Alam NA, Rowan AJ, Barclay E, Jaeger EE, Kelsell D, et al. Germline mutations in FH predispose to dominantly inherited uterine fibroids, skin leiomyomata and papillary renal cell cancer. Nat Genet. 2002;30(4):406-10.
- 264. Kerrigan JF, Aleck KA, Tarby TJ, Bird CR, Heidenreich RA. Fumaric aciduria: clinical and imaging features. Ann Neurol. 2000;47(5):583-8.
- 265. Wei MH, Toure O, Glenn GM, Pithukpakorn M, Neckers L, Stolle C, et al. Novel mutations in FH and expansion of the spectrum of phenotypes expressed in families with hereditary leiomyomatosis and renal cell cancer. J Med Genet. 2006;43(1):18-27.
- 266. Yang M, Soga T, Pollard PJ, Adam J. The emerging role of fumarate as an oncometabolite. Frontiers in oncology. 2012;2:85-.
- 267. Isaacs JS, Jung YJ, Mole DR, Lee S, Torres-Cabala C, Chung YL, et al. HIF overexpression correlates with biallelic loss of fumarate hydratase in renal cancer: novel role of fumarate in regulation of HIF stability. Cancer Cell. 2005;8(2):143-53.

- 268. Sciacovelli M, Gonçalves E, Johnson TI, Zecchini VR, da Costa ASH, Gaude E, et al. Fumarate is an epigenetic modifier that elicits epithelial-to-mesenchymal transition. Nature. 2016;537(7621):544-7.
- 269. Inigo M, Deja S, Burgess SC. Ins and Outs of the TCA Cycle: The Central Role of Anaplerosis. Annual Review of Nutrition. 2021;41(1):19-47.
- 270. Owen OE, Kalhan SC, Hanson RW. The key role of anaplerosis and cataplerosis for citric acid cycle function. J Biol Chem. 2002;277(34):30409-12.
- 271. Granner DK. In Pursuit of Genes of Glucose Metabolism. Journal of Biological Chemistry. 2015;290(37):22312-24.
- 272. Landau BR, Wahren J, Chandramouli V, Schumann WC, Ekberg K, Kalhan SC. Contributions of gluconeogenesis to glucose production in the fasted state. The Journal of Clinical Investigation. 1996;98(2):378-85.
- 273. Hanson RW, Patel YM. Phosphoenolpyruvate carboxykinase (GTP): the gene and the enzyme. Adv Enzymol Relat Areas Mol Biol. 1994;69:203-81.
- 274. Reshef L, Olswang Y, Cassuto H, Blum B, Croniger CM, Kalhan SC, et al. Glyceroneogenesis and the triglyceride/fatty acid cycle. J Biol Chem. 2003;278(33):30413-6.
- 275. Owen OE, Smalley KJ, D'Alessio DA, Mozzoli MA, Dawson EK. Protein, fat, and carbohydrate requirements during starvation: anaplerosis and cataplerosis. Am J Clin Nutr. 1998;68(1):12-34.
- 276. Cappel DA, Deja S, Duarte JAG, Kucejova B, Iñigo M, Fletcher JA, et al. Pyruvate-Carboxylase-Mediated Anaplerosis Promotes Antioxidant Capacity by Sustaining TCA Cycle and Redox Metabolism in Liver. Cell Metab. 2019;29(6):1291-305.e8.

- 277. von Glutz G, Walter P. Regulation of pyruvate carboxylation by acetyl-CoA in rat liver mitochondria. FEBS Lett. 1976;72(2):299-303.
- 278. Sellers K, Fox MP, Bousamra M, 2nd, Slone SP, Higashi RM, Miller DM, et al. Pyruvate carboxylase is critical for non-small-cell lung cancer proliferation. J Clin Invest. 2015;125(2):687-98.
- 279. Phannasil P, Thuwajit C, Warnnissorn M, Wallace JC, MacDonald MJ, Jitrapakdee S. Pyruvate Carboxylase Is Up-Regulated in Breast Cancer and Essential to Support Growth and Invasion of MDA-MB-231 Cells. PLoS One. 2015;10(6):e0129848.
- 280. Strickaert A, Corbet C, Spinette SA, Craciun L, Dom G, Andry G, et al. Reprogramming of Energy Metabolism: Increased Expression and Roles of Pyruvate Carboxylase in Papillary Thyroid Cancer. Thyroid. 2019;29(6):845-57.
- 281. Leithner K, Hrzenjak A, Trötzmüller M, Moustafa T, Köfeler HC, Wohlkoenig C, et al. PCK2 activation mediates an adaptive response to glucose depletion in lung cancer. Oncogene. 2015;34(8):1044-50.
- 282. Méndez-Lucas A, Hyroššová P, Novellasdemunt L, Viñals F, Perales JC. Mitochondrial phosphoenolpyruvate carboxykinase (PEPCK-M) is a pro-survival, endoplasmic reticulum (ER) stress response gene involved in tumor cell adaptation to nutrient availability. J Biol Chem. 2014;289(32):22090-102.
- 283. Vincent EE, Sergushichev A, Griss T, Gingras MC, Samborska B, Ntimbane T, et al. Mitochondrial Phosphoenolpyruvate Carboxykinase Regulates Metabolic Adaptation and Enables Glucose-Independent Tumor Growth. Mol Cell. 2015;60(2):195-207.
- 284. Stein WH, Moore S. The free amino acids of human blood plasma. J Biol Chem. 1954;211(2):915-26.

- 285. Mayers JR, Vander Heiden MG. Famine versus feast: understanding the metabolism of tumors in vivo. Trends in biochemical sciences. 2015;40(3):130-40.
- 286. Taylor L, Curthoys NP. Glutamine metabolism: Role in acid-base balance*. Biochem Mol Biol Educ. 2004;32(5):291-304.
- 287. Rennie MJ, Ahmed A, Khogali SE, Low SY, Hundal HS, Taylor PM. Glutamine metabolism and transport in skeletal muscle and heart and their clinical relevance. J Nutr. 1996;126(4 Suppl):1142s-9s.
- 288. Lacey JM, Wilmore DW. Is glutamine a conditionally essential amino acid? Nutr Rev. 1990;48(8):297-309.
- 289. Yoo HC, Yu YC, Sung Y, Han JM. Glutamine reliance in cell metabolism. Exp Mol Med. 2020;52(9):1496-516.
- 290. Amores-Sánchez MI, Medina MA. Glutamine, as a precursor of glutathione, and oxidative stress. Mol Genet Metab. 1999;67(2):100-5.
- 291. Bhutia YD, Babu E, Ramachandran S, Ganapathy V. Amino Acid transporters in cancer and their relevance to "glutamine addiction": novel targets for the design of a new class of anticancer drugs. Cancer Res. 2015;75(9):1782-8.
- 292. Scalise M, Pochini L, Galluccio M, Console L, Indiveri C. Glutamine Transport and Mitochondrial Metabolism in Cancer Cell Growth. Front Oncol. 2017;7:306.
- 293. Pochini L, Scalise M, Galluccio M, Indiveri C. Membrane transporters for the special amino acid glutamine: structure/function relationships and relevance to human health. Front Chem. 2014;2:61-.
- 294. Curthoys NP, Watford M. Regulation of Glutaminase Activity and Glutamine Metabolism. Annual Review of Nutrition. 1995;15(1):133-59.

- 295. Krebs HA. Metabolism of amino-acids: The synthesis of glutamine from glutamic acid and ammonia, and the enzymic hydrolysis of glutamine in animal tissues. The Biochemical journal. 1935;29(8):1951-69.
- 296. Corbet C, Feron O. Cancer cell metabolism and mitochondria: Nutrient plasticity for TCA cycle fueling. Biochim Biophys Acta Rev Cancer. 2017;1868(1):7-15.
- 297. Daye D, Wellen KE. Metabolic reprogramming in cancer: unraveling the role of glutamine in tumorigenesis. Semin Cell Dev Biol. 2012;23(4):362-9.
- 298. Choi BH, Coloff JL. The Diverse Functions of Non-Essential Amino Acids in Cancer. Cancers (Basel). 2019;11(5).
- 299. Stine ZE, Dang CV. Glutamine Skipping the Q into Mitochondria. Trends Mol Med. 2020;26(1):6-7.
- 300. Altman BJ, Stine ZE, Dang CV. From Krebs to clinic: glutamine metabolism to cancer therapy. Nature Reviews Cancer. 2016;16(10):619-34.
- 301. Eagle H. The minimum vitamin requirements of the L and HeLa cells in tissue culture, the production of specific vitamin deficiencies, and their cure. J Exp Med. 1955;102(5):595-600.
- 302. Wise DR, Thompson CB. Glutamine addiction: a new therapeutic target in cancer. Trends in biochemical sciences. 2010;35(8):427-33.
- 303. Wang R, Dillon CP, Shi LZ, Milasta S, Carter R, Finkelstein D, et al. The transcription factor Myc controls metabolic reprogramming upon T lymphocyte activation. Immunity. 2011;35(6):871-82.
- 304. Le A, Lane AN, Hamaker M, Bose S, Gouw A, Barbi J, et al. Glucose-independent glutamine metabolism via TCA cycling for proliferation and survival in B cells. Cell Metab. 2012;15(1):110-21.

- 305. Le A, Lane AN, Hamaker M, Bose S, Gouw A, Barbi J, et al. Glucose-independent glutamine metabolism via TCA cycling for proliferation and survival in B cells. Cell metabolism. 2012;15(1):110-21.
- 306. Son J, Lyssiotis CA, Ying H, Wang X, Hua S, Ligorio M, et al. Glutamine supports pancreatic cancer growth through a KRAS-regulated metabolic pathway. Nature. 2013;496(7443):101-5.
- 307. Chen Q, Kirk K, Shurubor YI, Zhao D, Arreguin AJ, Shahi I, et al. Rewiring of Glutamine Metabolism Is a Bioenergetic Adaptation of Human Cells with Mitochondrial DNA Mutations. Cell Metab. 2018;27(5):1007-25.e5.
- 308. Seltzer MJ, Bennett BD, Joshi AD, Gao P, Thomas AG, Ferraris DV, et al. Inhibition of glutaminase preferentially slows growth of glioma cells with mutant IDH1. Cancer Res. 2010;70(22):8981-7.
- 309. Frezza C, Zheng L, Folger O, Rajagopalan KN, MacKenzie ED, Jerby L, et al. Haem oxygenase is synthetically lethal with the tumour suppressor fumarate hydratase. Nature. 2011;477(7363):225-8.
- 310. Yoo H, Antoniewicz MR, Stephanopoulos G, Kelleher JK. Quantifying reductive carboxylation flux of glutamine to lipid in a brown adipocyte cell line. The Journal of biological chemistry. 2008;283(30):20621-7.
- 311. Birsoy K, Wang T, Chen WW, Freinkman E, Abu-Remaileh M, Sabatini DM. An essential role of the mitochondrial electron transport chain in cell proliferation is to enable aspartate synthesis. Cell. 2015;162(3):540-51.

- 312. Sullivan LB, Gui DY, Hosios AM, Bush LN, Freinkman E, Vander Heiden MG. Supporting aspartate biosynthesis is an essential function of respiration in proliferating cells. Cell. 2015;162(3):552-63.
- 313. Metallo CM, Gameiro PA, Bell EL, Mattaini KR, Yang J, Hiller K, et al. Reductive glutamine metabolism by IDH1 mediates lipogenesis under hypoxia. Nature. 2012;481(7381):380-4.
- 314. Scott DA, Richardson AD, Filipp FV, Knutzen CA, Chiang GG, Ronai ZeA, et al. Comparative metabolic flux profiling of melanoma cell lines: beyond the Warburg effect. The Journal of biological chemistry. 2011;286(49):42626-34.
- 315. Cheng T, Sudderth J, Yang C, Mullen AR, Jin ES, Matés JM, et al. Pyruvate carboxylase is required for glutamine-independent growth of tumor cells. Proceedings of the National Academy of Sciences of the United States of America. 2011;108(21):8674-9.
- 316. Bott AJ, Peng IC, Fan Y, Faubert B, Zhao L, Li J, et al. Oncogenic Myc Induces Expression of Glutamine Synthetase through Promoter Demethylation. Cell Metab. 2015;22(6):1068-77.
- 317. Tardito S, Oudin A, Ahmed SU, Fack F, Keunen O, Zheng L, et al. Glutamine synthetase activity fuels nucleotide biosynthesis and supports growth of glutamine-restricted glioblastoma. Nat Cell Biol. 2015;17(12):1556-68.
- 318. Osada T, Nagashima I, Tsuno NH, Kitayama J, Nagawa H. Prognostic significance of glutamine synthetase expression in unifocal advanced hepatocellular carcinoma. J Hepatol. 2000;33(2):247-53.
- 319. Zhao R-Z, Jiang S, Zhang L, Yu Z-B. Mitochondrial electron transport chain, ROS generation and uncoupling (Review). Int J Mol Med. 2019;44(1):3-15.

- 320. Jastroch M, Divakaruni AS, Mookerjee S, Treberg JR, Brand MD. Mitochondrial proton and electron leaks. Essays Biochem. 2010;47:53-67.
- 321. Brand MD. Uncoupling to survive? The role of mitochondrial inefficiency in ageing. Experimental Gerontology. 2000;35(6):811-20.
- 322. Carroll J, Fearnley IM, Skehel JM, Shannon RJ, Hirst J, Walker JE. Bovine complex I is a complex of 45 different subunits. J Biol Chem. 2006;281(43):32724-7.
- 323. Efremov RG, Sazanov LA. Structure of the membrane domain of respiratory complex I. Nature. 2011;476(7361):414-20.
- 324. Walker JE. The NADH:ubiquinone oxidoreductase (complex I) of respiratory chains. Q Rev Biophys. 1992;25(3):253-324.
- 325. Schapira AHV. Human complex I defects in neurodegenerative diseases. Biochimica et Biophysica Acta (BBA) Bioenergetics. 1998;1364(2):261-70.
- 326. Lake NJ, Compton AG, Rahman S, Thorburn DR. Leigh syndrome: One disorder, more than 75 monogenic causes. Ann Neurol. 2016;79(2):190-203.
- 327. Sazanov LA. Respiratory complex I: mechanistic and structural insights provided by the crystal structure of the hydrophilic domain. Biochemistry. 2007;46(9):2275-88.
- 328. Akouchekian M, Houshmand M, Akbari MH, Kamalidehghan B, Dehghan M. Analysis of mitochondrial ND1 gene in human colorectal cancer. J Res Med Sci. 2011;16(1):50-5.
- 329. Li L-D, Sun H-F, Liu X-X, Gao S-P, Jiang H-L, Hu X, et al. Down-Regulation of NDUFB9 Promotes Breast Cancer Cell Proliferation, Metastasis by Mediating Mitochondrial Metabolism. PloS one. 2015;10(12):e0144441-e.

- 330. Calabrese C, Iommarini L, Kurelac I, Calvaruso MA, Capristo M, Lollini P-L, et al. Respiratory complex I is essential to induce a Warburg profile in mitochondria-defective tumor cells. Cancer Metab. 2013;1(1):11-.
- 331. Sun F, Huo X, Zhai Y, Wang A, Xu J, Su D, et al. Crystal structure of mitochondrial respiratory membrane protein complex II. Cell. 2005;121(7):1043-57.
- 332. Bezawork-Geleta A, Rohlena J, Dong L, Pacak K, Neuzil J. Mitochondrial Complex II: At the Crossroads. Trends Biochem Sci. 2017;42(4):312-25.
- 333. Bandara AB, Drake JC, Brown DA. Complex II subunit SDHD is critical for cell growth and metabolism, which can be partially restored with a synthetic ubiquinone analog. BMC Mol Cell Biol. 2021;22(1):35.
- 334. Brière JJ, Favier J, El Ghouzzi V, Djouadi F, Bénit P, Gimenez AP, et al. Succinate dehydrogenase deficiency in human. Cell Mol Life Sci. 2005;62(19-20):2317-24.
- 335. Nolfi-Donegan D, Braganza A, Shiva S. Mitochondrial electron transport chain: Oxidative phosphorylation, oxidant production, and methods of measurement. Redox Biol. 2020;37:101674.
- 336. Koopman WJ, Nijtmans LG, Dieteren CE, Roestenberg P, Valsecchi F, Smeitink JA, et al. Mammalian mitochondrial complex I: biogenesis, regulation, and reactive oxygen species generation. Antioxid Redox Signal. 2010;12(12):1431-70.
- 337. Stipanuk MH, Caudill MA. Biochemical, Physiological and Molecular Aspects of Human Nutrition: W B Saunders Co; 2018.
- 338. Watmough NJ, Frerman FE. The electron transfer flavoprotein: Ubiquinone oxidoreductases. Biochimica et Biophysica Acta (BBA) Bioenergetics. 2010;1797(12):1910-6.

- 339. Schiff M, Froissart R, Olsen RKJ, Acquaviva C, Vianey-Saban C. Electron transfer flavoprotein deficiency: Functional and molecular aspects. Molecular Genetics and Metabolism. 2006;88(2):153-8.
- 340. El-Gharbawy A, Vockley J. Chapter 14 Nonmitochondrial Metabolic Cardioskeletal Myopathies. In: Jefferies JL, Blaxall BC, Robbins J, Towbin JA, editors. Cardioskeletal Myopathies in Children and Young Adults. Boston: Academic Press; 2017. p. 265-303.
- 341. Mráček T, Drahota Z, Houštěk J. The function and the role of the mitochondrial glycerol-3-phosphate dehydrogenase in mammalian tissues. Biochimica et Biophysica Acta (BBA) Bioenergetics. 2013;1827(3):401-10.
- 342. Löffler M, Jöckel J, Schuster G, Becker C. Dihydroorotat-ubiquinone oxidoreductase links mitochondria in the biosynthesis of pyrimidine nucleotides. Mol Cell Biochem. 1997;174(1-2):125-9.
- 343. Gao X, Wen X, Esser L, Quinn B, Yu L, Yu CA, et al. Structural basis for the quinone reduction in the bc1 complex: a comparative analysis of crystal structures of mitochondrial cytochrome bc1 with bound substrate and inhibitors at the Qi site. Biochemistry. 2003;42(30):9067-80.
- 344. Trumpower BL. A concerted, alternating sites mechanism of ubiquinol oxidation by the dimeric cytochrome bc(1) complex. Biochim Biophys Acta. 2002;1555(1-3):166-73.
- 345. Fernández-Vizarra E, Zeviani M. Nuclear gene mutations as the cause of mitochondrial complex III deficiency. Frontiers in Genetics. 2015;6(134).
- 346. Owens KM, Kulawiec M, Desouki MM, Vanniarajan A, Singh KK. Impaired OXPHOS complex III in breast cancer. PloS one. 2011;6(8):e23846-e.

- 347. Koopman WJH, Distelmaier F, Smeitink JAM, Willems PHGM. OXPHOS mutations and neurodegeneration. EMBO J. 2013;32(1):9-29.
- 348. Lu J, Sharma LK, Bai Y. Implications of mitochondrial DNA mutations and mitochondrial dysfunction in tumorigenesis. Cell Res. 2009;19(7):802-15.
- 349. Mick DU, Fox TD, Rehling P. Inventory control: cytochrome c oxidase assembly regulates mitochondrial translation. Nat Rev Mol Cell Biol. 2011;12(1):14-20.
- 350. Wikstrom MK. Proton pump coupled to cytochrome c oxidase in mitochondria. Nature. 1977;266(5599):271-3.
- 351. Srinivasan S, Guha M, Dong DW, Whelan KA, Ruthel G, Uchikado Y, et al. Disruption of cytochrome c oxidase function induces the Warburg effect and metabolic reprogramming. Oncogene. 2016;35(12):1585-95.
- 352. Chinopoulos C, Adam-Vizi V. Mitochondria as ATP consumers in cellular pathology. Biochim Biophys Acta. 2010;1802(1):221-7.
- 353. Nicholls DG, Budd SL. Mitochondria and neuronal survival. Physiol Rev. 2000;80(1):315-60.
- 354. Grzybowska-Szatkowska L, Slaska B, Rzymowska J, Brzozowska A, Floriańczyk B. Novel mitochondrial mutations in the ATP6 and ATP8 genes in patients with breast cancer. Mol Med Rep. 2014;10(4):1772-8.
- 355. Guo XG, Liu CT, Dai H, Guo QN. Mutations in the mitochondrial ATPase6 gene are frequent in human osteosarcoma. Exp Mol Pathol. 2013;94(1):285-8.
- 356. Petros JA, Baumann AK, Ruiz-Pesini E, Amin MB, Sun CQ, Hall J, et al. mtDNA mutations increase tumorigenicity in prostate cancer. Proceedings of the National Academy of Sciences of the United States of America. 2005;102(3):719-24.

- 357. Shin YK, Yoo BC, Chang HJ, Jeon E, Hong SH, Jung MS, et al. Down-regulation of mitochondrial F1F0-ATP synthase in human colon cancer cells with induced 5-fluorouracil resistance. Cancer Res. 2005;65(8):3162-70.
- 358. Kowaltowski AJ, de Souza-Pinto NC, Castilho RF, Vercesi AE. Mitochondria and reactive oxygen species. Free Radic Biol Med. 2009;47(4):333-43.
- 359. Brand MD. The sites and topology of mitochondrial superoxide production. Exp Gerontol. 2010;45(7-8):466-72.
- 360. Jabs T. Reactive oxygen intermediates as mediators of programmed cell death in plants and animals. Biochem Pharmacol. 1999;57(3):231-45.
- 361. Finkel T. Redox-dependent signal transduction. FEBS Lett. 2000;476(1-2):52-4.
- 362. Lebovitz RM, Zhang H, Vogel H, Cartwright J, Jr., Dionne L, Lu N, et al. Neurodegeneration, myocardial injury, and perinatal death in mitochondrial superoxide dismutase-deficient mice. Proc Natl Acad Sci U S A. 1996;93(18):9782-7.
- 363. Li Y, Huang TT, Carlson EJ, Melov S, Ursell PC, Olson JL, et al. Dilated cardiomyopathy and neonatal lethality in mutant mice lacking manganese superoxide dismutase. Nat Genet. 1995;11(4):376-81.
- 364. Bienert GP, Schjoerring JK, Jahn TP. Membrane transport of hydrogen peroxide. Biochim Biophys Acta. 2006;1758(8):994-1003.
- 365. Luo Y, Ma J, Lu W. The Significance of Mitochondrial Dysfunction in Cancer. Int J Mol Sci. 2020;21(16).
- 366. Schiliro C, Firestein BL. Mechanisms of Metabolic Reprogramming in Cancer Cells Supporting Enhanced Growth and Proliferation. Cells. 2021;10(5):1056.

- 367. Palmieri L, Pardo B, Lasorsa FM, del Arco A, Kobayashi K, Iijima M, et al. Citrin and aralar1 are Ca(2+)-stimulated aspartate/glutamate transporters in mitochondria. EMBO J. 2001;20(18):5060-9.
- 368. Sullivan LB, Luengo A, Danai LV, Bush LN, Diehl FF, Hosios AM, et al. Aspartate is an endogenous metabolic limitation for tumour growth. Nat Cell Biol. 2018;20(7):782-8.
- 369. Thornburg JM, Nelson KK, Clem BF, Lane AN, Arumugam S, Simmons A, et al. Targeting aspartate aminotransferase in breast cancer. Breast Cancer Res. 2008;10(5):R84.
- 370. Garcia-Bermudez J, Baudrier L, La K, Zhu XG, Fidelin J, Sviderskiy VO, et al. Aspartate is a limiting metabolite for cancer cell proliferation under hypoxia and in tumours. Nat Cell Biol. 2018;20(7):775-81.
- 371. Pavlova NN, Hui S, Ghergurovich JM, Fan J, Intlekofer AM, White RM, et al. As Extracellular Glutamine Levels Decline, Asparagine Becomes an Essential Amino Acid. Cell metabolism. 2018;27(2):428-38.e5.
- 372. Krall AS, Xu S, Graeber TG, Braas D, Christofk HR. Asparagine promotes cancer cell proliferation through use as an amino acid exchange factor. Nat Commun. 2016;7:11457.
- 373. Richards NG, Kilberg MS. Asparagine synthetase chemotherapy. Annu Rev Biochem. 2006;75:629-54.
- 374. Balasubramanian MN, Butterworth EA, Kilberg MS. Asparagine synthetase: regulation by cell stress and involvement in tumor biology. Am J Physiol Endocrinol Metab. 2013;304(8):E789-E99.
- 375. Butler M, van der Meer LT, van Leeuwen FN. Amino Acid Depletion Therapies: Starving Cancer Cells to Death. Trends Endocrinol Metab. 2021;32(6):367-81.

- 376. Chiu M, Taurino G, Bianchi MG, Kilberg MS, Bussolati O. Asparagine Synthetase in Cancer: Beyond Acute Lymphoblastic Leukemia. Front Oncol. 2019;9:1480.
- 377. Cools J. Improvements in the survival of children and adolescents with acute lymphoblastic leukemia. Haematologica. 2012;97(5):635.
- 378. Pieters R, Hunger SP, Boos J, Rizzari C, Silverman L, Baruchel A, et al. L-asparaginase treatment in acute lymphoblastic leukemia: a focus on Erwinia asparaginase. Cancer. 2011;117(2):238-49.
- 379. Asselin BL. The three asparaginases. Comparative pharmacology and optimal use in childhood leukemia. Adv Exp Med Biol. 1999;457:621-9.
- 380. Zhang J, Fan J, Venneti S, Cross JR, Takagi T, Bhinder B, et al. Asparagine plays a critical role in regulating cellular adaptation to glutamine depletion. Molecular cell. 2014;56(2):205-18.
- 381. Sircar K, Huang H, Hu L, Cogdell D, Dhillon J, Tzelepi V, et al. Integrative molecular profiling reveals asparagine synthetase is a target in castration-resistant prostate cancer. Am J Pathol. 2012;180(3):895-903.
- 382. Batool T, Makky EA, Jalal M, Yusoff MM. A Comprehensive Review on L-Asparaginase and Its Applications. Appl Biochem Biotechnol. 2016;178(5):900-23.
- 383. Cantor JR, Stone EM, Chantranupong L, Georgiou G. The human asparaginase-like protein 1 hASRGL1 is an Ntn hydrolase with beta-aspartyl peptidase activity. Biochemistry. 2009;48(46):11026-31.
- 384. Knott SRV, Wagenblast E, Khan S, Kim SY, Soto M, Wagner M, et al. Asparagine bioavailability governs metastasis in a model of breast cancer. Nature. 2018;554(7692):378-81.

- 385. Nakanishi T, Kekuda R, Fei YJ, Hatanaka T, Sugawara M, Martindale RG, et al. Cloning and functional characterization of a new subtype of the amino acid transport system N. Am J Physiol Cell Physiol. 2001;281(6):C1757-68.
- 386. Bröer S. The SLC38 family of sodium–amino acid co-transporters. Pflügers Archiv European Journal of Physiology. 2014;466(1):155-72.
- 387. Shuvalov O, Petukhov A, Daks A, Fedorova O, Vasileva E, Barlev NA. One-carbon metabolism and nucleotide biosynthesis as attractive targets for anticancer therapy. Oncotarget. 2017;8(14):23955-77.
- 388. Achouri Y, Rider MH, Schaftingen EV, Robbi M. Cloning, sequencing and expression of rat liver 3-phosphoglycerate dehydrogenase. Biochem J. 1997;323 (Pt 2)(Pt 2):365-70.
- 389. de Koning TJ, Snell K, Duran M, Berger R, Poll-The BT, Surtees R. L-serine in disease and development. Biochem J. 2003;371(Pt 3):653-61.
- 390. Kurmi K, Haigis MC. Nitrogen Metabolism in Cancer and Immunity. Trends Cell Biol. 2020;30(5):408-24.
- 391. Maddocks OD, Berkers CR, Mason SM, Zheng L, Blyth K, Gottlieb E, et al. Serine starvation induces stress and p53-dependent metabolic remodelling in cancer cells. Nature. 2013;493(7433):542-6.
- 392. Possemato R, Marks KM, Shaul YD, Pacold ME, Kim D, Birsoy K, et al. Functional genomics reveal that the serine synthesis pathway is essential in breast cancer. Nature. 2011;476(7360):346-50.
- 393. Locasale JW, Grassian AR, Melman T, Lyssiotis CA, Mattaini KR, Bass AJ, et al. Phosphoglycerate dehydrogenase diverts glycolytic flux and contributes to oncogenesis. Nat Genet. 2011;43(9):869-74.

- 394. Vié N, Copois V, Bascoul-Mollevi C, Denis V, Bec N, Robert B, et al. Overexpression of phosphoserine aminotransferase PSAT1 stimulates cell growth and increases chemoresistance of colon cancer cells. Mol Cancer. 2008;7:14.
- 395. Ye J, Fan J, Venneti S, Wan YW, Pawel BR, Zhang J, et al. Serine catabolism regulates mitochondrial redox control during hypoxia. Cancer Discov. 2014;4(12):1406-17.
- 396. Labuschagne CF, van den Broek NJ, Mackay GM, Vousden KH, Maddocks OD. Serine, but not glycine, supports one-carbon metabolism and proliferation of cancer cells. Cell Rep. 2014;7(4):1248-58.
- 397. Jain M, Nilsson R, Sharma S, Madhusudhan N, Kitami T, Souza AL, et al. Metabolite profiling identifies a key role for glycine in rapid cancer cell proliferation. Science (New York, NY). 2012;336(6084):1040-4.
- 398. Mattaini KR, Sullivan MR, Vander Heiden MG. The importance of serine metabolism in cancer. J Cell Biol. 2016;214(3):249-57.
- 399. Lewis CA, Parker SJ, Fiske BP, McCloskey D, Gui DY, Green CR, et al. Tracing compartmentalized NADPH metabolism in the cytosol and mitochondria of mammalian cells. Mol Cell. 2014;55(2):253-63.
- 400. Ducker GS, Rabinowitz JD. One-Carbon Metabolism in Health and Disease. Cell Metab. 2017;25(1):27-42.
- 401. Newman AC, Maddocks ODK. One-carbon metabolism in cancer. Br J Cancer. 2017;116(12):1499-504.
- 402. Tedeschi PM, Markert EK, Gounder M, Lin H, Dvorzhinski D, Dolfi SC, et al. Contribution of serine, folate and glycine metabolism to the ATP, NADPH and purine requirements of cancer cells. Cell Death Dis. 2013;4(10):e877.

- 403. Bruns H, Kazanavicius D, Schultze D, Saeedi MA, Yamanaka K, Strupas K, et al. Glycine inhibits angiogenesis in colorectal cancer: role of endothelial cells. Amino Acids. 2016;48(11):2549-58.
- 404. Rose ML, Cattley RC, Dunn C, Wong V, Li X, Thurman RG. Dietary glycine prevents the development of liver tumors caused by the peroxisome proliferator WY-14,643. Carcinogenesis. 1999;20(11):2075-81.
- 405. Rose ML, Madren J, Bunzendahl H, Thurman RG. Dietary glycine inhibits the growth of B16 melanoma tumors in mice. Carcinogenesis. 1999;20(5):793-8.
- 406. Nilsson R, Jain M, Madhusudhan N, Sheppard NG, Strittmatter L, Kampf C, et al. Metabolic enzyme expression highlights a key role for MTHFD2 and the mitochondrial folate pathway in cancer. Nat Commun. 2014;5:3128.
- 407. Pan S, Fan M, Liu Z, Li X, Wang H. Serine, glycine and one-carbon metabolism in cancer (Review). International journal of oncology. 2021;58(2):158-70.
- 408. Kim D, Fiske BP, Birsoy K, Freinkman E, Kami K, Possemato RL, et al. SHMT2 drives glioma cell survival in ischaemia but imposes a dependence on glycine clearance. Nature. 2015;520(7547):363-7.
- 409. Ouyang Y, Wu Q, Li J, Sun S, Sun S. S-adenosylmethionine: A metabolite critical to the regulation of autophagy. Cell Proliferation. 2020;53(11):e12891.
- 410. Serpa J. Cysteine as a Carbon Source, a Hot Spot in Cancer Cells Survival. Frontiers in oncology. 2020;10:947-.
- 411. Yu X, Long YC. Crosstalk between cystine and glutathione is critical for the regulation of amino acid signaling pathways and ferroptosis. Sci Rep. 2016;6(1):30033.

- 412. Luciano-Mateo F, Hernández-Aguilera A, Cabre N, Camps J, Fernández-Arroyo S, Lopez-Miranda J, et al. Nutrients in Energy and One-Carbon Metabolism: Learning from Metformin Users. Nutrients. 2017;9(2).
- 413. Ducker GS, Chen L, Morscher RJ, Ghergurovich JM, Esposito M, Teng X, et al. Reversal of Cytosolic One-Carbon Flux Compensates for Loss of the Mitochondrial Folate Pathway. Cell Metab. 2016;23(6):1140-53.
- 414. Lee D, Xu IM, Chiu DK, Lai RK, Tse AP, Lan Li L, et al. Folate cycle enzyme MTHFD1L confers metabolic advantages in hepatocellular carcinoma. J Clin Invest. 2017;127(5):1856-72.
- 415. Hoffman RM, Erbe RW. High in vivo rates of methionine biosynthesis in transformed human and malignant rat cells auxotrophic for methionine. Proc Natl Acad Sci U S A. 1976;73(5):1523-7.
- 416. Stern PH, Wallace CD, Hoffman RM. Altered methionine metabolism occurs in all members of a set of diverse human tumor cell lines. J Cell Physiol. 1984;119(1):29-34.
- 417. Halpern BC, Clark BR, Hardy DN, Halpern RM, Smith RA. The effect of replacement of methionine by homocystine on survival of malignant and normal adult mammalian cells in culture. Proc Natl Acad Sci U S A. 1974;71(4):1133-6.
- 418. Borrego SL, Fahrmann J, Datta R, Stringari C, Grapov D, Zeller M, et al. Metabolic changes associated with methionine stress sensitivity in MDA-MB-468 breast cancer cells. Cancer Metab. 2016;4:9-.
- 419. Wang Z, Yip LY, Lee JHJ, Wu Z, Chew HY, Chong PKW, et al. Methionine is a metabolic dependency of tumor-initiating cells. Nat Med. 2019;25(5):825-37.
- 420. Snaebjornsson MT, Janaki-Raman S, Schulze A. Greasing the Wheels of the Cancer Machine: The Role of Lipid Metabolism in Cancer. Cell Metab. 2020;31(1):62-76.

- 421. Fujimoto T, Parton RG. Not just fat: the structure and function of the lipid droplet. Cold Spring Harb Perspect Biol. 2011;3(3).
- 422. Henne WM, Reese ML, Goodman JM. The assembly of lipid droplets and their roles in challenged cells. EMBO J. 2018;37(12):e98947.
- 423. Röhrig F, Schulze A. The multifaceted roles of fatty acid synthesis in cancer. Nat Rev Cancer. 2016;16(11):732-49.
- 424. Koundouros N, Poulogiannis G. Reprogramming of fatty acid metabolism in cancer. British journal of cancer. 2020;122(1):4-22.
- 425. Rotondo F, Ho-Palma AC, Remesar X, Fernández-López JA, Romero MdM, Alemany M. Glycerol is synthesized and secreted by adipocytes to dispose of excess glucose, via glycerogenesis and increased acyl-glycerol turnover. Sci Rep. 2017;7(1):8983.
- 426. Fondy TP, Herwig KJ, Sollohub SJ, Rutherford DB. Isolation and structural properties of cytoplasmic glycerol-3-phosphate dehydrogenase from rat liver. Arch Biochem Biophys. 1971;145(2):583-90.
- 427. Chajès V, Cambot M, Moreau K, Lenoir GM, Joulin V. Acetyl-CoA carboxylase alpha is essential to breast cancer cell survival. Cancer Res. 2006;66(10):5287-94.
- 428. Flavin R, Peluso S, Nguyen PL, Loda M. Fatty acid synthase as a potential therapeutic target in cancer. Future Oncol. 2010;6(4):551-62.
- 429. Migita T, Narita T, Nomura K, Miyagi E, Inazuka F, Matsuura M, et al. ATP citrate lyase: activation and therapeutic implications in non-small cell lung cancer. Cancer Res. 2008;68(20):8547-54.

- 430. Milgraum LZ, Witters LA, Pasternack GR, Kuhajda FP. Enzymes of the fatty acid synthesis pathway are highly expressed in in situ breast carcinoma. Clin Cancer Res. 1997;3(11):2115-20.
- 431. Schug ZT, Peck B, Jones DT, Zhang Q, Grosskurth S, Alam IS, et al. Acetyl-CoA synthetase 2 promotes acetate utilization and maintains cancer cell growth under metabolic stress. Cancer cell. 2015;27(1):57-71.
- 432. Berg P. Acyl adenylates; an enzymatic mechanism of acetate activation. J Biol Chem. 1956;222(2):991-1013.
- 433. Medes G, Thomas A, Weinhouse S. Metabolism of neoplastic tissue. IV. A study of lipid synthesis in neoplastic tissue slices in vitro. Cancer Res. 1953;13(1):27-9.
- 434. Brown MS, Goldstein JL. A receptor-mediated pathway for cholesterol homeostasis. Science. 1986;232(4746):34-47.
- 435. Kazantzis M, Stahl A. Fatty acid transport proteins, implications in physiology and disease. Biochim Biophys Acta. 2012;1821(5):852-7.
- 436. Furuhashi M, Hotamisligil GS. Fatty acid-binding proteins: role in metabolic diseases and potential as drug targets. Nat Rev Drug Discov. 2008;7(6):489-503.
- 437. Wang W, Bai L, Li W, Cui J. The Lipid Metabolic Landscape of Cancers and New Therapeutic Perspectives. Frontiers in Oncology. 2020;10.
- 438. An Q, Lin R, Wang D, Wang C. Emerging roles of fatty acid metabolism in cancer and their targeted drug development. European Journal of Medicinal Chemistry. 2022;240:114613.
- 439. Munir R, Lisec J, Swinnen JV, Zaidi N. Lipid metabolism in cancer cells under metabolic stress. British Journal of Cancer. 2019;120(12):1090-8.

- 440. Pascual G, Avgustinova A, Mejetta S, Martín M, Castellanos A, Attolini CS, et al. Targeting metastasis-initiating cells through the fatty acid receptor CD36. Nature. 2017;541(7635):41-5.
- 441. Kamphorst JJ, Cross JR, Fan J, de Stanchina E, Mathew R, White EP, et al. Hypoxic and Ras-transformed cells support growth by scavenging unsaturated fatty acids from lysophospholipids. Proc Natl Acad Sci U S A. 2013;110(22):8882-7.
- 442. Bensaad K, Favaro E, Lewis CA, Peck B, Lord S, Collins JM, et al. Fatty acid uptake and lipid storage induced by HIF-1α contribute to cell growth and survival after hypoxia-reoxygenation. Cell Rep. 2014;9(1):349-65.
- 443. Koizume S, Miyagi Y. Lipid Droplets: A Key Cellular Organelle Associated with Cancer Cell Survival under Normoxia and Hypoxia. International journal of molecular sciences. 2016;17(9):1430.
- 444. Huang D, Li T, Li X, Zhang L, Sun L, He X, et al. HIF-1-mediated suppression of acyl-CoA dehydrogenases and fatty acid oxidation is critical for cancer progression. Cell Rep. 2014;8(6):1930-42.
- 445. Zaugg K, Yao Y, Reilly PT, Kannan K, Kiarash R, Mason J, et al. Carnitine palmitoyltransferase 1C promotes cell survival and tumor growth under conditions of metabolic stress. Genes Dev. 2011;25(10):1041-51.
- 446. Patra KC, Hay N. The pentose phosphate pathway and cancer. Trends Biochem Sci. 2014;39(8):347-54.
- 447. Jiang P, Du W, Wu M. Regulation of the pentose phosphate pathway in cancer. Protein & Cell. 2014;5(8):592-602.

- 448. Kloska SM, Pałczyński K, Marciniak T, Talaśka T, Miller M, Wysocki BJ, et al. Queueing theory model of pentose phosphate pathway. Sci Rep. 2022;12(1):4601.
- 449. Ayala A, Fabregat I, Machado A. The role of NADPH in the regulation of glucose-6-phosphate and 6-phosphogluconate dehydrogenases in rat adipose tissue. Mol Cell Biochem. 1991;105(1):1-5.
- 450. Jonas SK, Benedetto C, Flatman A, Hammond RH, Micheletti L, Riley C, et al. Increased activity of 6-phosphogluconate dehydrogenase and glucose-6-phosphate dehydrogenase in purified cell suspensions and single cells from the uterine cervix in cervical intraepithelial neoplasia. Br J Cancer. 1992;66(1):185-91.
- 451. Boros LG, Puigjaner J, Cascante M, Lee WN, Brandes JL, Bassilian S, et al. Oxythiamine and dehydroepiandrosterone inhibit the nonoxidative synthesis of ribose and tumor cell proliferation. Cancer Res. 1997;57(19):4242-8.
- 452. Liu H, Huang D, McArthur DL, Boros LG, Nissen N, Heaney AP. Fructose induces transketolase flux to promote pancreatic cancer growth. Cancer Res. 2010;70(15):6368-76.
- 453. Robinson AD, Eich ML, Varambally S. Dysregulation of de novo nucleotide biosynthetic pathway enzymes in cancer and targeting opportunities. Cancer Lett. 2020;470:134-40.
- 454. Ben-Sahra I, Manning BD. mTORC1 signaling and the metabolic control of cell growth. Curr Opin Cell Biol. 2017;45:72-82.
- 455. Traut TW. Physiological concentrations of purines and pyrimidines. Mol Cell Biochem. 1994;140(1):1-22.
- 456. Villa E, Ali ES, Sahu U, Ben-Sahra I. Cancer Cells Tune the Signaling Pathways to Empower de Novo Synthesis of Nucleotides. Cancers (Basel). 2019;11(5):688.

- 457. Cunningham JT, Moreno MV, Lodi A, Ronen SM, Ruggero D. Protein and nucleotide biosynthesis are coupled by a single rate-limiting enzyme, PRPS2, to drive cancer. Cell. 2014;157(5):1088-103.
- 458. Huang F, Ni M, Chalishazar MD, Huffman KE, Kim J, Cai L, et al. Inosine Monophosphate Dehydrogenase Dependence in a Subset of Small Cell Lung Cancers. Cell Metab. 2018;28(3):369-82.e5.
- 459. Evans DR, Guy HI. Mammalian pyrimidine biosynthesis: fresh insights into an ancient pathway. J Biol Chem. 2004;279(32):33035-8.
- 460. Lane AN, Fan TWM. Regulation of mammalian nucleotide metabolism and biosynthesis. Nucleic acids research. 2015;43(4):2466-85.
- 461. Cory JG, Sato A. Regulation of ribonucleotide reductase activity in mammalian cells. Mol Cell Biochem. 1983;53-54(1-2):257-66.
- 462. Sigoillot FD, Sigoillot SM, Guy HI. Breakdown of the regulatory control of pyrimidine biosynthesis in human breast cancer cells. Int J Cancer. 2004;109(4):491-8.
- 463. Semenza GL. HIF-1: upstream and downstream of cancer metabolism. Curr Opin Genet Dev. 2010;20(1):51-6.
- 464. Emami Nejad A, Najafgholian S, Rostami A, Sistani A, Shojaeifar S, Esparvarinha M, et al. The role of hypoxia in the tumor microenvironment and development of cancer stem cell: a novel approach to developing treatment. Cancer Cell International. 2021;21(1):62.
- 465. Muz B, de la Puente P, Azab F, Azab AK. The role of hypoxia in cancer progression, angiogenesis, metastasis, and resistance to therapy. Hypoxia (Auckl). 2015;3:83-92.

- 466. Nagao A, Kobayashi M, Koyasu S, Chow CCT, Harada H. HIF-1-Dependent Reprogramming of Glucose Metabolic Pathway of Cancer Cells and Its Therapeutic Significance. International journal of molecular sciences. 2019;20(2):238.
- 467. Semenza GL. Pharmacologic Targeting of Hypoxia-Inducible Factors. Annual Review of Pharmacology and Toxicology. 2019;59(1):379-403.
- 468. Hoefflin R, Harlander S, Schäfer S, Metzger P, Kuo F, Schönenberger D, et al. HIF- 1α and HIF- 2α differently regulate tumour development and inflammation of clear cell renal cell carcinoma in mice. Nature Communications. 2020;11(1):4111.
- 469. Lau KW, Tian YM, Raval RR, Ratcliffe PJ, Pugh CW. Target gene selectivity of hypoxia-inducible factor-α in renal cancer cells is conveyed by post-DNA-binding mechanisms. British Journal of Cancer. 2007;96(8):1284-92.
- 470. Semenza GL, Artemov D, Bedi A, Bhujwalla Z, Chiles K, Feldser D, et al. 'The Metabolism of Tumours': 70 Years Later. The Tumour Microenvironment: Causes and Consequences of Hypoxia and Acidity2001. p. 251-64.
- 471. Zhang H, Bosch-Marce M, Shimoda LA, Tan YS, Baek JH, Wesley JB, et al. Mitochondrial autophagy is an HIF-1-dependent adaptive metabolic response to hypoxia. J Biol Chem. 2008;283(16):10892-903.
- 472. Bellot G, Garcia-Medina R, Gounon P, Chiche J, Roux D, Pouysségur J, et al. Hypoxia-Induced Autophagy Is Mediated through Hypoxia-Inducible Factor Induction of BNIP3 and BNIP3L via Their BH3 Domains. Molecular and Cellular Biology. 2009;29(10):2570-81.
- 473. Gameiro PA, Yang J, Metelo AM, Pérez-Carro R, Baker R, Wang Z, et al. In vivo HIF-mediated reductive carboxylation is regulated by citrate levels and sensitizes VHL-deficient cells to glutamine deprivation. Cell Metab. 2013;17(3):372-85.

- 474. Sun RC, Denko NC. Hypoxic regulation of glutamine metabolism through HIF1 and SIAH2 supports lipid synthesis that is necessary for tumor growth. Cell Metab. 2014;19(2):285-92.
- 475. Chen H, Liu H, Qing G. Targeting oncogenic Myc as a strategy for cancer treatment. Signal Transduct Target Ther. 2018;3:5-.
- 476. Dong Y, Tu R, Liu H, Qing G. Regulation of cancer cell metabolism: oncogenic MYC in the driver's seat. Signal Transduct Target Ther. 2020;5(1):124.
- 477. Erisman MD, Rothberg PG, Diehl RE, Morse CC, Spandorfer JM, Astrin SM. Deregulation of c-myc gene expression in human colon carcinoma is not accompanied by amplification or rearrangement of the gene. Mol Cell Biol. 1985;5(8):1969-76.
- 478. Shachaf CM, Felsher DW. Tumor dormancy and MYC inactivation: pushing cancer to the brink of normalcy. Cancer Res. 2005;65(11):4471-4.
- 479. Soucek L, Whitfield J, Martins CP, Finch AJ, Murphy DJ, Sodir NM, et al. Modelling Myc inhibition as a cancer therapy. Nature. 2008;455(7213):679-83.
- 480. Morrish F, Neretti N, Sedivy JM, Hockenbery DM. The oncogene c-Myc coordinates regulation of metabolic networks to enable rapid cell cycle entry. Cell Cycle. 2008;7(8):1054-66.
- 481. Satoh K, Yachida S, Sugimoto M, Oshima M, Nakagawa T, Akamoto S, et al. Global metabolic reprogramming of colorectal cancer occurs at adenoma stage and is induced by MYC. Proceedings of the National Academy of Sciences. 2017;114(37):E7697-E706.
- 482. Kim JW, Zeller KI, Wang Y, Jegga AG, Aronow BJ, O'Donnell KA, et al. Evaluation of myc E-box phylogenetic footprints in glycolytic genes by chromatin immunoprecipitation assays. Mol Cell Biol. 2004;24(13):5923-36.

- 483. Gao P, Tchernyshyov I, Chang TC, Lee YS, Kita K, Ochi T, et al. c-Myc suppression of miR-23a/b enhances mitochondrial glutaminase expression and glutamine metabolism. Nature. 2009;458(7239):762-5.
- 484. Sun L, Song L, Wan Q, Wu G, Li X, Wang Y, et al. cMyc-mediated activation of serine biosynthesis pathway is critical for cancer progression under nutrient deprivation conditions. Cell Res. 2015;25(4):429-44.
- 485. Yue M, Jiang J, Gao P, Liu H, Qing G. Oncogenic MYC Activates a Feedforward Regulatory Loop Promoting Essential Amino Acid Metabolism and Tumorigenesis. Cell Rep. 2017;21(13):3819-32.
- 486. Wise DR, DeBerardinis RJ, Mancuso A, Sayed N, Zhang XY, Pfeiffer HK, et al. Myc regulates a transcriptional program that stimulates mitochondrial glutaminolysis and leads to glutamine addiction. Proc Natl Acad Sci U S A. 2008;105(48):18782-7.
- 487. Eberhardy SR, Farnham PJ. c-Myc mediates activation of the cad promoter via a post-RNA polymerase II recruitment mechanism. J Biol Chem. 2001;276(51):48562-71.
- 488. Mannava S, Grachtchouk V, Wheeler LJ, Im M, Zhuang D, Slavina EG, et al. Direct role of nucleotide metabolism in C-MYC-dependent proliferation of melanoma cells. Cell Cycle. 2008;7(15):2392-400.
- 489. Chiodi I, Perini C, Berardi D, Mondello C. Asparagine sustains cellular proliferation and c-Myc expression in glutamine-starved cancer cells. Oncol Rep. 2021;45(6).
- 490. Javeshghani S, Zakikhani M, Austin S, Bazile M, Blouin MJ, Topisirovic I, et al. Carbon source and myc expression influence the antiproliferative actions of metformin. Cancer Res. 2012;72(23):6257-67.

- 491. Liu J, Zhang C, Hu W, Feng Z. Tumor suppressor p53 and metabolism. J Mol Cell Biol. 2019;11(4):284-92.
- 492. Takayama T, Miyanishi K, Hayashi T, Sato Y, Niitsu Y. Colorectal cancer: genetics of development and metastasis. J Gastroenterol. 2006;41(3):185-92.
- 493. Jackson JG, Post SM, Lozano G. Regulation of tissue- and stimulus-specific cell fate decisions by p53 in vivo. J Pathol. 2011;223(2):127-36.
- 494. Schwartzenberg-Bar-Yoseph F, Armoni M, Karnieli E. The tumor suppressor p53 down-regulates glucose transporters GLUT1 and GLUT4 gene expression. Cancer Res. 2004;64(7):2627-33.
- 495. Kawauchi K, Araki K, Tobiume K, Tanaka N. p53 regulates glucose metabolism through an IKK-NF-kappaB pathway and inhibits cell transformation. Nat Cell Biol. 2008;10(5):611-8.
- 496. Wang L, Xiong H, Wu F, Zhang Y, Wang J, Zhao L, et al. Hexokinase 2-mediated Warburg effect is required for PTEN- and p53-deficiency-driven prostate cancer growth. Cell reports. 2014;8(5):1461-74.
- 497. Kondoh H, Lleonart ME, Gil J, Wang J, Degan P, Peters G, et al. Glycolytic enzymes can modulate cellular life span. Cancer Res. 2005;65(1):177-85.
- 498. Bensaad K, Tsuruta A, Selak MA, Vidal MN, Nakano K, Bartrons R, et al. TIGAR, a p53-inducible regulator of glycolysis and apoptosis. Cell. 2006;126(1):107-20.
- 499. Matoba S, Kang JG, Patino WD, Wragg A, Boehm M, Gavrilova O, et al. p53 regulates mitochondrial respiration. Science. 2006;312(5780):1650-3.
- 500. Cairns RA, Harris IS, Mak TW. Regulation of cancer cell metabolism. Nature Reviews Cancer. 2011;11(2):85-95.

- 501. Roberts PJ, Der CJ. Targeting the Raf-MEK-ERK mitogen-activated protein kinase cascade for the treatment of cancer. Oncogene. 2007;26(22):3291-310.
- 502. Chang F, Steelman LS, Lee JT, Shelton JG, Navolanic PM, Blalock WL, et al. Signal transduction mediated by the Ras/Raf/MEK/ERK pathway from cytokine receptors to transcription factors: potential targeting for therapeutic intervention. Leukemia. 2003;17(7):1263-93.
- 503. Yang W, Zheng Y, Xia Y, Ji H, Chen X, Guo F, et al. ERK1/2-dependent phosphorylation and nuclear translocation of PKM2 promotes the Warburg effect. Nat Cell Biol. 2012;14(12):1295-304.
- 504. Cox AD, Fesik SW, Kimmelman AC, Luo J, Der CJ. Drugging the undruggable RAS: Mission possible? Nature reviews Drug discovery. 2014;13(11):828-51.
- 505. Pylayeva-Gupta Y, Grabocka E, Bar-Sagi D. RAS oncogenes: weaving a tumorigenic web. Nature reviews Cancer. 2011;11(11):761-74.
- 506. Kimmelman AC. Metabolic Dependencies in RAS-Driven Cancers. Clinical cancer research: an official journal of the American Association for Cancer Research. 2015;21(8):1828-34.
- 507. Gaglio D, Metallo CM, Gameiro PA, Hiller K, Danna LS, Balestrieri C, et al. Oncogenic K-Ras decouples glucose and glutamine metabolism to support cancer cell growth. Mol Syst Biol. 2011;7:523-.
- 508. Ying H, Kimmelman AC, Lyssiotis CA, Hua S, Chu GC, Fletcher-Sananikone E, et al. Oncogenic Kras maintains pancreatic tumors through regulation of anabolic glucose metabolism. Cell. 2012;149(3):656-70.
- 509. Amendola CR, Mahaffey JP, Parker SJ, Ahearn IM, Chen W-C, Zhou M, et al. KRAS4A directly regulates hexokinase 1. Nature. 2019;576(7787):482-6.

- 510. Santana-Codina N, Roeth AA, Zhang Y, Yang A, Mashadova O, Asara JM, et al. Oncogenic KRAS supports pancreatic cancer through regulation of nucleotide synthesis. Nature communications. 2018;9(1):4945-.
- 511. Roskoski R. RAF protein-serine/threonine kinases: Structure and regulation. Biochemical and Biophysical Research Communications. 2010;399(3):313-7.
- 512. Guo YJ, Pan WW, Liu SB, Shen ZF, Xu Y, Hu LL. ERK/MAPK signalling pathway and tumorigenesis (Review). Exp Ther Med. 2020;19(3):1997-2007.
- 513. Davies H, Bignell GR, Cox C, Stephens P, Edkins S, Clegg S, et al. Mutations of the BRAF gene in human cancer. Nature. 2002;417(6892):949-54.
- 514. Papa S, Choy PM, Bubici C. The ERK and JNK pathways in the regulation of metabolic reprogramming. Oncogene. 2019;38(13):2223-40.
- 515. Parmenter TJ, Kleinschmidt M, Kinross KM, Bond ST, Li J, Kaadige MR, et al. Response of BRAF-mutant melanoma to BRAF inhibition is mediated by a network of transcriptional regulators of glycolysis. Cancer Discov. 2014;4(4):423-33.
- 516. Yun J, Rago C, Cheong I, Pagliarini R, Angenendt P, Rajagopalan H, et al. Glucose deprivation contributes to the development of KRAS pathway mutations in tumor cells. Science. 2009;325(5947):1555-9.
- 517. Hall A, Meyle KD, Lange MK, Klima M, Sanderhoff M, Dahl C, et al. Dysfunctional oxidative phosphorylation makes malignant melanoma cells addicted to glycolysis driven by the (V600E)BRAF oncogene. Oncotarget. 2013;4(4):584-99.
- 518. Haq R, Shoag J, Andreu-Perez P, Yokoyama S, Edelman H, Rowe GC, et al. Oncogenic BRAF regulates oxidative metabolism via PGC1α and MITF. Cancer cell. 2013;23(3):302-15.

- 519. Kahn BB, Alquier T, Carling D, Hardie DG. AMP-activated protein kinase: ancient energy gauge provides clues to modern understanding of metabolism. Cell Metab. 2005;1(1):15-25.
- 520. Shaw RJ. LKB1 and AMP-activated protein kinase control of mTOR signalling and growth. Acta Physiol (Oxf). 2009;196(1):65-80.
- 521. Hardie DG, Scott JW, Pan DA, Hudson ER. Management of cellular energy by the AMP-activated protein kinase system. FEBS Lett. 2003;546(1):113-20.
- 522. Carling D. The AMP-activated protein kinase cascade--a unifying system for energy control. Trends Biochem Sci. 2004;29(1):18-24.
- 523. Garcia D, Shaw RJ. AMPK: Mechanisms of Cellular Energy Sensing and Restoration of Metabolic Balance. Mol Cell. 2017;66(6):789-800.
- 524. Sanders MJ, Grondin PO, Hegarty BD, Snowden MA, Carling D. Investigating the mechanism for AMP activation of the AMP-activated protein kinase cascade. Biochem J. 2007;403(1):139-48.
- 525. Hardie DG, Carling D, Gamblin SJ. AMP-activated protein kinase: also regulated by ADP? Trends Biochem Sci. 2011;36(9):470-7.
- 526. Gowans GJ, Hawley SA, Ross FA, Hardie DG. AMP is a true physiological regulator of AMP-activated protein kinase by both allosteric activation and enhancing net phosphorylation. Cell metabolism. 2013;18(4):556-66.
- 527. Xiao B, Sanders MJ, Underwood E, Heath R, Mayer FV, Carmena D, et al. Structure of mammalian AMPK and its regulation by ADP. Nature. 2011;472(7342):230-3.
- 528. Hardie DG. AMP-activated/SNF1 protein kinases: conserved guardians of cellular energy. Nat Rev Mol Cell Biol. 2007;8(10):774-85.

- 529. Willows R, Navaratnam N, Lima A, Read J, Carling D. Effect of different γ -subunit isoforms on the regulation of AMPK. Biochemical Journal. 2017;474(10):1741-54.
- 530. Boudeau J, Miranda-Saavedra D, Barton GJ, Alessi DR. Emerging roles of pseudokinases. Trends Cell Biol. 2006;16(9):443-52.
- 531. Alessi DR, Sakamoto K, Bayascas JR. LKB1-dependent signaling pathways. Annu Rev Biochem. 2006;75:137-63.
- 532. Shackelford DB, Shaw RJ. The LKB1-AMPK pathway: metabolism and growth control in tumour suppression. Nat Rev Cancer. 2009;9(8):563-75.
- 533. Hurley RL, Anderson KA, Franzone JM, Kemp BE, Means AR, Witters LA. The Ca2+/calmodulin-dependent protein kinase kinases are AMP-activated protein kinase kinases. J Biol Chem. 2005;280(32):29060-6.
- 534. Marcelo KL, Means AR, York B. The Ca(2+)/Calmodulin/CaMKK2 Axis: Nature's Metabolic CaMshaft. Trends in endocrinology and metabolism: TEM. 2016;27(10):706-18.
- 535. Ghislat G, Patron M, Rizzuto R, Knecht E. Withdrawal of essential amino acids increases autophagy by a pathway involving Ca2+/calmodulin-dependent kinase kinase-β (CaMKK-β). J Biol Chem. 2012;287(46):38625-36.
- 536. Mungai PT, Waypa GB, Jairaman A, Prakriya M, Dokic D, Ball MK, et al. Hypoxia triggers AMPK activation through reactive oxygen species-mediated activation of calcium release-activated calcium channels. Molecular and cellular biology. 2011;31(17):3531-45.
- 537. Sallé-Lefort S, Miard S, Nolin MA, Boivin L, Paré M, Debigaré R, et al. Hypoxia upregulates Malat1 expression through a CaMKK/AMPK/HIF-1α axis. Int J Oncol. 2016;49(4):1731-6.

- 538. Zhang CS, Jiang B, Li M, Zhu M, Peng Y, Zhang YL, et al. The lysosomal v-ATPase-Ragulator complex is a common activator for AMPK and mTORC1, acting as a switch between catabolism and anabolism. Cell Metab. 2014;20(3):526-40.
- 539. Zhang YL, Guo H, Zhang CS, Lin SY, Yin Z, Peng Y, et al. AMP as a low-energy charge signal autonomously initiates assembly of AXIN-AMPK-LKB1 complex for AMPK activation. Cell Metab. 2013;18(4):546-55.
- 540. Shao D, Oka S, Liu T, Zhai P, Ago T, Sciarretta S, et al. A redox-dependent mechanism for regulation of AMPK activation by Thioredoxin1 during energy starvation. Cell Metab. 2014;19(2):232-45.
- 541. Zmijewski JW, Banerjee S, Bae H, Friggeri A, Lazarowski ER, Abraham E. Exposure to hydrogen peroxide induces oxidation and activation of AMP-activated protein kinase. J Biol Chem. 2010;285(43):33154-64.
- 542. Wu N, Zheng B, Shaywitz A, Dagon Y, Tower C, Bellinger G, et al. AMPK-dependent degradation of TXNIP upon energy stress leads to enhanced glucose uptake via GLUT1. Mol Cell. 2013;49(6):1167-75.
- 543. Bultot L, Guigas B, Von Wilamowitz-Moellendorff A, Maisin L, Vertommen D, Hussain N, et al. AMP-activated protein kinase phosphorylates and inactivates liver glycogen synthase. Biochem J. 2012;443(1):193-203.
- 544. Koo SH, Flechner L, Qi L, Zhang X, Screaton RA, Jeffries S, et al. The CREB coactivator TORC2 is a key regulator of fasting glucose metabolism. Nature. 2005;437(7062):1109-11.
- 545. Carling D, Zammit VA, Hardie DG. A common bicyclic protein kinase cascade inactivates the regulatory enzymes of fatty acid and cholesterol biosynthesis. FEBS Lett. 1987;223(2):217-22.

- 546. Inoki K, Zhu T, Guan KL. TSC2 mediates cellular energy response to control cell growth and survival. Cell. 2003;115(5):577-90.
- 547. Gwinn DM, Shackelford DB, Egan DF, Mihaylova MM, Mery A, Vasquez DS, et al. AMPK phosphorylation of raptor mediates a metabolic checkpoint. Mol Cell. 2008;30(2):214-26.
- 548. Leprivier G, Remke M, Rotblat B, Dubuc A, Mateo AR, Kool M, et al. The eEF2 kinase confers resistance to nutrient deprivation by blocking translation elongation. Cell. 2013;153(5):1064-79.
- 549. Browne GJ, Proud CG. A novel mTOR-regulated phosphorylation site in elongation factor 2 kinase modulates the activity of the kinase and its binding to calmodulin. Mol Cell Biol. 2004;24(7):2986-97.
- 550. Zadra G, Photopoulos C, Tyekucheva S, Heidari P, Weng QP, Fedele G, et al. A novel direct activator of AMPK inhibits prostate cancer growth by blocking lipogenesis. EMBO Mol Med. 2014;6(4):519-38.
- 551. Huang X, Wullschleger S, Shpiro N, McGuire VA, Sakamoto K, Woods YL, et al. Important role of the LKB1-AMPK pathway in suppressing tumorigenesis in PTEN-deficient mice. Biochem J. 2008;412(2):211-21.
- 552. Faubert B, Boily G, Izreig S, Griss T, Samborska B, Dong Z, et al. AMPK is a negative regulator of the Warburg effect and suppresses tumor growth in vivo. Cell Metab. 2013;17(1):113-24.
- 553. Faubert B, Vincent EE, Poffenberger MC, Jones RG. The AMP-activated protein kinase (AMPK) and cancer: many faces of a metabolic regulator. Cancer Lett. 2015;356(2 Pt A):165-70.
- 554. Jeon S-M, Chandel NS, Hay N. AMPK regulates NADPH homeostasis to promote tumour cell survival during energy stress. Nature. 2012;485(7400):661-5.

- 555. Vara-Ciruelos D, Russell FM, Hardie DG. The strange case of AMPK and cancer: Dr Jekyll or Mr Hyde? (†). Open Biol. 2019;9(7):190099.
- 556. Laplante M, Sabatini DM. mTOR signaling at a glance. J Cell Sci. 2009;122(Pt 20):3589-94.
- 557. Ruggero D, Sonenberg N. The Akt of translational control. Oncogene. 2005;24(50):7426-34.
- 558. Schlessinger J. Ligand-induced, receptor-mediated dimerization and activation of EGF receptor. Cell. 2002;110(6):669-72.
- 559. Lemmon MA, Schlessinger J. Cell signaling by receptor tyrosine kinases. Cell. 2010;141(7):1117-34.
- 560. Domchek SM, Auger KR, Chatterjee S, Burke TR, Jr., Shoelson SE. Inhibition of SH2 domain/phosphoprotein association by a nonhydrolyzable phosphonopeptide. Biochemistry. 1992;31(41):9865-70.
- 561. Alessi DR, James SR, Downes CP, Holmes AB, Gaffney PR, Reese CB, et al. Characterization of a 3-phosphoinositide-dependent protein kinase which phosphorylates and activates protein kinase Balpha. Curr Biol. 1997;7(4):261-9.
- 562. Stambolic V, Suzuki A, de la Pompa JL, Brothers GM, Mirtsos C, Sasaki T, et al. Negative regulation of PKB/Akt-dependent cell survival by the tumor suppressor PTEN. Cell. 1998;95(1):29-39.
- 563. Deprez J, Vertommen D, Alessi DR, Hue L, Rider MH. Phosphorylation and activation of heart 6-phosphofructo-2-kinase by protein kinase B and other protein kinases of the insulin signaling cascades. J Biol Chem. 1997;272(28):17269-75.

- 564. Kohn AD, Summers SA, Birnbaum MJ, Roth RA. Expression of a constitutively active Akt Ser/Thr kinase in 3T3-L1 adipocytes stimulates glucose uptake and glucose transporter 4 translocation. J Biol Chem. 1996;271(49):31372-8.
- 565. Uchenunu O, Pollak M, Topisirovic I, Hulea L. Oncogenic kinases and perturbations in protein synthesis machinery and energetics in neoplasia. J Mol Endocrinol. 2019;62(2):R83-r103.
- 566. Wullschleger S, Loewith R, Hall MN. TOR signaling in growth and metabolism. Cell. 2006;124(3):471-84.
- 567. Wang L, Harris TE, Lawrence JC. Regulation of proline-rich Akt substrate of 40 kDa (PRAS40) function by mammalian target of rapamycin complex 1 (mTORC1)-mediated phosphorylation. Journal of Biological Chemistry. 2008;283(23):15619-27.
- 568. Jacinto E, Facchinetti V, Liu D, Soto N, Wei S, Jung SY, et al. SIN1/MIP1 maintains rictormTOR complex integrity and regulates Akt phosphorylation and substrate specificity. Cell. 2006;127(1):125-37.
- 569. Yang Q, Inoki K, Ikenoue T, Guan K-L. Identification of Sin1 as an essential TORC2 component required for complex formation and kinase activity. Genes & development. 2006;20(20):2820-32.
- 570. Saxton RA, Sabatini DM. mTOR Signaling in Growth, Metabolism, and Disease. Cell. 2017;168(6):960-76.
- 571. Düvel K, Yecies JL, Menon S, Raman P, Lipovsky AI, Souza AL, et al. Activation of a metabolic gene regulatory network downstream of mTOR complex 1. Mol Cell. 2010;39(2):171-83.
- 572. Alessi DR, Pearce LR, García-Martínez JM. New insights into mTOR signaling: mTORC2 and beyond. Science signaling. 2009;2(67):pe27-pe.

- 573. Destefano MA, Jacinto E. Regulation of insulin receptor substrate-1 by mTORC2 (mammalian target of rapamycin complex 2). Biochem Soc Trans. 2013;41(4):896-901.
- 574. Jacinto E, Loewith R, Schmidt A, Lin S, Rüegg MA, Hall A, et al. Mammalian TOR complex 2 controls the actin cytoskeleton and is rapamycin insensitive. Nat Cell Biol. 2004;6(11):1122-8.
- 575. Sarbassov DD, Ali SM, Kim DH, Guertin DA, Latek RR, Erdjument-Bromage H, et al. Rictor, a novel binding partner of mTOR, defines a rapamycin-insensitive and raptor-independent pathway that regulates the cytoskeleton. Curr Biol. 2004;14(14):1296-302.
- 576. Gan X, Wang J, Wang C, Sommer E, Kozasa T, Srinivasula S, et al. PRR5L degradation promotes mTORC2-mediated PKC-δ phosphorylation and cell migration downstream of Gα12. Nat Cell Biol. 2012;14(7):686-96.
- 577. Li X, Gao T. mTORC2 phosphorylates protein kinase Cζ to regulate its stability and activity. EMBO Rep. 2014;15(2):191-8.
- 578. Thomanetz V, Angliker N, Cloëtta D, Lustenberger RM, Schweighauser M, Oliveri F, et al. Ablation of the mTORC2 component rictor in brain or Purkinje cells affects size and neuron morphology. J Cell Biol. 2013;201(2):293-308.
- 579. García-Martínez JM, Alessi DR. mTOR complex 2 (mTORC2) controls hydrophobic motif phosphorylation and activation of serum- and glucocorticoid-induced protein kinase 1 (SGK1). Biochem J. 2008;416(3):375-85.
- 580. Lu M, Wang J, Ives HE, Pearce D. mSIN1 protein mediates SGK1 protein interaction with mTORC2 protein complex and is required for selective activation of the epithelial sodium channel. J Biol Chem. 2011;286(35):30647-54.

- 581. Zech R, Kiontke S, Mueller U, Oeckinghaus A, Kümmel D. Structure of the Tuberous Sclerosis Complex 2 (TSC2) N Terminus Provides Insight into Complex Assembly and Tuberous Sclerosis Pathogenesis. The Journal of biological chemistry. 2016;291(38):20008-20.
- 582. Sancak Y, Thoreen CC, Peterson TR, Lindquist RA, Kang SA, Spooner E, et al. PRAS40 is an insulin-regulated inhibitor of the mTORC1 protein kinase. Mol Cell. 2007;25(6):903-15.
- 583. Long X, Lin Y, Ortiz-Vega S, Yonezawa K, Avruch J. Rheb binds and regulates the mTOR kinase. Curr Biol. 2005;15(8):702-13.
- 584. DeYoung MP, Horak P, Sofer A, Sgroi D, Ellisen LW. Hypoxia regulates TSC1/2-mTOR signaling and tumor suppression through REDD1-mediated 14-3-3 shuttling. Genes & development. 2008;22(2):239-51.
- 585. Dennis MD, Coleman CS, Berg A, Jefferson LS, Kimball SR. REDD1 enhances protein phosphatase 2A-mediated dephosphorylation of Akt to repress mTORC1 signaling. Sci Signal. 2014;7(335):ra68.
- 586. Li XH, Ha CT, Fu D, Xiao M. REDD1 protects osteoblast cells from gamma radiation-induced premature senescence. PLoS One. 2012;7(5):e36604.
- 587. Ma L, Chen Z, Erdjument-Bromage H, Tempst P, Pandolfi PP. Phosphorylation and functional inactivation of TSC2 by Erk implications for tuberous sclerosis and cancer pathogenesis. Cell. 2005;121(2):179-93.
- 588. Carriere A, Romeo Y, Acosta-Jaquez HA, Moreau J, Bonneil E, Thibault P, et al. ERK1/2 phosphorylate Raptor to promote Ras-dependent activation of mTOR complex 1 (mTORC1). J Biol Chem. 2011;286(1):567-77.
- 589. Hobbs GA, Der CJ, Rossman KL. RAS isoforms and mutations in cancer at a glance. J Cell Sci. 2016;129(7):1287-92.

- 590. Rajalingam K, Schreck R, Rapp UR, Albert S. Ras oncogenes and their downstream targets. Biochim Biophys Acta. 2007;1773(8):1177-95.
- 591. Ballif BA, Roux PP, Gerber SA, MacKeigan JP, Blenis J, Gygi SP. Quantitative phosphorylation profiling of the ERK/p90 ribosomal S6 kinase-signaling cassette and its targets, the tuberous sclerosis tumor suppressors. Proc Natl Acad Sci U S A. 2005;102(3):667-72.
- 592. Carrière A, Cargnello M, Julien LA, Gao H, Bonneil E, Thibault P, et al. Oncogenic MAPK signaling stimulates mTORC1 activity by promoting RSK-mediated raptor phosphorylation. Curr Biol. 2008;18(17):1269-77.
- 593. Romeo Y, Moreau J, Zindy PJ, Saba-El-Leil M, Lavoie G, Dandachi F, et al. RSK regulates activated BRAF signalling to mTORC1 and promotes melanoma growth. Oncogene. 2013;32(24):2917-26.
- 594. Roux PP, Ballif BA, Anjum R, Gygi SP, Blenis J. Tumor-promoting phorbol esters and activated Ras inactivate the tuberous sclerosis tumor suppressor complex via p90 ribosomal S6 kinase. Proc Natl Acad Sci U S A. 2004;101(37):13489-94.
- 595. Mendoza MC, Er EE, Blenis J. The Ras-ERK and PI3K-mTOR pathways: cross-talk and compensation. Trends Biochem Sci. 2011;36(6):320-8.
- 596. Lehr S, Kotzka J, Avci H, Sickmann A, Meyer HE, Herkner A, et al. Identification of major ERK-related phosphorylation sites in Gab1. Biochemistry. 2004;43(38):12133-40.
- 597. Zhang SQ, Tsiaras WG, Araki T, Wen G, Minichiello L, Klein R, et al. Receptor-specific regulation of phosphatidylinositol 3'-kinase activation by the protein tyrosine phosphatase Shp2. Mol Cell Biol. 2002;22(12):4062-72.
- 598. Zimmermann S, Moelling K. Phosphorylation and Regulation of Raf by Akt (Protein Kinase B). Science. 1999;286(5445):1741-4.

- 599. Moelling K, Schad K, Bosse M, Zimmermann S, Schweneker M. Regulation of Raf-Akt Cross-talk. J Biol Chem. 2002;277(34):31099-106.
- 600. Cheung M, Sharma A, Madhunapantula SV, Robertson GP. Akt3 and mutant V600E B-Raf cooperate to promote early melanoma development. Cancer Res. 2008;68(9):3429-39.
- 601. Shaw RJ, Cantley LC. Ras, PI(3)K and mTOR signalling controls tumour cell growth. Nature. 2006;441(7092):424-30.
- 602. Inoki K, Li Y, Xu T, Guan KL. Rheb GTPase is a direct target of TSC2 GAP activity and regulates mTOR signaling. Genes Dev. 2003;17(15):1829-34.
- 603. Efeyan A, Zoncu R, Chang S, Gumper I, Snitkin H, Wolfson RL, et al. Regulation of mTORC1 by the Rag GTPases is necessary for neonatal autophagy and survival. Nature. 2013;493(7434):679-83.
- 604. Kalender A, Selvaraj A, Kim SY, Gulati P, Brûlé S, Viollet B, et al. Metformin, independent of AMPK, inhibits mTORC1 in a rag GTPase-dependent manner. Cell Metab. 2010;11(5):390-401.
- 605. Kim E, Goraksha-Hicks P, Li L, Neufeld TP, Guan KL. Regulation of TORC1 by Rag GTPases in nutrient response. Nat Cell Biol. 2008;10(8):935-45.
- 606. Sancak Y, Peterson TR, Shaul YD, Lindquist RA, Thoreen CC, Bar-Peled L, et al. The Rag GTPases bind raptor and mediate amino acid signaling to mTORC1. Science. 2008;320(5882):1496-501.
- 607. Sancak Y, Bar-Peled L, Zoncu R, Markhard AL, Nada S, Sabatini DM. Ragulator-Rag complex targets mTORC1 to the lysosomal surface and is necessary for its activation by amino acids. Cell. 2010;141(2):290-303.

- 608. Bar-Peled L, Schweitzer LD, Zoncu R, Sabatini DM. Ragulator is a GEF for the rag GTPases that signal amino acid levels to mTORC1. Cell. 2012;150(6):1196-208.
- 609. Tsun ZY, Bar-Peled L, Chantranupong L, Zoncu R, Wang T, Kim C, et al. The folliculin tumor suppressor is a GAP for the RagC/D GTPases that signal amino acid levels to mTORC1. Mol Cell. 2013;52(4):495-505.
- 610. Petit CS, Roczniak-Ferguson A, Ferguson SM. Recruitment of folliculin to lysosomes supports the amino acid-dependent activation of Rag GTPases. J Cell Biol. 2013;202(7):1107-22.
- 611. Jewell JL, Kim YC, Russell RC, Yu FX, Park HW, Plouffe SW, et al. Metabolism. Differential regulation of mTORC1 by leucine and glutamine. Science. 2015;347(6218):194-8.
- 612. Meng D, Yang Q, Wang H, Melick CH, Navlani R, Frank AR, et al. Glutamine and asparagine activate mTORC1 independently of Rag GTPases. J Biol Chem. 2020;295(10):2890-9.
- 613. Stracka D, Jozefczuk S, Rudroff F, Sauer U, Hall MN. Nitrogen source activates TOR (target of rapamycin) complex 1 via glutamine and independently of Gtr/Rag proteins. J Biol Chem. 2014;289(36):25010-20.
- 614. Bar-Peled L, Chantranupong L, Cherniack AD, Chen WW, Ottina KA, Grabiner BC, et al. A Tumor suppressor complex with GAP activity for the Rag GTPases that signal amino acid sufficiency to mTORC1. Science. 2013;340(6136):1100-6.
- 615. Wolfson RL, Chantranupong L, Wyant GA, Gu X, Orozco JM, Shen K, et al. KICSTOR recruits GATOR1 to the lysosome and is necessary for nutrients to regulate mTORC1. Nature. 2017;543(7645):438-42.
- 616. Chantranupong L, Scaria SM, Saxton RA, Gygi MP, Shen K, Wyant GA, et al. The CASTOR Proteins Are Arginine Sensors for the mTORC1 Pathway. Cell. 2016;165(1):153-64.

- 617. Saxton RA, Chantranupong L, Knockenhauer KE, Schwartz TU, Sabatini DM. Mechanism of arginine sensing by CASTOR1 upstream of mTORC1. Nature. 2016;536(7615):229-33.
- 618. Parmigiani A, Nourbakhsh A, Ding B, Wang W, Kim YC, Akopiants K, et al. Sestrins inhibit mTORC1 kinase activation through the GATOR complex. Cell Rep. 2014;9(4):1281-91.
- 619. Saxton RA, Knockenhauer KE, Wolfson RL, Chantranupong L, Pacold ME, Wang T, et al. Structural basis for leucine sensing by the Sestrin2-mTORC1 pathway. Science. 2016;351(6268):53-8.
- 620. Wolfson RL, Chantranupong L, Saxton RA, Shen K, Scaria SM, Cantor JR, et al. Sestrin2 is a leucine sensor for the mTORC1 pathway. Science. 2016;351(6268):43-8.
- 621. Menon D, Salloum D, Bernfeld E, Gorodetsky E, Akselrod A, Frias MA, et al. Lipid sensing by mTOR complexes via de novo synthesis of phosphatidic acid. J Biol Chem. 2017;292(15):6303-11.
- 622. Hoxhaj G, Hughes-Hallett J, Timson RC, Ilagan E, Yuan M, Asara JM, et al. The mTORC1 Signaling Network Senses Changes in Cellular Purine Nucleotide Levels. Cell Rep. 2017;21(5):1331-46.
- 623. Dalle Pezze P, Sonntag AG, Thien A, Prentzell MT, Gödel M, Fischer S, et al. A dynamic network model of mTOR signaling reveals TSC-independent mTORC2 regulation. Science signaling. 2012;5(217):ra25-ra.
- 624. Liu P, Gan W, Chin YR, Ogura K, Guo J, Zhang J, et al. PtdIns(3,4,5)P3-Dependent Activation of the mTORC2 Kinase Complex. Cancer Discov. 2015;5(11):1194-209.
- 625. Zinzalla V, Stracka D, Oppliger W, Hall MN. Activation of mTORC2 by association with the ribosome. Cell. 2011;144(5):757-68.

- 626. Yang G, Murashige DS, Humphrey SJ, James DE. A Positive Feedback Loop between Akt and mTORC2 via SIN1 Phosphorylation. Cell Rep. 2015;12(6):937-43.
- 627. Harrington LS, Findlay GM, Gray A, Tolkacheva T, Wigfield S, Rebholz H, et al. The TSC1-2 tumor suppressor controls insulin-PI3K signaling via regulation of IRS proteins. J Cell Biol. 2004;166(2):213-23.
- 628. Shah OJ, Wang Z, Hunter T. Inappropriate activation of the TSC/Rheb/mTOR/S6K cassette induces IRS1/2 depletion, insulin resistance, and cell survival deficiencies. Curr Biol. 2004;14(18):1650-6.
- 629. Shepherd PR, Withers DJ, Siddle K. Phosphoinositide 3-kinase: the key switch mechanism in insulin signalling. Biochem J. 1998;333 (Pt 3)(Pt 3):471-90.
- 630. Hsu PP, Kang SA, Rameseder J, Zhang Y, Ottina KA, Lim D, et al. The mTOR-regulated phosphoproteome reveals a mechanism of mTORC1-mediated inhibition of growth factor signaling. Science. 2011;332(6035):1317-22.
- 631. Yu Y, Yoon SO, Poulogiannis G, Yang Q, Ma XM, Villén J, et al. Phosphoproteomic analysis identifies Grb10 as an mTORC1 substrate that negatively regulates insulin signaling. Science. 2011;332(6035):1322-6.
- 632. Kazyken D, Magnuson B, Bodur C, Acosta-Jaquez HA, Zhang D, Tong X, et al. AMPK directly activates mTORC2 to promote cell survival during acute energetic stress. Sci Signal. 2019;12(585).
- 633. Jacinto E. Amplifying mTORC2 signals through AMPK during energetic stress. Sci Signal. 2019;12(585).
- 634. Sengupta S, Peterson TR, Laplante M, Oh S, Sabatini DM. mTORC1 controls fasting-induced ketogenesis and its modulation by ageing. Nature. 2010;468(7327):1100-4.

- 635. Mori H, Inoki K, Opland D, Münzberg H, Villanueva EC, Faouzi M, et al. Critical roles for the TSC-mTOR pathway in β -cell function. Am J Physiol Endocrinol Metab. 2009;297(5):E1013-22.
- 636. Shigeyama Y, Kobayashi T, Kido Y, Hashimoto N, Asahara S, Matsuda T, et al. Biphasic response of pancreatic beta-cell mass to ablation of tuberous sclerosis complex 2 in mice. Mol Cell Biol. 2008;28(9):2971-9.
- 637. Khamzina L, Veilleux A, Bergeron S, Marette A. Increased activation of the mammalian target of rapamycin pathway in liver and skeletal muscle of obese rats: possible involvement in obesity-linked insulin resistance. Endocrinology. 2005;146(3):1473-81.
- 638. Um SH, Frigerio F, Watanabe M, Picard F, Joaquin M, Sticker M, et al. Absence of S6K1 protects against age- and diet-induced obesity while enhancing insulin sensitivity. Nature. 2004;431(7005):200-5.
- 639. Ardestani A, Lupse B, Kido Y, Leibowitz G, Maedler K. mTORC1 Signaling: A Double-Edged Sword in Diabetic β Cells. Cell Metab. 2018;27(2):314-31.
- 640. Yuan T, Rafizadeh S, Gorrepati KD, Lupse B, Oberholzer J, Maedler K, et al. Reciprocal regulation of mTOR complexes in pancreatic islets from humans with type 2 diabetes. Diabetologia. 2017;60(4):668-78.
- 641. Hagiwara A, Cornu M, Cybulski N, Polak P, Betz C, Trapani F, et al. Hepatic mTORC2 activates glycolysis and lipogenesis through Akt, glucokinase, and SREBP1c. Cell Metab. 2012;15(5):725-38.
- 642. Yuan M, Pino E, Wu L, Kacergis M, Soukas AA. Identification of Akt-independent regulation of hepatic lipogenesis by mammalian target of rapamycin (mTOR) complex 2. J Biol Chem. 2012;287(35):29579-88.

- 643. Lamming DW, Ye L, Katajisto P, Goncalves MD, Saitoh M, Stevens DM, et al. Rapamycin-induced insulin resistance is mediated by mTORC2 loss and uncoupled from longevity. Science. 2012;335(6076):1638-43.
- 644. Kumar A, Harris TE, Keller SR, Choi KM, Magnuson MA, Lawrence JC, Jr. Musclespecific deletion of rictor impairs insulin-stimulated glucose transport and enhances Basal glycogen synthase activity. Mol Cell Biol. 2008;28(1):61-70.
- 645. Kumar A, Lawrence JC, Jr., Jung DY, Ko HJ, Keller SR, Kim JK, et al. Fat cell-specific ablation of rictor in mice impairs insulin-regulated fat cell and whole-body glucose and lipid metabolism. Diabetes. 2010;59(6):1397-406.
- 646. Lamming DW, Sabatini DM. A Central role for mTOR in lipid homeostasis. Cell Metab. 2013;18(4):465-9.
- 647. Szwed A, Kim E, Jacinto E. Regulation and metabolic functions of mTORC1 and mTORC2. Physiological Reviews. 2021;101(3):1371-426.
- 648. Porstmann T, Santos CR, Griffiths B, Cully M, Wu M, Leevers S, et al. SREBP activity is regulated by mTORC1 and contributes to Akt-dependent cell growth. Cell Metab. 2008;8(3):224-36.
- 649. Wan M, Leavens KF, Saleh D, Easton RM, Guertin DA, Peterson TR, et al. Postprandial hepatic lipid metabolism requires signaling through Akt2 independent of the transcription factors FoxA2, FoxO1, and SREBP1c. Cell Metab. 2011;14(4):516-27.
- 650. Lee PL, Tang Y, Li H, Guertin DA. Raptor/mTORC1 loss in adipocytes causes progressive lipodystrophy and fatty liver disease. Mol Metab. 2016;5(6):422-32.

- 651. Polak P, Cybulski N, Feige JN, Auwerx J, Rüegg MA, Hall MN. Adipose-specific knockout of raptor results in lean mice with enhanced mitochondrial respiration. Cell Metab. 2008;8(5):399-410.
- 652. Cybulski N, Polak P, Auwerx J, Rüegg MA, Hall MN. mTOR complex 2 in adipose tissue negatively controls whole-body growth. Proc Natl Acad Sci U S A. 2009;106(24):9902-7.
- 653. Bodine SC, Stitt TN, Gonzalez M, Kline WO, Stover GL, Bauerlein R, et al. Akt/mTOR pathway is a crucial regulator of skeletal muscle hypertrophy and can prevent muscle atrophy in vivo. Nat Cell Biol. 2001;3(11):1014-9.
- 654. Castets P, Lin S, Rion N, Di Fulvio S, Romanino K, Guridi M, et al. Sustained activation of mTORC1 in skeletal muscle inhibits constitutive and starvation-induced autophagy and causes a severe, late-onset myopathy. Cell Metab. 2013;17(5):731-44.
- 655. Peng Y, Wang Y, Zhou C, Mei W, Zeng C. PI3K/Akt/mTOR Pathway and Its Role in Cancer Therapeutics: Are We Making Headway? Front Oncol. 2022;12:819128.
- 656. Zhang Y, Kwok-Shing Ng P, Kucherlapati M, Chen F, Liu Y, Tsang YH, et al. A Pan-Cancer Proteogenomic Atlas of PI3K/AKT/mTOR Pathway Alterations. Cancer Cell. 2017;31(6):820-32.e3.
- 657. Carpten JD, Faber AL, Horn C, Donoho GP, Briggs SL, Robbins CM, et al. A transforming mutation in the pleckstrin homology domain of AKT1 in cancer. Nature. 2007;448(7152):439-44.
- 658. Liu P, Cheng H, Roberts TM, Zhao JJ. Targeting the phosphoinositide 3-kinase pathway in cancer. Nature Reviews Drug Discovery. 2009;8(8):627-44.
- 659. Grabiner BC, Nardi V, Birsoy K, Possemato R, Shen K, Sinha S, et al. A diverse array of cancer-associated MTOR mutations are hyperactivating and can predict rapamycin sensitivity. Cancer Discov. 2014;4(5):554-63.

- 660. Mossmann D, Park S, Hall MN. mTOR signalling and cellular metabolism are mutual determinants in cancer. Nature Reviews Cancer. 2018;18(12):744-57.
- 661. Brunn GJ, Hudson CC, Sekulić A, Williams JM, Hosoi H, Houghton PJ, et al. Phosphorylation of the translational repressor PHAS-I by the mammalian target of rapamycin. Science. 1997;277(5322):99-101.
- 662. Gingras AC, Raught B, Gygi SP, Niedzwiecka A, Miron M, Burley SK, et al. Hierarchical phosphorylation of the translation inhibitor 4E-BP1. Genes Dev. 2001;15(21):2852-64.
- 663. Roux PP, Topisirovic I. Regulation of mRNA translation by signaling pathways. Cold Spring Harbor perspectives in biology. 2012;4(11):a012252.
- 664. Sonenberg N, Hinnebusch AG. Regulation of translation initiation in eukaryotes: mechanisms and biological targets. Cell. 2009;136(4):731-45.
- 665. Gingras AC, Gygi SP, Raught B, Polakiewicz RD, Abraham RT, Hoekstra MF, et al. Regulation of 4E-BP1 phosphorylation: a novel two-step mechanism. Genes Dev. 1999;13(11):1422-37.
- 666. Hinnebusch AG. The Scanning Mechanism of Eukaryotic Translation Initiation. Annual Review of Biochemistry. 2014;83(1):779-812.
- 667. Hinnebusch AG. Structural Insights into the Mechanism of Scanning and Start Codon Recognition in Eukaryotic Translation Initiation. Trends in Biochemical Sciences. 2017;42(8):589-611.
- 668. Merrick WC, Pavitt GD. Protein Synthesis Initiation in Eukaryotic Cells. Cold Spring Harb Perspect Biol. 2018;10(12).
- 669. Shatsky IN, Terenin IM, Smirnova VV, Andreev DE. Cap-Independent Translation: What's in a Name? Trends Biochem Sci. 2018;43(11):882-95.

- 670. Wang X, Li W, Williams M, Terada N, Alessi DR, Proud CG. Regulation of elongation factor 2 kinase by p90(RSK1) and p70 S6 kinase. EMBO J. 2001;20(16):4370-9.
- 671. Redpath NT, Foulstone EJ, Proud CG. Regulation of translation elongation factor-2 by insulin via a rapamycin-sensitive signalling pathway. EMBO J. 1996;15(9):2291-7.
- 672. Buttgereit F, Brand MD. A hierarchy of ATP-consuming processes in mammalian cells. Biochem J. 1995;312 (Pt 1)(Pt 1):163-7.
- 673. Morita M, Gravel SP, Hulea L, Larsson O, Pollak M, St-Pierre J, et al. mTOR coordinates protein synthesis, mitochondrial activity and proliferation. Cell Cycle. 2015;14(4):473-80.
- 674. Meyuhas O, Dreazen A. Ribosomal protein S6 kinase from TOP mRNAs to cell size. Prog Mol Biol Transl Sci. 2009;90:109-53.
- 675. Larsson O, Morita M, Topisirovic I, Alain T, Blouin MJ, Pollak M, et al. Distinct perturbation of the translatome by the antidiabetic drug metformin. Proc Natl Acad Sci U S A. 2012;109(23):8977-82.
- 676. Hsieh AC, Liu Y, Edlind MP, Ingolia NT, Janes MR, Sher A, et al. The translational landscape of mTOR signalling steers cancer initiation and metastasis. Nature. 2012;485(7396):55-61.
- 677. Hsieh AC, Costa M, Zollo O, Davis C, Feldman ME, Testa JR, et al. Genetic dissection of the oncogenic mTOR pathway reveals druggable addiction to translational control via 4EBP-eIF4E. Cancer Cell. 2010;17(3):249-61.
- 678. Thoreen CC, Chantranupong L, Keys HR, Wang T, Gray NS, Sabatini DM. A unifying model for mTORC1-mediated regulation of mRNA translation. Nature. 2012;485(7396):109-13.

- 679. Morita M, Gravel SP, Chénard V, Sikström K, Zheng L, Alain T, et al. mTORC1 controls mitochondrial activity and biogenesis through 4E-BP-dependent translational regulation. Cell Metab. 2013;18(5):698-711.
- 680. Gandin V, Masvidal L, Hulea L, Gravel SP, Cargnello M, McLaughlan S, et al. nanoCAGE reveals 5' UTR features that define specific modes of translation of functionally related MTOR-sensitive mRNAs. Genome Res. 2016;26(5):636-48.
- 681. Elfakess R, Sinvani H, Haimov O, Svitkin Y, Sonenberg N, Dikstein R. Unique translation initiation of mRNAs-containing TISU element. Nucleic Acids Res. 2011;39(17):7598-609.
- 682. Csibi A, Lee G, Yoon SO, Tong H, Ilter D, Elia I, et al. The mTORC1/S6K1 pathway regulates glutamine metabolism through the eIF4B-dependent control of c-Myc translation. Curr Biol. 2014;24(19):2274-80.
- 683. Csibi A, Fendt SM, Li C, Poulogiannis G, Choo AY, Chapski DJ, et al. The mTORC1 pathway stimulates glutamine metabolism and cell proliferation by repressing SIRT4. Cell. 2013;153(4):840-54.
- 684. Masui K, Tanaka K, Akhavan D, Babic I, Gini B, Matsutani T, et al. mTOR complex 2 controls glycolytic metabolism in glioblastoma through FoxO acetylation and upregulation of c-Myc. Cell Metab. 2013;18(5):726-39.
- 685. van der Vos KE, Eliasson P, Proikas-Cezanne T, Vervoort SJ, van Boxtel R, Putker M, et al. Modulation of glutamine metabolism by the PI(3)K-PKB-FOXO network regulates autophagy. Nat Cell Biol. 2012;14(8):829-37.
- 686. Dodd KM, Yang J, Shen MH, Sampson JR, Tee AR. mTORC1 drives HIF-1α and VEGF-A signalling via multiple mechanisms involving 4E-BP1, S6K1 and STAT3. Oncogene. 2015;34(17):2239-50.

- 687. He L, Gomes AP, Wang X, Yoon SO, Lee G, Nagiec MJ, et al. mTORC1 Promotes Metabolic Reprogramming by the Suppression of GSK3-Dependent Foxk1 Phosphorylation. Mol Cell. 2018;70(5):949-60.e4.
- 688. Brugarolas JB, Vazquez F, Reddy A, Sellers WR, Kaelin WG, Jr. TSC2 regulates VEGF through mTOR-dependent and -independent pathways. Cancer Cell. 2003;4(2):147-58.
- 689. Laughner E, Taghavi P, Chiles K, Mahon PC, Semenza GL. HER2 (neu) signaling increases the rate of hypoxia-inducible factor 1alpha (HIF-1alpha) synthesis: novel mechanism for HIF-1-mediated vascular endothelial growth factor expression. Mol Cell Biol. 2001;21(12):3995-4004.
- 690. West MJ, Stoneley M, Willis AE. Translational induction of the c-myc oncogene via activation of the FRAP/TOR signalling pathway. Oncogene. 1998;17(6):769-80.
- 691. Kalkat M, De Melo J, Hickman KA, Lourenco C, Redel C, Resetca D, et al. MYC Deregulation in Primary Human Cancers. Genes (Basel). 2017;8(6).
- 692. Goetzman ES, Prochownik EV. The Role for Myc in Coordinating Glycolysis, Oxidative Phosphorylation, Glutaminolysis, and Fatty Acid Metabolism in Normal and Neoplastic Tissues. Front Endocrinol (Lausanne). 2018;9:129.
- 693. Betz C, Stracka D, Prescianotto-Baschong C, Frieden M, Demaurex N, Hall MN. Feature Article: mTOR complex 2-Akt signaling at mitochondria-associated endoplasmic reticulum membranes (MAM) regulates mitochondrial physiology. Proc Natl Acad Sci U S A. 2013;110(31):12526-34.
- 694. Gottlob K, Majewski N, Kennedy S, Kandel E, Robey RB, Hay N. Inhibition of early apoptotic events by Akt/PKB is dependent on the first committed step of glycolysis and mitochondrial hexokinase. Genes Dev. 2001;15(11):1406-18.

- 695. Elstrom RL, Bauer DE, Buzzai M, Karnauskas R, Harris MH, Plas DR, et al. Akt stimulates aerobic glycolysis in cancer cells. Cancer Res. 2004;64(11):3892-9.
- 696. Schieke SM, Phillips D, McCoy JP, Jr., Aponte AM, Shen RF, Balaban RS, et al. The mammalian target of rapamycin (mTOR) pathway regulates mitochondrial oxygen consumption and oxidative capacity. J Biol Chem. 2006;281(37):27643-52.
- 697. Yang K, Shrestha S, Zeng H, Karmaus PW, Neale G, Vogel P, et al. T cell exit from quiescence and differentiation into Th2 cells depend on Raptor-mTORC1-mediated metabolic reprogramming. Immunity. 2013;39(6):1043-56.
- 698. Bentzinger CF, Romanino K, Cloëtta D, Lin S, Mascarenhas JB, Oliveri F, et al. Skeletal muscle-specific ablation of raptor, but not of rictor, causes metabolic changes and results in muscle dystrophy. Cell Metab. 2008;8(5):411-24.
- 699. Cunningham JT, Rodgers JT, Arlow DH, Vazquez F, Mootha VK, Puigserver P. mTOR controls mitochondrial oxidative function through a YY1-PGC-1alpha transcriptional complex. Nature. 2007;450(7170):736-40.
- 700. Rosario FJ, Gupta MB, Myatt L, Powell TL, Glenn JP, Cox L, et al. Mechanistic Target of Rapamycin Complex 1 Promotes the Expression of Genes Encoding Electron Transport Chain Proteins and Stimulates Oxidative Phosphorylation in Primary Human Trophoblast Cells by Regulating Mitochondrial Biogenesis. Sci Rep. 2019;9(1):246.
- 701. Feldman ME, Apsel B, Uotila A, Loewith R, Knight ZA, Ruggero D, et al. Active-site inhibitors of mTOR target rapamycin-resistant outputs of mTORC1 and mTORC2. PLoS Biol. 2009;7(2):e38.

702. Thoreen CC, Kang SA, Chang JW, Liu Q, Zhang J, Gao Y, et al. An ATP-competitive mammalian target of rapamycin inhibitor reveals rapamycin-resistant functions of mTORC1. J Biol Chem. 2009;284(12):8023-32.

CHAPTER 2: Mitochondrial complex IV defects induce metabolic and signaling perturbations that expose potential vulnerabilities in HCT116 cells

Oro Uchenunu^{1,2*}, Alexander V. Zhdanov^{3*}, Phillipe Hutton¹, Predrag Jovanovic^{1,2}, Ye Wang¹, Dmitry E. Andreev^{4,5}, Laura Hulea⁶, David J. Papadopoli^{1,7}, Daina Avizonis⁸, Pavel V. Baranov³, Michael N. Pollak^{1,2,7**}, Dmitri B. Papkovsky^{3**} and Ivan Topisirovic^{1,2,7,9**}.

*equal contribution

¹ Lady Davis Institute for Medical Research, Jewish General Hospital, Montréal, QC H3T1E2, Canada.

² Department of Experimental Medicine, McGill University, Montreal QC H4A3T2, Canada.

³ School of Biochemistry and Cell Biology, University College Cork, Cork, Ireland.

⁴ Shemyakin-Ovchinnikov Institute of Bioorganic Chemistry, Moscow, Russia, 117997

⁵ Belozersky Institute of Physico-Chemical Biology, Lomonosov Moscow State University,

Moscow, Russia, 119992

⁶ Département de Médecine, Département de Biochimie et Médecine Moléculaire, Université de Montréal, Maisonneuve-Rosemont Hospital Research Centre, Montréal, QC, Canada

⁷ Gerald Bronfman Department of Oncology, McGill University, Montreal QC H4A3T2, Canada.

 $^8\,\mathrm{Goodman}$ Cancer Research Centre, McGill University, Montreal, QC H3A 1A3, Canada.

⁹ Department of Biochemistry, McGill University, Montreal, QC H4A 3T2, Canada.

**Correspondence

D.B. Papkovsky, School of Biochemistry and Cell Biology, University College Cork, Cork, Ireland.

Tel: +353-21-490-1698; E-mail: d.papkovsky@ucc.ie

M.N. Pollak and I. Topisirovic, Lady Davis Institute for Medical Research, Jewish General Hospital, Montréal, QC H3T1E2, Canada.

Tel: +514-340-8222; E-mail: michael.pollak@mcgill.ca and ivan.topisirovic@mcgill.ca

2.1 ABSTRACT

Mutations in genes encoding cytochrome c oxidase (COX; mitochondrial complex IV) subunits and assembly factors (e.g., SCO1, SCO2, COA6) are linked to severe metabolic syndromes. Notwithstanding that SCO2 is under transcriptional control of tumor suppressor p53, the role of mitochondrial complex IV dysfunction in cancer metabolism remains obscure. Herein, we demonstrate that the loss of SCO2 in HCT116 colorectal cancer cells leads to significant metabolic and signaling perturbations. Specifically, abrogation of SCO2 increased NAD+ regenerating reactions and decreased glucose oxidation through citric acid cycle while enhancing pyruvate carboxylation. This was accompanied by a reduction in amino acid levels and the accumulation of lipid droplets. In addition, SCO2 loss resulted in hyperactivation of the IGF1R/AKT axis with paradoxical downregulation of mTOR signaling which was accompanied by increased AMPK activity. Accordingly, abrogation of SCO2 expression appears to increase the sensitivity of cells to IGF1R and AKT, but not mTOR inhibitors. Finally, the loss of SCO2 was associated with reduced proliferation and enhanced migration of HCT116 cells. Collectively, herein we describe potential adaptive signaling and metabolic perturbations triggered by mitochondrial complex IV dysfunction.

2.2 INTRODUCTION

Driven by genetic, epigenetic, environmental and other factors, malfunctions of citric acid cycle (CAC) enzymes, OXPHOS supercomplexes and other mitochondrial proteins have been

implicated in neoplastic transformation, tumor progression and/or therapeutic responses (1, 2). This is exemplified by inactivation of fumarate hydratase (FH), succinate dehydrogenase (SDH) or neomorphic mutations in isocitrate dehydrogenase (IDH) that result in accumulation of fumarate, succinate and 2-hydroxyglutarate, respectively (3-7). These metabolites are thought to contribute to tumorigenesis and tumor progression by interfering with several classes of α -ketoglutarate-dependent enzymes that govern key cellular functions (8). Cytochrome c oxidase (COX) assembly protein 2 (SCO2) is essential to the functioning of COX (mitochondrial complex IV). The loss of function or deletion of *SCO2* leads to abrogation of COX assembly and activity (9).

Though non-lethal diseases associated with deficiencies of COX are rare (10, 11), cell models bearing the relevant mutations are useful for understanding metabolic re-arrangements caused by mitochondrial complex IV deficiencies. To this end, studies on colon cancer HCT116 cell line devoid of *SCO2* (HCT116 *SCO2* cells) showed that COX deficiency is associated with decrease in O₂ consumption and slower proliferation. In addition, SCO2-deficient cells exhibit an increase in NADH, reactive oxygen species (ROS) and glycolysis, which are accompanied by reversed activity of F₁Fo ATP-synthase (12-14). These perturbations are paralleled by dramatic changes in gene expression including induction of the factors implicated in epithelial-to-mesenchymal transition (EMT) (12-15). Importantly, HCT116 *SCO2* cells are more resilient to hypoxia than their SCO2-proficient counterparts (13), which in conjunction with induction of EMT phenotypes, suggests that dysfunction of mitochondrial complex IV may play a central role in metastatic progression. *SCO2* expression is regulated by p53 (12). Metabolic perturbations caused by the loss of *TP53* function are thus thought to be at least in part mediated by the downregulation of *SCO2* (12). The loss of p53 function was reported to result in the reduction of oxidative

phosphorylation (OXPHOS) and a compensatory increase in glycolysis (12) which is thought to be mediated by increase in hexokinase 2 (HK2) (16) and phosphoglycerate mutase (PGM) (17) as well as the reduction in TIGAR levels (18). Deletion of the SCO2 gene via homologous recombination in wild type TP53 HCT116 cells recapitulates the metabolic rewiring towards glycolysis that is observed in p53-deficient cells (12). However, it was also reported that wild type TP53 glioma and colon cancer cells adapt to hypoxia by at least in part inducing SCO2 expression (19). Moreover, the correlation between SCO2 levels and cancer prognosis remains unclear. For instance, low expression of SCO2 was associated with poor prognosis in breast and ovarian cancer patients (20-22). In contrast, TCGA analysis revealed amplification and subsequent increase in SCO2 levels in metastatic cancers harboring TP53 mutations, wherein high SCO2 levels correlated with poor prognosis (23). Collectively these findings demonstrate that notwithstanding that SCO2 is likely to play a major role in p53-dependent metabolic reprogramming and thus determine the fate of cancer cells, the underpinning mechanisms and associated clinical correlates remain incompletely understood. In the attempt to address these gaps in knowledge, we systematically examined metabolic perturbations induced by SCO2 loss in HCT116 cells. As expected, dysfunction of mitochondrial complex IV in SCO2-/- HCT116 cells resulted in dramatic metabolic reprogramming including elevated dependence on glucose and altered pyruvate and amino acid metabolism. These metabolic perturbations were accompanied by increased migration and sustained proliferation under extremely low (<0.1%) oxygen levels. Accordingly, SCO2 deletion in HCT116 cells increases survival under hypoxia compared to the wildtype (WT) cells (13). Moreover, loss of SCO2 resulted in activation of IGF1R/AKT axis and elevated sensitivity to the IGF1R and AKT inhibitors.

2.3 RESULTS

2.3.1 SCO2 loss results in metabolic rewiring of HCT116 cells that is characterized by increased NAD+ regeneration

Mitochondrial complex IV deficiency caused by SCO2 loss leads to impairment of the electron transport chain, decreased pyruvate oxidation and increased lactate production (13, 14). To identify metabolic pathways that are altered by abrogation of SCO2, we first quantified intracellular and extracellular steady-state levels of key metabolites. As expected, the loss or depletion of SCO2 in HCT116 or A549 cells, respectively increased glucose uptake (Fig. 2.1A, Fig. S2.1A), extracellular lactate levels (Fig. 2.1B, Fig. S2.1B) and glycolytic intermediates including dihydroxyacetone phosphate (DHAP), 3-phosphoglycerol (3-PG) phosphoglycerol (2-PG) (Fig. 2.1C). This is in agreement with previous observations that SCO2 deletion or OXPHOS inhibition using biguanides increases levels of 3-PG and lactate production in order to regenerate NAD+ necessary for maintaining glycolysis (13, 24, 25). The re-introduction of exogenous SCO2 into SCO2-/- HCT116 cells attenuated increased glucose uptake and lactate secretion thus confirming that SCO2 attenuates glycolysis (Fig. S2.1C-D). Of note, notwithstanding repeated attempts, we could not achieve the rescue of SCO2 expression to the levels of the endogenous protein (Fig. S2.1E). Taken together, loss of SCO2 in HCT116 cells increases their dependence on glucose metabolism.

In contrast to DHAP, pyruvate levels were found to be lower in $SCO2^{-/-}$ relative to WT HCT116 cells (Fig. 2.1C). This is likely due to the diversion of carbon units from the glycolytic pathway to glycerol biosynthesis via 3-phosphoglycerol (3-PG) as 3-PG was found to be higher in $SCO2^{-/-}$ than in WT HCT116 cells (Fig. 2.1C). This is indicative of enhanced cytosolic glycerol-3-phosphate dehydrogenase (GPD1) activity which not only produces glycerol but also NAD+ (26). We hypothesize that this reaction in addition to the conversion of pyruvate to lactate is

necessary for maintaining glycolysis in the HCT116 SCO2-/- cells. Indeed, the intracellular lactate/pyruvate ratio, which is traditionally used as a proxy for cytosolic NADH/NAD+ ratio and glycolytic activity (27) was elevated in the SCO2-/- as compared to WT HCT116 cells (Fig. 2.1D). Since pyruvate oxidation is initiated by the pyruvate dehydrogenase (PDH), we investigated whether the SCO2 status affects the levels and/or phosphorylation of PDH subunits. Pyruvate dehydrogenase kinases (PDK1-4) when stimulated by ATP, acetyl-CoA or NADH phosphorylate and inactivate PDH thus deflecting pyruvate from CAC under conditions of mitochondrial dysfunction and hypoxia (28). Surprisingly, we noted that both PDK1 levels and the phosphorylation of PDH subunit PDHE1-α1 (S293) are decreased in SCO2-/- cells relative to WT HCT116 cells in both normoxia and hypoxia (Fig. 2.1E). This was despite the fact that NADH levels are higher in SCO2-/- than in WT HCT116 cells (13). Considering that PDK1 expression is stimulated by hypoxia inducible factor (HIF)-1 and 2α, we next determined HIF-2α levels. HIF- 2α induction under severe hypoxia (<0.1% O₂) was comparable between the cell lines (Fig. 2.1E). PDK1 levels and PDHE1-α1 phosphorylation were however more strongly induced in WT as compared to HCT116 SCO2^{-/-} cells (Fig. 2.1E). Collectively, these findings show that although the loss of SCO2 increased NADH levels (13), PDK1 activity is reduced in SCO2-/- cells. Intriguingly, the decreased phosphorylation level of the PDHE1-α1 subunit in HCT116 SCO2^{-/-} cells suggests that pyruvate oxidation via PDH is elevated relative to WT cells. Collectively, these findings show that despite the loss of SCO2 which increased NADH levels (13), PDK1 activity is reduced in SCO2^{-/-} cells. Hence, although pyruvate oxidation may be elevated in HCT116 SCO2^{-/-} cells, this cannot be explained by NADH-mediated regulation of PDK1 activity. Recent studies demonstrated that one of the major functions of mitochondrial respiration is to produce sufficient amount of aspartate required to drive proliferation of cancer cells (29, 30). To this end, it is thought that the most of cellular aspartate is derived from oxaloacetate produced in oxidative CAC (31). Consistent with the disruption of the oxidative CAC in *SCO2*^{-/-} HCT116 cells, steady-state aspartate levels were dramatically reduced in *SCO2*^{-/-} as compared to WT HCT116 cells (Fig. 2.2A). However, stable isotope tracer analysis (SITA) using ¹³C-labelled glucose show that in *SCO2*^{-/-} HCT116 cells, pyruvate may primarily undergo carboxylation followed by transamination to produce aspartate as illustrated by increase in m+3 fractions of malate, fumarate and aspartate isotopomers (Fig. 2.2B-C). In turn, the levels of the m+2 citrate, α-KG, fumarate, and malate isotopomers were markedly reduced in *SCO2*^{-/-} compared to WT HCT116 (Fig. 2.2C). These findings suggest that increased carboxylation of pyruvate may represent a compensatory mechanism for a decrease in CAC-derived aspartate in *SCO2*^{-/-} HCT116 cells. This, in addition to increased lactate production and contribution of 3-PG to glycerol synthesis may explain reduction in pyruvate levels in SCO2-deficient HCT116 cells.

2.3.2 Abrogation of SCO2 in HCT116 cells leads to alterations in acetyl-CoA and lipid metabolism

Pyruvate is oxidized through PDH to produce acetyl-coenzyme A (acetyl-CoA), a 2-carbon unit that enters the CAC and yields NADH (32). Notwithstanding observed reduction in PDK1 activity in HCT116 cells devoid of SCO2 (Fig. 2.1E), PDH is sensitive to product inhibition by NADH (33). Considering that NADH levels are elevated in *SCO2*^{-/-} vs. WT HCT116 cells (13) while SCO2 loss decreased pyruvate oxidation through the CAC (Fig. 2.2B-C), we hypothesized that SCO2 deletion is paralleled by a decrease in acetyl-CoA levels. Despite our inability to measure acetyl-CoA directly, we analyzed the effects of *SCO2* loss on acetyl-CoA-dependent pathways. Herein, we observed decreased levels of histone and α-tubulin lysine N-acetylation in *SCO2*^{-/-} relative to WT HCT116 cells in both normoxia and moderate hypoxia (3% O₂) (Fig. 2.3A).

Thus, although the phosphorylation of S293 residue of PDHE1-α1 subunit often negatively correlates with PDH activity this is not the case for HCT116 SCO2-/- cells. Moreover, PDH can be inhibited when phosphorylated at either S232 or S300 residues of PDHE1-α1 subunit by PDK1-4 (34-36). Considering that acetyl-CoA carboxylation which generates malonyl-CoA is the ratelimiting step in fatty acid (FA) synthesis (37), we next monitored acetyl-CoA carboxylase (ACC) activity. Relative to WT, SCO2-/- HCT116 cells exhibited increased activity of AMP-activated protein kinase (AMPK) that phosphorylates (S79) and inactivates ACC (Fig. 2.3B). Moreover, the levels of citrate, which allosterically activates ACC, were markedly decreased in SCO2^{-/-} as compared to WT HCT116 cells (Fig. 2.3C). Reduction of FA synthesis in SCO2-/- HCT116 as compared to WT cells also aligns with the increase in both the steady-state and m+3 levels of 2and 3-PG, which are triacylglycerol (TAG) precursors (Fig. 2.1C, Fig. 2.2C). Collectively, these data suggest that FA synthesis is reduced in SCO2-deficient vs. proficient cells. However, in contrast to WT cells, numerous Nile Red positive lipid droplets (LD), which are depots of TAGs, were observed in SCO2^{-/-} but not in WT HCT116 cells (Fig. 2.3D). SCO2-deficient mice have increased fat mass associated with reduced β-oxidation (38). Altogether, these findings suggest that the SCO2 loss-induced decrease in mitochondrial β -oxidation is incompletely compensated by reduction in FA synthesis via suppression of ACC. Of note, we excluded the possibility that LDs contain FA that were imported from growth media by culturing cells in the presence of normal or FA-free FBS for 20 days, which did not affect the size or number of LDs (Fig. S2.2A). Importantly, HCT116 WT cells phenocopied the accumulation of LDs observed in SCO2-deficient cells when grown continuously under severe hypoxia (<0.1% O₂) (Fig. S2.2B) or in the presence of complex III inhibitors antimycin A (Ant A) or myxothiazol (Myx) (Fig. S2.2C). Chronically

hypoxic HCT116 *SCO2*-/- cells also increased LD deposition, suggesting that in the presence of O₂ some FA may be metabolized likely through the peroxisomal β-oxidation (39).

2.3.3 Complex IV dysfunction in HCT116 cells results in increased succinate and 2-hydroxyglutarate levels

Steady-state metabolite analysis also revealed dramatic accumulation of succinate and 2hydroxyglutarate (2-HG) in SCO2-/- vs. WT HCT116 cells (Fig. 2.4A). As succinate is known to accumulate upon complex II inhibition (40-43) as well as following treatment with the complex III inhibitor Ant A (44), we reasoned that the increased succinate observed in cells devoid of SCO2 was due to the impairment of the electron transport chain (ETC) and subsequent decrease in the activity of mitochondrial complex II (SDH). Indeed, steady state fumarate and malate levels were decreased, thus suggesting reduced utilization of succinate through CAC in SCO2-/- as compared to WT HCT116 cells (Fig. 2.4A). In addition, 2-HG accumulated in HCT116 cells devoid of SCO2. While we could not distinguish the enantiomer of 2-HG that was elevated in HCT116 SCO2-/cells, sequencing analysis of IDH1 and IDH2 mRNAs in WT and HCT116 SCO2-/- did not reveal neomorphic mutations (arginine residues R100, R109, R132 for IDH1, and R140, R149, R172 for IDH2) known to give rise to D-2-HG (Fig. S2.3A) (45). Low pH, reduced oxidation of αketoglutarate (α-KG) and increased NADH levels have been shown to enhance L-2-HG synthesis chiefly via lactate (LDH) and malate dehydrogenases (MDH) (46, 47). Although we did not detect differences in cellular pH between WT and SCO2-/- HCT116 cells (Fig. S2.3B), the overall reductive state caused by ETC dysfunction and the lack of *IDH1* or *IDH2* mutations, suggest that it is likely that L-2-HG accumulates in HCT116 SCO2-/- cells (48).

2.3.4 SCO2 loss in HCT116 cells affects amino-acid metabolism

Amino acid metabolism is partly dependent on mitochondrial function. The CAC intermediates are used to biosynthesize amino acids including aspartate, asparagine, proline and glutamate (49). Moreover, as noted above, the essential role of mitochondrial respiration in producing aspartate to fuel neoplastic growth has been described (29, 30, 50). To this end, it was shown that the inhibition of mitochondrial complex I with metformin not only reduced the NAD+/NADH ratio but also suppressed aspartate biosynthesis (50). Consistently, we observed a decrease in proline, glutamate and asparagine levels in SCO2^{-/-} vs. WT HCT116 cells (Fig. 2.4B). In turn, levels of cysteine were higher in SCO2-deficient vs. proficient HCT116 cells (Fig. 2.4B). Considering that cysteine is a rate-limiting substrate in glutathione synthesis (51) and that the loss of SCO2 results in increased ROS production (13), the observed increase in cysteine levels in SCO2-/- HCT116 cells may be indicative of potential compensatory mechanisms that are triggered to protect cells from ROSinduced damage. In line with this, increased cysteine levels may be required to support the turnover of mitochondrial cysteine-rich proteins that also contribute to the antioxidant defense machinery (52). Accordingly, the levels of mitochondrial ROS scavenger superoxide dismutase 2 (SOD2) were elevated in SCO2-/- compared to WT HCT116 cells (Fig. S2.4A).

Cancer cells use glutamine as an anaplerotic source for the CAC (53, 54). The loss of SCO2 in HCT116 cells reduced intracellular glutamine levels compared to WT cells. Inhibition of OXPHOS results in reductive glutamine metabolism and consequent reductive carboxylation of α -KG to produce aspartate which is necessary for cancer cell proliferation (29, 30). A high α -KG/citrate ratio, commonly observed in cancer cells with mitochondrial dysfunction, is an indirect indication of reductive glutamine metabolism (55). Notwithstanding that the glutamine levels were lower in $SCO2^{-/-}$ as compared to WT HCT116 cells, the α -KG/citrate ratio was dramatically

elevated in SCO2-deficient cells (Fig. 2.4B-C). Hence, although the deletion of *SCO2* decreased intracellular glutamine level in HCT116 cells, these data suggest that most of the glutamine is likely to be reductively metabolized in HCT116 *SCO2*-/- cells (Fig. 2.4B). Altogether, these data suggest that the loss of SCO2 causes major perturbations in amino acid metabolism.

2.3.5 Loss of mitochondrial complex IV function leads to induction of IGF1R/AKT axis with paradoxical reduction in mTOR signaling

To better understand the mechanism of metabolic adaptations to the disruption of mitochondrial complex IV function, we next investigated the effects of SCO2 abrogation on mTOR signaling, which acts a major conductor of metabolic programs in the cell (56). Notably, phosphorylation of AKT catalytic site (T308) and hydrophobic motif (S473) were increased in SCO2-/- as compared to WT HCT116 cells (Fig. 2.5A). Accordingly, SCO2-/- HCT116 cells exhibited higher AKTdependent phosphorylation (S9) of GSK3β (Fig. 2.5A), thus indicating that AKT activity is higher in SCO2-deficient vs. proficient cells. Importantly, HCT116 WT cells treated with complex III inhibitors AntA and Myx showed similar increase in phosphorylation of AKT (S473) (Fig. 2.5B). Collectively, this indicates that disruption of terminal ETC complexes (III and IV) may result in compensatory AKT activation. Notably, the increase in AKT activity coincided with upregulation of insulin-like growth factor 1 receptor (IGF1R) mRNA and IGF1Rβ protein in SCO2-/- vs. WT HCT116 cells (Fig. 2.5A and 2.5C), implying that the loss of mitochondrial complex IV function may lead to increased signaling through the IGF1R/AKT axis. Similar induction of IGF1R mRNA levels was observed in WT HCT116 cells maintained at 0.1% O₂ (Fig. 2.5C). Upregulated signaling via the IGF1R/AKT axis in SCO2-/- HCT116 cells was also paralleled by an increase in the amount of IGF1 bound to IGF1R (Fig. 2.5D).

Surprisingly, despite increased AKT activity, *SCO2* loss in HCT116 cells led to a decrease in mTORC1 activity, as illustrated by reduction in phosphorylation of its downstream substrate 4E-binding protein 1 (4E-BP1; S65), and ribosomal protein S6 (rpS6; S240/244) which is a substrate of mTOR-dependent S6 kinases (S6Ks) (Fig. 2.5A). In turn, AMPK phosphorylation was increased in *SCO2*-/- relative to HCT116 WT cells (Fig. 2.3B). Given that AMPK is a negative regulator of mTORC1 (57, 58) this may explain the reduction of mTORC1 signaling upon *SCO2* loss, despite increase in AKT activity. Altogether, these findings show that the impairment of mitochondrial complex IV function leads to increase in AKT and AMPK activity, which is accompanied by a decrease in mTORC1 signaling.

mTORC1 stimulates cell proliferation (59). *SCO2* loss-induced reduction in mTORC1 activity was therefore consistent with decreased proliferation of SCO2-deficient vs. proficient cells (Fig. 2.5E). Consistent with previous findings (13), the proliferation of *SCO2*-/- HCT116 cells was less affected by exposure to 0.1% O₂ in comparison to WT HCT116 cells (Fig. 2.5E). These observed phenotypes appeared not to be limited to HCT116 cells. *SCO2* depletion in A549, HeLa and HT29 cells resulted in increased AKT phosphorylation (S473) and decreased phosphorylation of downstream mTORC1 substrates (Fig. S2.5A-C). Consistent with the findings in HCT116 cells, *SCO2* depletion also reduced proliferation of A549, HeLa and HT29 cells (Fig. S2.5D-F). Next, we re-expressed *SCO2* in *SCO2*-/- HCT116 cells to exclude potential inadvertent effects caused by cellular adaptation to *SCO2* loss. Notwithstanding that as indicated above exogenous SCO2 protein levels were significantly lower than the levels of endogenous SCO2 protein (Fig. S2.1E, S2.5G), re-expression of *SCO2* in *SCO2*-/- HCT116 cells resulted in partial rescue of cellular proliferation as compared to vector infected *SCO2*-/- HCT116 cells (Fig. S2.5H). Re-expression of *SCO2* also partially rescued mTORC1 signaling as illustrated by increase in 4E-BP1 phosphorylation in

SCO2-/- HCT116 cells expressing *SCO2* relative to control, vector infected *SCO2*-/- HCT116 cells (Fig. S2.5G).

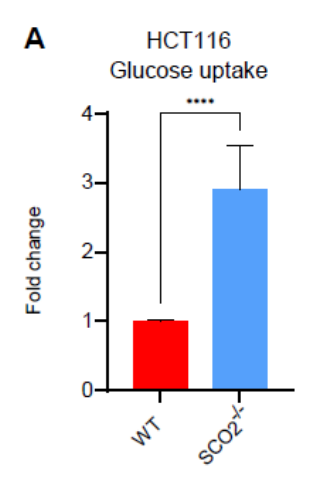
2.3.6 SCO2 loss leads to increased cell migration and altered expression of EMT markers in HCT116 cells.

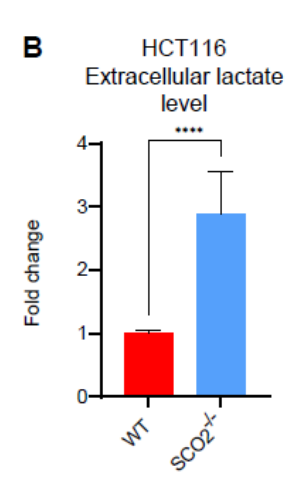
Mitochondrial dysfunction resulting in increased ROS and/or accumulation of oncometabolites such as 2-HG has been linked to elevated expression of EMT markers, increased cell migration and higher metastatic potential of cancer cells (60, 61). Accordingly, previous studies have shown higher levels of ROS and the mesenchymal marker, vimentin, in SCO2-/- compared to HCT116 WT cells (13, 14). To this end, we next monitored the effects of SCO2 loss on migration and expression of epithelial (E-cadherin) and mesenchymal (vimentin) markers using HCT116 cell model. These studies revealed that the loss of SCO2 enhances migration of HCT116 cells (Fig. 2.5F). In addition to increased vimentin levels, SCO2-deficient HCT116 cells exhibited a decrease in E-cadherin levels as compared to WT HCT116 cells (Fig. 2.5G). Also the loss of SCO2 in HCT116 correlated with elevated ZEB1 mRNA levels (Fig. 2.5H), which encodes a key regulator of EMT (62). Moreover, re-expression of SCO2 in SCO2-/- HCT116 cells attenuated migration, reduced vimentin levels while increasing E-cadherin abundance (Fig. S2.5I-J). We observed that SCO2-deficient HCT116 cells exhibit attenuated mTORC1 signaling as compared to their SCO2proficient counterparts (Fig. 2.5A). Inhibition of mTOR was shown to coincide with elevated phosphorylation of the α subunit of eukaryotic translation initiation factor 2 (eIF2) and increased cell migration (63, 64). However, the phosphorylation of eIF2\alpha (S51) was not affected by the SCO2 status in the HCT116 cells (Fig. S2.5K). Hence, although SCO2 deletion in HCT116 cells reduced proliferation, it increased their migratory potential whereby this effect was independent of eIF2α phosphorylation.

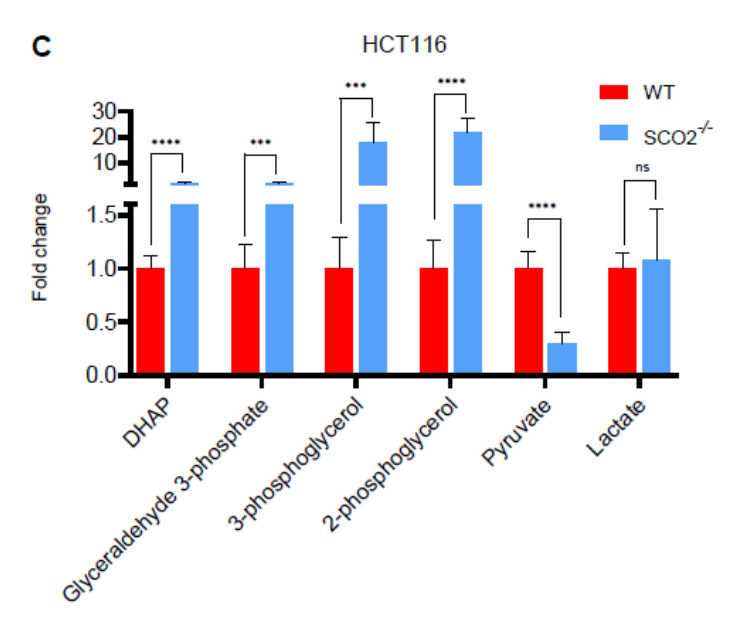
2.3.7 SCO2-deficient HCT116 cells exhibit increased susceptibility to IGF1R and AKT inhibitors.

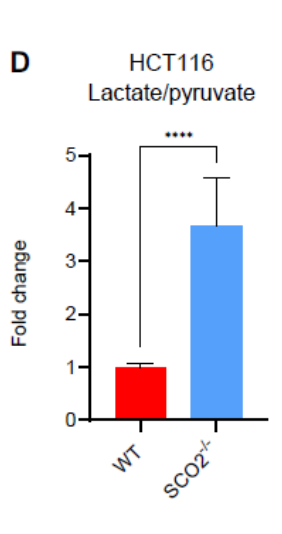
Considering that the disruption of mitochondrial complex IV activity is paralleled by the increase in IGF1R\beta levels and AKT activity (Fig. 2.5A), we next investigated the effects of IGF1R and AKT inhibitors on the fate of transformed cells as a function of their SCO2 status. As compared to control (vehicle) treatment, allosteric pan-AKT inhibitor MK2206 reduced proliferation (Fig. 2.6A), attenuated progression from G1 to S phase of cell cycle (Fig. 2.6B) and decreased survival (Fig. 2.6C) of SCO2^{-/-} HCT116 cells more pronouncedly than in WT cells. Of note, depletion of SCO2 also potentiated anti-proliferative effects of MK2206 in A549 and HT29 cells as compared to the control, scrambled shRNA infected cells (Fig. S2.6A-B) albeit to a lesser extent than the complete SCO2 knock-out in HCT116 cells (Fig. 2.6A). Moreover, MK2206 reduced levels of glycolytic intermediates including DHAP and 3-PG in HCT116 SCO2-/- cells to a greater extent than in control cells (Fig. S2.7A-B). Notably, comparable reduction of phosphorylated AKT levels was observed between WT and SCO2-/- HCT116 cells thus excluding potential differences in AKT inhibition by MK2206 between the cell lines (Fig. 2.6D). The effect of MK2206 on mTORC1, as monitored by rpS6 (S240/244) and 4E-BP1 (S65) phosphorylation levels, were greater in SCO2proficient vs. deficient HCT116 cells which is consistent with higher basal mTORC1 activity in the former cell line (Fig. 2.6D). In turn, although the allosteric (rapamycin) and active-site (torin 1) mTOR inhibitors abolished mTORC1 signaling in both cell lines as evidenced by the reduction in rpS6 (S240/244) and 4E-BP1 (S65) phosphorylation, their anti-proliferative effects were lesser in SCO2^{-/-} as compared to WT HCT116 cells (Fig. 2.6D-F). SCO2 depletion also attenuated antiproliferative effects of mTOR inhibitors in A549 and HT29 cells (Fig. S2.8A-D). Similar to AKT inhibition, IGF1R/insulin receptor inhibitor, OSI-906 (linsitinib), reduced 4E-BP1 (S65) phosphorylation and proliferation of HCT116 *SCO2*-/- cells to a greater extent compared to WT cells (Fig. 2.6G-H). These findings suggest that the loss of *SCO2* may render HCT116 cells "addicted" to the IGF1R/AKT axis. In turn, HCT116 *SCO2*-/- cells exhibit reduced mTORC1 signaling, which may explain their decreased sensitivity to mTOR inhibitors. Collectively, these results suggest that uncoupling of IGF1R/AKT and mTORC1 signaling may be required for adaptation of HCT116 cells to *SCO2* loss. mTOR is major stimulator of anabolic processes such as lipid and protein synthesis (65, 66). This alludes to a model whereby activation of IGF1R/AKT axis promotes survival of cancer cells with complex IV dysfunction by driving glycolysis, while concomitant suppression of mTOR is required to decrease energy consumption and thus compensate for disrupted mitochondrial ATP production.

2.4 FIGURES









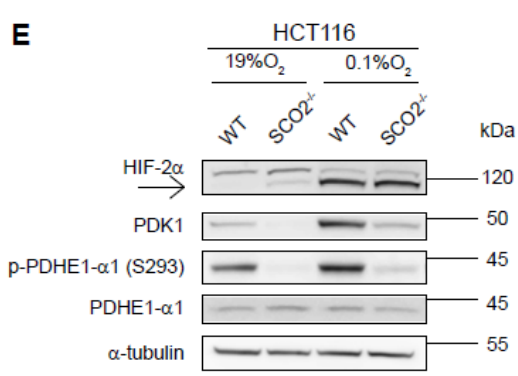


Fig. 2.1. SCO2 loss in HCT116 cells rewires glucose metabolism while decreasing PDHE1-α1 phosphorylation. A-B, Glucose uptake (A) and extracellular lactate levels (B) were determined using BioProfiler analyzer. Data are represented as mean fold change relative to the control, WT HCT116 cells (set to 1) +/- standard deviation (SD). ****p<0.0001 (Unpaired 2-tailed t-test; n=5 independent experiments with 3 technical replicates in each). C. Intracellular levels of indicated metabolites in WT or HCT116 SCO2-/- cells. Metabolite levels were monitored by GC-MS. Data are presented as mean fold change relative to HCT116 WT cells (set to 1) +/- SD. *p<0.05, **p<0.01, ***p<0.001, ****p<0.0001 (Unpaired 2-tailed t-test; n=3 independent experiments with 3 technical replicates in each). **D.** Intracellular lactate/pyruvate ratio in WT or HCT116 SCO2⁻¹ ^{/-} cells. Intracellular lactate and pyruvate levels were determined by GC-MS. Obtained lactate/pyruvate ratio in WT HCT116 cells were set to 1. Data are presented as mean fold change of n=3 independent experiments with 3 technical replicates in each. E. Levels and phosphorylation status of indicated proteins in WT or SCO2-/- HCT116 cells were monitored by Western blotting. α-tubulin served as a loading control. As indicated, cells were grown for 10 days under 19% and 0.1% O₂. Shown are representative Western blots from 3 independent experiments. Quantifications of Western Blots are shown in Fig. S2.9.

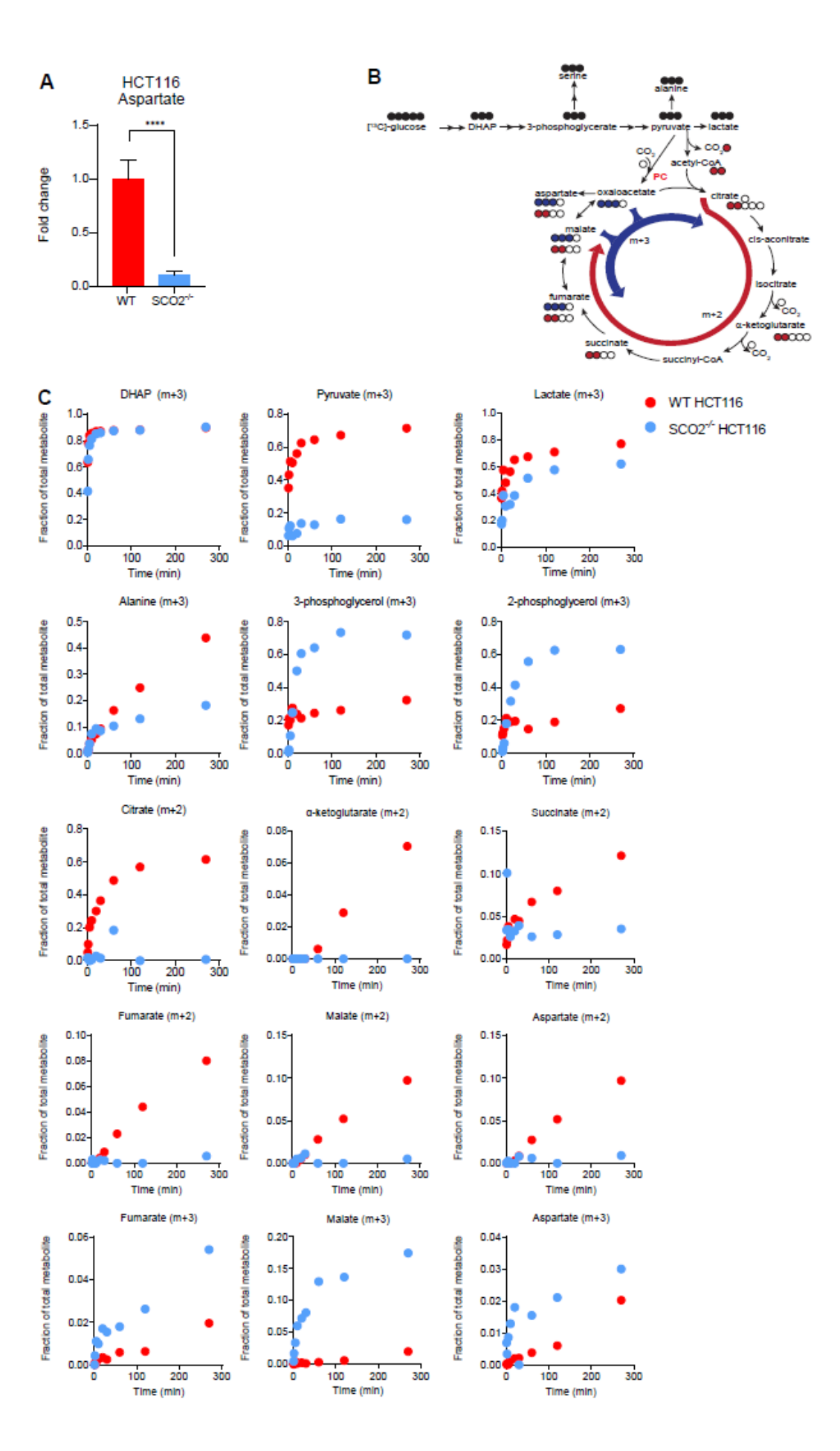
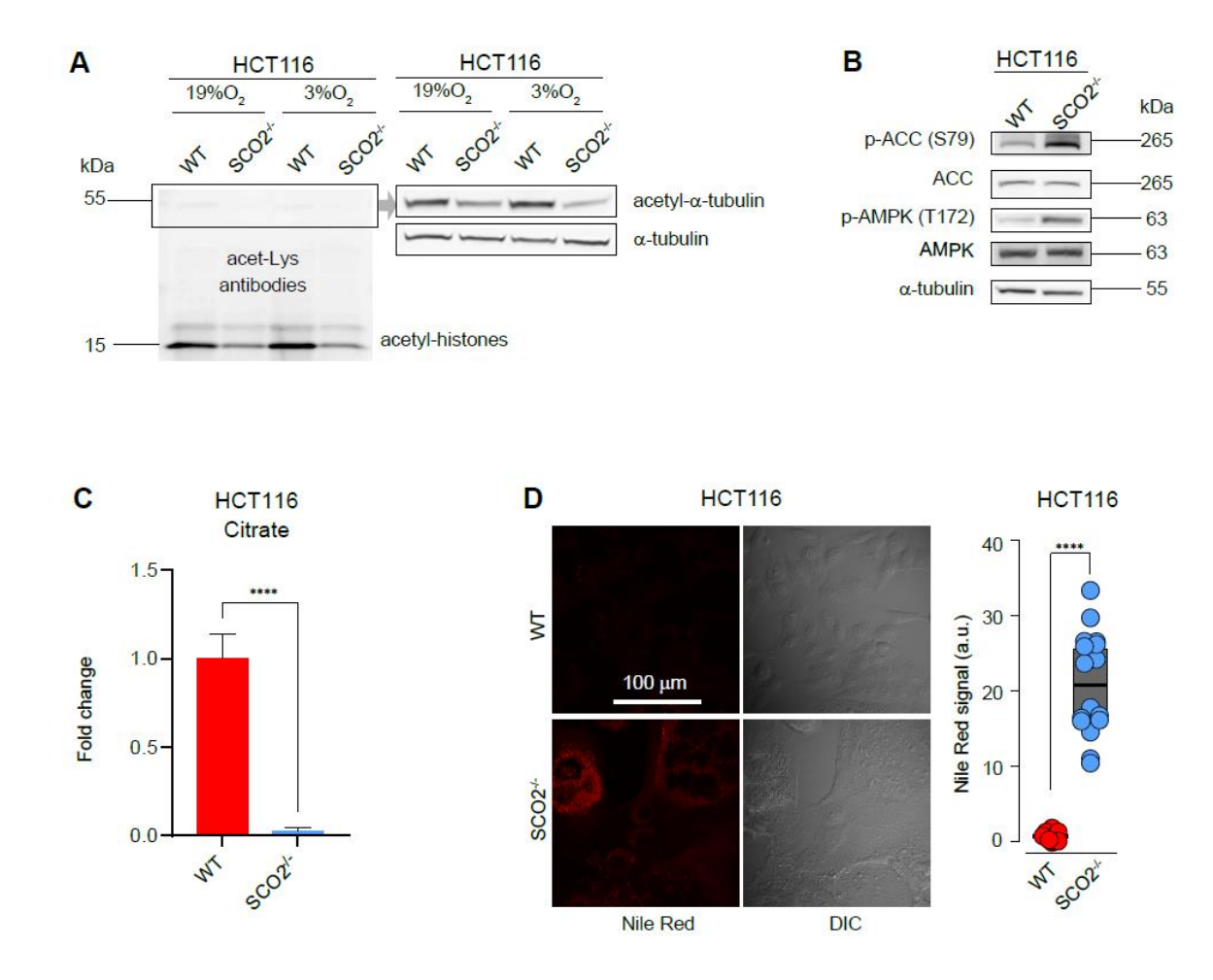
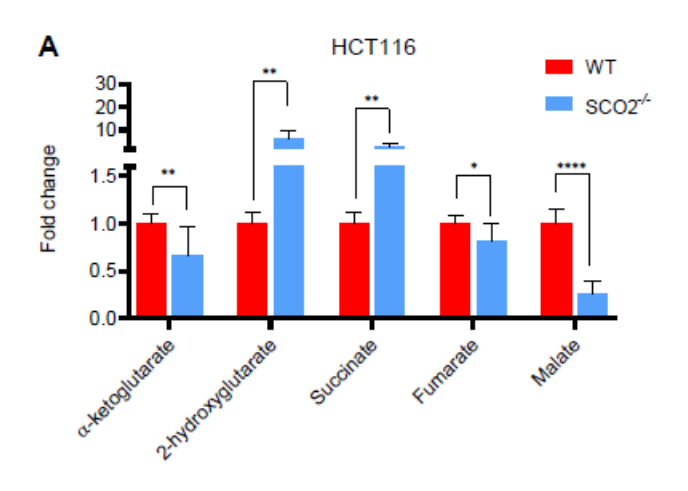


Fig. 2.2. SCO2 loss in HCT116 cells reduces pyruvate oxidation while increasing pyruvate reduction and carboxylation. A. Intracellular levels of aspartate in WT and SCO2^{-/-} HCT116 cells. Aspartate levels were determined by GC-MS. Results are represented as mean fold change +/- SD in which the values calculated for WT HCT116 cells were set to 1. ****p<0.0001 (Unpaired 2-tailed t-test; n=3 independent experiments with 3 technical replicates in each). B. Schematic diagram of ¹³C incorporation into metabolites after incubation with ¹³C₆-glucose. Red arrow represents the incorporation of two ¹³C units via the oxidative carboxylation of CAC. Blue arrow represents the carboxylation of pyruvate via pyruvate carboxylase (PC) whereby resulting metabolites have three ¹³C units. C. Mass spectrometry analysis of glucose-derived metabolites (glucose flux) in SCO2^{-/-} and WT HCT116 cells. Cells were grown in the presence of ¹³C₆-glucose for 1, 2, 5, 10, 20, 30, 60, 120 and 270 min. Representative plots of 3 independent experiments are shown.



independent experiments with 3 technical replicates in each). **D.** Confocal microscopy of lipid droplets in WT and *SCO2*-/- HCT116 cells using Nile Red staining. Fluorescence images are stacks of 5 focal planes taken with a 0.5 μm step, with single-plane DIC images on the right (n=3 independent experiments). Results of a representative experiment (N = 16 cells for each cell line) are normalized to the mean fluorescence intensity in WT HCT116 cells and shown as individual data points in arbitrary units (a.u.); mean value in WT HCT116 cells was set to 1 a.u. ****p<0.0001 (Unpaired 2-tailed t-test). Quantifications of Western Blots are shown in Fig. S2.9.



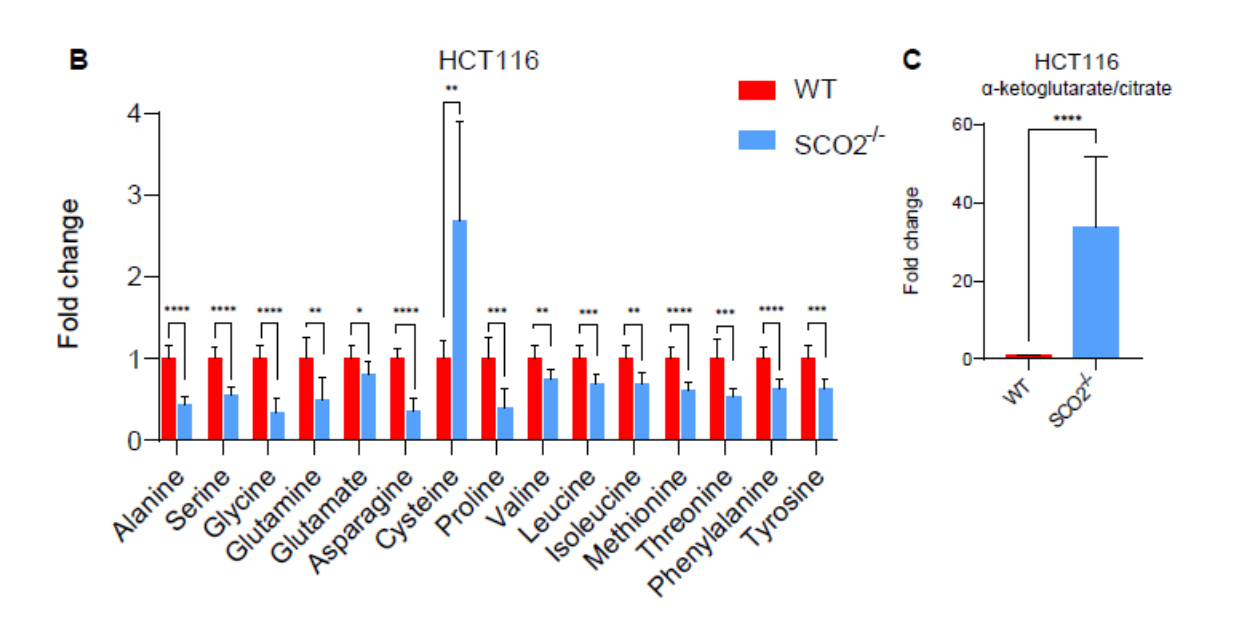


Fig. 2.4. SCO2 abrogation in HCT116 cells results in asymmetry in CAC intermediates and decrease in the levels of the most amino acids. A-B, Intracellular levels of metabolites in WT and $SCO2^{-/-}$ HCT116 cells were monitored by GC-MS showing decreased levels of malate, fumarate, α -ketoglutarate while succinate level increased in $SCO2^{-/-}$ HCT116 cells. Data are

represented as mean fold change +/- SD relative to WT HCT116 cells wherein values for each metabolite are set to 1. *p<0.05, **p<0.01, ***p<0.001, ****p<0.001 (Unpaired 2-tailed t-test; n=3 independent experiments with 3 technical replicates in each). **C.** Intracellular α -ketoglutarate/citrate ratio in WT and $SCO2^{-/-}$ HCT116 cells was determined from the levels of respective metabolites detected by GC-MS. The values obtained for WT HCT116 cells were set at 1 and the results were represented as means of the ratios from 3 independent experiments with 3 technical replicates each +/- SD. ****p<0.0001 (Unpaired 2-tailed t-test).

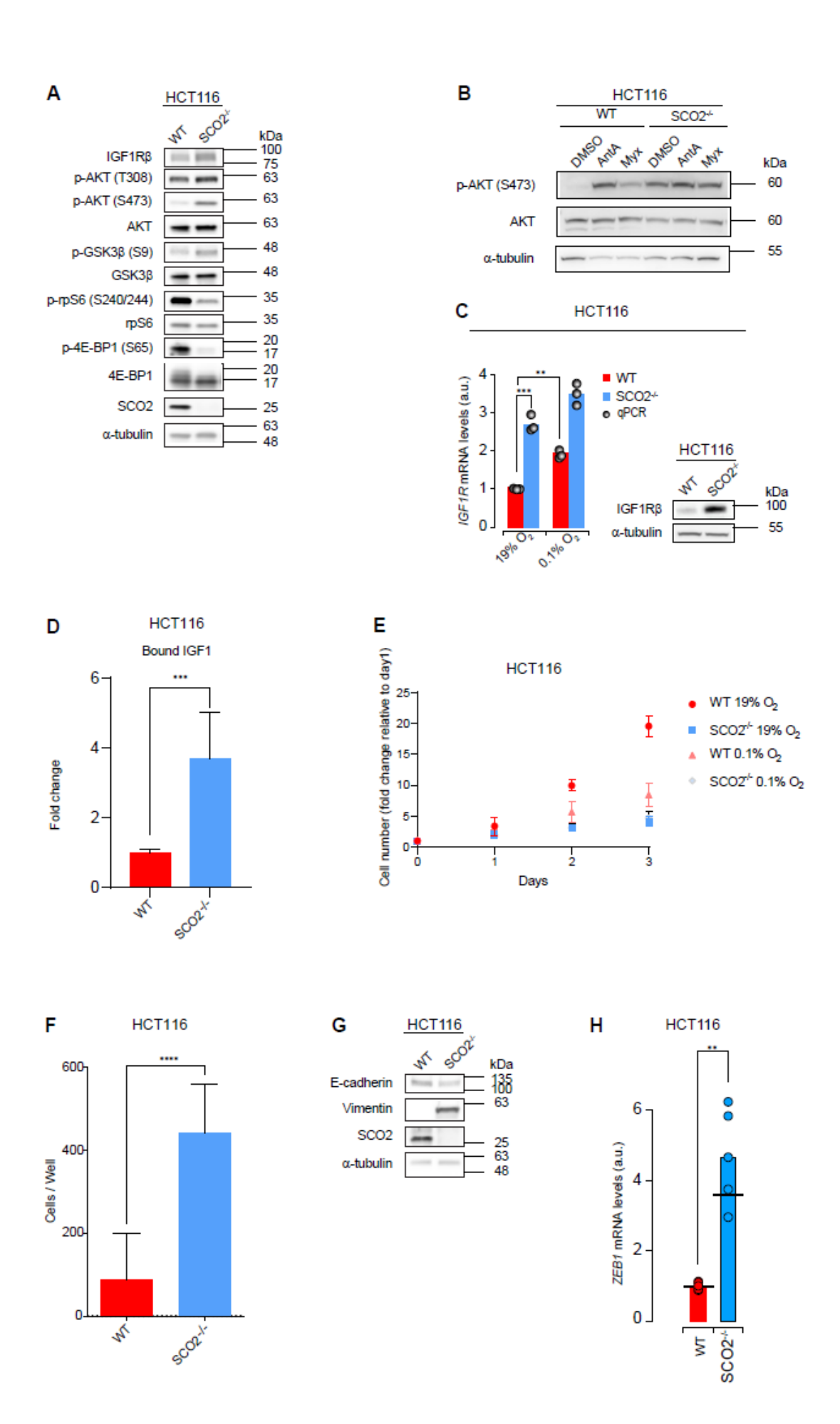


Fig. 2.5. SCO2 loss in HCT116 cells leads to activation of AKT and AMPK, suppression of mTORC1, reduction in cell proliferation and increased cell migration. A. Levels and phosphorylation status of indicated proteins were monitored by Western blotting in WT and SCO2 - HCT116 cells. α-tubulin served as a loading control. Shown are representative Western blots from 3 independent replicates. **B.** WT HCT116 cells were treated with antimycin A (Ant A, 5 µM) or myxothiazol (Myx, 2 µM) treated for 8 days. Western blot analysis was employed to assess the levels and phosphorylation status of indicated proteins. α-tubulin served as a loading control. Representative blots from 3 independent experiments are shown C. IGF1R mRNA and IGF1Rβ protein levels were determined by RT-qPCR and Western blotting respectively. As indicated WT and SCO2-/- HCT116 cells were maintained under 19% or 0.1% O2 for 8 days. RT-qPCR data are presented as mean values of 3 independent experiments (columns) and individual data points; mean values obtained for HCT116 WT maintained under 19% oxygen was set to 1 a.u. **p<0.01, ***p<0.001 (Unpaired 2-tailed t-test). Representative Western blots from 3 independent experiments are shown. α -tubulin was used as a loading control. **D.** Levels of bound IGF1 were calculated by monitoring free IGF1 levels in extracellular media of WT and SCO2-/- HCT116 cells using ELISA. Data is represented as a mean fold change +/- SD relative to WT HCT116 cells (set at 1). ****p<0.0001 (Unpaired 2-tailed t-test; n=3 independent replicates with 3 technical replicates each). E. Numbers of viable WT (red) and SCO2^{-/-} (blue) HCT116 cells grown 0.1% (triangles) or 19% O2 (squares) for indicated times was monitored by trypan blue exclusion using automated cell counter. Results are presented as the mean value +/- SD relative to WT or SCO2-/-HCT116 cell number grown in normoxia at day 1 which was set to 1 (n=4 independent experiments with 3 technical replicates each). **F.** Transwell migration assay of WT and SCO2^{-/-} HCT116 cells. The columns represent the mean summarized cell counts of four fields from a single transwell

migration chamber. Data are presented as the mean value +/- SD ****p<0.0001 (Unpaired 2-tailed t-test; n=3 independent experiments with 2 technical replicates each). **G.** Levels of indicated proteins were monitored by Western blotting. α-tubulin was used as a loading control. Representative blots from 3 independent experiments are shown. **H.** *ZEB1* mRNA levels in WT and *SCO2*-/- HCT116 cells were analyzed by RT-qPCR. Results are presented as mean values of 3 independent experiments (columns) and individual data points. Mean values obtained for WT HCT116 cells was set to 1 a.u. **p<0.01, ***p<0.001 (Unpaired 2-tailed t-test). Quantifications of Western Blots are shown in Fig. S2.9.

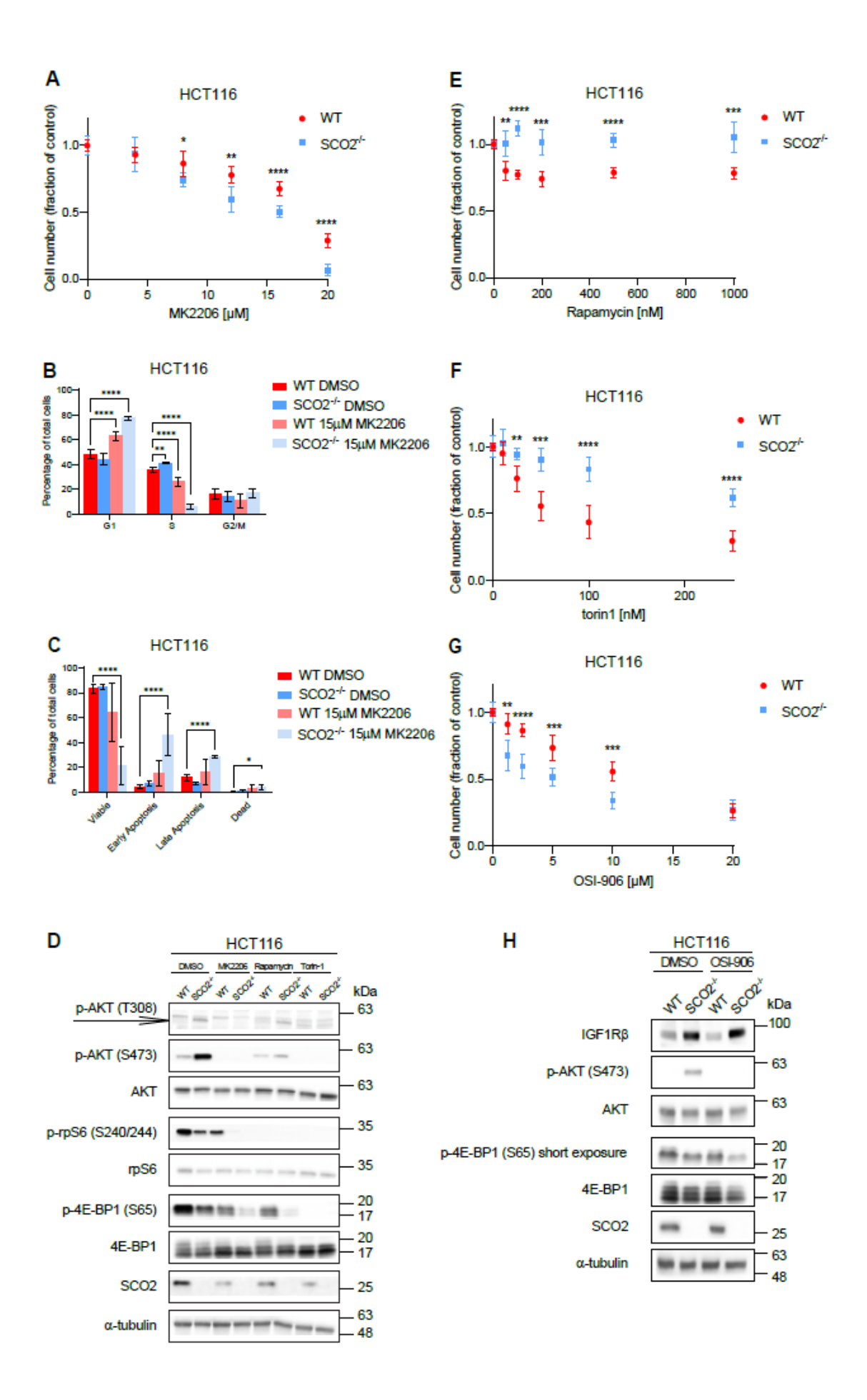


Fig. 2.6. Complex IV deficiency increases sensitivity of HCT116 cells to IGF1R and AKT, but not mTOR inhibitors. A. WT and SCO2-/- HCT116 cells were treated with indicated concentrations of pan-AKT inhibitor MK2206 or a vehicle (DMSO) for 3 days. The number of viable cells at each time point was obtained using trypan blue exclusion and automated cell counter. Data are represented as the mean fraction of cells relative to the corresponding DMSOtreated controls which were set to 1. Experiments were carried out in 3 independent replicates (2 technical replicates each time). Bars represent +/- SD values. B. Cell cycle distribution of WT and HCT116 SCO2-/- cells treated with MK2206 (15 µM) or a vehicle (DMSO) for 24 h was determined by flow cytometry. The data are presented as mean percent values of the total cell population +/- the SD. *p<0.05, **p<0.01, ***p<0.001, ****p<0.001 (One-way ANOVA; Dunnette's posthoc test with WT HCT116 DMSO-treated cells as control; n=2 independent experiments with 3 technical replicates in each). C. WT and SCO2-/- HCT116 cells were treated with MK2206 (15 µM) for 48 h, stained with AnnexinV-FITC and PI subsequently monitored by flow cytometry. Percent of live, early apoptotic, late apoptotic and dead cells are shown relative to the total cell population. The data are presented as mean values +/- the SD. *p<0.05, **p<0.01, ***p<0.001, ****p<0.0001 (One-way ANOVA; Dunnette's posthoc test with WT HCT116 DMSO-treated cells as control; n=2 independent experiments with 3 technical replicates each). **D.** Western blot analysis of indicated proteins isolated from WT and HCT116 SCO2-/- cells treated with MK2206 (15 μ M), rapamycin (50 nM), torin 1 (250 nM), or a vehicle (DMSO) for 24 h. Representative blots from 2 independent experiments are shown. α-tubulin served as a loading control. **E-G,** WT and SCO2^{-/-} HCT116 cells were treated with indicated concentrations of mTOR [rapamycin (**E**) or torin 1 (**F**)], INSR/IGF1R inhibitors [OSI-906 (**G**)] or a vehicle (DMSO) for 3 days. Numbers of viable cells in each condition were determined by trypan blue exclusion using

automated cell counter. Data are represented as the mean fraction of cells relative to DMSO treated controls +/- SD. Experiments were carried out in independent triplicate with 2 technical replicates each. **H.** WT and *SCO2*-/- HCT116 cells were treated with OS1-906 (10 μM) or a vehicle (DMSO) for 24 h. Levels and phosphorylation status of indicated proteins was determined by Western blotting. α-tubulin served as a loading control. Representative blots from 3 independent experiments are shown. Quantifications of Western Blots are shown in Fig. S2.9.

2.5 SUPPLEMENTAL FIGURES

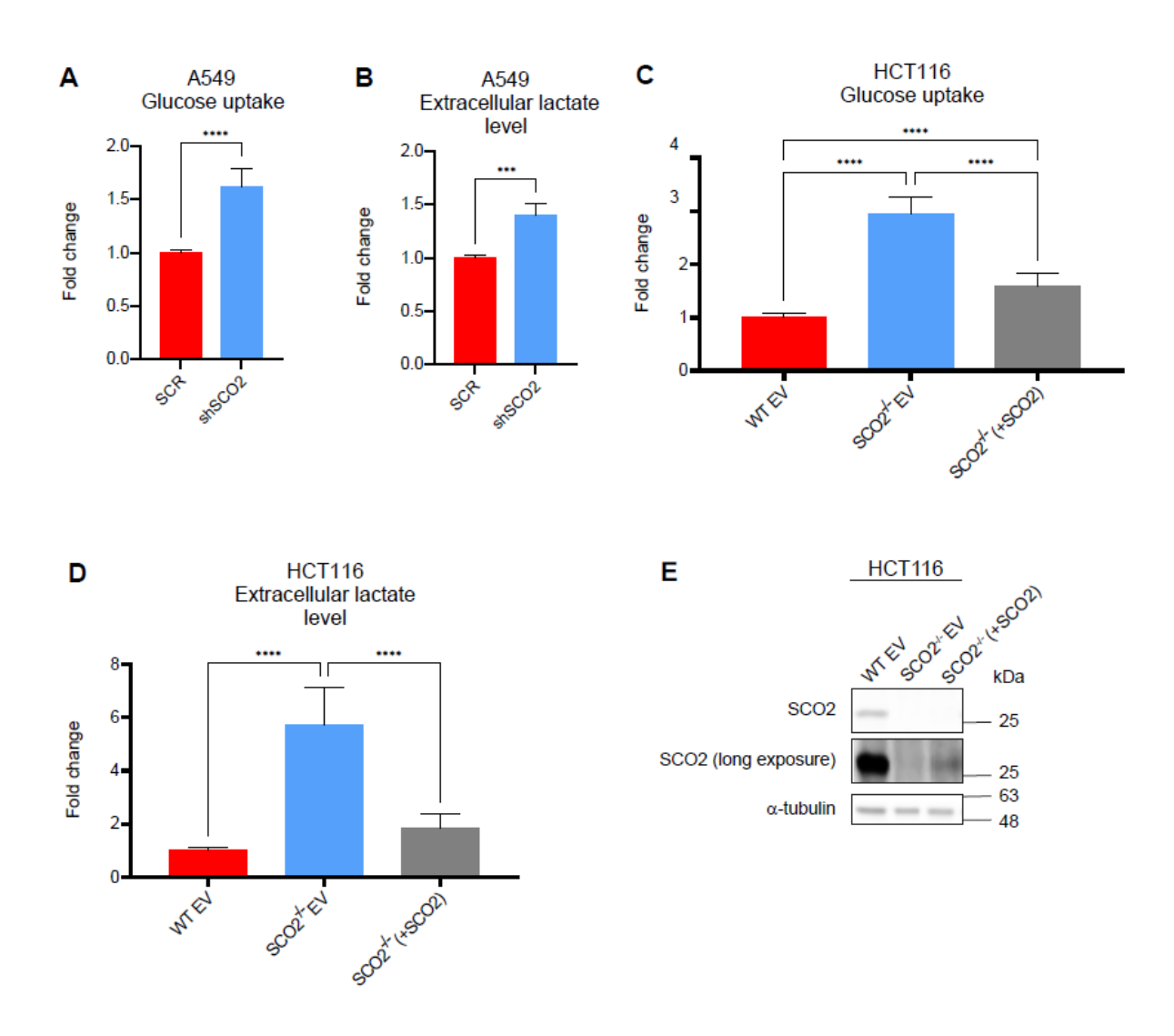


Fig. S2.1. *SCO2* **regulates glucose metabolism. A-D,** Glucose uptake (**A** and **C**) and extracellular lactate levels (**B** and **D**) were monitored using BioProfiler analyzer in the indicated cell lines. Data are represented as mean fold change relative to the scrambled shRNA (SCR) control in A549 cells (**A-B**) or empty vector (EV) control in HCT116 cells (**C-D**) [SCR A549 and WT EV HCT116; set to 1 +/- standard deviation (SD)]. ****p<0.0001, ***p<0.001 ((**A-B**) Unpaired 2-tailed t-test; n=2 independent experiments with 3 technical replicates each. (**C-D**) One-way ANOVA; Tukey's multiple comparison post-hoc test; n=4 independent experiments with 1-3 technical replicates in each). **E.** Level of SCO2 in WT and *SCO2*-/- HCT116 cells infected with an empty vector (EV) or *SCO2*-/- HCT116 cells where *SCO2* was re-expressed (+SCO2) was monitored by Western blotting (N=3 independent experiments). α-tubulin served as a loading control. Quantifications of the Western blots are provided in Fig. S2.9.

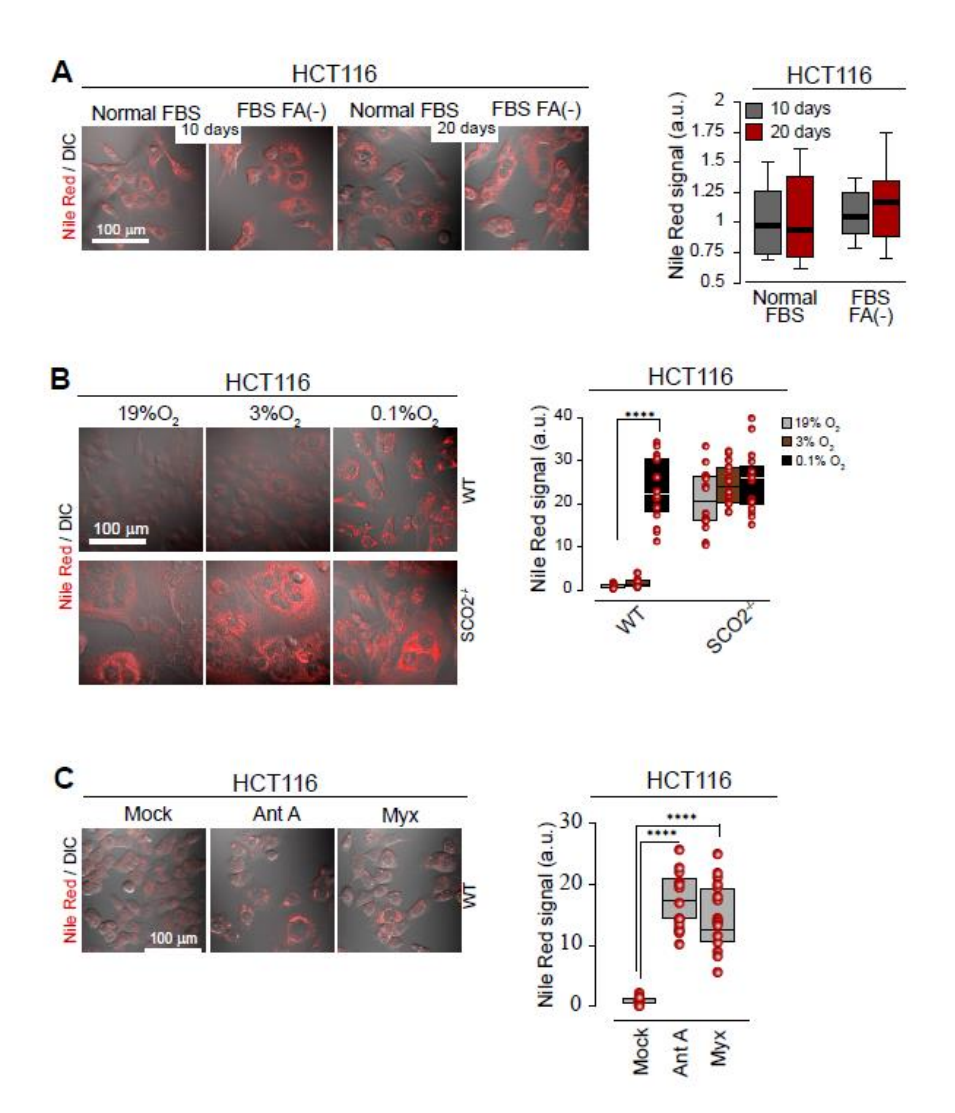


Fig. S2.2. Inhibition of complex III or IV of the electron transport chain results in lipid droplet accumulation in HCT116 cells. A-C, Confocal microscopy of lipid droplets using Nile Red staining with the fluorescent images composed of stacks of 5 focal planes taken with 0.5 μm step subsequently superimposed with single-plane DIC images (N= 20 cells for each condition). **A.** *SCO2*^{-/-} HCT116 cells were grown for 10 and 20 days in the presence of regular fatty acid (FA+) and FA-deficient FBS (FA-). **B.** *SCO2*^{-/-} and WT HCT116 cells were maintained for 10 days at 19%, 3% or 0.1% O₂. **C.** WT HCT116 cells were treated with complex III inhibitors antimycin A (Ant A, 5 mM) or myxothiazol (Myx, 2 mM) for 10 days. All results are presented as median and

interquartile range (boxes) (**A-C**) along with individual data points (**B-C**). Mean value obtained for WT HCT116 cells was set to 1 a.u. ****p<0.0001 (Unpaired 2-tailed t-test).

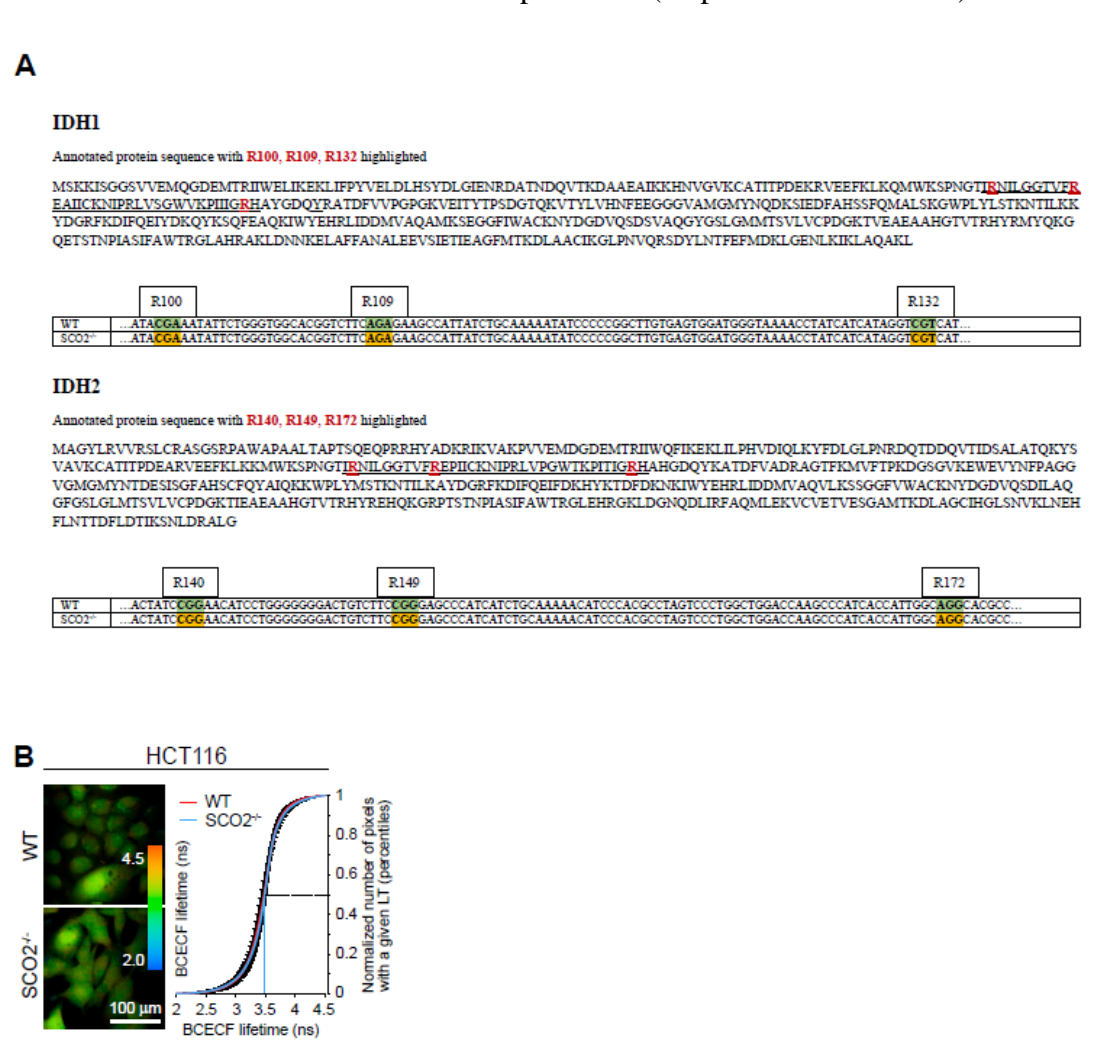


Fig. S2.3. HCT116 cells are devoid of mutations in *IDH1* **and** *IDH2* **genes while the loss of** *SCO2* **does not affect intracellular pH. A.** Sequence analysis of *IDH1* and *IDH2* genes in WT and *SCO2*-/- HCT116 cells. Complete amino acid sequences of IDH1 and IDH2 proteins and DNA fragments containing the known mutations (R140, R149 and R172) that underlie D-2-HG production by IDH is provided. The absence of mutations was confirmed by RNAseq analysis (n=

2 independent experiments). **B.** The effects of *SCO2* on intracellular pH were assessed via confocal Fluorescence Lifetime Imaging (FLIM) of 2'-7'-bis(carboxyethyl)-5(6)-carboxyfluorescein (BCECF) staining. Images are stacks of three focal planes taken with a 1 μm step. Right panel shows cumulative distributions of BCECF lifetime values in cells localized in the entire field of view (256×256 pixels); dotted lines demonstrate lifetime values that correspond to the 50th percentile (median) of the lifetime distribution (n=3 independent experiments).

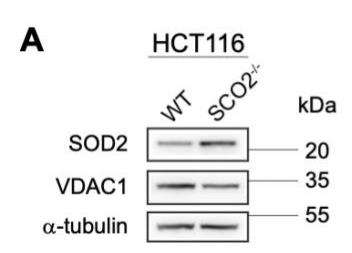


Fig. S2.4. SCO2 deletion in HCT116 cells increases expression of SOD2. A. Levels of indicated proteins were monitored by Western blotting. VDAC1 and α -tubulin served as loading controls. The experiments are representative of 3 independent replicates. Quantifications of the Western blots are provided in Fig. S2.9.

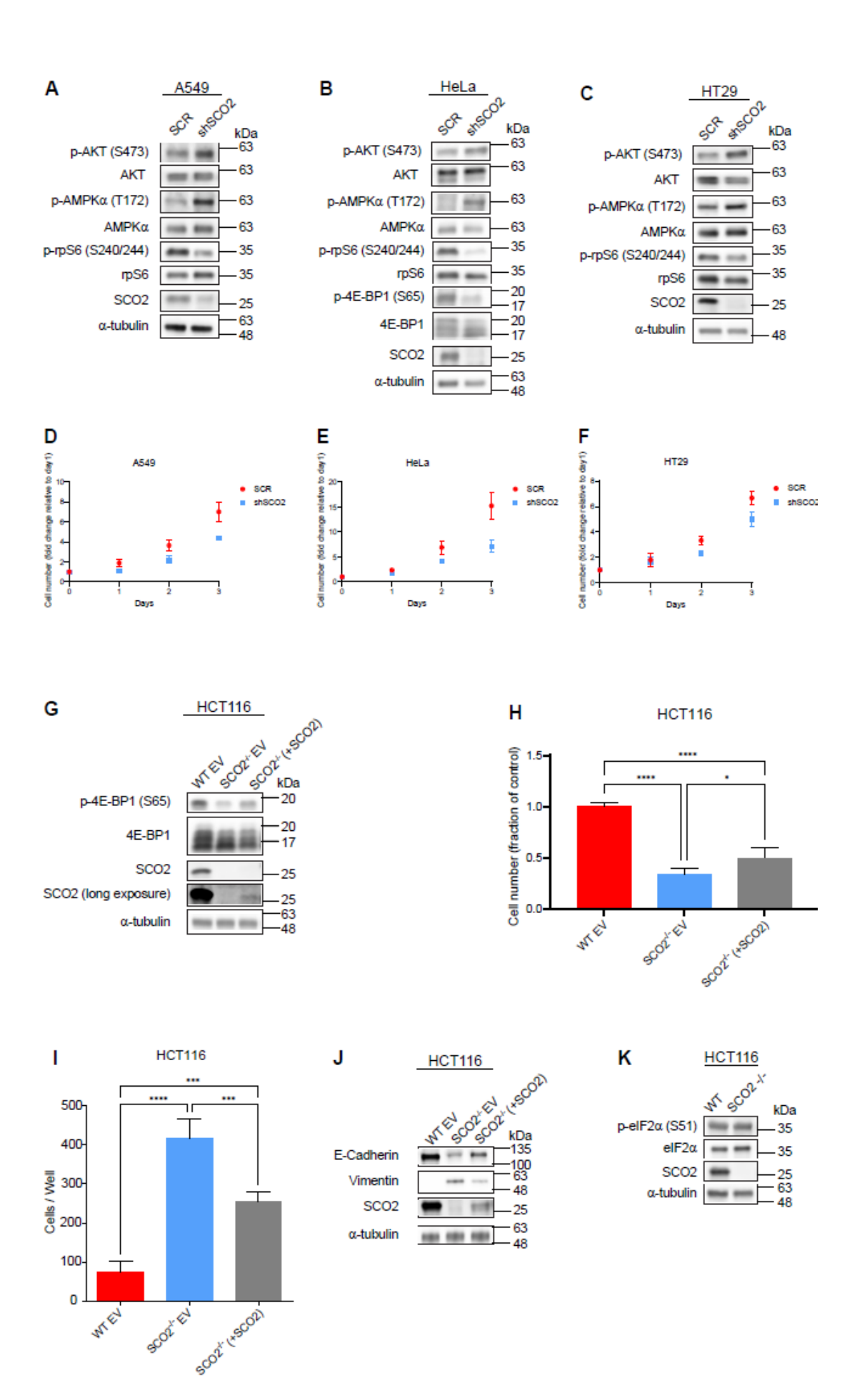


Fig. S2.5. SCO2 loss rewires signaling, reduces proliferation and bolsters migration A-C, Levels and phosphorylation status of indicated proteins were monitored by Western blotting after lentiviral knockdown of SCO2 (shSCO2) in A549 (A), HeLa (B) and HT29 (C) cells. In parallel, A549 (A), HeLa (B) and HT29 (C) cells were infected with scrambled shRNA (SCR). Shown are the representative Western blots from 3 (A549 and HeLa) or 2 (HT29) independent experiments. α-tubulin was used as a loading control. **D-F**. Numbers of viable SCR (red) and shSCO2 (blue) infected A549 (**D**), HeLa (**E**) and HT29 (**F**) cells grown for indicated times were determined by trypan blue exclusion using automated cell counter. Results are presented as the mean value +/-SD whereby the number of SCR cells at day 1 was set to 1 (n=2 independent experiments with 3 technical replicates each for A549, n=4 independent experiments with 3 technical replicates each for HeLa, n=3 independent experiments with 3 technical replicates each for HT29). G. Levels and phosphorylation status of indicated proteins in WT EV, SCO2-/- EV and SCO2-/- (+SCO2) HCT116 cells were monitored by Western blotting. α-tubulin served as a loading control. Shown are representative Western blots from 3 independent experiments. **H**. Numbers of WT and SCO2^{-/-} HCT116 cells infected with empty vector (EV) and SCO2-/- HCT116 cells re-expressing SCO2 (+SCO2) grown for 3 days were assessed using trypan blue exclusion using automated cell counter. Results are presented as the mean value +/- SD relative to WT EV HCT116 cell number which was set to 1 (n=2 independent experiments with 2-3 technical replicates each). I. Transwell migration assay of WT EV, SCO2-/-EV and SCO2-/-(+SCO2) HCT116 cells. Presented are the mean summarized cell counts of four fields from a single transwell migration chamber +/- SD (****p<0.0001; ***p<0.001 One-way ANOVA; Tukey's multiple comparison post-hoc test; n=2 independent experiments with 2 technical replicates in each). J. Levels and phosphorylation status of indicated proteins were monitored by Western blotting in WT EV, SCO2-/- EV and SCO2-/-

(+SCO2) HCT116 cells. α-tubulin served as a loading control. Shown are representative Western blots from 3 independent experiments. **K.** Levels and phosphorylation status of indicated proteins were monitored by Western blotting in WT and *SCO2*-/- HCT116 cells. α-tubulin served as a loading control. Shown are representative Western blots from 4 independent experiments. Quantifications of the Western blots are provided in Fig. S2.9.

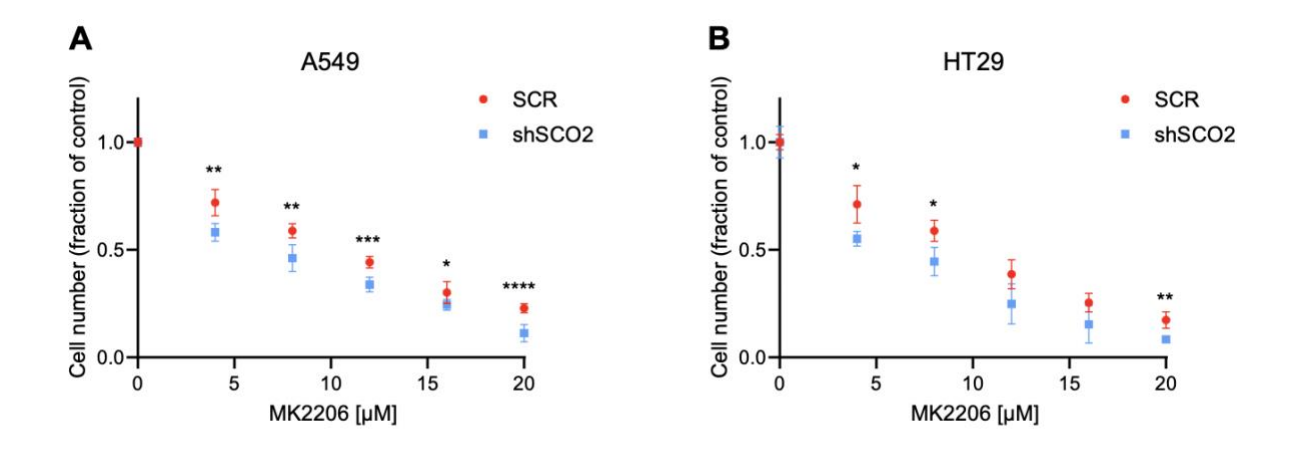


Fig. S2.6. Reduced complex IV activity increases sensitivity cancer cells to AKT inhibitor. A-B. A549 (A) and HT29 (B) cells were infected with scrambled shRNA (SCR) or SCO2 shRNA (shSCO2). The cells were treated with indicated concentrations of pan-AKT inhibitor MK2206 or a vehicle (DMSO) for 3 days. The number of viable cells were determined using trypan blue exclusion and automated cell counter. Data are presented as the mean fraction of cells relative to the corresponding DMSO-treated controls which were set to 1. Experiments were carried out in at

least 2 independent replicates (with 2 technical replicates each). Bars represent SD values. Data are represented as mean fold change +/- SD relative to vehicle (DMSO) treated cells. *p<0.05, **p<0.01, ***p<0.001, ****p<0.001 (Unpaired 2-tailed t-tests were carried out at each drug concentration tested).

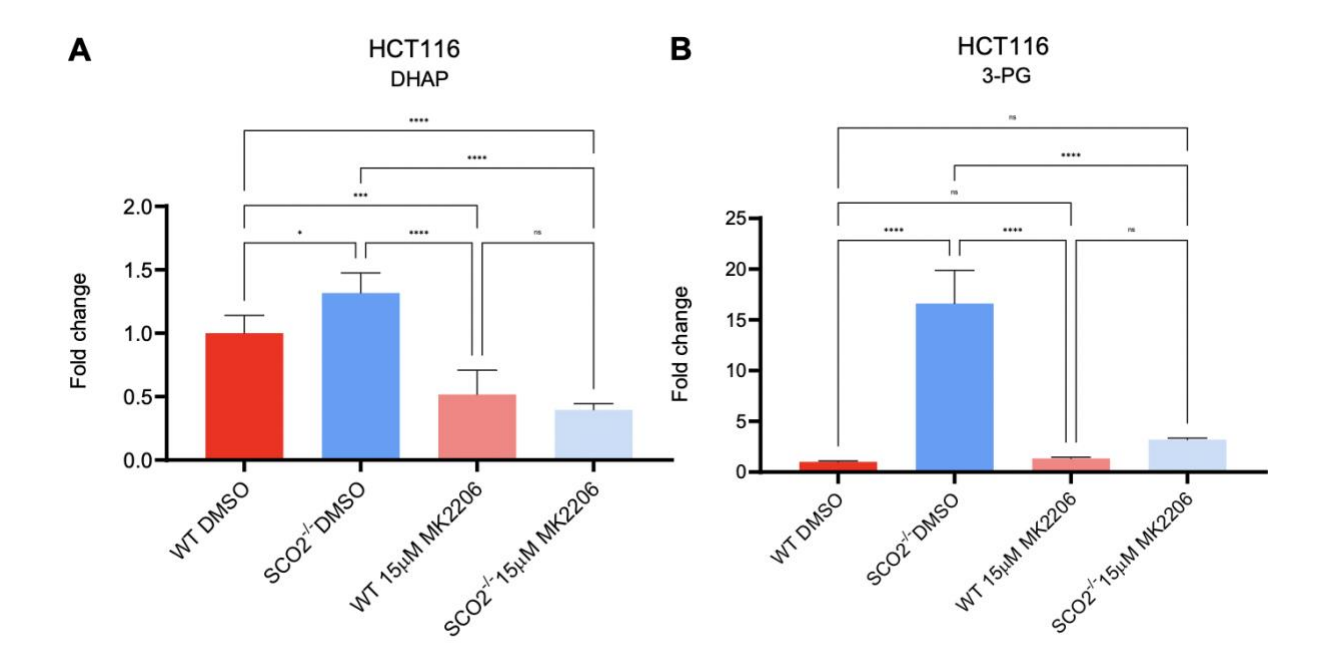
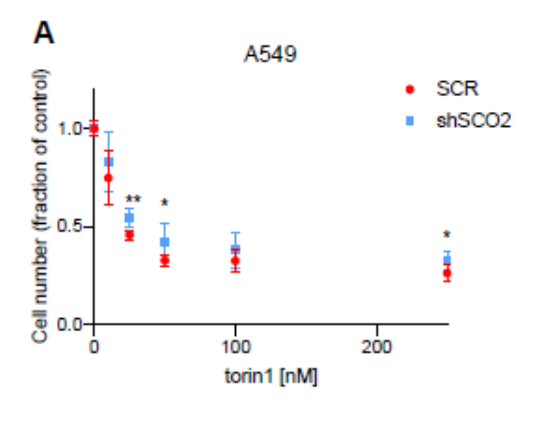
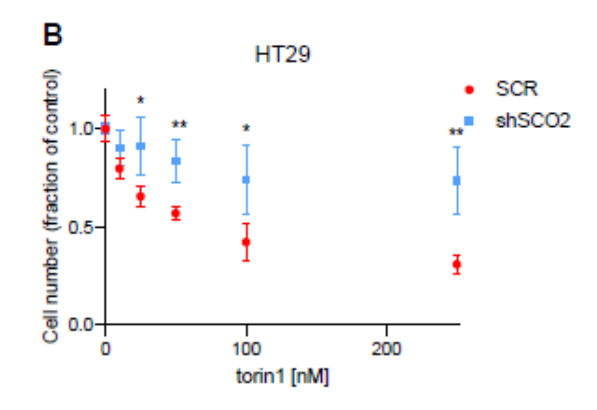
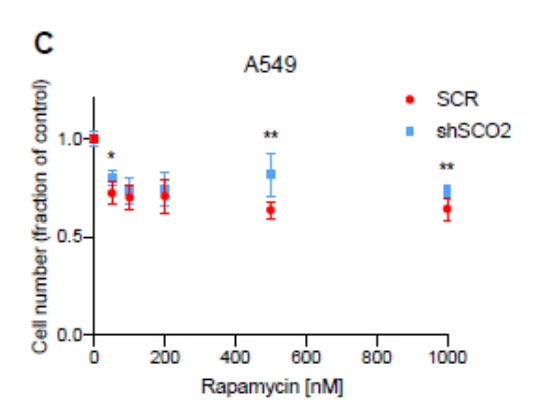


Fig. S2.7. Inhibition of AKT dampens the compensatory increase in glycolysis caused by the deletion of SCO2 in HCT116 cells. A-B, Intracellular levels of DHAP (A) and 3-PG (B) in WT or $SCO2^{-/-}$ HCT116 cells. Cells were seeded and treated with MK2206 (15 μ M) for 24 h. Metabolite levels were monitored by GC-MS. Data are represented as mean fold change +/- SD relative to vehicle (DMSO) treated WT HCT116 cells. *p<0.05, **p<0.01, ***p<0.001,

****p<0.0001 (One-way ANOVA; Tukey's multiple comparison post-hoc test; n= 2 independent experiments with 3 technical replicates in each).







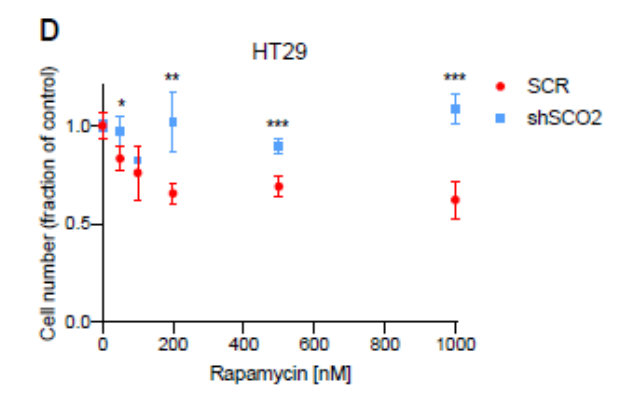
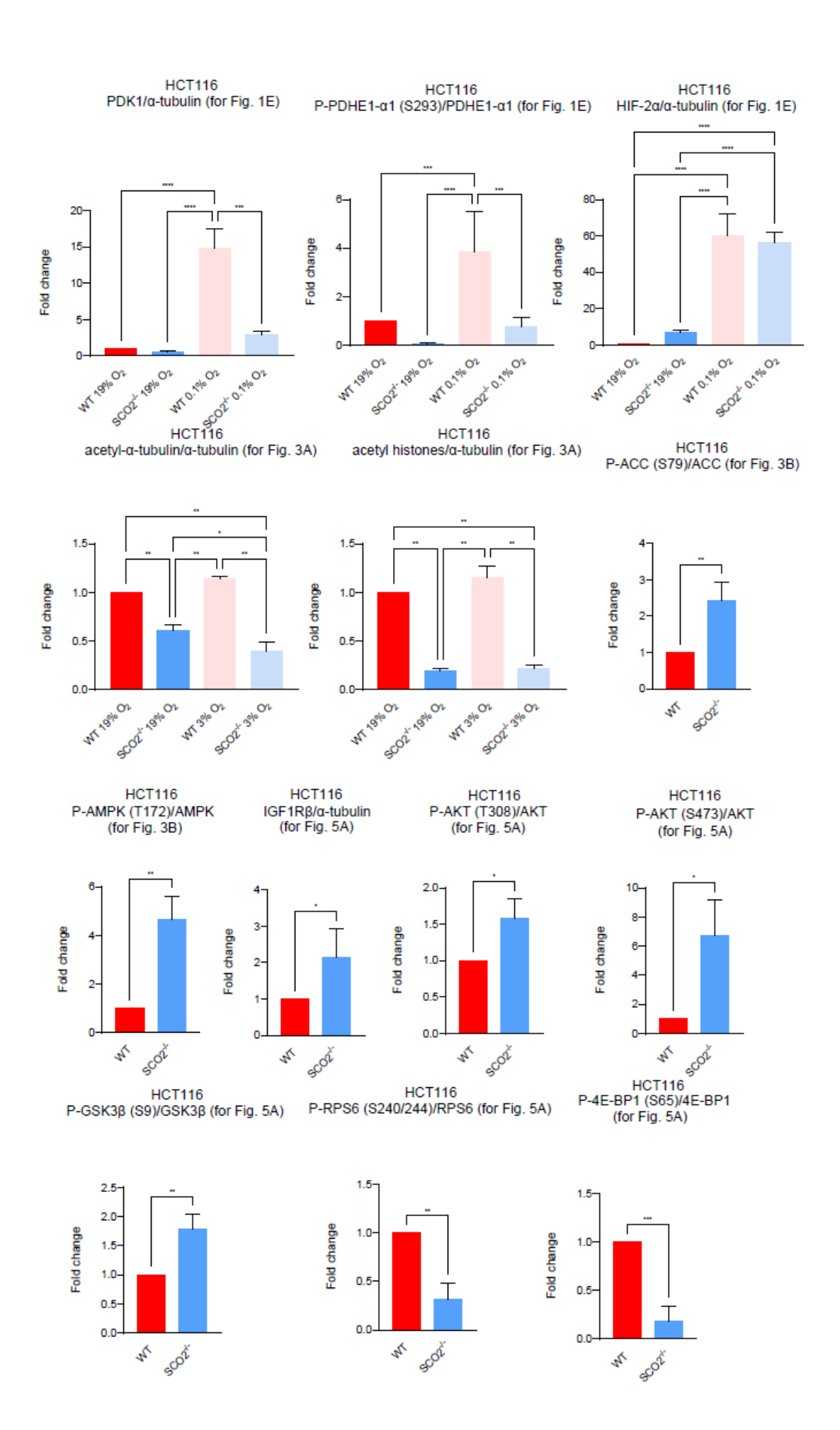
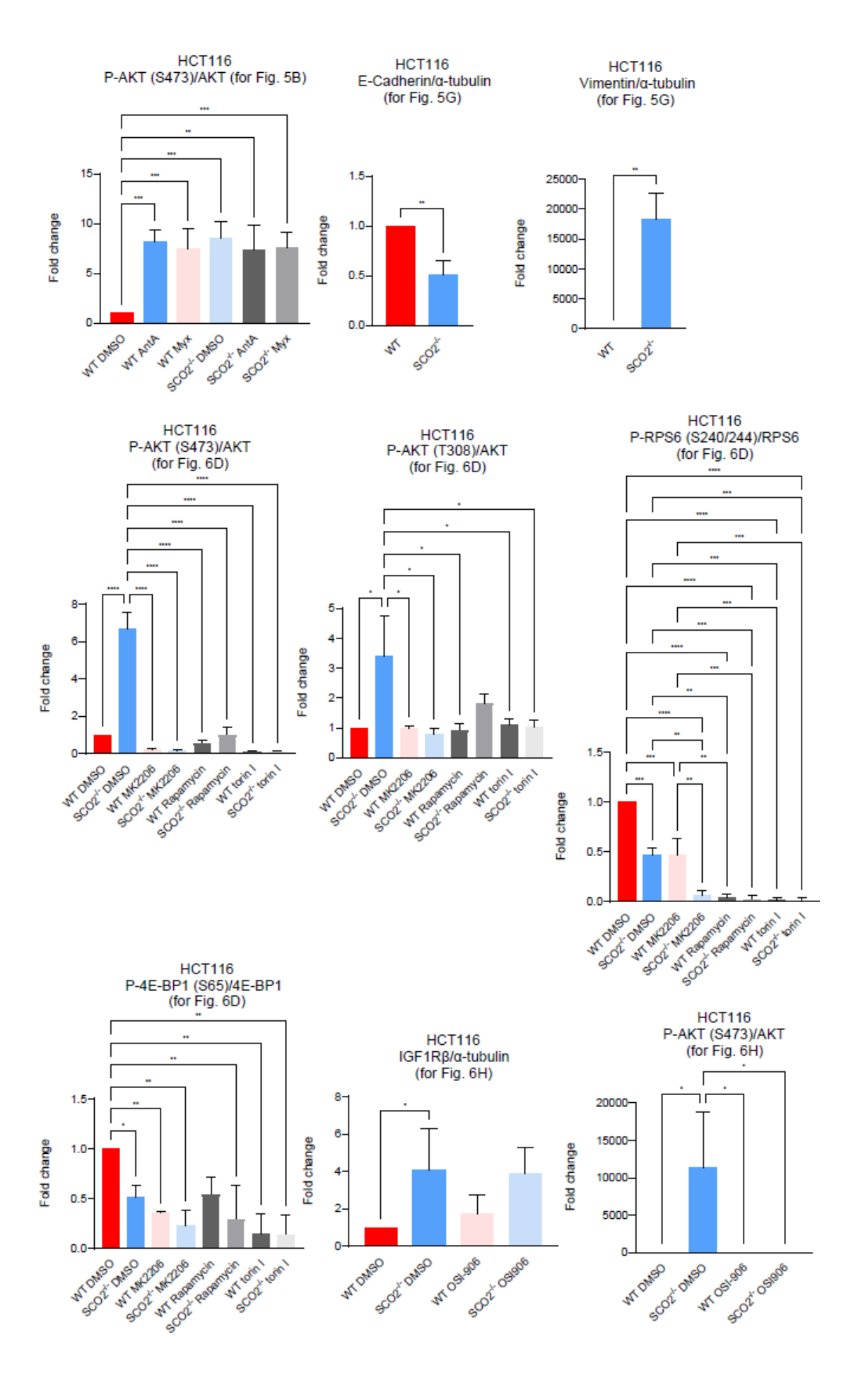
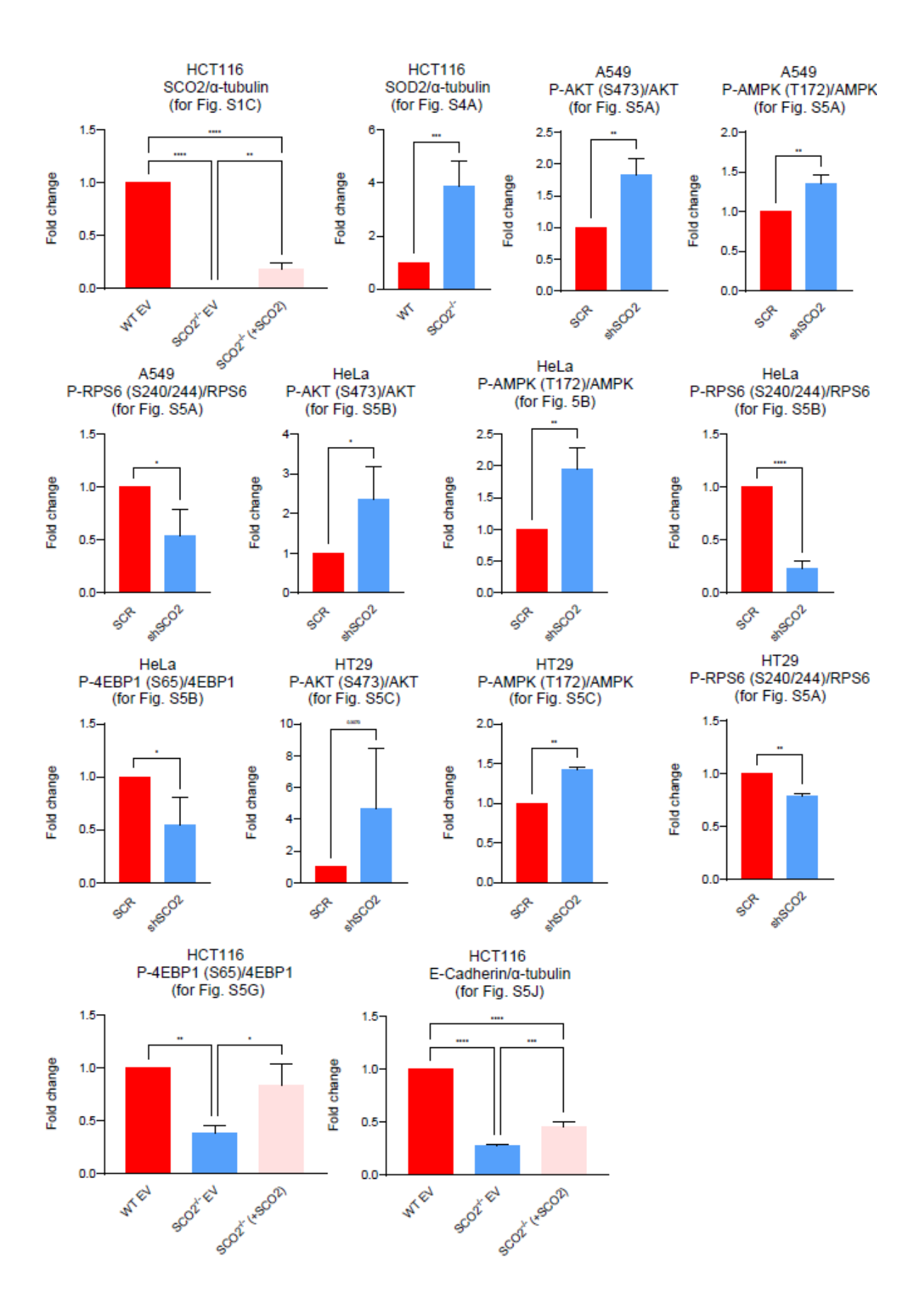


Fig. S2.8. Depletion of mitochondrial complex IV activity reduces sensitivity of cancer cells to mTOR inhibitors. A549 (A-B) and HT29 (C-D) cells were infected with scrambled shRNA (SCR) or SCO2 shRNA (shSCO2). The cells were treated with indicated concentrations of rapamycin (A, C) or torin 1 (B, D) or a vehicle (DMSO) for 3 days. Numbers of viable cells in each condition were determined by trypan blue exclusion using automated cell counter. Data are represented as the mean fraction of cells relative to DMSO treated controls +/- SD. Experiments were carried out in at least two independent times with 2 technical replicates each. Error bars represent SD values. *p<0.05, **p<0.01, ***p<0.001, ****p<0.0001 (Unpaired 2-tailed t-tests were carried out at each drug concentration tested).







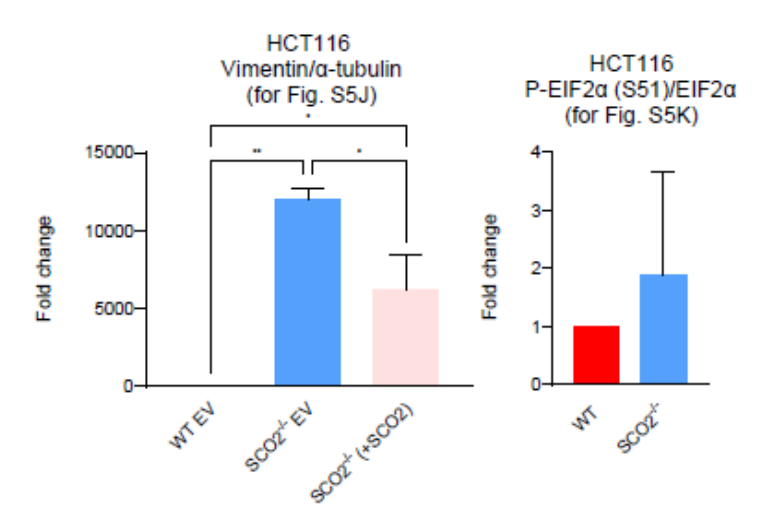
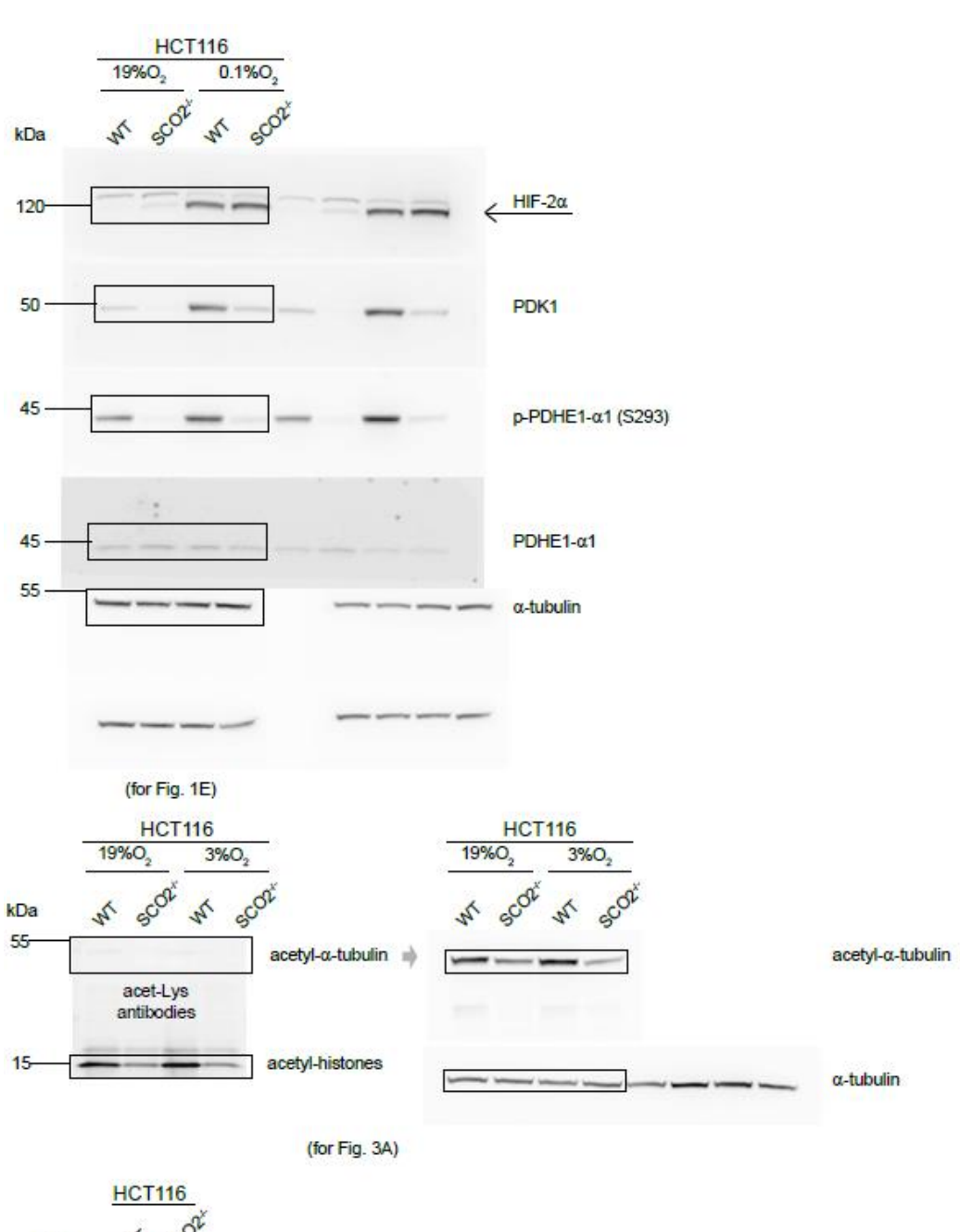
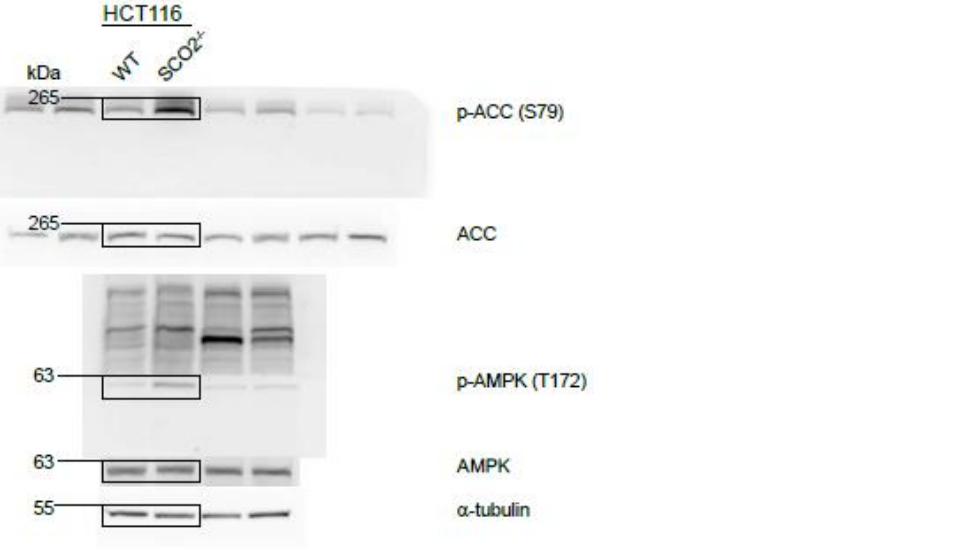


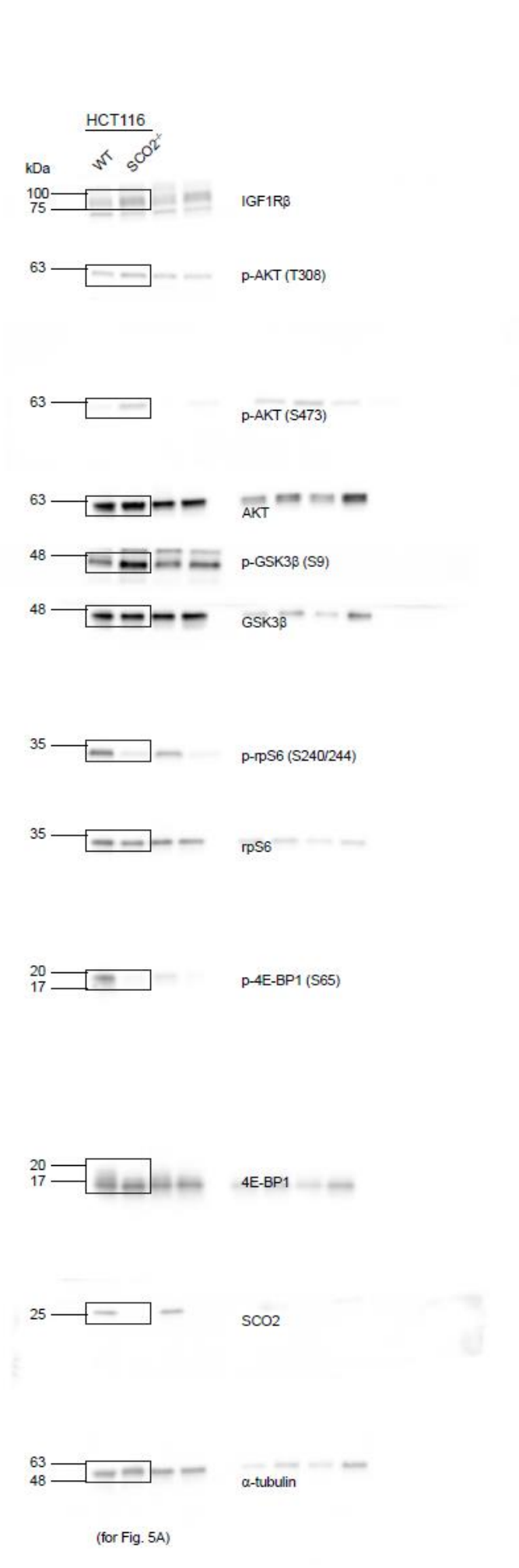
Fig. S2.9. Densitometry analysis of Western blots. Results represent mean fold changes in densitometry signals relative to the indicated controls. Signals for phospho-proteins and proteins of interest were normalized over corresponding total proteins or α -tubulin, respectively as

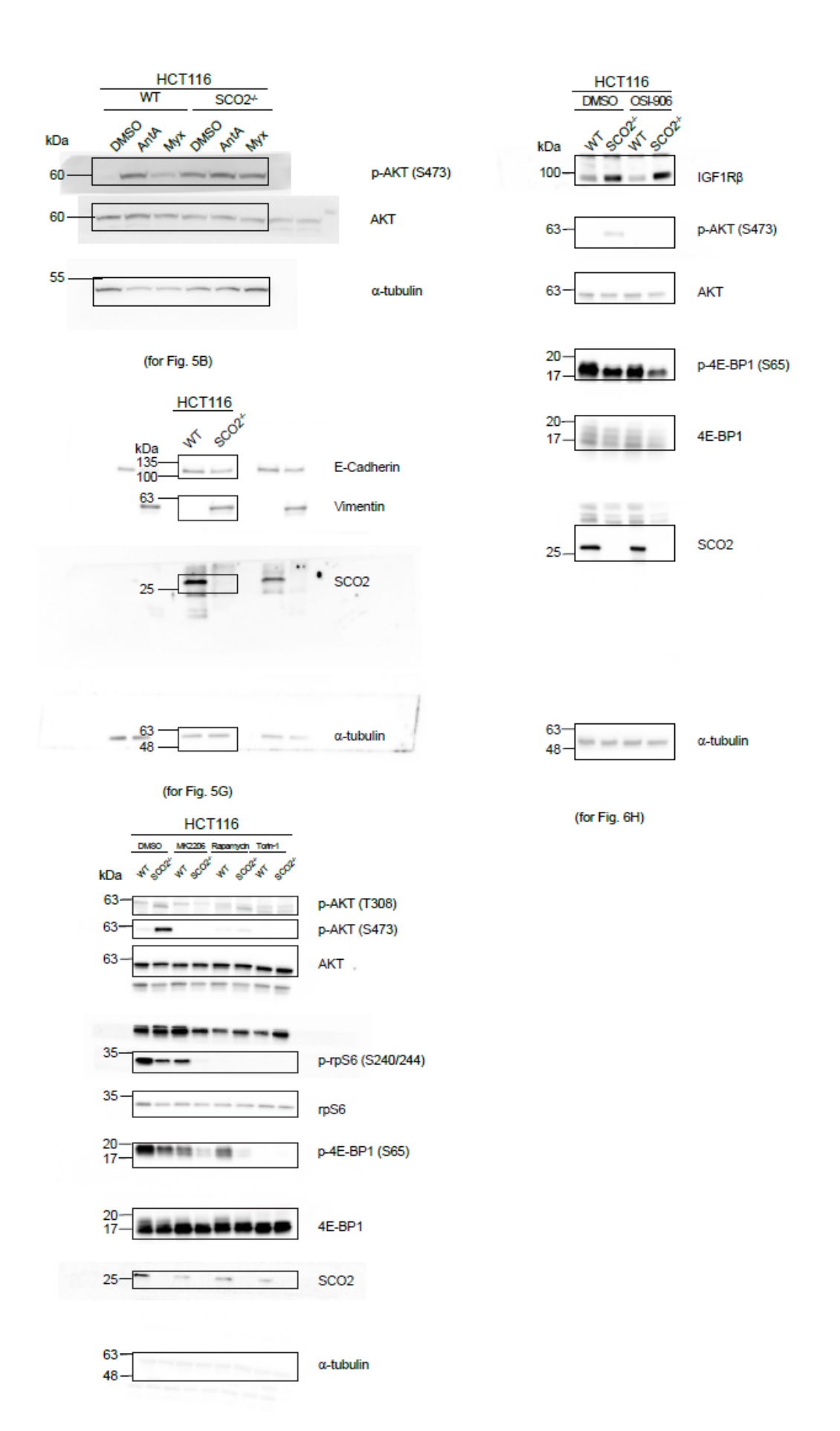
indicated. The experiments were repeated at least in independent duplicates; *p<0.05, **p<0.01, ****p<0.001, ****p<0.0001 (Unpaired 2-tailed t-test, 1-way ANOVAs, and 2-way ANOVAs were done when two, three or more than three variables were investigated, respectively).



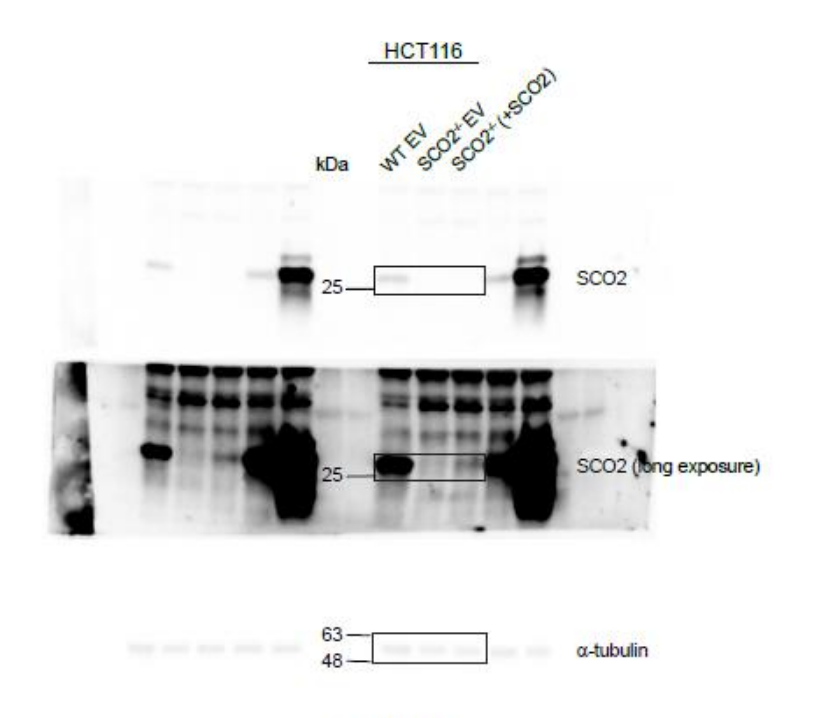


(for Fig. 3B)

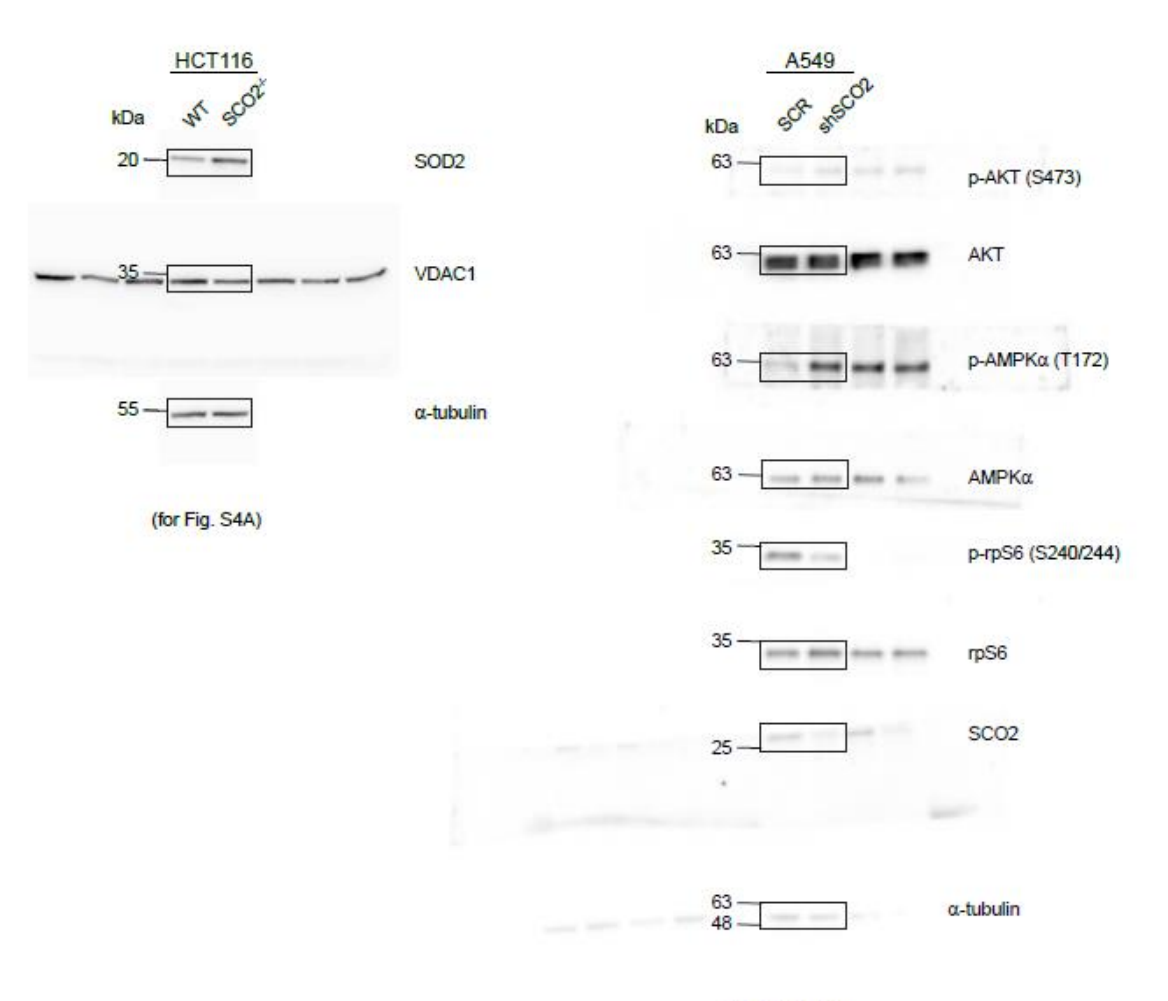




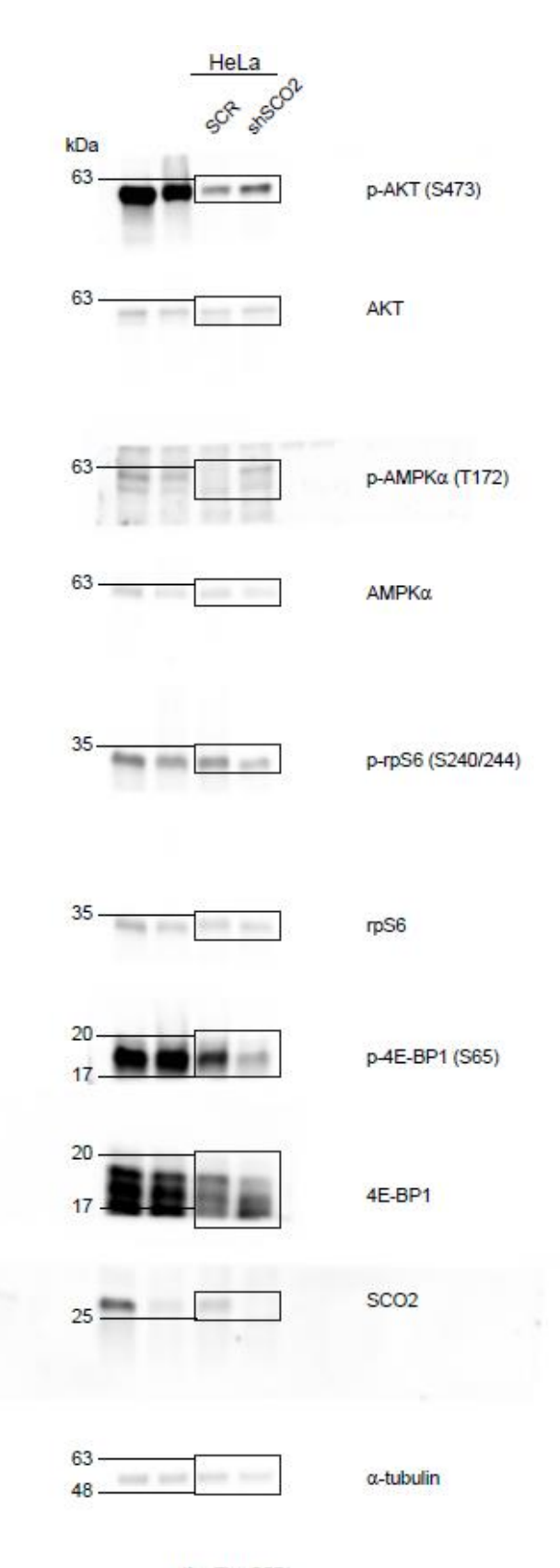
(for Fig. 6D)



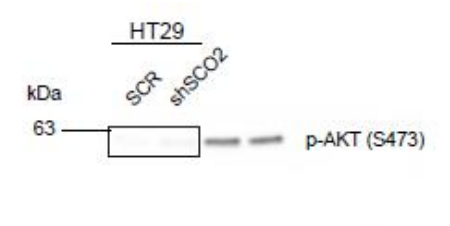
(for Fig. S1E)



(for Fig. S5A)



(for Fig. S5B)

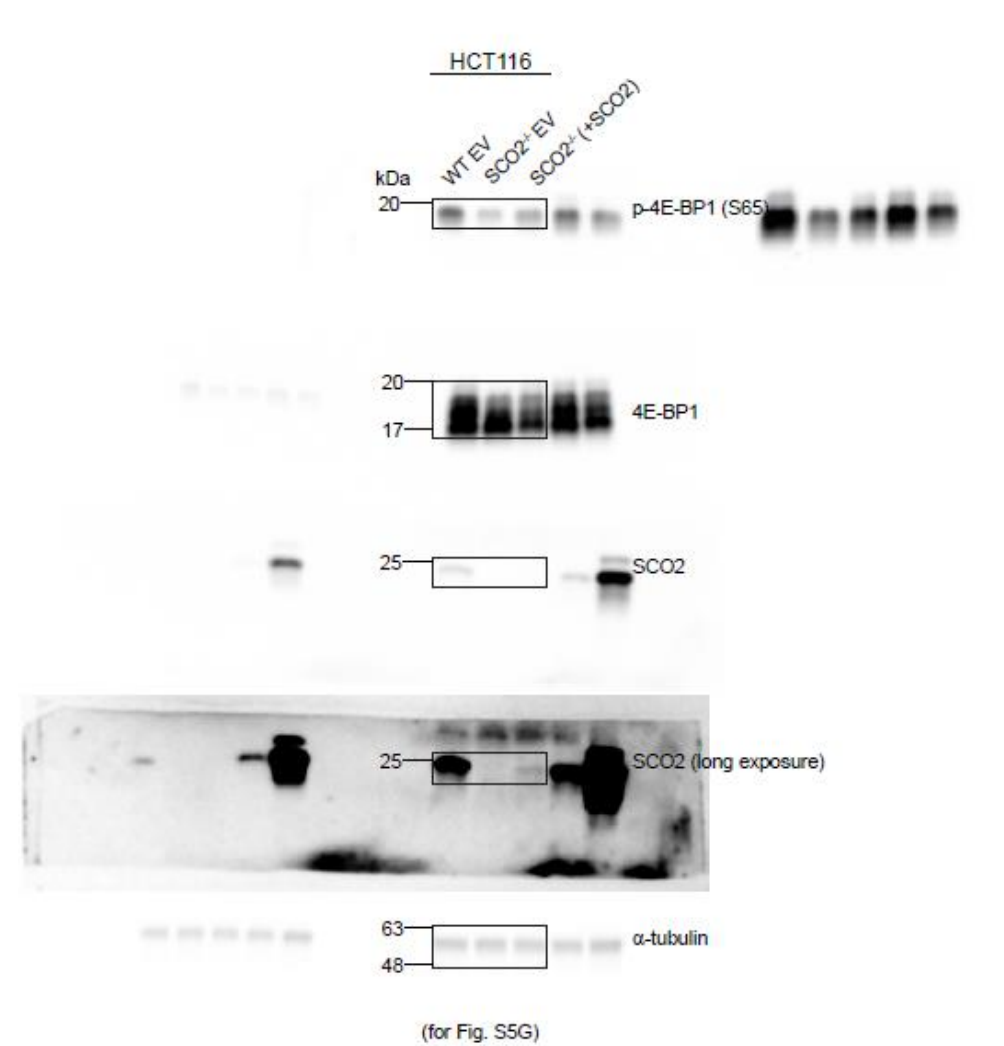


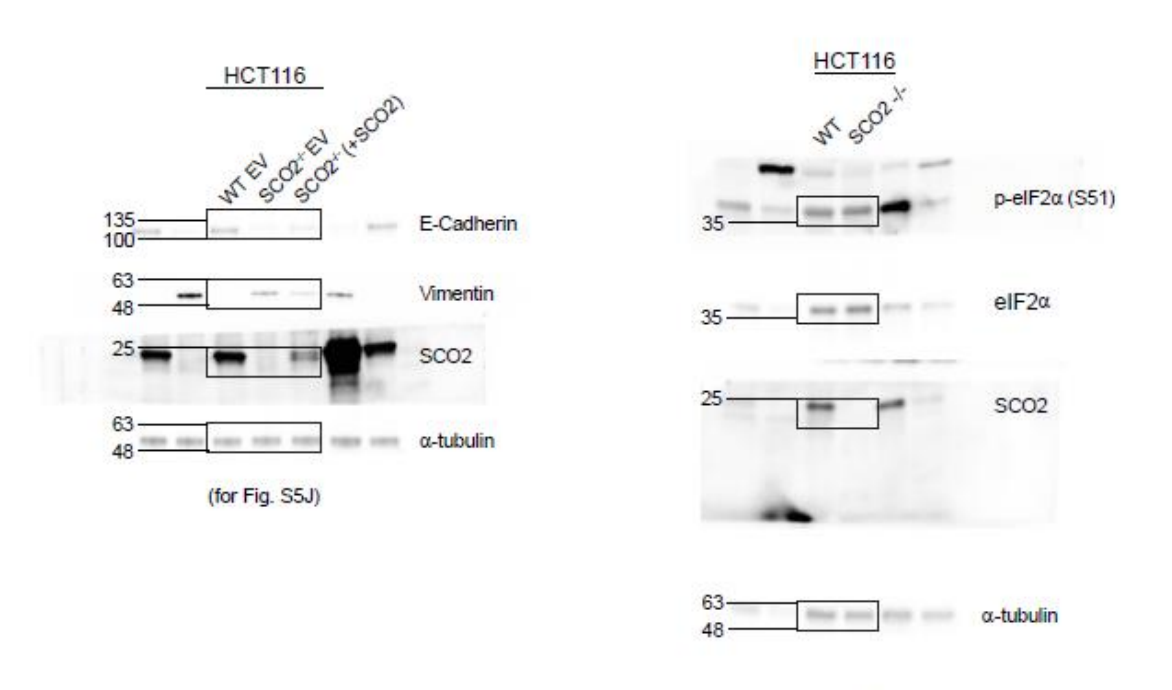






(for Fig. S5C)





(for Fig. S5K)

Fig. S2.10. Images and scans of Western blot films that are incorporated in the manuscript.

The boxes around the indicated protein bands show the approximate area of the x-ray films and nitrocellulose membrane images included in the figures.

2.6 DISCUSSION

Metabolic reprogramming of cancer cells allows them to adapt to changes in nutrient and oxygen availability and therapeutic insults (67, 68). To this end, it is considered that metabolic rewiring not only fulfils the energetic requirements of cancer cells, but also provides building blocks and maintains redox buffering capacity required to fuel growth and survival of cancer cells (67, 68). Herein, we report that disruption of mitochondrial complex IV function by SCO2 loss is compensated by dramatic perturbations in metabolome and signaling. Most notably, SCO2 loss in HCT116 cells leads to increase in glycolysis (12). This not only enables HCT116 cells with dysfunctional complex IV to meet the biosynthetic demands by providing carbon atoms but also allows for the regeneration of NAD+ which is necessary to maintain glycolysis and redox homeostasis. Indeed, although SCO2 loss leads to overall increase in NADH levels in HCT116 cells (13), SCO2-/- HCT116 cells upregulate NAD+ regenerating reactions. This is consistent with previous findings suggesting that conversion of pyruvate to lactate and the simultaneous production of NAD+ from NADH by lactate dehydrogenase are essential in the context of mitochondrial dysfunction (69). Moreover, SCO2-/- HCT116 cells appear to exhibit increased activity of GPD1, as illustrated by the alterations in steady-state metabolite levels and increased glucose flux to 3-PG. Notably, although mitochondrial glycerophosphate dehydrogenase (GPD2) has been implicated in the reoxidation of cytosolic NADH via the ETC in prostate cancer (70), due to compromised mitochondrial functions this mechanisms is unlikely to be at play in SCO2deficient HCT116 cells. Hence, GPD1 is most likely involved in maintaining NAD+/NADH ratio in HCT116 $SCO2^{-/-}$ cells. In addition, we observed large accumulation of lipids in HCT116 $SCO2^{-/-}$ cells as compared to their WT counterparts. Lipid accumulation in SCO2-deficient cells was not caused by increased lipogenesis or FA uptake, thus indicating that the observed phenotype likely stems from impediments in β -oxidation of FA in the mitochondria. Finally, SCO2 loss resulted in a reduction of most of the CAC intermediates and amino acids, which was paralleled by an increase in succinate and 2-HG. Although we did not formally test whether accumulation of these metabolites is sufficient to disrupt function of α -ketoglutarate-dependent enzymes (e.g. HIF- α prolyl hydroxylase, histone, DNA and RNA demethylases) (41, 67), these findings suggest that SCO2 loss may result in epigenetic, transcriptional and epitranscriptional reprogramming.

Notably, the observed alterations in metabolic programs in SCO2-deficient HCT116 cells were paralleled by significant rewiring characterized by increased IGF1R/AKT activity that was accompanied by a reduction in mTORC1 signaling. This, at least in part, may be explained by elevated AMPK activity in SCO2-deficient HCT116 cells. Accordingly, SCO2-HCT116 cells showed heightened sensitivity to IGF1R and AKT inhibitors, while they were less sensitive to mTOR inhibitors relative to SCO2-proficient cells. Previous studies demonstrated that AKT upregulates glycolysis (71). Since the loss of SCO2 renders HCT116 cells heavily dependent on glycolysis to produce ATP and regenerate NAD+, it is plausible that these cells are more sensitive to IGF1R and AKT inhibitors because of their inhibitory effects on glycolysis. Strikingly, similar induction in AKT phosphorylation was observed in WT HCT116 cells treated with mitochondrial complex III inhibitors or subjected to hypoxia. Comparable to HCT116 SCO2-cells, the decreased expression of SCO2 in HeLa and A549 increased AKT activity while downregulating mTORC1. Although the precise mechanism(s) of induction of IGF1R/AKT axis in the context of

mitochondrial complex III or IV disruption remains elusive, these findings suggest that mitochondrial dysfunction may lead to critical reliance of neoplastic cells on AKT.

AMPK acts as a negative regulator of mTORC1, and it has recently been described that it may stimulate mTORC2 (72) and be activated by ROS (73). This suggests that AMPK upregulation in HCT116 SCO2-/- cells may dampen mTORC1 signaling while sustaining mTORC2 and AKT activity. Indeed, we observed that disruption of SCO2 results in marked increase in S473 AKT phosphorylation which is indicative of increased mTORC2 activity (74). In addition, mTORC2 may also exert AKT-independent effects of glucose metabolism as reported in glioblastoma (75). Of note, HCT116 SCO2-/- cells produce ATP mainly in cytosol and have the ATP/protein ratio similar to that in WT cells (14), thus suggesting that AMP/ATP or ADP/ATP ratio may not play a major role in AMPK activation in this context. In turn, cytosolic Ca²⁺ levels are elevated in SCO2-/- as compared to HCT116 WT cells (14) thereby suggesting that Ca²⁺/calmodulin dependent protein kinase kinase (CAMKK) may activate AMPK in cells exhibiting complex IV dysfunction. Also, AMPK has been found to be hyperactivated by CAMKK in mouse embryonic fibroblasts (MEFs) devoid of LKB1 kinase when subjected to oxidative stress (76). Considering that we observed similar phenotypes between cells with functional (HCT116) or dysfunctional LKB1 (A549, HeLa), it is likely that mechanisms other than LKB1 play a major role in AMPK activation in the context of mitochondrial complex IV dysfunction. Intriguingly, despite several attempts, we failed to knock down AMPK α1 and/or α2 subunits in HCT116 SCO2 /- cells or deplete SCO2 in AMPK $\alpha 1/\alpha 2^{-/-}$ mouse embryonic fibroblasts (MEFs) due to massive cell death. Notwithstanding that future investigations are required to establish the precise mechanism(s) of adaptation of cancer cells to the abrogated complex IV activity, these observations may suggest an important role for AMPK in this process.

Recent studies show that ROS plays pivotal roles in facilitating EMT and cell motility (77). HCT116 *SCO2*-/- cells were previously shown to have elevated ROS levels (13). A prior study showed that ZEB1 represses E-cadherin and induces vimentin (62). Furthermore, elevated levels of 2-HG have been reported to increase the expression of *ZEB1* by inhibiting histone demethylase, which in turn decreased the expression of E-cadherin while concurrently increasing the expression of vimentin in HCT116 cells (78). Similarly, elevated levels of 2-HG were observed to stimulate migration, invasion of HCT116 cells and associated with distant metastasis (78). Collectively these findings suggest that metabolic and signaling adaptation to mitochondrial dysfunction caused by *SCO2* loss result in increased migratory potential of HCT116 cells.

Since *SCO2* represents one of the major metabolic targets of p53, together with the previous work, our study suggests that complex IV dysfunction plays a major role in metabolic perturbations of malignancies with defective p53 function. Importantly, we demonstrate that despite reducing proliferation in cell culture models, *SCO2* loss results in alterations in expression of EMT markers and increased migration of HCT116 cells. Considering the positive correlation of these phenomena and metastatic spread of cancer (79, 80), these findings suggest that alterations in *SCO2* and dysfunction of mitochondrial complex IV may increase the metastatic potential of cancer cells. Nonetheless, we acknowledge that our study has significant limitations as it was carried out on a very limited number of cell lines, while the precise mechanisms of signaling and metabolic perturbations remain elusive. Expanding these studies across various cancer cell lines and *in vivo* is therefore warranted to establish the general role of SCO2 and disruption of complex IV function in metabolic reprogramming and accompanied signaling rewiring in neoplasia and its impact on cancer cell phenotypes.

2.7 METHODS

2.7.1 Cell lines and culture conditions

SCO2^{-/-} and WT HCT116 cells were provided by Dr. Paul M. Hwang (15). A549, HT29 and HeLa cells were obtained and authenticated by ATCC. All cells were cultured in McCoy's 5A medium supplemented with 10% heat-inactivated fetal bovine serum (FBS), 1% penicillin/streptomycin, 10 mM HEPES and 2 mM L-Glutamine, (provided by either MilliporeSigma or Wisent). Cells were maintained at 37°C, 5% CO₂ and 19% O₂, unless otherwise indicated.

2.7.2 Lentiviral infection of SCO2 shRNA and expression constructs

Stable knockdown of *SCO2* in A549, HT29 and HeLa cells was generated using pLKO.1 lentiviral shSCO2-containing vector (TRCN236560) obtained from Mission TRC genome-wide shRNA collections (MilliporeSigma). Non-mammalian shRNA control plasmid DNA was used as a negative control (MilliporeSigma: SHC002).

For *SCO2* cDNA generation, RNA was extracted from HCT116 cells using Trizol (ThermoFisher Scientific) according to manufacturer's instructions. Subsequently, cDNA was synthesized by SuperScript III Reverse Transcriptase (Invitrogen) and PCR amplified using Phusion High-Fidelity DNA polymerase (New England BioLabs) and the following primers:

Forward primer: 5' TATGCAACCGGTATGTTTGGTGGAGGTGGAGTTCTGAGC 3'

Reverse Primer: 5' TTGCAAGAATTCTCAAGACAGGACACTGCGGAAAGCCGC 3'

PCR cycling conditions: Initial denaturation was done at 98 °C for 3 min, 35 cycles of 98 °C for 30 secs, 60 °C for 30 s and 72 °C for 40 s and the final extension was done at 72 °C for 10 min.

Human *SCO2* cDNA was cloned into pLKO.1-puro empty vector control plasmid DNA (SHC001) using EcoRI and AgeI restriction enzymes (New England BioLabs). pLKO.1-puro empty vector (SHC001) was used as a negative control for the exogenous expression of *SCO2*.

Lentiviruses were produced as follows: HEK293T cells were co-transfected with 12 μg of shSCO2-containing plasmid (to knockdown *SCO2* in HeLa, HT29 and A549 cells) or *SCO2*-containing plasmid (to re-express *SCO2* in HCT116 *SCO2*-/- cells), 8 μg of psPAX2 packaging plasmid and 4 μg of pMD2.G plasmid using jetPRIME transfection agent according to the manufacturer's protocol (Polyplus transfection). The media was changed 24h later and collected 48h post-transfection. The media was filtered through 0.45 μm filter (Fisher Scientific). The virus-containing media was mixed with fresh media at 1:1 ratio and added to already seeded A549, HT29 and HeLa cells. 4 μg/mL polybrene (MilliporeSigma) was added to the cells. Cells were re-infected the following day using freshly collected and filtered virus-containing media. 48h later, selection was done using 2 μg/mL of puromycin (Bio Basic).

2.7.3 Flow cytometry analysis of cell cycle

HCT116 *SCO2*-/- and WT cells were seeded on 6-well plates and treated for 24 h MK2206 (15 μM) or vehicle (DMSO). The cells were then trypsinized, washed in PBS (Wisent) and then stained with 50 μg/mL propidium iodide (PI) in cold hypotonic buffer (0.1% sodium citrate and 0.1% Triton X-100 in water). Approximately 2.5×10⁵ cells per condition were stained with 0.5 mL of the PI stain and analyzed on a LSR Fortessa cytometer (Becton Dickinson). Fluorescence was detected by excitation at 561nm and acquisition on the 610/20-A channel in linear scale. The distribution of cell cycle population was analyzed using the ModFit LT software.

2.7.4 Flow cytometry analysis of apoptosis

HCT116 *SCO2*-/- and WT cells were seeded on 6-well plates and treated for 48h with MK2206 (15 μM) or vehicle (DMSO). Cells were trypsinized, counted and 1×10⁵ cells were stained using Annexin V-FITC and PI for 20 min in the dark as per the manufacturer's instructions (FITC Annexin V Apoptosis Detection Kit; Becton Dickinson). Samples were then analyzed with a LSR

Fortessa cytometer (Becton Dickinson). Fluorescence was detected by excitation at 488 nm and acquisition on the 530/30-A channel for FITC-Annexin V and by excitation at 561 nm and acquisition on the 610/20-A channel for PI. Cell populations were separated as follows: viable cells – Annexin V-/PI-; early apoptosis - Annexin V+/PI-; late apoptosis Annexin V+/PI+; dead Annexin V-/PI+; and expressed as % of total single cells.

2.7.5 GC-MS for Stable Isotope Tracer Analysis (SITA)

3×10⁵ SCO2^{-/-} and WT HCT116 cells were seeded on 6-well plates to obtain 80% confluency 24 h later. For stable isotope tracer analysis (SITA), the supplemented McCoy's 5A medium was aspirated and replaced with fresh Dulbecco's Modified Eagle's Medium (DMEM) without glucose, glutamine and pyruvate, supplemented with 10% heat-inactivated FBS, 1% P/S, 2mM Lglutamine and 16.65 mM glucose to equilibrate the cells for 2 h. The equilibration media was replaced with DMEM containing 16.65 mM [U-¹³C]-glucose (Cambridge Isotope laboratories). Cells were incubated in this 'labelling media' for 1 min, 2 min, 5 min, 10 min, 20 min, 30 min, 1 h, 2 h and 4.5 h. The 6-well plates were taken out of the incubator and placed immediately on ice. The labelling media was aspirated, and cells were washed 3X with pre-chilled isotonic saline solution (on ice) and quenched on dry ice by adding 600 µL of 80% methanol pre-chilled to -20°C. Cells were scraped from the plates and transferred to microcentrifuge tubes pre-chilled to -20 °C. Cell suspensions were lysed using a sonicator at 4 °C (10 minutes, 30 sec on, 30 sec off, high power setting with a Diagenode Bioruptor). This was repeated to ensure complete recovery of metabolites. Cell debris were discarded after centrifugation (16000 g, 4°C), supernatants were transferred to pre-chilled tubes and dried in a CentriVap cold trap (Labconco) overnight at 4°C. Dried pellets were dissolved in 30 µL of pyridine containing methoxyamine-HCl (10 mg/mL) (MilliporeSigma) using a sonicator and vortex. Samples were incubated for 30 min at 70°C and then transferred to injection vials containing 70 µL of *N-tert*-butyldimethylsilyl-*N*-methyltrifluoroacetamide (MTBSTFA). Sample mixtures were further incubated at 70 °C for 1 h. 1 µL of each sample was injected for GC–MS analysis. GC–MS instrumentation and software were all from Agilent. GC–MS methods and mass isotopomer distribution analyses were conducted as described (81). Data analyses were performed using the Agilent ChemStation and MassHunter software (Agilent).

2.7.6 GC-MS for Steady State metabolite analysis

3×10⁵ HCT116 SCO2^{-/-} and WT cells were seeded on 6-well plates to obtain cells at 80% confluency 24 h later. The plates were quickly placed on ice after incubation period was over. Media were aspirated and cells were washed 3X with chilled isotonic saline solution. Subsequently, 300 µL of 80% methanol pre-chilled to -20 °C was added to the cells. Cells were scraped from the wells and transferred to microcentrifuge tubes pre-chilled to -20 °C. 300 µL more of the 80% methanol was added to the leftover cells in the wells, scraped, collected and pooled with the previously collected 300 µL fraction. Cells were lysed, centrifuged and then the supernatants transferred into prechilled microcentrifuge tubes as previously described for SITA. The collected supernatants were spiked with 750 ng of myristic acid-D₂₇ (Millipore Sigma) to serve as an internal standard. Supernatants were dried overnight and derivatized as previously described for SITA. 1 µL of the derivatized samples was injected for GC–MS analysis. The instrumentation and software used were identical to those used for SITA. Each metabolite was normalized to the peak intensity of myristic acid-D₂₇ and the average protein content derived from cells seeded in parallel and identical conditions to those collected for GC-MS steady state analysis. Data were expressed as fold change relative to WT HCT116 cells.

2.7.7 Glucose and lactate release assays

5×10⁵ cells were seeded in triplicates in 6-well plates in 2 mL of media. The media were collected 24 h later. Cells were trypsinized and counted using an automated cell counter (Invitrogen). Media were spun down at 16000 g for 10 min and the supernatants transferred into microcentrifuge tubes. Glucose and lactate concentrations in the media were measured using a BioProfile 400 analyzer (Nova Biomedical). Total uptake and release were calculated by subtracting the concentrations from baseline glucose and lactate concentrations measured in samples of media incubated under identical conditions in 6-well plates without cells. Molar concentrations of the metabolites were normalized per cell and presented relative to the control.

2.7.8 Cell proliferation assays

 1×10^5 cells were seeded in 6-well plates and incubated for 24 h. The media were replaced with treatment media containing MK2206, OSI-906, rapamycin, torin 1 or DMSO as a negative control and incubated for 72h. Treatment media were aspirated, and the cells were trypsinized. Complete media were added to stop the trypsinization. Samples were collected, stained with trypan blue to exclude dead cells and counted using an automated cell counter (Invitrogen). For hypoxic treatments, 1×10^5 cells were seeded in 6-well plates and placed in hypoxic chamber set to 0.1% O₂. Cells were counted daily over a span of 3 days in parallel to cells seeded and placed at 19% O₂.

2.7.9 Western blotting and antibodies

Cells were washed with ice-cold PBS and lysed for 20 min on ice in buffer A (Pierce RIPA) or B [50 mM Tris/HCL (pH 7.4), 5 mM NaF, 5 mM Na pyrophosphate, 1 mM EDTA, 1 mM EGTA, 250 mM mannitol, 1% (v/v) triton X-100, 1 mM DTT], both supplemented with 1× complete protease inhibitors and 1× PhosSTOP. The lysates were clarified at 4°C (10 min at 16,000 g), and

protein concentrations in the supernatants were determined using BCATM kit. Samples were boiled in 1× Laemmli buffer at 95°C for 5 min, proteins were separated by SDS-PAGE (10-40 µg per lane) and transferred using wet mini-transfer system HoeferTM TE 22 (Hoefer, CA) either onto 0.45 µm ImmobilonTM-P PVDF membranes (buffer A) or 0.45 µm nitrocellulose membranes (buffer B). In most cases, membranes were blocked in 5% BSA w/v in TBST buffer (0.1% Tween 20 in 1× TBS) for 1h, and then incubated with primary antibodies, which were prepared at 1:1000 dilution in 5% BSA in TBST (16 h at 4 °C). Antibodies against α-tubulin and HIF-2α (1:1000 dilution), and the corresponding blocking solution were prepared using 5% (w/v) non-fat dry milk in TBST. Membranes were washed with TBST (3-5×5-10 min) and incubated for 1h with HRPconjugated secondary antibodies, which were prepared at 1:5000 or 1:2500 in 5% milk/TBST. Primary antibodies against 4E-BP1#9644, p-4E-BP1 (S65) #9456, ACC #3662, anti p-ACC (S79) #3661, eIF2α #2103S, p-eIF2α (S51) #9721S, α-tubulin #2125, acetyl-α-tubulin (Lys40) #5335, AKT #4691, p-AKT (S473) #4060, p-AKT (T308) #13038, #4056 and #9275, AMPKα #5832 and 2532, p-AMPKα (T172) #50081 and # 2535, E-cadherin #3195, IGF1Rβ #9750, mTOR #2972, p-mTOR (Ser2448) #2971, rpS6 #2217, p-rpS6 (S240/244) #2215, Snail #3879, Vimentin #5741 were all from Cell Signaling Technologies (Danvers, MA); VDAC1 #sc-8828 and rpS6 #sc-74459 from Santa Cruz Biotechnologies (Dallas, TX); SCO2 #PA5-76209 from Thermo Fisher Scientific, HIF-2α # AF2886 from R&D Systems (Minneapolis, MN), SOD2 #ab16956, PDH E1α # Ab110330 and p-PDH E1-α (Ser293) #Ab92696 from Abcam (Cambridge, UK), acetyl-lysine #ST1027 and α-tubulin #T5168 from MilliporeSigma. Secondary HRP-conjugated mouse antigoat/sheep IgG #A9452, mouse anti-rabbit IgG #A1949, goat anti-mouse IgG #A0168 were from MilliporeSigma. After washing the membranes with TBST (3-5×5-10 min), specific protein bands were revealed by chemiluminescence using ECLTM Prime reagent on the LAS-3000 imager

(Fujifilm, Japan). As requested by reviewers, we performed densitometric analysis using ImageJ software. Herein, for each replicate intensities obtained for the bands of the proteins or phosphoproteins of interest were normalized against corresponding loading controls and total proteins, respectively. Resulting quantification (mean values across replicates +/- standard deviation) are provided in Fig. S9 while x-ray film scans and images of the immunoblots are included in Fig. S10.

2.7.10 Transwell migration assay

Cells were serum starved overnight (16 h) and plated onto 12-well-transwell migration inserts of 8 µm pore diameter (VWR) at 2.5 X 10⁵ cells per well. 10% FBS-supplemented media was added to the lower chamber as the chemo-attractant and incubated for 24 h. Cells were fixed with 10% buffered formalin and stained with crystal-violet. Migrated cells were imaged under 200X light microscope. Four separate images (fields) were taken of each well. Each data point represents the summarized cell count of four fields from a single transwell migration chamber.

2.7.11 Generation of mRNA-seq libraries and *IDH1* and 2 mRNA sequencing analysis

The libraries for mRNA sequencing analysis were generated as in (82). Libraries were sequenced on an Illumina HiSeq 2000 system at the Beijing Genomics Institute (China).

2.7.12 Isolation of RNA and RT-PCR Analysis

Isolation of total RNA and reverse transcription reaction were performed using RNeasy® plus universal mini kit (Qiagen), high-capacity cDNA reverse transcription kit (Applied Biosystems). qPCR was conducted using SensiFASTTM SYBR® Lo-ROX kit (Bioline) on the AB7300 machine and analyzed using the 7300 System SDS Software (Applied Biosystems); reaction was controlled for the absence of genomic DNA amplification. Each experiment was carried out in independent triplicate. Primers were designed using Primer-BLAST program

(http://www.ncbi.nlm.nih.gov/tools/primer-blast/) for human B-actin genes encoding (NM 001101.5, 5'-CGGCTACAGCTTCACCACCACG 5'forward: and reverse: AGGCTGGAAGAGTGCCTCAGGG) and IGF1R (NM 000875.5, forward: 5'-CGGGGAGAGAGCCTCCTGTGA and reverse: 5'-GCTGTTGGAGCCGCAGGCAT) and ZEB1 (NM 001128128.2, forward: 5'-GAAGACAAACTGCATATTGTGGAAG and reverse: 5'-CATCCTGCTTCATCTGCCTGA).

2.7.13 Live cell staining and confocal microscopy

Loading of the cells with fluorescent indicators was performed for 30 min using 1 μM BCECF (whole cell pH probe) or 2 μg/ml Nile Red (NR, lipid droplet stain) prepared in OptiMEM I medium. Live cell imaging was performed as follows: Fluorescence lifetime imaging (FLIM) of BCECF was performed at 37°C on an upright laser scanning Axio Examiner Z1 (Carl Zeiss) microscope equipped with 20x/1.0 W-Plan Apochromat dipping objective. Fluorescence decays were collected using a picosecond 488 nm laser (with emission collected at 512-536 nm), DCS-120 confocal (TCSPC) scanner, photon counting detector and SPCM software (Becker & Hickl GmbH). Data were analyzed with SPCImage (B&H) and Excel software. Fluorescence lifetime (LT) of BCECF was calculated using monoexponential fitting. The LT distribution histograms were obtained for 3 individual focal planes within each field of view (256×256-pixel matrixes). Cumulative LT distribution histograms were produced according to the algorithm developed in (83).

The NR staining was analyzed on an Olympus FV1000 confocal laser-scanning microscope with controlled CO₂, humidity and temperature. Fluorescence signals were collected with a UPLSAPO 60X/1.35 oil immersion Super Apochromat objective using 543 nm excitation and 550-650 nm emission wavelengths. The resulting z-stacked fluorescence and single plane differential

interference contrast (DIC) images were processed using FV1000 Viewer software (Olympus) and Adobe Photoshop.

2.7.14 IGF1 ELISA

 1×10^6 SCO2^{-/-} and WT HCT116 cells were seeded in duplicates in 2 mL of media in 6-well plates and incubated for 24h. The media were collected 24h later and the cells were trypsinized and counted using an automated cell counter (Invitrogen). Media samples were spun down at 16000 g for 10 min and the supernatants were transferred into microcentrifuge tubes. ELISA was used to measure the concentrations of free IGF1 present in the media samples (Ansh Labs) according to the manufacturer's instructions. Briefly, media samples were added to IGF1 antibody coated microtiter wells. The wells were then washed and then incubated with horseradish peroxidase labelled antibody conjugate. At the end of the incubation period, a substrate solution was added to the wells until the color was adequately developed. After incubation with the substrate solution, an acidic stopping solution was added. Dual wavelength absorbance measurements were taken at 450 nm and at 630 nm. IGF1 concentrations were determined using a calibration curve. IGF1 bound to the cells were calculated by subtracting the concentrations of free IGF1 concentrations from baseline concentrations measured in samples of media incubated under identical conditions in 6-well plates without cells. Molar concentrations of the metabolites were normalized per cell and presented relative to the control.

2.7.15 Statistical analysis

Statistical analysis was performed using the results of 2-5 independent experiments. To ensure the accuracy and fidelity of the data, the experiments, when possible, were performed in several technical replicates.

The differences between *SCO2*-/- and WT HCT116 cells (at different treatment conditions) in NR fluorescence, protein and mRNA levels, and other measured parameters were evaluated using unpaired 2-tailed t-test and non-parametrical Mann-Whitney U-test. Unpaired 2-tailed t-tests, two-way ANOVA (Dunnette's) multiple comparison posthoc test) and one-way ANOVA (Tukey's and Dunnette's multiple comparison posthoc tests) analyses were done on Prism (GraphPad).

2.7.16 Data Accessibility

Raw data are deposited at Mendeley (https://data.mendeley.com/datasets/pyr8t5ng6r/draft?a=754177d8-d6f3-4de6-85b9-645dd4136d2f).

2.8 ACKNOWLEDGEMENTS

We are thankful to Shannon McLaughlan, Dr. Matthew Leibovitch, Ranveer Palia, Dr. Ana Paula Ventura-Silva (University College Dublin, Ireland) and to the members of Papkovsky's, Pollak's and Topisirovic's laboratories for helpful discussions and technical assistance. In addition, we are indebted to Dr. Vuk Stambolic (University of Toronto) and Dr. Scot Leary (University of Saskatchewan) for invaluable advice. This research was funded by the Terry Fox Foundation (TFF) Oncometabolism Team Grant TFF-242122 and TFF-116128 to M.P. and I.T., Canadian Institutes for Health Research (CIHR) PJT-175050 to IT, the Russian Science Foundation grant 20-14-00121 for D.E.A., the Science Foundation Ireland grant SFI/12/RC/2276_P2 to D.B.P. and SFI-HRB-Wellcome Trust Investigator in Science award 210692/Z/18/ to P.V.B. O.U. was supported by Fellowship from Fonds de Recherche du Québec-Santé (FRQS). A.V.Z. was supported by SFI/12/RC/2276_P2 grant, D.J.P. is supported by a CIHR Postdoctoral Fellowship. P.J. is supported by TD Fellowship. I.T. is supported by FRQS Senior Investigator award. L.H. is supported by FRQS Junior 1 Investigator award. Metabolic analysis was performed at The

Rosalind and Morris Goodman Cancer Research Centre's Metabolomics Core Facility, which is supported by the Canada Foundation for Innovation, The Dr. John R. and Clara M. Fraser Memorial Trust, the Terry Fox Foundation (TFF Oncometabolism Team Grant; TFF-242122) and McGill University.

2.9 AUTHOR CONTRIBUTIONS

Author contributions: O.U., A.V.Z, D.B.P., M.N.P. and I.T. conceived the study. O.U., A.V.Z., designed and conducted experiments on gene expression, cell functioning, migration, signaling and metabolism. D.E.A and P.V.B. carried out RNA-sequence analysis. L.H. D.A., D.J.P assisted with metabolic experiments. P.J. carried out the transwell migration assay and analysis. Y.W. and P.H. carried out ELISA and Western blotting experiments. A.V.Z and O.U. wrote the initial draft of the manuscript. D.B.P., M.N.P. and I.T. provided funding. All authors contributed to the interpretation of the data and editing the final version of the manuscript.

2.10 REFERENCES

- 1. Vasan K, Werner M, Chandel NS. Mitochondrial Metabolism as a Target for Cancer Therapy. Cell Metab. 2020;32(3):341-52.
- 2. Hollinshead KER, Parker SJ, Eapen VV, Encarnacion-Rosado J, Sohn A, Oncu T, et al. Respiratory Supercomplexes Promote Mitochondrial Efficiency and Growth in Severely Hypoxic Pancreatic Cancer. Cell Rep. 2020;33(1):108231.
- 3. Astuti D, Latif F, Dallol A, Dahia PL, Douglas F, George E, et al. Gene mutations in the succinate dehydrogenase subunit SDHB cause susceptibility to familial pheochromocytoma and to familial paraganglioma. Am J Hum Genet. 2001;69(1):49-54.
- 4. Balss J, Meyer J, Mueller W, Korshunov A, Hartmann C, von Deimling A. Analysis of the IDH1 codon 132 mutation in brain tumors. Acta Neuropathol. 2008;116(6):597-602.

- 5. Dang L, White DW, Gross S, Bennett BD, Bittinger MA, Driggers EM, et al. Cancer-associated IDH1 mutations produce 2-hydroxyglutarate. Nature. 2010;465(7300):966.
- 6. Janeway KA, Kim SY, Lodish M, Nosé V, Rustin P, Gaal J, et al. Defects in succinate dehydrogenase in gastrointestinal stromal tumors lacking KIT and PDGFRA mutations. Proc Natl Acad Sci U S A. 2011;108(1):314-8.
- 7. Tomlinson IP, Alam NA, Rowan AJ, Barclay E, Jaeger EE, Kelsell D, et al. Germline mutations in FH predispose to dominantly inherited uterine fibroids, skin leiomyomata and papillary renal cell cancer. Nat Genet. 2002;30(4):406-10.
- 8. Baksh SC, Finley LWS. Metabolic Coordination of Cell Fate by a-Ketoglutarate-Dependent Dioxygenases. Trends in Cell Biology. 2021;31(1):24-36.
- 9. Leary SC, Cobine PA, Kaufman BA, Guercin GH, Mattman A, Palaty J, et al. The human cytochrome c oxidase assembly factors SCO1 and SCO2 have regulatory roles in the maintenance of cellular copper homeostasis. Cell Metab. 2007;5(1):9-20.
- Chinnery PF, Keogh MJ. Clinical Mitochondrial Medicine: Cambridge University Press;
 2018.
- 11. Ghezzi D, Zeviani M. Human diseases associated with defects in assembly of OXPHOS complexes. Essays Biochem. 2018;62(3):271-86.
- 12. Matoba S, Kang JG, Patino WD, Wragg A, Boehm M, Gavrilova O, et al. p53 regulates mitochondrial respiration. Science. 2006;312(5780):1650-3.
- 13. Sung HJ, Ma W, Wang PY, Hynes J, O'Riordan TC, Combs CA, et al. Mitochondrial respiration protects against oxygen-associated DNA damage. Nat Commun. 2010;1:5.

- 14. Zhdanov AV, Andreev DE, Baranov PV, Papkovsky DB. Low energy costs of F1Fo ATP synthase reversal in colon carcinoma cells deficient in mitochondrial complex IV. Free Radic Biol Med. 2017;106:184-95.
- 15. Matsumoto T, Wang PY, Ma W, Sung HJ, Matoba S, Hwang PM. Polo-like kinases mediate cell survival in mitochondrial dysfunction. Proc Natl Acad Sci U S A. 2009;106(34):14542-6.
- 16. Wang L, Xiong H, Wu F, Zhang Y, Wang J, Zhao L, et al. Hexokinase 2-mediated Warburg effect is required for PTEN- and p53-deficiency-driven prostate cancer growth. Cell reports. 2014;8(5):1461-74.
- 17. Kondoh H, Lleonart ME, Gil J, Wang J, Degan P, Peters G, et al. Glycolytic enzymes can modulate cellular life span. Cancer Res. 2005;65(1):177-85.
- 18. Bensaad K, Tsuruta A, Selak MA, Vidal MN, Nakano K, Bartrons R, et al. TIGAR, a p53-inducible regulator of glycolysis and apoptosis. Cell. 2006;126(1):107-20.
- 19. Wanka C, Brucker DP, Bähr O, Ronellenfitsch M, Weller M, Steinbach JP, et al. Synthesis of cytochrome C oxidase 2: a p53-dependent metabolic regulator that promotes respiratory function and protects glioma and colon cancer cells from hypoxia-induced cell death. Oncogene. 2012;31(33):3764-76.
- 20. Gyorffy B, Lánczky A, Szállási Z. Implementing an online tool for genome-wide validation of survival-associated biomarkers in ovarian-cancer using microarray data from 1287 patients. Endocr Relat Cancer. 2012;19(2):197-208.
- 21. Won KY, Lim SJ, Kim GY, Kim YW, Han SA, Song JY, et al. Regulatory role of p53 in cancer metabolism via SCO2 and TIGAR in human breast cancer. Hum Pathol. 2012;43(2):221-

8.

- 22. Alldredge J, Randall L, De Robles G, Agrawal A, Mercola D, Liu M, et al. Transcriptome Analysis of Ovarian and Uterine Clear Cell Malignancies. Frontiers in oncology. 2020;10:598579-
- 23. Nath A, Chan C. Genetic alterations in fatty acid transport and metabolism genes are associated with metastatic progression and poor prognosis of human cancers. Sci Rep. 2016;6:18669.
- 24. Hulea L, Gravel SP, Morita M, Cargnello M, Uchenunu O, Im YK, et al. Translational and HIF-1α-Dependent Metabolic Reprogramming Underpin Metabolic Plasticity and Responses to Kinase Inhibitors and Biguanides. Cell Metab. 2018;28(6):817-32.e8.
- 25. Janzer A, German NJ, Gonzalez-Herrera KN, Asara JM, Haigis MC, Struhl K. Metformin and phenformin deplete tricarboxylic acid cycle and glycolytic intermediates during cell transformation and NTPs in cancer stem cells. Proceedings of the National Academy of Sciences of the United States of America. 2014;111(29):10574-9.
- 26. Brisson D, Vohl MC, St-Pierre J, Hudson TJ, Gaudet D. Glycerol: a neglected variable in metabolic processes? Bioessays. 2001;23(6):534-42.
- 27. Williamson DH, Lund P, Krebs HA. The redox state of free nicotinamide-adenine dinucleotide in the cytoplasm and mitochondria of rat liver. Biochem J. 1967;103(2):514-27.
- 28. Pettit FH, Pelley JW, Reed LJ. Regulation of pyruvate dehydrogenase kinase and phosphatase by acetyl-CoA/CoA and NADH/NAD ratios. Biochem Biophys Res Commun. 1975;65(2):575-82.
- 29. Birsoy K, Wang T, Chen WW, Freinkman E, Abu-Remaileh M, Sabatini DM. An essential role of the mitochondrial electron transport chain in cell proliferation is to enable aspartate synthesis. Cell. 2015;162(3):540-51.

- 30. Sullivan LB, Gui DY, Hosios AM, Bush LN, Freinkman E, Vander Heiden MG. Supporting aspartate biosynthesis is an essential function of respiration in proliferating cells. Cell. 2015;162(3):552-63.
- 31. Chen WW, Freinkman E, Wang T, Birsoy K, Sabatini DM. Absolute Quantification of Matrix Metabolites Reveals the Dynamics of Mitochondrial Metabolism. Cell. 2016;166(5):1324-37.e11.
- 32. Patel MS, Nemeria NS, Furey W, Jordan F. The pyruvate dehydrogenase complexes: structure-based function and regulation. The Journal of biological chemistry. 2014;289(24):16615-23.
- 33. Denton RM, Randle PJ, Bridges BJ, Cooper RH, Kerbey AL, Pask HT, et al. Regulation of mammalian pyruvate dehydrogenase. Mol Cell Biochem. 1975;9(1):27-53.
- 34. Rardin MJ, Wiley SE, Naviaux RK, Murphy AN, Dixon JE. Monitoring phosphorylation of the pyruvate dehydrogenase complex. Anal Biochem. 2009;389(2):157-64.
- 35. Korotchkina LG, Patel MS. Site specificity of four pyruvate dehydrogenase kinase isoenzymes toward the three phosphorylation sites of human pyruvate dehydrogenase. J Biol Chem. 2001;276(40):37223-9.
- 36. Kolobova E, Tuganova A, Boulatnikov I, Popov KM. Regulation of pyruvate dehydrogenase activity through phosphorylation at multiple sites. Biochem J. 2001;358(Pt 1):69-77.
- 37. Donaldson WE. Regulation of fatty acid synthesis. Fed Proc. 1979;38(12):2617-21.
- 38. Hill S, Deepa SS, Sataranatarajan K, Premkumar P, Pulliam D, Liu Y, et al. Sco2 deficient mice develop increased adiposity and insulin resistance. Mol Cell Endocrinol. 2017;455:103-14.

- 39. Schönenberger MJ, Kovacs WJ. Hypoxia signaling pathways: modulators of oxygenrelated organelles. Frontiers in cell and developmental biology. 2015;3:42.
- 40. Tretter L, Patocs A, Chinopoulos C. Succinate, an intermediate in metabolism, signal transduction, ROS, hypoxia, and tumorigenesis. Biochim Biophys Acta. 2016;1857(8):1086-101.
- 41. Selak MA, Armour SM, MacKenzie ED, Boulahbel H, Watson DG, Mansfield KD, et al. Succinate links TCA cycle dysfunction to oncogenesis by inhibiting HIF-alpha prolyl hydroxylase. Cancer Cell. 2005;7(1):77-85.
- 42. Hobert JA, Mester JL, Moline J, Eng C. Elevated plasma succinate in PTEN, SDHB, and SDHD mutation-positive individuals. Genet Med. 2012;14(6):616-9.
- 43. Letouzé E, Martinelli C, Loriot C, Burnichon N, Abermil N, Ottolenghi C, et al. SDH mutations establish a hypermethylator phenotype in paraganglioma. Cancer Cell. 2013;23(6):739-52.
- 44. Mamer O, Gravel SP, Choinière L, Chénard V, St-Pierre J, Avizonis D. The complete targeted profile of the organic acid intermediates of the citric acid cycle using a single stable isotope dilution analysis, sodium borodeuteride reduction and selected ion monitoring GC/MS. Metabolomics. 2013;9(5):1019-30.
- 45. Ward PS, Patel J, Wise DR, Abdel-Wahab O, Bennett BD, Coller HA, et al. The common feature of leukemia-associated IDH1 and IDH2 mutations is a neomorphic enzyme activity converting alpha-ketoglutarate to 2-hydroxyglutarate. Cancer Cell. 2010;17(3):225-34.
- 46. Intlekofer AM, Wang B, Liu H, Shah H, Carmona-Fontaine C, Rustenburg AS, et al. L-2-Hydroxyglutarate production arises from noncanonical enzyme function at acidic pH. Nature chemical biology. 2017;13(5):494-500.

- 47. Intlekofer AM, Dematteo RG, Venneti S, Finley LW, Lu C, Judkins AR, et al. Hypoxia Induces Production of L-2-Hydroxyglutarate. Cell Metab. 2015;22(2):304-11.
- 48. Ye D, Guan K-L, Xiong Y. Metabolism, activity, and targeting of D-and L-2-hydroxyglutarates. Trends in cancer. 2018;4(2):151-65.
- 49. Vander Heiden MG, DeBerardinis RJ. Understanding the Intersections between Metabolism and Cancer Biology. Cell. 2017;168(4):657-69.
- 50. Gui DY, Sullivan LB, Luengo A, Hosios AM, Bush LN, Gitego N, et al. Environment Dictates Dependence on Mitochondrial Complex I for NAD+ and Aspartate Production and Determines Cancer Cell Sensitivity to Metformin. Cell Metab. 2016;24(5):716-27.
- 51. Lu SC. Regulation of glutathione synthesis. Mol Aspects Med. 2009;30(1-2):42-59.
- 52. Requejo R, Hurd TR, Costa NJ, Murphy MP. Cysteine residues exposed on protein surfaces are the dominant intramitochondrial thiol and may protect against oxidative damage. Febs j. 2010;277(6):1465-80.
- 53. Earle WR, Evans VJ, Hawkins NM, Peppers EV, Westfall BB. Effect of glutamine on the growth and metabolism of liver cells in vitro. J Natl Cancer Inst. 1956;17(2):131-8.
- 54. Zhao Y, Zhao X, Chen V, Feng Y, Wang L, Croniger C, et al. Colorectal cancers utilize glutamine as an anaplerotic substrate of the TCA cycle in vivo. Sci Rep. 2019;9(1):19180.
- 55. Fendt S-M, Bell EL, Keibler MA, Olenchock BA, Mayers JR, Wasylenko TM, et al. Reductive glutamine metabolism is a function of the α -ketoglutarate to citrate ratio in cells. Nature Communications. 2013;4(1):2236.
- 56. Liu GY, Sabatini DM. mTOR at the nexus of nutrition, growth, ageing and disease. Nat Rev Mol Cell Biol. 2020;21(4):183-203.

- 57. Gwinn DM, Shackelford DB, Egan DF, Mihaylova MM, Mery A, Vasquez DS, et al. AMPK phosphorylation of raptor mediates a metabolic checkpoint. Mol Cell. 2008;30(2):214-26.
- 58. Inoki K, Zhu T, Guan KL. TSC2 mediates cellular energy response to control cell growth and survival. Cell. 2003;115(5):577-90.
- 59. Dowling RJ, Topisirovic I, Alain T, Bidinosti M, Fonseca BD, Petroulakis E, et al. mTORC1-mediated cell proliferation, but not cell growth, controlled by the 4E-BPs. Science. 2010;328(5982):1172-6.
- 60. Denisenko TV, Gorbunova AS, Zhivotovsky B. Mitochondrial Involvement in Migration, Invasion and Metastasis. Frontiers in Cell and Developmental Biology. 2019;7(355).
- 61. Guerra F, Guaragnella N, Arbini AA, Bucci C, Giannattasio S, Moro L. Mitochondrial Dysfunction: A Novel Potential Driver of Epithelial-to-Mesenchymal Transition in Cancer. Frontiers in Oncology. 2017;7(295).
- 62. Sánchez-Tilló E, Lázaro A, Torrent R, Cuatrecasas M, Vaquero EC, Castells A, et al. ZEB1 represses E-cadherin and induces an EMT by recruiting the SWI/SNF chromatin-remodeling protein BRG1. Oncogene. 2010;29(24):3490-500.
- 63. Harvey RF, Pöyry TAA, Stoneley M, Willis AE. Signaling from mTOR to eIF2α mediates cell migration in response to the chemotherapeutic doxorubicin. Sci Signal. 2019;12(612).
- 64. Gandin V, Masvidal L, Cargnello M, Gyenis L, McLaughlan S, Cai Y, et al. mTORC1 and CK2 coordinate ternary and eIF4F complex assembly. Nature communications. 2016;7:11127-.
- 65. Laplante M, Sabatini DM. An emerging role of mTOR in lipid biosynthesis. Curr Biol. 2009;19(22):R1046-52.
- 66. Wang X, Proud CG. The mTOR pathway in the control of protein synthesis. Physiology (Bethesda). 2006;21:362-9.

- 67. Faubert B, Solmonson A, DeBerardinis RJ. Metabolic reprogramming and cancer progression. Science. 2020;368(6487).
- 68. DeBerardinis RJ, Lum JJ, Hatzivassiliou G, Thompson CB. The biology of cancer: metabolic reprogramming fuels cell growth and proliferation. Cell Metab. 2008;7(1):11-20.
- 69. Fan J, Hitosugi T, Chung TW, Xie J, Ge Q, Gu TL, et al. Tyrosine phosphorylation of lactate dehydrogenase A is important for NADH/NAD(+) redox homeostasis in cancer cells. Mol Cell Biol. 2011;31(24):4938-50.
- 70. Chowdhury SK, Gemin A, Singh G. High activity of mitochondrial glycerophosphate dehydrogenase and glycerophosphate-dependent ROS production in prostate cancer cell lines. Biochem Biophys Res Commun. 2005;333(4):1139-45.
- 71. Elstrom RL, Bauer DE, Buzzai M, Karnauskas R, Harris MH, Plas DR, et al. Akt stimulates aerobic glycolysis in cancer cells. Cancer Res. 2004;64(11):3892-9.
- 72. Kazyken D, Magnuson B, Bodur C, Acosta-Jaquez HA, Zhang D, Tong X, et al. AMPK directly activates mTORC2 to promote cell survival during acute energetic stress. Sci Signal. 2019;12(585).
- 73. Rabinovitch RC, Samborska B, Faubert B, Ma EH, Gravel SP, Andrzejewski S, et al. AMPK Maintains Cellular Metabolic Homeostasis through Regulation of Mitochondrial Reactive Oxygen Species. Cell Rep. 2017;21(1):1-9.
- 74. Sarbassov DD, Guertin DA, Ali SM, Sabatini DM. Phosphorylation and regulation of Akt/PKB by the rictor-mTOR complex. Science. 2005;307(5712):1098-101.
- 75. Masui K, Tanaka K, Akhavan D, Babic I, Gini B, Matsutani T, et al. mTOR complex 2 controls glycolytic metabolism in glioblastoma through FoxO acetylation and upregulation of c-Myc. Cell Metab. 2013;18(5):726-39.

- 76. Woods A, Dickerson K, Heath R, Hong SP, Momcilovic M, Johnstone SR, et al. Ca2+/calmodulin-dependent protein kinase kinase-beta acts upstream of AMP-activated protein kinase in mammalian cells. Cell Metab. 2005;2(1):21-33.
- 77. Jiang J, Wang K, Chen Y, Chen H, Nice EC, Huang C. Redox regulation in tumor cell epithelial—mesenchymal transition: molecular basis and therapeutic strategy. Signal Transduct Target Ther. 2017;2(1):17036.
- 78. Colvin H, Nishida N, Konno M, Haraguchi N, Takahashi H, Nishimura J, et al. Oncometabolite D-2-Hydroxyglurate Directly Induces Epithelial-Mesenchymal Transition and is Associated with Distant Metastasis in Colorectal Cancer. Sci Rep. 2016;6:36289-.
- 79. Craene BD, Berx G. Regulatory networks defining EMT during cancer initiation and progression. Nature Reviews Cancer. 2013;13(2):97-110.
- 80. Yang J, Weinberg RA. Epithelial-mesenchymal transition: at the crossroads of development and tumor metastasis. Dev Cell. 2008;14(6):818-29.
- 81. Gravel S-P, Avizonis D, St-Pierre J. Metabolomics Analyses of Cancer Cells in Controlled Microenvironments. Methods Mol Biol. 2016;1458:273-90.
- 82. Andreev DE, O'Connor PB, Fahey C, Kenny EM, Terenin IM, Dmitriev SE, et al. Translation of 5' leaders is pervasive in genes resistant to eIF2 repression. Elife. 2015;4:e03971.
- 83. Zhdanov AV, Okkelman IA, Golubeva AV, Doerr B, Hyland NP, Melgar S, et al. Quantitative analysis of mucosal oxygenation using ex vivo imaging of healthy and inflamed mammalian colon tissue. Cellular and Molecular Life Sciences. 2017;74(1):141-51.

2.11 BRIDGING TEXT

This chapter investigates metabolic adaptations caused by mitochondrial dysfunction due to the inactivation of SCO2 in cancer cells. Loss of SCO2 induces energy stress which cancer cells adapt to by activating compensatory metabolic pathways (e.g., NAD+ regenerating pathways and pyruvate carboxylation). Metabolic reprogramming mediated by SCO2 deletion is accompanied by rewiring of the IGF1R/AKT axis and paradoxical decrease in mTORC1 signaling. This is paralleled by increased sensitivity of colorectal cancer cells to IGF1 and AKT inhibitors. This study therefore suggests that metabolic adaptations following energy stress may create rewiring of signaling pathways that may result in targetable vulnerabilities of cancer cells.

Considering these findings, and recent recognition of perturbations in energy metabolism as a hallmark of cancer cells, in chapter 3, we sought to define potential metabolic vulnerabilities of CRC cells. Herein, we induced energy stress by treating cells with mitochondrial complex I inhibitor (i.e., phenformin) or nutrient depletion (i.e., glutamine deprivation). Different stressors were used to discern the metabolic pathways activated by phenformin or glutamine starvation in genetically heterogenous CRC cell lines but not in normal colon epithelial cells. These studies build on those carried out in the chapter 2 and have the overarching objective to identify potential commonalities in metabolic perturbations of genetically distinct CRC cells to various energetic stressors.

CHAPTER 3: Energy stress induces metabolic reprogramming in colorectal cancer

Oro Uchenunu^{1,2}, Michael Pollak^{1,2,3}, Ivan Topisirovic^{1,2,3,4}

¹ Lady Davis Institute for Medical Research, Jewish General Hospital, Montréal, QC H3T1E2,

Canada.

² Department of Experimental Medicine, McGill University, Montreal QC H4A3T2, Canada.

³ Gerald Bronfman Department of Oncology, McGill University, Montreal QC H4A3T2, Canada.

⁴ Department of Biochemistry, McGill University, Montreal, QC H4A 3T2, Canada.

3.1 ABSTRACT

Intratumor heterogeneity is commonly observed in colorectal cancers (CRCs) as evidenced by different genetic makeup of cancer cells in the same tumor bed. Intratumor heterogeneity represents a major challenge for therapeutic approaches to target neoplasia. This is because most targeted anti-cancer therapies, although effective in eradicating cancer cells that harbor specific mutations, are ineffective against selected subclonal populations that are inherently resistant and/or acquire resistance by losing their dependence on targeted mutation. Regardless of their genetic makeup, cancer cells must undergo metabolic reprogramming to survive energy stress. To this end, identifying mechanisms of metabolic adaptations of cancer cells that are independent of their genetic makeup holds a promise to overcome issues related to therapeutic challenges imposed by intratumor genetic heterogeneity. To address this, we metabolically profiled colorectal cancer (CRC) cell lines in the context of glutamine deprivation or phenformin treatment to comprehensively map the metabolic pathways that underlie adaptation to energy stress. We show that CRC cells are more sensitive to the antiproliferative effects of phenformin, or glutamine

deprivation compared to normal colon epithelial cells. Phenformin treatment and glutamine starvation downregulate mTORC1 signaling which concurrently suppress protein synthesis in transformed colon cells. Although phenformin and glutamine depletion lead to distinct metabolic profiles in HCT116 and HT29 cells, α-ketoglutarate carboxylation appears to be a common and potentially targetable metabolic vulnerability that may be exploited by combining biguanides with inhibitors of glutamine metabolism. Altogether, our studies provide initial evidence for potential commonalities in metabolic adaptations of CRC cell lines and lay foundation for further studies on a broader panel of CRC cell lines and *in vivo* models of CRC.

3.2 INTRODUCTION

Colorectal cancer (CRC) is the second leading cause of cancer-related deaths and third most prevalent cancer amongst men and women globally (1). CRC death rates decreased in 2016 compared to 1970 in highly developed countries because of the rapid development of diagnosing technologies and improved therapeutics over the years (2). However, it is projected that by 2035, the incidence of CRC would rise to 2.5 million while the mortality rates of colon and rectal cancers will increase by 71.5% and 60% respectively worldwide (3). Genetic, lifestyle and environmental factors have been closely associated with the incidence and death rates of CRC, but the mechanisms underpinning the progression of CRC as well as potential molecular targets to treat this disease are still incompletely understood.

Despite the recent developments, nearly 70% of CRC patients develop liver metastasis which is the primary cause of mortality (4-6). The treatment protocol for CRC typically involves a combination of approaches including surgery, radiotherapy, systemic chemotherapy, targeted therapy and/or immunotherapy (2). However, there are limitations to the different approaches in managing CRC such as systemic toxicity, comorbidities, poor efficacy and acquired resistance (7,

8). Clinical management of CRC has been improved by the advent of targeted therapies (8). To this end, the aberrant expression of EGFR and VEGFR, activating mutations in PI3KCA, KRAS and BRAF, mutations in p53 are regarded as biomarkers which dictate the advancement of CRC and predict the responsiveness to targeted therapeutics (7, 8). While targeted therapy has been effective in hindering the progression of certain cancers such as the use of imatinib to treat BCR-ABL chronic myeloid leukemia (9), targeted approaches have yet to meet their expectations in CRC (7, 10-13).

Although cetuximab, a monoclonal antibody specific for EGFR is occasionally used to treat chemorefractory metastatic CRC, resistance to this drug develops via a number of mechanisms including constitutive activation of KRAS (14, 15). Malignant cell populations with activating gene mutations downstream of EGFR may be present at frequencies too low to be detected by insensitive techniques during genetic profiling of tumors (16). Consequently, the analyses of tumor biopsies may fail to capture the extensive molecular complexities of genetic heterogenous tumors thus leading to ineffective treatment strategies (11). Intratumor and/or intermetastatic tumor genetic heterogeneity are commonly observed in solid tumors including CRC (11, 17-24). Genetic heterogeneity of tumors, which evolves as subclonal tumor cell populations change spatially and temporally during the development and progression of the disease, are often associated with shorter overall survival and adverse treatment outcomes of CRC (25-27). In addition, targeted therapies are thought to exert selection pressure that may allow better adapted malignant clonal cell populations to expand (28). This drawback in current targeted approaches needs to be addressed to effectively treat CRC.

During neoplastic growth, tumors rapidly outstrip their vasculature which results in hypoxic and nutrient-deficient tumor microenvironment (29-32). Therefore, in advanced solid

tumors, neoplastic cells are exposed to metabolic stress that they must overcome to meet their bioenergetic and/or biosynthetic demands (33). To achieve this, neoplastic cells rewire their energy metabolism to sustain proliferation and survival (34). Since the discovery of the Warburg effect, numerous studies have illustrated metabolic reprogramming in cancer under contexts of various oncogenic mutations and tumor microenvironment conditions (34). To this end, metabolic reprogramming is now regarded as a hallmark of cancer (34). Glucose and glutamine are the two most predominantly used nutrients for energy production and biosynthesis of macromolecules in cells (35, 36). Tumor cells consume more glucose and glutamine than the cells populating nonproliferating normal tissues (37). While CRC cells have been shown to survive glucosedeprived conditions, glutamine has been demonstrated to be required for their survival (38). Nonetheless, this apparent preference of glutamine over glucose as a biomass and bioenergetic source for CRC remains incompletely understood.

Metformin, a biguanide used as a first-line therapy for type 2 diabetes, exhibits antineoplastic effects across numerous cancer cell lines and models (39, 40). In addition, clinical studies revealed that metformin may be associated with reduced risk of colorectal adenoma incidence and CRC-specific mortality in diabetic patients with CRC (41, 42). In addition to its systemic effects that include decrease in insulin levels, metformin is thought to exert cell autonomous antitumoral effects by inhibiting mitochondrial complex I of the electron transport chain which leads to decreased ATP synthesis and an increase in the cellular AMP:ATP ratio (43). The elevated AMP:ATP ratio activates the cellular energy sensor, AMP-activated protein kinase (AMPK) which stimulates ATP generating catabolic processes such as fatty acid β -oxidation while suppressing energy consuming processes including protein synthesis in order to restore energy homeostasis (44, 45). Cells with impaired ability to activate AMPK due to the loss of LKB1 are

unable to restore ATP levels in response to biguanide-induced energetic stress (46, 47). Thus, cancer cells with defective LKB1-AMPK signaling are more sensitive to metformin compared to tumor cells that can activate AMPK (46). Taken together, AMPK activation seems to represent an adaptive response to biguanides that allows cells to bypass energy crisis. We previously showed that biguanides induce compensatory metabolic adaptations such as glucose addiction (48, 49). These adaptations represent potential drug targetable "metabolic vulnerabilities" that may be exploitable for treating CRC.

As all tumor cells require energy to proliferate, we hypothesize that the systematic mapping of the metabolic pathways that enable genetically distinct CRC cells adapt to glutamine deprivation and phenformin (a biguanide that is more potent than metformin) will highlight potentially clinically targetable metabolic vulnerabilities. Given that biguanides and nutrient depletion induce energy stress (50-52), we sought to investigate their effects as independent stressors of CRC cells. Specifically, we set out to identify potential common adaptive metabolic alterations in genetically diverse CRC cell lines subjected to energy stress caused by glutamine depletion or phenformin. We observed that CRC cells were more sensitive to the antiproliferative effects of phenformin and glutamine deprivation than normal colon epithelial cells. As expected, phenformin and glutamine starvation inhibited mTORC1 signaling which was associated with reduced global protein synthesis. Although phenformin led to distinct metabolic profiles in HCT116 and HT29 cells, glutamine deprivation resulted in relatively similar metabolic perturbations characterized by increased levels of intracellular amino acids in both cell lines. Moreover, phenformin and glutamine deprivation of CRC cells reveal that reductive α-ketoglutarate carboxylation may be a common mechanism underpinning adaptation of CRC cells to metabolic stress.

3.3 RESULTS

3.3.1 Metabolic stress reduces proliferation of transformed colorectal cell lines more strongly than non-transformed colon epithelial cells

Well-defined cancer cell lines that are frequently used as cell culture models have been shown to exhibit intra-cell line genetic variability (53, 54). Therefore, focusing on a single CRC cell line of defined genetic background may be insufficient to comprehensively recapitulate the intratumor genetic heterogeneity observed in patients and in vivo CRC models (55, 56). In order to simulate intratumor heterogeneity of CRC, and to mitigate cell line associated biases, we employed 2 genetically different human colon adenocarcinoma cell lines: HCT116 and HT29. One of the primary goals behind the study was to elucidate energy-stress response networks shared between different CRC cell lines (Fig. 3.1A). Both HCT116 (Fig. 3.1B) and HT29 (Fig. 3.1C) cells were treated with increasing concentrations of phenformin. Although the antiproliferative effects of biguanides across various cancer cell lines have been previously documented (49, 57-59), it was important to determine the phenformin concentration that inhibited proliferation by 50% of the control cells (i.e., IC₅₀). To facilitate direct comparisons of phenformin-induced metabolic perturbations between the cell lines we treated HCT116 and HT29 cells with the IC50 of phenformin (determined to be 0.6mM for both cells lines) (Fig. 3.1B-C). In addition to HCT116 and HT29 cells, SV40-transformed colorectal cell line (CCD841CoTr) derived from the same tissue as the normal epithelial colon cell line (CCD841CoN) were also treated with phenformin (Fig. 3.1D). At most of the tested concentrations, phenformin minimally reduced proliferation of CCD841CoN compared to CCD841CoTr cells (Fig. 3.1D). This confirms previous findings that phenformin has only a marginal effect on proliferation and survival of non-malignant cells (49).

We next assessed the dependence of CRC cell lines on glucose. Herein, we cultured HCT116 and HT29 cells in DMEM supplemented with FBS and different concentrations of glucose (Fig. 3.1E-F). Of note, this concentration range encompasses the normal blood glucose level (5 mM) and recommended cell culture (25 mM) levels. While glucose concentration below 2 mM dramatically reduced proliferation of both CRC cell lines, when cultured in 5mM of glucose, proliferation of HCT116 and HT29 was reduced by ~ 40% (Fig 3.1E) or was largely unaffected (Fig 3.1F) as compared to 25 mM glucose, respectively. Previous studies demonstrated that glutamine anaplerosis into citric acid cycle (CAC) may play an important role in normal colon but also in CRC (38, 60, 61). The core regions of solid tumors however often display glutamine deficiency (62). Therefore, we investigated glutamine dependencies in CRC cell lines. As expected, the proliferation of HCT116 (Fig 3.1G) and HT29 (Fig 3.1H) cells positively correlated with increasing glutamine concentration whereby the IC₅₀ were determined to be 0.4mM for both cell lines. Although CCD841CoN cells exhibited no proliferative advantage over CCD841CoTr cells at any of the tested glutamine concentrations (Fig 3.11), the proliferation of CCD841CoN cells was reduced by ~50% in the absence of glutamine in the media as compared to ~90% and 80% reduction in proliferation of HCT116 (Fig 3.1G) and HT29 (Fig 3.1H) cells, respectively. Collectively, these data suggest that CRC cells exhibit heightened sensitivity to the inhibitors of mitochondrial functions as compared to non-transformed colon epithelial cells, and that, at least in some contexts, CRC cells exhibit increased dependency on exogenous glutamine.

3.3.2 Phenformin and glutamine depletion downregulate mTORC1 activity and inhibit protein synthesis in CRC cell lines.

Since AMPK and mTORC1 act as sensors for nutrient availability cellular energy status, we next monitored AMPK/mTORC1 signaling at early (2 h) and late (16 h) time points after inducing

energy stress. Consistent with previous findings (63, 64), phenformin increased AMPK activity as illustrated by the phosphorylation of its α subunit (at T172) in both HCT116 (Fig 3.2A) and HT29 (Fig 3.2B) cells. Phenformin induced AMPK activity as early as 2 h in HCT116 cells which was augmented after 16 h of treatment (Fig 3.2A). In turn, induction of AMPK by phenformin was evident only after 16 h of treatment in HT29 cells (Fig 3.2B). Consistent with the role of AMPK in suppressing mTORC1 (65), increase in AMPK activity correlated with reduced mTORC1 signaling in both cell lines (Fig 3.2A-B). This was illustrated by the reduced phosphorylation of mTORC1 substrate, 4E-binding protein 1 (4E-BP1; S65) (Fig 3.2A), and mTORC1-dependent S6 kinases (S6Ks) substrate ribosomal protein S6 (RPS6; S240/244) (Fig. 3.2A-B). In contrast to phenformin treatment, glutamine deprivation did not result in appreciable effects on AMPK phosphorylation levels in both HCT116 (Fig 3.2B) and HT29 (Fig 3.2D) cells. Nonetheless, long term (16 h) deprivation of glutamine suppressed mTORC1 signaling as illustrated by the diminished phosphorylation of 4E-BP1 (S65) and RPS6 (S240/244) (Fig 3.2C-D). This suggests that glutamine deprivation represses mTORC1 activity independently of AMPK. However, glutamine-derived α-ketoglutarate level may be depleted which prevents GTP loading of RAGB and subsequent activation of mTORC1 via prolyl hydroxylases (PHDs) (66). Alternatively, glutamine may activate mTORC1 independently of RAGs via adenosine diphosphate ribosylation factor-1 (ARF1) GTPase (67). Notwithstanding that future investigations are required to determine the temporal changes of mTORC1 signaling in response to glutamine starvation, the data imply that the time taken to deplete intracellular glutamine pools cause a time lag between the observed mTORC1 inhibition and the depletion of exogenous glutamine levels.

Considering that mRNA translation is one of the most energetically demanding processes in the cell which is also regulated by AMPK and mTORC1 (68, 69), we assessed whether global

protein synthesis was affected by phenformin and glutamine deprivation. Phenformin inhibited global mRNA translation as illustrated by reduced polysome formation that is reflected by decreased polysome/80S monosome ratios in HCT116 (Fig 3.2E) and HT29 cells (Fig 3.2F). Similar to phenformin treatment, 16 h of glutamine depletion suppressed global mRNA translation in both HCT116 (Fig 3.2G) and HT29 cells (Fig 3.2H). Overall, these findings are consistent with previous observations suggesting that downregulation of mTORC1 activity and global protein synthesis plays a central role in adaptation to metabolic stress (49).

3.3.3 Phenformin induces metabolic perturbations in CRC cells.

Aberrant AMPK and mTOR signaling has been implicated in the metabolic reprogramming of cancer cells (70). Furthermore, mTOR inhibitors have been shown to modulate cell metabolism by suppressing the translation of mRNAs encoding metabolic enzymes and mitochondrial factors (49, 71-73). Thus, we determined the impact of phenformin on steady-state intracellular metabolites in order to identify metabolic pathways that are perturbed in CRC cells in response to metabolic stress. As expected (74), phenformin reduced the intracellular levels of CAC intermediates including citrate, succinate, fumarate and malate in HCT116 cells as compared to the control, vehicle treated cells (Fig 2.3A) Also consistent with prior findings (48), in HCT116 cells phenformin increased the levels of α -ketoglutarate and α -ketoglutarate/citrate ratio which is associated with the induction of reductive glutamine metabolism (75) (Fig 3.3A). Furthermore, the steady-state level of 2-hydroxyglutarate (2-HG) was elevated while γ-amino-butyric acid (GABA) was depleted in HCT116 cells treated with phenformin relative to the vehicle treated control (Fig 3.3A). Considering that 2-HG is synthesized from α-ketoglutarate while the GABA shunt represents anaplerotic CAC route via succinate (76, 77), these findings are consistent with observed phenformin-induced increase in α -ketoglutarate and decrease in succinate, respectively.

Since the synthesis of amino acids such as aspartate and alanine are dependent on mitochondrial activity (78-80), we expected that phenformin treatment will lead to reduction in intracellular steady-state levels of these amino acids. Indeed, a marked reduction in alanine and aspartate levels was observed in phenformin-treated HCT116 cells (Fig 3.3A). Although phenformin induced comparable perturbations in some steady-state metabolite levels in HT29 and HCT116 cells (e.g., citrate, succinate, α-ketoglutarate, 2-HG, GABA, aspartate and alanine), several differences in the phenformin-induced alterations of metabolite levels between these cell lines were noted (Fig 3.3B-C). For instance, fumarate and malate which were significantly elevated after 2 h exposure to phenformin were reduced to control levels after 16 h in HT29 (Fig 3.3B), but not HCT116 cells (Fig 3.3A). These findings suggest potential temporal differences in phenformin-induced metabolomes of HCT116 and HT29 cells (Fig 3.3C). Although the underpinning mechanisms remain to be established, these metabolic distinctions in the effects of phenformin on the metabolome of HCT116 and HT29 cells may be a reflection of genomic differences between the cell lines.

3.3.4 Glutamine deprivation depletes CAC intermediates while simultaneously increasing the levels of most amino acids in transformed colorectal cell lines.

CRC cells were reported to critically depend on glutamine as an anaplerotic substrate for CAC (61, 81). Moreover, biguanides induce glutaminolysis to support lipogenesis and aspartate synthesis (48, 49, 78, 82). Thus, we sought to investigate time-dependent metabolic perturbations of glutamine-deprived HCT116 and HT29 cells. In accordance with its role in supporting the CAC, glutamine depletion reduced the levels of CAC intermediates (i.e., citrate, malate, succinate, fumarate and malate) in HCT116 cells (Fig 3.4A). In contrast to energy stress induced by phenformin, long term glutamine deprivation of HCT116 cells decreased the α-

ketoglutarate/citrate ratio which is indicative of decreased reductive carboxylation of αketoglutarate (75). Intriguingly, 2 h of glutamine deprivation increased levels of both essential (e.g., valine, leucine, isoleucine, methionine, threonine, phenylalanine, tyrosine and histidine) and non-essential (e.g., cysteine, proline, serine and glycine) amino acids in HCT116 cells (Fig 3.4A). On the contrary, the levels a few amino acids such as alanine, glutamate, aspartate and asparagine were greatly depleted due to glutamine starvation (Fig 3.4A). Most of these observations were not limited to HCT116 cells. HT29 cells deprived of glutamine exhibited similar alterations in the levels of amino acids with concurrent decreases in CAC intermediates and α-ketoglutarate/citrate ratio (Fig 3.4B). Nonetheless, the effects of glutamine starvation on steady-state proline levels were remarkably different between HCT116 and HT29 cells (Fig 3.4A-B). Namely, while glutamine starvation led to an increase in proline levels in HCT116 cells, it was associated with a decrease in proline abundance in HT29 cells (Fig 3.4B-C). Although the cause of this apparent discrepancy in the effects of glutamine deprivation on proline levels between HCT116 and HT29 cells remains unclear, it is plausible that this and other observed discrepancies may stem from differences in the mechanisms that drive metabolic rewiring in these cell lines. For example, MYC has been demonstrated to promote proline biosynthesis from glutamine via glutamate by increasing the expression of enzymes in the pathway such as P5CS and P5C reductase (PYCR) (83). Considering that MYC expression is elevated in 50% of CRC (84), it is conceivable that differential expression of MYC (85) in HCT116 and HT29 glutamine-deprived cells may explain differences in proline levels.

3.4 FIGURES

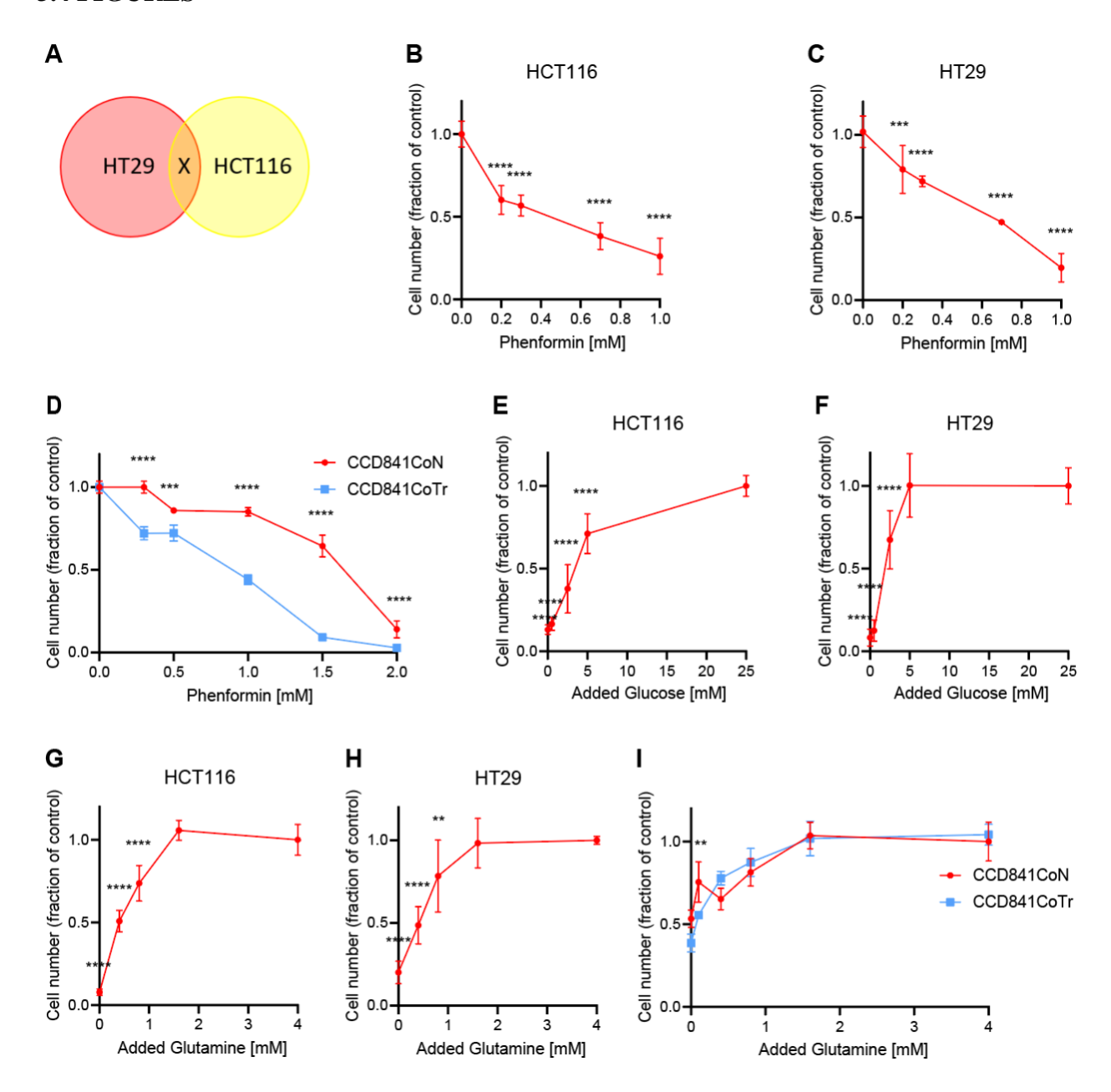


Fig. 3.1 Antiproliferative effects of nutrient deprivation and phenformin on epithelial colon cells. **A.** Venn diagram representing metabolic vulnerabilities after inducing energy stress in HCT116 and HT29. "X" denotes overlapping metabolic changes induced by energy stress in both HCT116 and HT29. **B-D.** HCT116 (**B**), HT29 (**C**), CCD841CoN and CCD841CoTr (**D**) cells were treated with indicated concentrations of phenformin or a vehicle (water) for 3 days. The number

of viable cells was determined using trypan blue exclusion and automated cell counter. Data are shown as the mean fraction of cells relative to the corresponding water-treated controls which were set at 1. The experiments were carried out in independent triplicates (with at least 2 technical replicates each time). Bars represent +/- SD values. E-F. HCT116 (E) and HT29 (F) cells were grown in media containing the indicated concentrations of glucose or vehicle (water) for 3 days. The number of live cells was determined using trypan blue exclusion and automated cell counter. Data are represented as the mean fraction of cells relative to the corresponding water-treated controls which were set at 1. The experiments were carried out in independent triplicates (with at least 2 technical replicates each time). Bars represent +/- SD values. G-I. HCT116 (G), HT29 (H), CCD841CoN and CCD841CoTr (I) cells were grown in media containing the indicated concentrations of glutamine or vehicle (water) for 3 days. The number of viable cells was determined using trypan blue exclusion and automated cell counter. Data are shown as the mean fraction of cells relative to the corresponding water-treated controls which were set at 1. The experiments were carried out in at least independent duplicates (with 2 technical replicates each time). Bars represent +/- SD values. *p<0.05, **p<0.01, ***p<0.001, ****p<0.0001 (**B-C** and **E-H,** One-way ANOVA; Dunnette's posthoc test with water-treated cells as control; **D** and **I,** Twoway ANOVA; Tukey's posthoc test with water-treated cells as control).

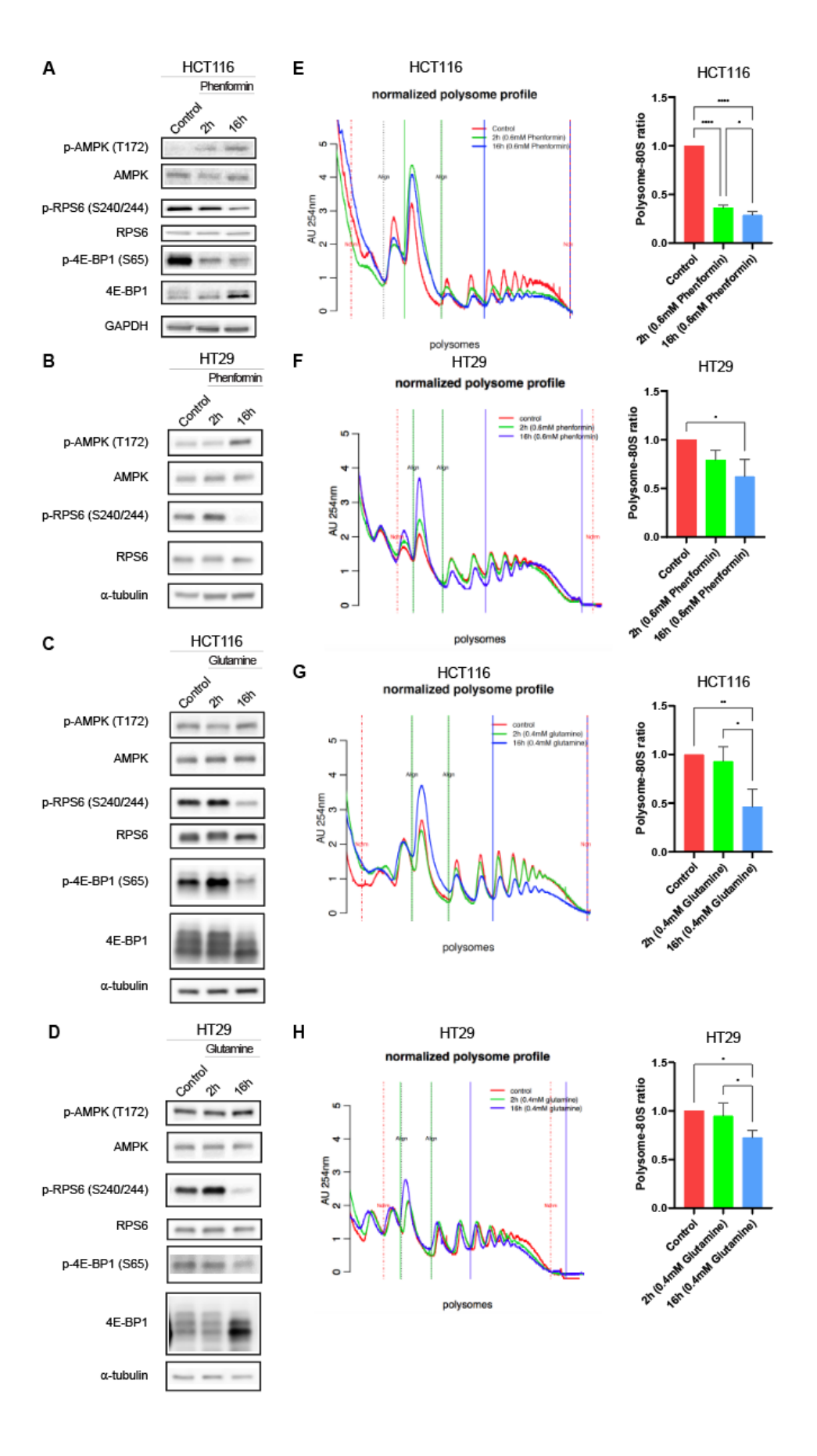


Fig. 3.2 Suppression of global mRNA translation is associated with the time course inhibition of mTORC1 signaling by phenformin and glutamine deprivation in CRC

A-B. Western blot analysis of indicated proteins isolated from HCT116 (A) and HT29 (B) cells treated with phenformin (0.6 mM) or a vehicle (water) for 2 h or 16 h. Representative blots from 3 independent experiments are shown. GAPDH and α -tubulin served as a loading control. **C-D.** HCT116 (C) and HT29 (D) cells were grown in media supplemented with FBS and 0.4 mM glutamine or 4 mM glutamine (water-treated control) for 2 h or 16 h. Levels and phosphorylation status of indicated proteins was determined by Western blotting. α-tubulin served as a loading control. The blots are representative of 3 independent experiments. E-H. HCT116 (E) and HT29 (**F**) cells were treated with phenformin (0.6 mM) or vehicle (water) for 2 h or 16 h. **G-H.** HCT116 (G) and HT29 (H) cells were in media supplemented with 0.4 mM glutamine or control (4 mM glutamine) for 2 h or 16 h. Polysome fractions were obtained by ultracentrifugation using 5-50% sucrose gradients. Representative images of the polysome fraction absorbance profiles (254 nm) are shown. Polysome to 80S monosome ratios were calculated by comparing the area of the 80S peak to the cumulative area under the polysome peaks. The ratios of the areas were made relative to the corresponding control cells which were set at 1 as displayed on the right of the corresponding polysome profiles. The experiments were carried out in independent triplicates. Bars represent +/-SD values. *p<0.05, **p<0.01, ***p<0.001, ****p<0.0001 (**E-H.** One-way ANOVA; Dunnette's posthoc test with water-treated cells as control).

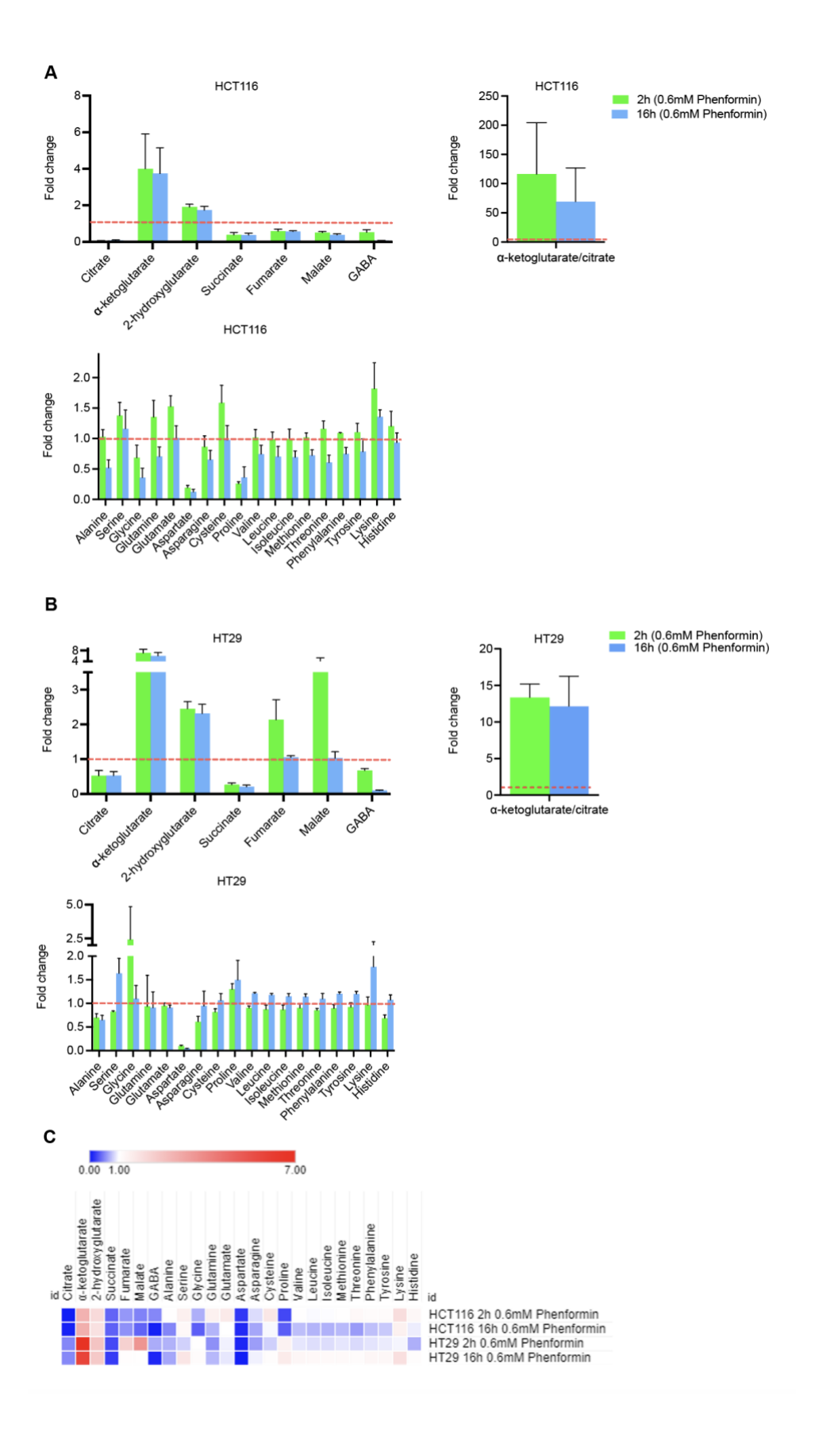


Fig. 3.3 Phenformin alters the metabolome of genetically heterogenous CRC cell lines. A-B. Intracellular levels of CAC-related metabolites and amino acids in HCT116 (**A**) and HT29 (**B**) cells were measured by GC-MS. The cells were treated as indicated and data are represented as mean fold change +/- SD relative to control cells wherein values for each metabolite are set to 1 and displayed as the red-dashed line (N=3 independent experiments with technical triplicates each time). Intracellular α -ketoglutarate/citrate ratios in HCT116 (**A**) and HT29 (**B**) cells were determined from the steady state levels of α -ketoglutarate and citrate. The ratios calculated for the water-treated control cells were set at 1 (red-dashed line) and the results were represented as means of the ratios +/- SD for the phenformin-treated cells of 3 independent experiments with 3 technical replicates each. **C.** Heatmap of the intracellular metabolites shown in Fig. **A** and **B**. The colors vary from blue (for metabolites whose levels were decreased in treatment conditions vs. control) to red (for metabolites whose levels were increased in treatment conditions vs. control).

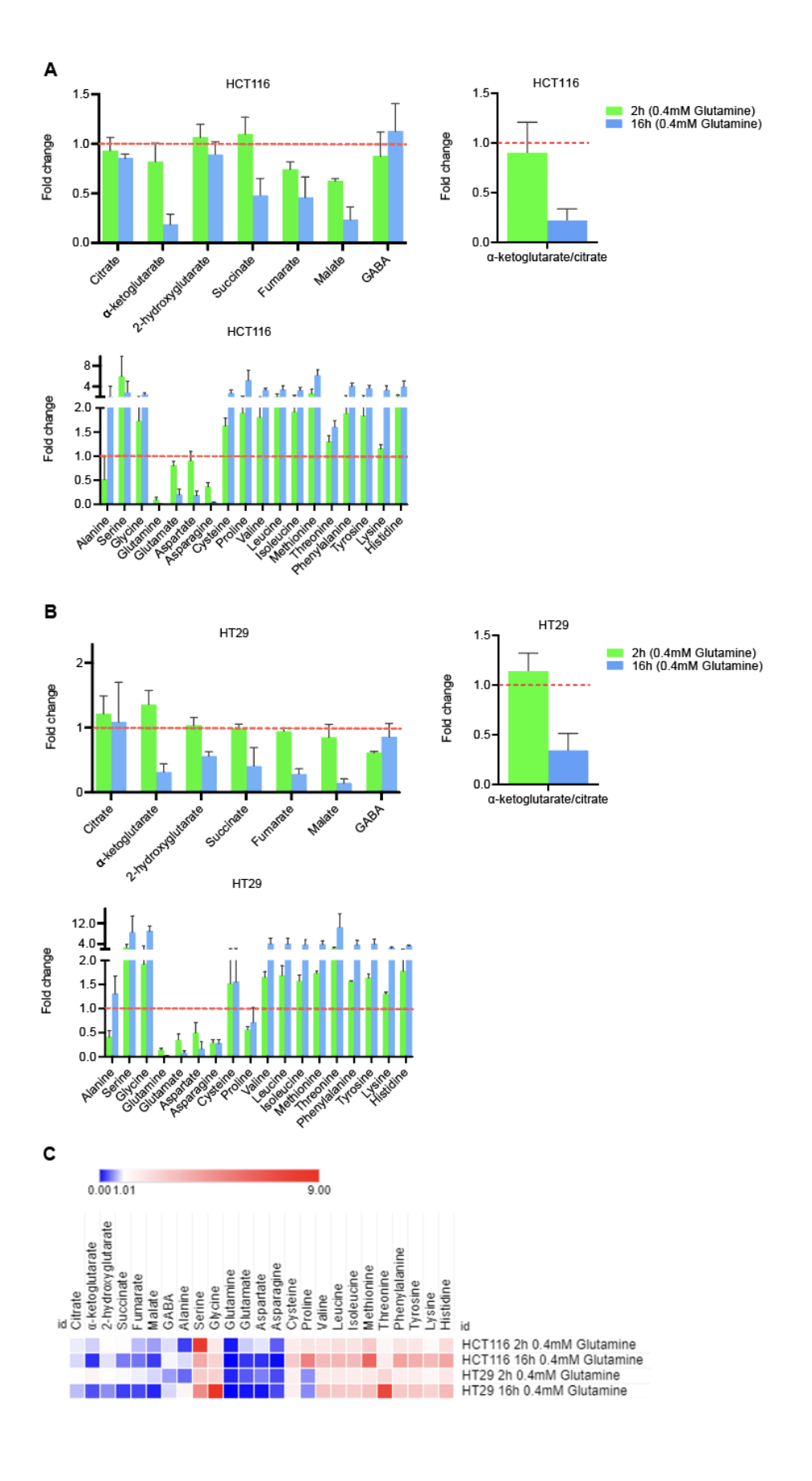


Fig. 3.4 Glutamine deprivation reduces the levels of CAC intermediates but increases the levels of most amino acids in genetically distinct CRC cell lines. A-B. Intracellular levels of metabolites in HCT116 (A) and HT29 (B) cells were detected by GC-MS. The cells were treated as indicated and data are shown as mean fold change +/- SD relative to water-treated cells wherein values for each metabolite are set to 1 and displayed as the red-dashed line (N=3 independent experiments with technical triplicates each time). Intracellular α -ketoglutarate/citrate ratios in HCT116 (A) and HT29 (B) cells were calculated from the steady state levels of α -ketoglutarate and citrate. The ratios determined for the water-treated control cells were set at 1 (red-dashed line) and the results are presented as means of the ratios +/- SD for the treated cells from 3 independent experiments with 3 technical replicates each. C. Heatmap of the intracellular metabolites shown in Fig. A and B. The colors vary from blue (for metabolites whose levels were decreased in treatment conditions vs. control) to red (for metabolites whose levels were increased in treatment conditions vs. control).

3.5 DISCUSSION

Oxygen and nutrient availability vary during tumor development (86), whereby both factors become limiting in poorly vascularized solid tumors (86). In response to the energy stress, cancer cells undergo metabolic reprogramming in order to meet their bioenergetic and biosynthetic demands (86). Previously published studies demonstrated that energy stress caused by phenformin has only a minimal impact on proliferation of non-transformed breast epithelial NMuMG cells as compared to NMuMG cells transformed with oncogenic Neu/ErbB2 (V664E) (referred to as NT2197) (49). Consistent with this finding, HCT116 and HT29 cells exhibited greater sensitivity to energy stress caused by phenformin relative to normal epithelial colon cells (CCD841CoN). This is evident as phenformin IC50 is lower in transformed colorectal cells (i.e., 0.9mM for

CCD841CoTr and 0.6 mM for both HCT116 and HT29) than in normal colon cells (i.e., 1.7 mM in CCD841CoN). Conversely, the IC₅₀ value for glutamine is higher in transformed colorectal cells (i.e., 0.4 mM in both HCT116 and HT29) than in normal colon cells (i.e., 0 mM in CCD841CoN).

Several driver mutations underlie tumor evolution and response to therapeutic insults in CRC. mutations (APC; present in 80% of CRC), KRAS (35%-These 45%), p53 (50%), PIK3CA (20%–30%), and BRAF (10%) result in aberrant activation of the mTOR pathway (87-89). HCT116 and HT29 cells have missense mutations (P449T for HT29 and H1047R for HCT116) in PIK3CA (90) which lead to the constitutively active PI3K-AKT-MTOR signaling (91, 92). However, HCT116 and HT29 cells differ in the status of other driver mutations implicated in metabolic reprogramming. For instance, KRAS (G13D) is mutated only in HCT116 cells (93). In addition, HT29 cells have mutations in BRAF (V600E and T119S) and p53 (R273H) which are absent in HCT116 cells (90, 94-98). Despite BRAF and KRAS mutations promoting similar physiological phenotypes, they have been reported to induce different metabolic dependencies in CRC (96). Corroborating prior works on the effects of biguanides across several cancer cell lines (49, 73, 99, 100), we establish that regardless of the genetic differences between HCT116 and HT29 cells, the downregulation of mTORC1 activity and consequently, protein synthesis by phenformin may at least be partly mediated by AMPK. However, it is worth mentioning that in addition to AMPK-dependent mechanisms, inhibition of mTORC1 by biguanides may be mediated via RAG GTPases and/or REDD1 (100-102). Thus, future genetic approaches whereby expression of REDD1, RAG GTPases or AMPK subunits is modulated is required to discern the precise mechanism by which phenformin inhibits mTORC1 signaling HCT116 and HT29 cells. Our data seem to validate reports that glutamine deprivation inhibits mTORC1 independent of AMPK activity (103). The inhibitory effects of glutamine deprivation on mTORC1 activity seem to be mediated via RAGB (66). In turn, glutamine appears to stimulate mTORC1 via ADP-ribosylation factor 1 (ARF1) (67, 104). Based on this, further investigation is required to highlight the mechanisms by which glutamine starvation inhibits mTORC1 activity in the context of CRC. In addition to reducing global protein synthesis, biguanides and nutrient deprivation have also been shown to preferentially affect translation of specific subsets of mRNAs while only marginally affecting others (49, 73, 105). Future applications of ribosome and/or polysome profiling methods coupled with RNAseq are therefore warranted to catalogue mRNAs whose translation is perturbed in response to metabolic stress in the context of CRC.

Biguanides inhibit mitochondrial functions which leads to compensatory increase in glycolysis (48, 49, 106). Although the biguanide-induced increase in glycolysis is well-defined, the effect of biguanides on the levels of CAC intermediates appear to be context dependent (48, 49, 59, 74, 107, 108). To this end, although phenformin induced comparable changes in the levels of α-ketoglutarate, citrate and succinate in HCT116 and HT29 cells, the effects of phenformin on fumarate and malate appeared to be diminished with time in HT29 but not HCT116 cells. However, to fully establish potential discrepancies in the effects of phenformin on the metabolome of HT29 and HCT116 cells it is necessary to perform future metabolic flux analysis using stable isotope tracer labeling with ¹³C-labelled substrates (such as glucose, glutamine or pyruvate). This and previously published studies (48, 49), suggest that phenformin induces reductive carboxylation of α-ketoglutarate. Given that glutamine is a major anaplerotic source (109, 110), CAC intermediate levels are expected to decrease once the intracellular glutamine levels become limiting. Importantly, glutamine deprivation appears to differentially affect CRC cell lines, whereby the effects of glutamine removal from the cell culture media led to dramatic inhibition of proliferation of HCT116 and HT29 but not CCD841CoTr cells. Notably, cells overexpressing the MYC proto-oncogene (e.g., HT29) or oncogenic KRAS (e.g., HCT116) or PI3KCA mutations (e.g., HCT116 and HT29) have been shown to be highly dependent on glutamine (61, 111-114). It is therefore plausible that the context of cancer-driving mutation(s) dictate(s) glutamine "addiction" of cancer cells, whereby SV40-transformed CCD841CoTr cells show lesser dependence on glutamine. Collectively, these data are in good keeping with previous findings (61, 111-114) suggesting that the driver mutations of CRC may direct metabolic adaptations to metabolic stress caused by glutamine starvation or drugs interfering with mitochondrial functions.

Amino acid starvation leads to elevated levels of deacetylated tRNAs due to the failure of tRNA synthetase to aminoacylate tRNA when intracellular amino acid pools are insufficient (115, 116). Subsequently, the deacetylated tRNA molecules bind and activate GCN2 kinase (116). Once activated, GCN2 phosphorylates eIF2\alpha which is paralleled by reduction in global mRNA translation with concomitant increase in translation of a small subset of mRNAs enriched in those encoding stress-responsive transcription factors including ATF4 (116). We observed similar alterations in the intracellular levels of most essential amino acids (EAAs) and nonessential amino acids (NEAAs) in glutamine-deprived HCT116 and HT29 cells. This is consistent with recent findings demonstrating that cancer cells cultured in glutamine-deficient media significantly elevate the levels of amino acids via increased uptake of exogenous amino acids mediated by ATF4 transcriptional reprogramming (109, 110, 117, 118). Specifically, it was shown that glutamine deprivation triggers the general amino acid control (GAAC) pathway wherein ATF4 expression is upregulated (118, 119). In turn, ATF4 stimulates expression of genes encoding amino acid transporters (e.g., SLC7A5) which is associated with a time-dependent reactivation of mTORC1 and inhibition of autophagy (117, 118). Although glutamine-deprived cells also upregulate amino acid biosynthesis enzymes (e.g., asparagine synthetase) via GCN2/eIF2α/ATF4 axis, they seem to

be unable to generate sufficient asparagine from the intracellular glutamine pools (109, 120). However, in contrast with the prior studies demonstrating that mTORC1 is reactivated in glutamine-starved cells (118), we observed no restoration of mTORC1 activity during 16 h of glutamine deprivation. Intriguingly, no observable changes to the levels of amino acids levels were detected when cells were grown in glutamine-deficient media that was supplemented with asparagine (109). Consistent with this, α-ketoglutarate or asparagine supplementation in glutamine-deficient media also rescued cell proliferation, restored mTORC1 activity and protein synthesis in glioblastoma and breast cancer cell lines (109, 110). Taken together, glutamine and/or asparagine appear to be required to sustain the mTORC1 activity in cancer cell lines, including CRC cells. In addition to enhanced amino acid uptake, it is plausible that the increase in the intracellular levels of EAA and NEAA in phenformin-treated or glutamine-deprived cells is caused by the induction of autophagy (121, 122). To this end, in the future we will set out to determine the role of autophagy in adaptation of CRC cells to energy stress induced by glutamine deprivation or biguanides.

CAC anaplerosis via α -ketoglutarate derived from glutamine is more pronounced in the tumors than in adjacent normal colon tissues (61). Thus, phenformin and drugs inhibiting glutaminolysis may have an optimal therapeutic index for treating CRC. Phenformin increases the reductive carboxylation of α -ketoglutarate, while glutamine deprivation impedes it. This suggests that combining biguanides and inhibitors of glutaminolysis may result in synergistic antineoplastic effects. Indeed, our findings have potential implications for therapeutic strategies targeting glutamine metabolism in CRC, as the efficacy of biguanides as antineoplastic drugs could be bolstered by combining it with inhibitors of glutamine metabolism.

Accordingly, CRC stem cells show greater sensitivity to metformin in glutamine-depleted media but not in glucose-deprived media (123). Furthermore, glutaminase C inhibitor (compound 968) enhanced the antineoplastic effects of metformin (123). In addition, CB-839 (a noncompetitive allosteric GLS1 inhibitor) exhibits marked antiproliferative effects across several cancer models (124-126) and prevents metabolic adaptation to MLN128 (an mTOR inhibitor) (127). Although our study provides pioneering insights into metabolic profiles of CRC in the context of metabolic stress. Future efforts to integrate energy stress-induced changes in gene expression, signaling and metabolome are warranted to establish the networks that underpin adaptive mechanisms of CRC cells and unravel potentially targetable metabolic vulnerabilities.

3.6 METHODS

3.6.1 Cell lines and culture conditions

HCT116, HT29, CCD841CoN and CCD841CoTr were obtained from ATCC. All cells were cultured in complete DMEM (i.e., DMEM supplemented with 10% heat-inactivated fetal bovine serum (FBS) and 1% penicillin/streptomycin) (DMEM, FBS and penicillin/streptomycin were provided by Wisent). HCT116, HT29, CCD841CoN were maintained at 37 °C, 5% CO₂ and 19% O₂ while CCD841CoTr was incubated at 33 °C, 5% CO₂ and 19% O₂.

3.6.2 Glutamine deprivation

For western blotting, polysome profiling and GC-MS analysis, cells were seeded in complete DMEM 24 h before glutamine deprivation treatments. The cells were washed twice using DMEM without glutamine. After discarding the wash media, the cells were treated with DMEM containing 0.4mM glutamine supplemented with 10% heat-inactivated FBS and 1% penicillin/streptomycin. 1.8mL, 10.8mL and 27mL of treatment media were used for cells seeded in 6-well, 100mm and 150mm plates respectively.

3.6.3 Phenformin treatment

Cells seeded for western blotting, polysome profiling and GC-MS analysis were cultured in complete DMEM media 24 h prior to treatment. The cells were washed twice with DMEM without glucose. After discarding the wash media, cells were treated with DMEM containing 10mM glucose supplemented with 10% heat-inactivated FBS, 1% penicillin/streptomycin and 0.6mM phenformin hydrochloride (Sigma). 1.8mL, 10.8mL and 27mL of the treatment media were used for cells seeded in 6-well, 100mm and 150mm plates respectively.

3.6.4 Metabolomics analysis

4.5×10⁵ HCT116 and 5.7×10⁵ HT29 cells were cultured on 6-well plates in technical triplicates to obtain cells approximately 80% confluency 48 h later. Cells were then treated with phenformin or deprived of glutamine for 2 h and 16 h. The plates were quickly placed on ice as soon as the treatment period was over. Media were discarded with an aspirator and the cells were washed with prechilled isotonic saline solution three times. Afterwards, the cells while on the plates were quenched on dry ice. 300 µL of 80% methanol pre-chilled to -20 °C was added to the cells which were subsequently scraped from the wells and transferred into pre-chilled microcentrifuge tubes. This process was repeated with an additional 300 µL of 80% methanol and pooled with the previously collected 300 µL fraction. The cells were lysed at 4 °C (10 minutes, 30 sec on, 30 sec off, high power setting twice with a Diagenode Bioruptor). Cell debris were precipitated and discarded after centrifugation (16000 g, 4°C) while the supernatants were transferred into prechilled tubes, spiked with 750 ng of myristic acid-D₂₇ (Millipore Sigma) and dried in a CentriVap cold trap (Labconco) overnight at 4°C. Subsequently, the dried pellets were solubilized in 30 µL of pyridine containing methoxyamine-HCl (10 mg/mL) (MilliporeSigma) using a sonicator and vortex. The samples were heated to 70°C for 30 min and then moved into GC-MS injection vials containing 70 µL of N-tert-Butyldimethylsilyl-N-methyltrifluoroacetamide (MTBSTFA). After homogenizing, the sample samples were reheated at 70 °C for 1 h. 1 µL of the derivatized samples was injected for GC–MS analysis. All GC–MS instrumentation and software (ChemStation and MassHunter) were from Agilent. Each metabolite was normalized to the peak intensity of myristic acid-D₂₇ and the average cell number derived from the cells seeded in parallel and identical conditions to those collected for GC-MS steady state analysis. Data were expressed as fold change relative to the control cells.

3.6.5 Cell proliferation assays

1×10⁵ cells were seeded in technical duplicates in 6-well plates and incubated for 24 h. The seeding media were aspirated and substituted with treatment media for 72 h. Different concentrations of phenformin tested were prepared using DMEM containing 10 mM glucose supplemented with 10% heat-inactivated FBS and 1% penicillin/streptomycin. After the treatment period was over, the media were aspirated, and trypsin was added to the cells. Trypsinization was stopped by adding complete media to the wells after observing the cells were dislodged from the surface of the plates. The cell sample mixtures were collected and stained with trypan blue. Live cells were counted using an automated cell counter (Invitrogen).

3.6.6 Western blotting and antibodies

2.7×10⁶ HCT116 and 3.4×10⁶ HT29 cells were seeded in complete DMEM on 100mm plates. The seeding media were discarded 24 h later. Cells were then treated as previously described for glutamine deprivation and phenformin treatment. At the end of treatment period, the treatment media were aspirated, and the cells washed twice with ice-cold PBS while on ice. The cells were scrapped from the plates, collected into pre-chilled tubes and centrifuged (600 g at 4°C). The supernatants were carefully removed, the cell pellets were resuspended in lysis buffer [50 mM]

Tris/HCL (pH 7.4), 5 mM NaF, 5 mM Na pyrophosphate, 1 mM EDTA, 1 mM EGTA, 250 mM mannitol, 1% (v/v) triton X-100, 1 mM DTT, 1× complete protease inhibitors and 1× PhosSTOP] and placed on ice for 20 min. The cell lysates were centrifuged (10 min at 16,000 g and 4°C), and the supernatant subsequently transferred into clean microfuge tubes. After calculating protein concentrations by using BCATM kit, the samples were boiled in 1× Laemmli buffer at 95°C for 5 min to denture and reduce the proteins. The proteins were separated by SDS-PAGE and transferred using wet mini-transfer system onto 0.45 µm nitrocellulose membranes. Membranes were placed in blocking buffer solution (5% BSA w/v in TBST buffer (0.1% Tween 20 in 1× TBS)) for 1 h at room temperature and then incubated with the appropriate primary antibodies which were diluted at 1:1000 in 5% BSA in TBST (overnight at 4 °C). The membranes were washed with TBST (3x 10 min at room temperature) and incubated for 1 h with HRP-conjugated secondary antibodies diluted at 1:5000 or 1:2500 in 5% skimmed milk w/v in TBST. Primary antibodies against 4E-BP1#9644, p-4E-BP1 (S65) #9456, α-tubulin #2125, GAPDH #2118, AMPKα #5832 and 2532, p-AMPKα (T172) #50081 and # 2535, p-rpS6 (S240/244) #2215 were all from Cell Signaling Technologies (Danvers, MA); rpS6 #sc-74459 from Santa Cruz Biotechnologies (Dallas, TX). Secondary HRP-conjugated mouse anti-rabbit IgG #A1949, goat anti-mouse IgG #A0168 were from MilliporeSigma. The membranes were washed (3X for 10 min at room temperature), ECL (Bio-Rad) mixture was added on the membranes and protein signals were revealed as chemiluminescent bands using Azure C300 Chemiluminescent Western Blot Imaging System (Azure Biosystems).

3.6.7 Polysome Profiling

6.8×10⁶ HCT116 and 8.5×10⁶ HT29 cells were seeded in complete DMEM on three 150mm plates per treatment condition. The cells were treated as previously described for glutamine deprivation

and phenformin treatment. As soon as incubation period was over, the cells were harvested as described (128). A linear 5% to 50% sucrose gradient was prepared and used to isolate the polysomes described in (128). Trizol (Thermo Fisher Scientific) was added to each fraction according to manufacturer's instructions and stored at -80 °C. Experiments were carried out in independent triplicates.

3.6.8 Statistical analysis

Statistical analysis was performed using data from 2-3 independent experiments. To ensure the precision, accuracy and fidelity of the data, the experiments, when possible, were done with at least duplicates. Two-way ANOVA (Dunnette's) multiple comparison posthoc test) and one-way ANOVA (Tukey's and Dunnette's multiple comparison posthoc tests) analyses were done on Prism (GraphPad).

3.7 REFERENCES

- 1. Sawicki T, Ruszkowska M, Danielewicz A, Niedźwiedzka E, Arłukowicz T, Przybyłowicz KE. A Review of Colorectal Cancer in Terms of Epidemiology, Risk Factors, Development, Symptoms and Diagnosis. Cancers. 2021;13(9):2025.
- 2. Dekker E, Tanis PJ, Vleugels JLA, Kasi PM, Wallace MB. Colorectal cancer. The Lancet. 2019;394(10207):1467-80.
- 3. Douaiher J, Ravipati A, Grams B, Chowdhury S, Alatise O, Are C. Colorectal cancerglobal burden, trends, and geographical variations. J Surg Oncol. 2017;115(5):619-30.
- 4. Knijn N, van Erning FN, Overbeek LIH, Punt CJA, Lemmens VEPP, Hugen N, et al. Limited effect of lymph node status on the metastatic pattern in colorectal cancer. Oncotarget. 2016;7(22):31699-707.

- 5. Hess KR, Varadhachary GR, Taylor SH, Wei W, Raber MN, Lenzi R, et al. Metastatic patterns in adenocarcinoma. Cancer. 2006;106(7):1624-33.
- 6. Welch JP, Donaldson GA. The clinical correlation of an autopsy study of recurrent colorectal cancer. Ann Surg. 1979;189(4):496-502.
- 7. Xie Y-H, Chen Y-X, Fang J-Y. Comprehensive review of targeted therapy for colorectal cancer. Signal Transduct Target Ther. 2020;5(1):22.
- 8. Florescu-Ţenea RM, Kamal AM, Mitruţ P, Mitruţ R, Ilie DS, Nicolaescu AC, et al. Colorectal Cancer: An Update on Treatment Options and Future Perspectives. Curr Health Sci J. 2019;45(2):134-41.
- 9. Druker BJ, Guilhot F, O'Brien SG, Gathmann I, Kantarjian H, Gattermann N, et al. Five-year follow-up of patients receiving imatinib for chronic myeloid leukemia. N Engl J Med. 2006;355(23):2408-17.
- 10. Vermaat JS, Nijman IJ, Koudijs MJ, Gerritse FL, Scherer SJ, Mokry M, et al. Primary colorectal cancers and their subsequent hepatic metastases are genetically different: implications for selection of patients for targeted treatment. Clin Cancer Res. 2012;18(3):688-99.
- 11. Misale S, Di Nicolantonio F, Sartore-Bianchi A, Siena S, Bardelli A. Resistance to anti-EGFR therapy in colorectal cancer: from heterogeneity to convergent evolution. Cancer Discov. 2014;4(11):1269-80.
- 12. Wan L, Pantel K, Kang Y. Tumor metastasis: moving new biological insights into the clinic. Nature Medicine. 2013;19(11):1450-64.
- 13. Gasch C, Bauernhofer T, Pichler M, Langer-Freitag S, Reeh M, Seifert AM, et al. Heterogeneity of epidermal growth factor receptor status and mutations of KRAS/PIK3CA in circulating tumor cells of patients with colorectal cancer. Clin Chem. 2013;59(1):252-60.

- 14. Lièvre A, Bachet JB, Le Corre D, Boige V, Landi B, Emile JF, et al. KRAS mutation status is predictive of response to cetuximab therapy in colorectal cancer. Cancer Res. 2006;66(8):3992-5.
- 15. Benvenuti S, Sartore-Bianchi A, Di Nicolantonio F, Zanon C, Moroni M, Veronese S, et al. Oncogenic activation of the RAS/RAF signaling pathway impairs the response of metastatic colorectal cancers to anti-epidermal growth factor receptor antibody therapies. Cancer Res. 2007;67(6):2643-8.
- 16. Swanton C. Intratumor heterogeneity: evolution through space and time. Cancer Res. 2012;72(19):4875-82.
- 17. Gerlinger M, Rowan AJ, Horswell S, Math M, Larkin J, Endesfelder D, et al. Intratumor heterogeneity and branched evolution revealed by multiregion sequencing. N Engl J Med. 2012;366(10):883-92.
- 18. Richman SD, Chambers P, Seymour MT, Daly C, Grant S, Hemmings G, et al. Intratumoral Heterogeneity of <i>KRAS</i> and <i>BRAF</i> Mutation Status in Patients with Advanced Colorectal Cancer (aCRC) and Cost-Effectiveness of Multiple Sample Testing. Analytical Cellular Pathology. 2011;34:393521.
- 19. Reinartz R, Wang S, Kebir S, Silver DJ, Wieland A, Zheng T, et al. Functional Subclone Profiling for Prediction of Treatment-Induced Intratumor Population Shifts and Discovery of Rational Drug Combinations in Human Glioblastoma. Clinical cancer research: an official journal of the American Association for Cancer Research. 2017;23(2):562-74.
- 20. Kim TM, Jung SH, An CH, Lee SH, Baek IP, Kim MS, et al. Subclonal Genomic Architectures of Primary and Metastatic Colorectal Cancer Based on Intratumoral Genetic Heterogeneity. Clin Cancer Res. 2015;21(19):4461-72.

- 21. Lee SY, Haq F, Kim D, Jun C, Jo HJ, Ahn SM, et al. Comparative genomic analysis of primary and synchronous metastatic colorectal cancers. PLoS One. 2014;9(3):e90459.
- 22. Parsons BL. Many different tumor types have polyclonal tumor origin: Evidence and implications. Mutation Research/Reviews in Mutation Research. 2008;659(3):232-47.
- 23. Yachida S, Jones S, Bozic I, Antal T, Leary R, Fu B, et al. Distant metastasis occurs late during the genetic evolution of pancreatic cancer. Nature. 2010;467(7319):1114-7.
- 24. Liu J, Dang H, Wang XW. The significance of intertumor and intratumor heterogeneity in liver cancer. Experimental & Molecular Medicine. 2018;50(1):e416-e.
- 25. Menck K, Wlochowitz D, Wachter A, Conradi L-C, Wolff A, Scheel AH, et al. High-Throughput Profiling of Colorectal Cancer Liver Metastases Reveals Intra- and Inter-Patient Heterogeneity in the EGFR and WNT Pathways Associated with Clinical Outcome. Cancers. 2022;14(9):2084.
- 26. Sveen A, Løes IM, Alagaratnam S, Nilsen G, Høland M, Lingjærde OC, et al. Intra-patient Inter-metastatic Genetic Heterogeneity in Colorectal Cancer as a Key Determinant of Survival after Curative Liver Resection. PLOS Genetics. 2016;12(7):e1006225.
- 27. Bedard PL, Hansen AR, Ratain MJ, Siu LL. Tumour heterogeneity in the clinic. Nature. 2013;501(7467):355-64.
- 28. Zheng Z, Yu T, Zhao X, Gao X, Zhao Y, Liu G. Intratumor heterogeneity: A new perspective on colorectal cancer research. Cancer Med. 2020;9(20):7637-45.
- 29. Nussenbaum F, Herman IM. Tumor angiogenesis: insights and innovations. J Oncol. 2010;2010:132641-.
- 30. Jain RK. Transport of molecules in the tumor interstitium: a review. Cancer Res. 1987;47(12):3039-51.

- 31. Carmeliet P, Jain RK. Angiogenesis in cancer and other diseases. Nature. 2000;407(6801):249-57.
- 32. Kreuzaler P, Panina Y, Segal J, Yuneva M. Adapt and conquer: Metabolic flexibility in cancer growth, invasion and evasion. Molecular Metabolism. 2020;33:83-101.
- 33. Vaupel P, Kallinowski F, Okunieff P. Blood flow, oxygen and nutrient supply, and metabolic microenvironment of human tumors: a review. Cancer Res. 1989;49(23):6449-65.
- 34. Hanahan D, Weinberg RA. Hallmarks of cancer: the next generation. Cell. 2011;144(5):646-74.
- 35. Cantor JR, Sabatini DM. Cancer cell metabolism: one hallmark, many faces. Cancer Discov. 2012;2(10):881-98.
- 36. Pavlova NN, Thompson CB. The Emerging Hallmarks of Cancer Metabolism. Cell Metab. 2016;23(1):27-47.
- 37. Kodama M, Oshikawa K, Shimizu H, Yoshioka S, Takahashi M, Izumi Y, et al. A shift in glutamine nitrogen metabolism contributes to the malignant progression of cancer. Nature Communications. 2020;11(1):1320.
- 38. Miyo M, Konno M, Nishida N, Sueda T, Noguchi K, Matsui H, et al. Metabolic Adaptation to Nutritional Stress in Human Colorectal Cancer. Sci Rep. 2016;6(1):38415.
- 39. Ben Sahra I, Le Marchand-Brustel Y, Tanti JF, Bost F. Metformin in cancer therapy: a new perspective for an old antidiabetic drug? Mol Cancer Ther. 2010;9(5):1092-9.
- 40. Zhao H, Swanson KD, Zheng B. Therapeutic Repurposing of Biguanides in Cancer. Trends Cancer. 2021;7(8):714-30.
- 41. Lee JH, Kim TI, Jeon SM, Hong SP, Cheon JH, Kim WH. The effects of metformin on the survival of colorectal cancer patients with diabetes mellitus. Int J Cancer. 2012;131(3):752-9.

- 42. Lee JH, Jeon SM, Hong SP, Cheon JH, Kim TI, Kim WH. Metformin use is associated with a decreased incidence of colorectal adenomas in diabetic patients with previous colorectal cancer. Dig Liver Dis. 2012;44(12):1042-7.
- 43. El-Mir MY, Nogueira V, Fontaine E, Avéret N, Rigoulet M, Leverve X. Dimethylbiguanide inhibits cell respiration via an indirect effect targeted on the respiratory chain complex I. J Biol Chem. 2000;275(1):223-8.
- 44. Towler MC, Hardie DG. AMP-activated protein kinase in metabolic control and insulin signaling. Circ Res. 2007;100(3):328-41.
- 45. Hardie DG. AMP-activated/SNF1 protein kinases: conserved guardians of cellular energy. Nat Rev Mol Cell Biol. 2007;8(10):774-85.
- 46. Algire C, Amrein L, Bazile M, David S, Zakikhani M, Pollak M. Diet and tumor LKB1 expression interact to determine sensitivity to anti-neoplastic effects of metformin in vivo. Oncogene. 2011;30(10):1174-82.
- 47. Foretz M, Hébrard S, Leclerc J, Zarrinpashneh E, Soty M, Mithieux G, et al. Metformin inhibits hepatic gluconeogenesis in mice independently of the LKB1/AMPK pathway via a decrease in hepatic energy state. J Clin Invest. 2010;120(7):2355-69.
- 48. Gravel SP, Hulea L, Toban N, Birman E, Blouin MJ, Zakikhani M, et al. Serine deprivation enhances antineoplastic activity of biguanides. Cancer Res. 2014;74(24):7521-33.
- 49. Hulea L, Gravel SP, Morita M, Cargnello M, Uchenunu O, Im YK, et al. Translational and HIF-1α-Dependent Metabolic Reprogramming Underpin Metabolic Plasticity and Responses to Kinase Inhibitors and Biguanides. Cell Metab. 2018;28(6):817-32.e8.

- 50. Birsoy K, Possemato R, Lorbeer FK, Bayraktar EC, Thiru P, Yucel B, et al. Metabolic determinants of cancer cell sensitivity to glucose limitation and biguanides. Nature. 2014;508(7494):108-12.
- 51. DeBerardinis RJ, Chandel NS. Fundamentals of cancer metabolism. Sci Adv. 2016;2(5):e1600200.
- 52. Butler M, van der Meer LT, van Leeuwen FN. Amino Acid Depletion Therapies: Starving Cancer Cells to Death. Trends Endocrinol Metab. 2021;32(6):367-81.
- 53. Ben-David U, Siranosian B, Ha G, Tang H, Oren Y, Hinohara K, et al. Genetic and transcriptional evolution alters cancer cell line drug response. Nature. 2018;560(7718):325-30.
- 54. Li J, Settivari RS, LeBaron MJ. Genetic instability of in vitro cell lines: Implications for genetic toxicity testing. Environmental and Molecular Mutagenesis. 2019;60(6):559-62.
- 55. Kinker GS, Greenwald AC, Tal R, Orlova Z, Cuoco MS, McFarland JM, et al. Pan-cancer single-cell RNA-seq identifies recurring programs of cellular heterogeneity. Nature Genetics. 2020;52(11):1208-18.
- 56. Gambardella G, Viscido G, Tumaini B, Isacchi A, Bosotti R, di Bernardo D. A single-cell analysis of breast cancer cell lines to study tumour heterogeneity and drug response. Nature Communications. 2022;13(1):1714.
- 57. Jackson AL, Sun W, Kilgore J, Guo H, Fang Z, Yin Y, et al. Phenformin has anti-tumorigenic effects in human ovarian cancer cells and in an orthotopic mouse model of serous ovarian cancer. Oncotarget. 2017;8(59):100113-27.
- 58. Nayak AP, Kapur A, Barroilhet L, Patankar MS. Oxidative Phosphorylation: A Target for Novel Therapeutic Strategies Against Ovarian Cancer. Cancers. 2018;10(9):337.

- 59. Janzer A, German NJ, Gonzalez-Herrera KN, Asara JM, Haigis MC, Struhl K. Metformin and phenformin deplete tricarboxylic acid cycle and glycolytic intermediates during cell transformation and NTPs in cancer stem cells. Proceedings of the National Academy of Sciences of the United States of America. 2014;111(29):10574-9.
- 60. Hui S, Ghergurovich JM, Morscher RJ, Jang C, Teng X, Lu W, et al. Glucose feeds the TCA cycle via circulating lactate. Nature. 2017;551(7678):115-8.
- 61. Zhao Y, Zhao X, Chen V, Feng Y, Wang L, Croniger C, et al. Colorectal cancers utilize glutamine as an anaplerotic substrate of the TCA cycle in vivo. Sci Rep. 2019;9(1):19180.
- 62. Pan M, Reid MA, Lowman XH, Kulkarni RP, Tran TQ, Liu X, et al. Regional glutamine deficiency in tumours promotes dedifferentiation through inhibition of histone demethylation. Nat Cell Biol. 2016;18(10):1090-101.
- 63. Zhou G, Myers R, Li Y, Chen Y, Shen X, Fenyk-Melody J, et al. Role of AMP-activated protein kinase in mechanism of metformin action. J Clin Invest. 2001;108(8):1167-74.
- 64. Fryer LG, Parbu-Patel A, Carling D. The Anti-diabetic drugs rosiglitazone and metformin stimulate AMP-activated protein kinase through distinct signaling pathways. J Biol Chem. 2002;277(28):25226-32.
- 65. Gwinn DM, Shackelford DB, Egan DF, Mihaylova MM, Mery A, Vasquez DS, et al. AMPK phosphorylation of raptor mediates a metabolic checkpoint. Mol Cell. 2008;30(2):214-26.
- 66. Durán RV, Oppliger W, Robitaille AM, Heiserich L, Skendaj R, Gottlieb E, et al. Glutaminolysis activates Rag-mTORC1 signaling. Mol Cell. 2012;47(3):349-58.
- 67. Jewell JL, Kim YC, Russell RC, Yu FX, Park HW, Plouffe SW, et al. Metabolism. Differential regulation of mTORC1 by leucine and glutamine. Science. 2015;347(6218):194-8.

- 68. Buttgereit F, Brand MD. A hierarchy of ATP-consuming processes in mammalian cells. Biochem J. 1995;312 (Pt 1)(Pt 1):163-7.
- 69. Morita M, Gravel SP, Hulea L, Larsson O, Pollak M, St-Pierre J, et al. mTOR coordinates protein synthesis, mitochondrial activity and proliferation. Cell Cycle. 2015;14(4):473-80.
- 70. Saxton RA, Sabatini DM. mTOR Signaling in Growth, Metabolism, and Disease. Cell. 2017;168(6):960-76.
- 71. Ramanathan A, Schreiber SL. Direct control of mitochondrial function by mTOR. Proc Natl Acad Sci U S A. 2009;106(52):22229-32.
- 72. Morita M, Gravel SP, Chénard V, Sikström K, Zheng L, Alain T, et al. mTORC1 controls mitochondrial activity and biogenesis through 4E-BP-dependent translational regulation. Cell Metab. 2013;18(5):698-711.
- 73. Larsson O, Morita M, Topisirovic I, Alain T, Blouin MJ, Pollak M, et al. Distinct perturbation of the translatome by the antidiabetic drug metformin. Proc Natl Acad Sci U S A. 2012;109(23):8977-82.
- 74. Liu X, Romero Iris L, Litchfield Lacey M, Lengyel E, Locasale Jason W. Metformin Targets Central Carbon Metabolism and Reveals Mitochondrial Requirements in Human Cancers. Cell Metabolism. 2016;24(5):728-39.
- 75. Fendt S-M, Bell EL, Keibler MA, Olenchock BA, Mayers JR, Wasylenko TM, et al. Reductive glutamine metabolism is a function of the α -ketoglutarate to citrate ratio in cells. Nature Communications. 2013;4(1):2236.
- 76. Ye D, Guan K-L, Xiong Y. Metabolism, activity, and targeting of D-and L-2-hydroxyglutarates. Trends in cancer. 2018;4(2):151-65.

- 77. Tannahill GM, Curtis AM, Adamik J, Palsson-McDermott EM, McGettrick AF, Goel G, et al. Succinate is an inflammatory signal that induces IL-1 β through HIF-1 α . Nature. 2013;496(7444):238-42.
- 78. Birsoy K, Wang T, Chen WW, Freinkman E, Abu-Remaileh M, Sabatini DM. An essential role of the mitochondrial electron transport chain in cell proliferation is to enable aspartate synthesis. Cell. 2015;162(3):540-51.
- 79. Sullivan LB, Gui DY, Hosios AM, Bush LN, Freinkman E, Vander Heiden MG. Supporting aspartate biosynthesis is an essential function of respiration in proliferating cells. Cell. 2015;162(3):552-63.
- 80. Vettore L, Westbrook RL, Tennant DA. New aspects of amino acid metabolism in cancer. British Journal of Cancer. 2020;122(2):150-6.
- 81. Song Z, Wei B, Lu C, Li P, Chen L. Glutaminase sustains cell survival via the regulation of glycolysis and glutaminolysis in colorectal cancer. Oncol Lett. 2017;14(3):3117-23.
- 82. Fendt SM, Bell EL, Keibler MA, Davidson SM, Wirth GJ, Fiske B, et al. Metformin decreases glucose oxidation and increases the dependency of prostate cancer cells on reductive glutamine metabolism. Cancer Res. 2013;73(14):4429-38.
- 83. Liu W, Le A, Hancock C, Lane AN, Dang CV, Fan TW, et al. Reprogramming of proline and glutamine metabolism contributes to the proliferative and metabolic responses regulated by oncogenic transcription factor c-MYC. Proc Natl Acad Sci U S A. 2012;109(23):8983-8.
- 84. Rochlitz CF, Herrmann R, de Kant E. Overexpression and amplification of c-myc during progression of human colorectal cancer. Oncology. 1996;53(6):448-54.

- 85. Tortolina L, Duffy DJ, Maffei M, Castagnino N, Carmody AM, Kolch W, et al. Advances in dynamic modeling of colorectal cancer signaling-network regions, a path toward targeted therapies. Oncotarget. 2015;6(7):5041-58.
- 86. Nakazawa MS, Keith B, Simon MC. Oxygen availability and metabolic adaptations. Nature reviews Cancer. 2016;16(10):663-73.
- 87. Markowitz SD, Bertagnolli MM. Molecular origins of cancer: Molecular basis of colorectal cancer. N Engl J Med. 2009;361(25):2449-60.
- 88. Faller WJ, Jackson TJ, Knight JRP, Ridgway RA, Jamieson T, Karim SA, et al. mTORC1-mediated translational elongation limits intestinal tumour initiation and growth. Nature. 2015;517(7535):497-500.
- 89. Wang X-W, Zhang Y-J. Targeting mTOR network in colorectal cancer therapy. World journal of gastroenterology. 2014;20(15):4178-88.
- 90. Barretina J, Caponigro G, Stransky N, Venkatesan K, Margolin AA, Kim S, et al. The Cancer Cell Line Encyclopedia enables predictive modelling of anticancer drug sensitivity. Nature. 2012;483(7391):603-7.
- 91. Hoxhaj G, Manning BD. The PI3K-AKT network at the interface of oncogenic signalling and cancer metabolism. Nature reviews Cancer. 2020;20(2):74-88.
- 92. Lien EC, Lyssiotis CA, Cantley LC. Metabolic Reprogramming by the PI3K-Akt-mTOR Pathway in Cancer. In: Cramer T, A. Schmitt C, editors. Metabolism in Cancer. Cham: Springer International Publishing; 2016. p. 39-72.
- 93. Berg KCG, Eide PW, Eilertsen IA, Johannessen B, Bruun J, Danielsen SA, et al. Multiomics of 34 colorectal cancer cell lines a resource for biomedical studies. Molecular Cancer. 2017;16(1):116.

- 94. Matoba S, Kang JG, Patino WD, Wragg A, Boehm M, Gavrilova O, et al. p53 regulates mitochondrial respiration. Science. 2006;312(5780):1650-3.
- 95. Hutton JE, Wang X, Zimmerman LJ, Slebos RJ, Trenary IA, Young JD, et al. Oncogenic KRAS and BRAF Drive Metabolic Reprogramming in Colorectal Cancer. Mol Cell Proteomics. 2016;15(9):2924-38.
- 96. Fritsche-Guenther R, Zasada C, Mastrobuoni G, Royla N, Rainer R, Roßner F, et al. Alterations of mTOR signaling impact metabolic stress resistance in colorectal carcinomas with BRAF and KRAS mutations. Sci Rep. 2018;8(1):9204.
- 97. Mayers JR, Torrence ME, Danai LV, Papagiannakopoulos T, Davidson SM, Bauer MR, et al. Tissue of origin dictates branched-chain amino acid metabolism in mutant Kras-driven cancers. Science. 2016;353(6304):1161-5.
- 98. Charitou T, Srihari S, Lynn MA, Jarboui M-A, Fasterius E, Moldovan M, et al. Transcriptional and metabolic rewiring of colorectal cancer cells expressing the oncogenic KRASG13D mutation. British Journal of Cancer. 2019;121(1):37-50.
- 99. Mogavero A, Maiorana MV, Zanutto S, Varinelli L, Bozzi F, Belfiore A, et al. Metformin transiently inhibits colorectal cancer cell proliferation as a result of either AMPK activation or increased ROS production. Sci Rep. 2017;7(1):15992.
- 100. Jang S-K, Hong S-E, Lee D-H, Kim J-Y, Kim JY, Ye S-K, et al. Inhibition of mTORC1 through ATF4-induced REDD1 and Sestrin2 expression by Metformin. BMC Cancer. 2021;21(1):803.
- 101. Kalender A, Selvaraj A, Kim SY, Gulati P, Brûlé S, Viollet B, et al. Metformin, independent of AMPK, inhibits mTORC1 in a rag GTPase-dependent manner. Cell Metab. 2010;11(5):390-401.

- 102. Ben Sahra I, Regazzetti C, Robert G, Laurent K, Le Marchand-Brustel Y, Auberger P, et al. Metformin, independent of AMPK, induces mTOR inhibition and cell-cycle arrest through REDD1. Cancer research. 2011;71(13):4366-72.
- 103. Kim SG, Hoffman GR, Poulogiannis G, Buel GR, Jang YJ, Lee KW, et al. Metabolic stress controls mTORC1 lysosomal localization and dimerization by regulating the TTT-RUVBL1/2 complex. Mol Cell. 2013;49(1):172-85.
- 104. Meng D, Yang Q, Wang H, Melick CH, Navlani R, Frank AR, et al. Glutamine and asparagine activate mTORC1 independently of Rag GTPases. J Biol Chem. 2020;295(10):2890-9.
- 105. Gameiro PA, Struhl K. Nutrient Deprivation Elicits a Transcriptional and Translational Inflammatory Response Coupled to Decreased Protein Synthesis. Cell reports. 2018;24(6):1415-24.
- 106. Javeshghani S, Zakikhani M, Austin S, Bazile M, Blouin MJ, Topisirovic I, et al. Carbon source and myc expression influence the antiproliferative actions of metformin. Cancer Res. 2012;72(23):6257-67.
- 107. Andrzejewski S, Gravel S-P, Pollak M, St-Pierre J. Metformin directly acts on mitochondria to alter cellular bioenergetics. Cancer Metab. 2014;2(1):12.
- 108. Hohnholt MC, Blumrich* E-M, Waagepetersen HS, Dringen R. The antidiabetic drug metformin decreases mitochondrial respiration and tricarboxylic acid cycle activity in cultured primary rat astrocytes. Journal of Neuroscience Research. 2017;95(11):2307-20.
- 109. Pavlova NN, Hui S, Ghergurovich JM, Fan J, Intlekofer AM, White RM, et al. As Extracellular Glutamine Levels Decline, Asparagine Becomes an Essential Amino Acid. Cell metabolism. 2018;27(2):428-38.e5.

- 110. Zhang J, Fan J, Venneti S, Cross JR, Takagi T, Bhinder B, et al. Asparagine plays a critical role in regulating cellular adaptation to glutamine depletion. Molecular cell. 2014;56(2):205-18.
- 111. Qing G, Li B, Vu A, Skuli N, Walton ZE, Liu X, et al. ATF4 regulates MYC-mediated neuroblastoma cell death upon glutamine deprivation. Cancer Cell. 2012;22(5):631-44.
- 112. Wise DR, DeBerardinis RJ, Mancuso A, Sayed N, Zhang XY, Pfeiffer HK, et al. Myc regulates a transcriptional program that stimulates mitochondrial glutaminolysis and leads to glutamine addiction. Proc Natl Acad Sci U S A. 2008;105(48):18782-7.
- 113. Son J, Lyssiotis CA, Ying H, Wang X, Hua S, Ligorio M, et al. Glutamine supports pancreatic cancer growth through a KRAS-regulated metabolic pathway. Nature. 2013;496(7443):101-5.
- 114. Hao Y, Samuels Y, Li Q, Krokowski D, Guan B-J, Wang C, et al. Oncogenic PIK3CA mutations reprogram glutamine metabolism in colorectal cancer. Nature Communications. 2016;7(1):11971.
- 115. Anda S, Zach R, Grallert B. Activation of Gcn2 in response to different stresses. PLOS ONE. 2017;12(8):e0182143.
- 116. Masson GR. Towards a model of GCN2 activation. Biochemical Society transactions. 2019;47(5):1481-8.
- 117. Zhang N, Yang X, Yuan F, Zhang L, Wang Y, Wang L, et al. Increased Amino Acid Uptake Supports Autophagy-Deficient Cell Survival upon Glutamine Deprivation. Cell Rep. 2018;23(10):3006-20.
- 118. Chen R, Zou Y, Mao D, Sun D, Gao G, Shi J, et al. The general amino acid control pathway regulates mTOR and autophagy during serum/glutamine starvation. J Cell Biol. 2014;206(2):173-82.

- 119. Hinnebusch AG. Translational regulation of GCN4 and the general amino acid control of yeast. Annu Rev Microbiol. 2005;59:407-50.
- 120. Ye J, Kumanova M, Hart LS, Sloane K, Zhang H, De Panis DN, et al. The GCN2-ATF4 pathway is critical for tumour cell survival and proliferation in response to nutrient deprivation. EMBO J. 2010;29(12):2082-96.
- 121. Seo JW, Choi J, Lee SY, Sung S, Yoo HJ, Kang MJ, et al. Autophagy is required for PDAC glutamine metabolism. Sci Rep. 2016;6:37594.
- 122. De Santi M, Baldelli G, Diotallevi A, Galluzzi L, Schiavano GF, Brandi G. Metformin prevents cell tumorigenesis through autophagy-related cell death. Sci Rep. 2019;9(1):66.
- 123. Kim JH, Lee KJ, Seo Y, Kwon J-H, Yoon JP, Kang JY, et al. Effects of metformin on colorectal cancer stem cells depend on alterations in glutamine metabolism. Sci Rep. 2018;8(1):409.
- 124. Gross MI, Demo SD, Dennison JB, Chen L, Chernov-Rogan T, Goyal B, et al. Antitumor activity of the glutaminase inhibitor CB-839 in triple-negative breast cancer. Mol Cancer Ther. 2014;13(4):890-901.
- 125. Galan-Cobo A, Sitthideatphaiboon P, Qu X, Poteete A, Pisegna MA, Tong P, et al. LKB1 and KEAP1/NRF2 Pathways Cooperatively Promote Metabolic Reprogramming with Enhanced Glutamine Dependence in KRAS-Mutant Lung Adenocarcinoma. Cancer Res. 2019;79(13):3251-67.
- 126. Peterse EFP, Niessen B, Addie RD, de Jong Y, Cleven AHG, Kruisselbrink AB, et al. Targeting glutaminolysis in chondrosarcoma in context of the IDH1/2 mutation. Br J Cancer. 2018;118(8):1074-83.

- 127. Momcilovic M, Bailey ST, Lee JT, Fishbein MC, Braas D, Go J, et al. The GSK3 Signaling Axis Regulates Adaptive Glutamine Metabolism in Lung Squamous Cell Carcinoma. Cancer Cell. 2018;33(5):905-21.e5.
- 128. Gandin V, Sikstrom K, Alain T, Morita M, McLaughlan S, Larsson O, et al. Polysome fractionation and analysis of mammalian translatomes on a genome-wide scale. Journal of visualized experiments: JoVE. 2014(87).

CHAPTER 4: DISCUSSION

4.1 Rewiring of signaling and metabolic networks underpins metabolic plasticity and adaptation of cancer cells to energy stress.

Although Otto Warburg first described metabolic reprogramming in cancer cells over a century ago, the recent resurgence of interest in studying cancer metabolism that were spurred by the latest technological developments established dysregulated cellular energetics as a hallmark of cancer (1, 2). Metabolic reprogramming is often coupled with the other hallmarks of cancers such as sustained proliferation, resistance toward apoptosis, and epigenetic remodeling (3). For instance, this is evident as the sustained proliferation of tumor cells is a bioenergetically and biosynthetically demanding process, whereby neoplastic cells must adapt their metabolomes to survive and thrive in nutrient and oxygen depleted environment (2). In essence, cancer cells must be metabolically flexible and plastic to balance energy-producing and energy-consuming processes while withstanding adverse stressors emanating from tumor microenvironment. Commonly altered metabolic processes that support tumor growth and progression include glycolysis, lipid metabolism, glutamine metabolism, mitochondrial metabolism and redox homeostasis. Initial research in cancer metabolism predominantly focused on processes that incorporate nutrients into the biomass (e.g., nucleotides, amino acids, and lipids) needed for proliferation (4). This established glucose and glutamine as the major sources for central carbon metabolism needed for cancer cell bioenergetic and biosynthetic processes (3, 4). In terms of bioenergetics, cancer cells often compensate for deficiency of either glucose or glutamine by augmenting the use of the available nutrient considering that the metabolism of both nutrients through the citric acid cycle (CAC) generates reducing equivalents for ATP production via oxidative phosphorylation (OXPHOS) (3-5). Cancer cells predominantly use reduced carbon to

biosynthesize a vast array of macromolecules including fatty acids, nucleotides and non-essential amino acids through the transformation of nutrients into distinct intermediates that serve as substrates for these biomolecules (3). Aerobic glycolysis produces less ATP albeit rapidly from substrate-level phosphorylation than OXPHOS (4). However, it is proposed that aerobic glycolysis maintains redox balance and facilitates anabolic pathways by providing carbon units to support cancer cell survival (3, 4, 6). Most biosynthetic reactions such as fatty acid synthesis are fueled by the reducing equivalent, NADPH (3). While NADPH is mainly produced through the oxidation of glucose via the pentose phosphate pathway, NADH is predominantly generated from glycolysis and CAC to drive OXPHOS (3). Cancer cell plasticity is necessary to allocate portions of carbon atoms derived from nutrients such as glucose and/or glutamine to various bioenergetic and biosynthetic processes (3). Overall, this illustrates how metabolic flexibility allows cancer cells to adapt to energetic stress, while fueling neoplastic growth and disease progression.

Compared to aerobic glycolysis which has been extensively studied in the context of tumorigenesis and disease dissemination, the importance of OXPHOS in tumor metabolism has been mostly underappreciated despite studies demonstrating that OXPHOS is a pivotal source for ATP production in various types of cancers such as lymphoma, melanoma and glioblastoma (7). Mitochondrial metabolism is not only necessary for sustaining the biosynthetic and bioenergetic activities of the CAC but also maintaining mitochondrial membrane potential which is required for proliferation (8). Although neoplastic cells often display distinct metabolic features defined by their tissue of origin, metabolic plasticity enables cancer cells to adjust their dependence between aerobic glycolysis and OXPHOS during cancer progression, in response to therapeutic insults or alterations in tumor microenvironment (7, 9-11). For example, when primary melanoma lesions (which are characterized as "oxidative tumors") intravasate into circulation OXPHOS is

suppressed (9, 12). However, OXPHOS is upregulated after colonization of the metastatic site by the tumor cells (i.e., melanoma lung metastases) (9, 12).

CAC anaplerosis fueled by glucose and glutamine provides intermediates and reducing equivalents needed for *de novo* biosynthetic processes (3). However, not all biosynthetic reactions dependent on glutamine can be supported by glucose (3). This is because in addition to being a carbon source, glutamine supplies reduced nitrogen which is required for biosynthesizing non-essential amino acids and nucleotides (3). However, when glutamine is scarce cancer cells have been demonstrated to use branched-chain amino acids (BCAAs) as a nitrogen source (13). Overall, metabolic flexibility and plasticity allow cancer cells to meet their bioenergetic and biosynthetic needs which are vital to tumor growth, proliferation and survival. Recent discoveries indicate that cancer cell metabolism is dependent on various factors including (i) the availability of metabolic fuels, (ii) their metabolic plasticity and flexibility, and (iii) the tumor microenvironmental conditions [e.g., hypoxia, acidosis, etc. (14)].

Activation of oncogenes (e.g., *KRAS* and *PI3KCA*) or inactivation of tumor suppressors such as *PTEN* and *TP53* impact on key metabolic processes including glutamine metabolism, glycolysis and OXPHOS (15-19). As such, oncogenic mutations inadvertently result in metabolic dependencies while concurrently exposing metabolic vulnerabilities that could be targeted by therapeutic interventions. The precise mechanisms of how oncogenic lesions influence cellular metabolomes and how metabolic perturbations are orchestrated with the alterations in gene expression and signaling programs are still largely elusive. Major nutrient-sensing mTOR pathway is frequently dysregulated across a broad spectrum of neoplasia (20, 21). Aberrant mTOR signaling is emerging as a major factor implicated in metabolic rewiring of neoplasia [reviewed in (20-23)]. For example, we showed that mTORC1/4E-BP signaling axis coordinate reprograming of

mRNA translation, mitochondrial functions and metabolic rewiring via controlling biosynthesis of the components of mitochondrial complexes and NEAAs including serine, asparagine and aspartate, respectively (24, 25). Similar interactions between mRNA translation machinery and metabolic programs are thought to be mediated by the GCN2/eIF2 α /ATF4 signaling axis (26, 27). The GCN2/eIF2 α /ATF4 axis mediates an adaptive stress response to amino acid deprivation by upregulating expression of genes involved in amino acid synthesis and transport (26, 28). Recent studies highlight that the crosstalk between these pathways and AMPK may play a major role in the coordination of metabolic and post-transcriptional gene expression programs in cancer cells thus endowing cancer cells with sufficient flexibility to adapt to a variety of stressor (29-31). These and similar post-transcriptional mechanisms are anticipated to collaborate with transcriptional programs directed by tumor promoting (e.g., c-MYC, HIF- 1α) or tumor suppressive transcription factors (e.g., p53) in shaping malignant metabolomes (32-36) (36). In turn, it is becoming apparent that metabolites including succinate, fumarate and 2-hydroxyglutarate affect gene expression by abrogating epigenetic and epitranscriptomic programs via interfering with histone, DNA and RNA demethylases (37). Collectively, these findings provide initial insights into the complexity of cellular networks that orchestrate signaling, gene expression and metabolic rewiring of neoplasia and indicate that future studies are warranted to dissect precise mechanisms that govern these processes.

Through my primary projects, I sought to capture metabolic perturbations induced by energetic stress in attempt to reveal potential targetable metabolic vulnerabilities in cancer. To this end, we show that glutamine deprivation or impaired mitochondrial complex I or IV activities result in energetic stress which is accompanied by a downregulation of mTORC1 signaling. However, while energetic stress due to complex I or IV dysfunction is associated with

compensatory increase in glycolysis and activation of AMPK, glutamine starvation had no apparent effect on AMPK. Based on this and previous literature (38), it appears that glutamine depletion inhibits mTORC1 activity independently of AMPK. Furthermore, we show that the inactivation of complex IV results in a paradoxical hyperactivation of AKT which we assume promotes survival of cancer cells by upregulating ATP producing processes (i.e., glycolysis), while minimally consuming energy via concomitant suppression of mTORC1 signaling. Consistently, HCT116 with impaired complex IV function exhibited heightened sensitivity to AKT inhibitors, while they were less sensitive to mTOR inhibitors, as compared to control cells with undisrupted complex IV function. Although the mechanism of activation of AKT accompanied by the paradoxical suppression of mTORC1 remains elusive, it is plausible that associated activation of AMPK dampens the AKT-dependent activation of mTORC1. Indeed, repeated attempts to abrogate expression or deplete AMPK subunits in HCT116 cells with defective complex IV resulted in massive cell death. This suggests that AMPK activity is essential for rewiring signaling pathways and survival of cells with impaired complex IV function.

In addition to rewiring of signaling pathways, we also observed that different types of stressors lead to distinct metabolic rewiring. For example, our data in conjunction with previous studies (39-45) revealed that rewiring of glutamine metabolism plays a major role in adaptation of cancer cells to aberrant ETC function. Consistent with findings showing that reductive glutamine metabolism is a function of the intracellular levels of α -ketoglutarate to citrate (46), we observed that impeding mitochondrial complex I or IV activity increases reductive glutamine metabolism. Although stable isotope tracer analysis with 13 C-glutamine is required to delineate how intracellular carbon flux is altered in response to the different energetic stressors, these findings

suggest that reductive glutamine metabolism may play a major role in adaptation of cancer cells to energy crisis caused by aberrant mitochondrial function.

4.2 Pharmacological strategies to target metabolic vulnerabilities in cancer

Metabolic reprograming is thought to play a central role in tumorigenesis and tumor progression, whereby specific metabolic programs are thought to distinguish malignant from normal cells (11). Hence, targeting cancer-specific metabolic vulnerabilities should provide a sufficient therapeutic window to selectively eradicate neoplastic cells while exerting minimal toxicity in normal cells and tissues.

In addition to being the most abundant amino acid in the plasma, glutamine is metabolized by malignant cells at rates that appear to be higher than any other amino acid (10-100 times more than other amino acids) (47, 48). Although glutamine is often regarded as a nonessential amino acid, many types of cancers are dependent on extracellular glutamine, such as non-small cell lung cancer (NSCLC) and glioblastoma (49, 50). Furthermore, there is ample evidence suggesting that during stress, the need for glutamine seemingly exceeds the biosynthetic capacity of cells to provide sufficient amounts of de novo synthesized glutamine (51). Hence, glutamine is more accurately classified as a "conditionally essential amino acid" (51). Accordingly, the results of this thesis demonstrate the critical dependence of CRC cell lines on glutamine. For example, glutamine deprivation leads to reduction in mTORC1 activity and global protein synthesis which is paralleled with dramatically reduced proliferation of CRC cells. Although transformed colon cells showed no proliferative disadvantage compared to their parental non-transformed cells at any of the tested glutamine concentrations, future studies are required to elucidate the differences in glutamine metabolism between normal colon cells and CRC cells. In addition, our results in combination with studies from other groups (39-45) suggest that reductive glutamine metabolism may

constitute a targetable metabolic vulnerability in cancer cells that exhibit mitochondrial dysfunction. Based on this, I will discuss current and/or potential strategies to target glutamine metabolism in the context of my primary studies.

4.2.1 Pharmacological inhibition of glutamine uptake

The glutamine analog, γ-l-glutamyl-p-nitroanilide (GPNA), has been shown to have antitumor effects in glutamine-dependent NSCLC and triple-negative basal-like breast cancer (TNBC) cell lines (52, 53). Pharmacological treatment of tumor cells with GPNA not only reduced glutamine uptake, but also inhibited mTOR signaling and cell proliferation (52, 53). The effects of GPNA were proposed to be mediated through the inhibition of the glutamine transporter, SLC1A5 (52, 53). Moreover, SLC1A5 inhibitor 2-amino-4a more potent bis(aryloxybenzyl)aminobutanoic acid (AABA; also referred to as V-9302) was demonstrated to reduce the viability of several cancer cell lines including breast, lung and CRC and attenuated the growth of corresponding xenografts tumor in mice (54). Consistent with the findings on the effects of glutamine deprivation on CRC cell lines reported in this thesis, V-9302 exposure decrease mTOR activity and diminish cancer cell proliferation (54).

Interestingly, subsequent studies showed that GPNA and V-9302 may exert their antineoplastic effects independently of SLC1A5 and that they may be reliant on different glutamine (SLC38A2) and leucine transporters (SLC7A5) (55-57). Given that GPNA is a substrate of a key enzyme in glutathione metabolism, γ-glutamyltransferase (GGT), additional reports suggested that the antitumor properties of GPNA in lung cancer were mediated by GGT (58). Specifically, it was proposed that GGT-catalyzes hydrolysis of GPNA into cytotoxic p-nitroaniline thus inducing apoptosis without exerting a major effect on glutamine uptake in lung cancer cells (58). Taken together, these data suggest that the anticancer activities of GPNA may

be context-dependent and more pleiotropic than previously thought. To this end, the antineoplastic effects of GPNA may be mediated by a combination of reduction in glutamine uptake and induction of oxidative stress. Deciphering of the molecular mechanisms of GPNA and V-9302 is further complicated by the intricate metabolic network involved in amino acid homeostasis. This is due to the existence of multiple amino acid transporters that import and export one or more amino acids (59). It was initially suggested that SLC7A5 is functionally coupled with SLC1A5 wherein glutamine imported by SLC1A5 is subsequently exchanged for essential amino acids (EAAs) (e.g., leucine) by SLC7A5 (60, 61). According to this model, leucine and other branch chained amino acids were thought to mediate the effects of glutamine on mTOR activation (60, 61). However, the pharmacological inhibition of SLC7A5 and SLC38A2 with V-9032, and abrogation of SLC1A5 led to a recently revised model of amino acid homeostasis (62). Herein it is thought that glutamine along with other NEAAs are predominantly accumulated in the cytosol by SLC38A1 which are then rapidly exchanged for other extracellular neutral NEAAs via SLC7A5 and SLC1A5 (62). The inhibition of SLC7A5 results in a rescue response thereby upregulating SLC38A2 and SLC1A4 (62, 63). This therefore suggests that SLC38A2 and SLC1A4 are functionally redundant (63). This model is corroborated by the findings showing that the knockout of SLC1A5 in liver, colon and lung adenocarcinoma cell lines failed to repress mTORC1 signaling or proliferation because of amino acid transporter redundancies (64, 65). However, a recent study using human head and neck squamous cell carcinoma cell cultures and xenografts showed that abrogating SLC1A5 alone was sufficient to increase oxidative stress, suppress mTORC1 signaling and attenuate tumor growth (64). Collectively, with new emerging findings demonstrating redundancies in the various amino acid transporters, the mechanisms of antineoplastic actions of glutamine transporter inhibitors remain obscure.

4.2.2 Pharmacological inhibition of glutaminolysis

Intracellular glutamine is converted to glutamate by glutaminases (GLS). Glutamate is an important precursor of glutathione which protects cells from oxidative stress (66). Glutamate can then be deamidated either through (GLUD1) or transaminases such as (GOT or GPT) to produce α -ketoglutarate which is incorporated into the citric acid cycle (CAC) (67, 68). Other than its incorporation into the CAC for the subsequent production of ATP, glutamine-derived α -ketoglutarate can be used for *de novo* fatty acid synthesis (indirectly through citrate), aspartate and nucleotide synthesis (ultimately through oxaloacetate) (67, 68).

Over the last decade, small-molecule allosteric inhibitors of GLS have been developed as anticancer therapies. These include compound 968, BPTES (bis-2-(5-phenylacetamido-1,2,4thiadiazol-2-yl) ethyl sulfide), and CB-839 (69). GLS inhibitors differ in enzyme specificity and potency. While CB-839 and BPTES have the same molecular scaffold and are specific for GLS1, compound 968 is a pan-glutaminase inhibitor with moderate selectivity for GLS2 (69-72). Notably, compound 968 was demonstrated to suppress the proliferation of BPTES/CB-839resistant luminal breast cancer cell lines (72). The increased sensitivity of luminal A breast cancer cell lines to compound 968 was reported to be dependent on the upregulation and preference of GLS2 over GLS1 for glutaminolysis (72). The antiproliferative effect of CB-839 in TNBCs with upregulated GLS1 was associated with elevated glutamine uptake, decreased glutamine catabolism and diminished OXPHOS (73). Consistent with this, GLS inhibition of TNBC suppressed mTORC1 activity and induced ATF4 expression (74). Importantly, although the inhibition of glutaminolysis increases intracellular levels of glutamine while glutamine deprivation or treatment with glutamine transporter inhibitors deplete glutamine levels, abrogating any of the two reduces mTORC1 signaling and decreases cell proliferation (54, 74). Unlike GLS1, the function of GLS2

remains unclear and appears to be context-dependent. For instance, while *GLS2* is transcriptionally upregulated by p53 (75) and has been considered a tumor suppressor in liver cancer and glioblastoma, it was also shown to be regulated by N-MYC in neuroblastoma (76, 77). These apparently conflicting roles of GLS2 have hampered efforts in developing selective inhibitors against it.

In pre-clinical studies, BPTES is the most frequently used highly selective glutaminase inhibitor (78). However, it is less potent than its analog, CB-839, and its poor aqueous solubility restricts its application in *in vivo* models (78). To this end, CB-839 has been the only one tested in numerous clinical trials for many types of cancers including non-Hodgkin's lymphoma (NCT0207188), acute myeloid leukemia (NCT02071927), clear cell renal carcinoma (ccRCC) CRC (NCT02861300), TNBC (NCT03057600) (NCT02771626), and lung cancer (NCT02771626, NCT03831932, NCT03831932, NCT04250545). Although CB-839 used as a single-agent anticancer therapy profoundly inhibits glutaminolysis and arrest tumor cell growth in preclinical models, metabolic plasticity of cancer cells appears to significantly limit their efficacy (79) (80, 81). To this end, instead of relying solely on glutamine and specific glutamine transporters/glutaminolytic enzymes, cancer cells may switch to other metabolic routes that can be used as surrogate pathways to overcome therapeutic insults targeting glutamine metabolism (7). This in combination with a relatively modest success of therapeutic approaches targeting glutamine metabolism suggest that CB-839 and/or glutamine transporter inhibitors are unlikely to be effective as monotherapies.

4.2.3 Drug combinations with glutamine metabolism inhibitors

The mTOR signaling pathway regulates metabolism while integrating extracellular and intracellular signals emerging from the environment, nutrient availability and energetic status (82).

Importantly, mTOR inhibitors decrease energy consumption due to inhibition of global mRNA translation that is associated with reduced energy production (25). In this manner, mTOR inhibitors cause metabolic dormancy in cancer cells which explains their cytostatic effects observed in the clinic (25).

Strikingly, it was observed that CB-839 synergizes with the mTOR inhibitors AZD8055 and PP242 to reduce the proliferation of TNBC and glioblastoma cells (74, 83). Accordingly, the resistance to mTOR inhibitors in glioblastoma has been attributed to compensatory glutamine metabolism wherein GLS expression was upregulated by PP242 and led to concomitant increases in the intracellular levels of glutamate and α-ketoglutarate (83). Although these studies illustrated synergy between glutaminase inhibitors and active site mTOR inhibitors, they fail to address whether the synergistic effects are predicated on inhibiting mTORC1, mTORC2 or both. More recently it was demonstrated that glutamine deprivation, GLS knockdown, or exposure to CB-839 increased ROS levels, suppressed nucleotide synthesis and induced replication stress in a subset of ovarian cancer cells (84). The cells were more dependent on poly (ADP-ribose) polymerase (PARP) DNA repair and thus, sensitive to the PARP inhibitor, Olaparib (84). Moreover, DNA damage stimulated after treatment with certain cytotoxic drugs leads to abnormally high levels of PARP-mediated ribosylation, which is an energy costly process (85, 86). Taken together, these findings suggest that targeting multiple cellular processes increases the efficacy of drugs targeting glutamine metabolism which is likely due to the ability of these drug combinations to limit metabolic plasticity of neoplasia (84). Notwithstanding these promising preclinical results, future clinical trials are required to establish the efficacies of drug combinations targeting glutamine metabolism with other therapeutic modalities in cancer patients.

4.2.4 Therapeutics targeting OXPHOS in cancer

It has been shown that tumor cells devoid of mitochondrial DNA (mtDNA) lack tumorigenic potential, and form tumors only after acquiring healthy mtDNA from the host stromal cells (87). This was paralleled by restoration of respiratory activities in the tumor cells (87). This and similar studies illustrate the pivotal role of mitochondria in tumorigenesis and expose mitochondria as potential targets for anticancer drugs. The work in this thesis demonstrated that the inactivation of complex I or IV led to increased glucose uptake, glycolysis and reductive glutamine metabolism to compensate for the metabolic defects caused by mitochondrial (16, 24, 42, 88). This suggests that impairment in mitochondrial functions and consequent activation of compensatory metabolic pathways may constitute druggable metabolic vulnerabilities.

The anticancer activities of biguanides like metformin have been reported in numerous studies [reviewed in (89)]. Notably, results presented in this thesis confirmed previous findings that the antiproliferative effects of biguanides are more pronounced in malignant cells as compared to non-transformed cells (24), which together with proven safety of biguanides in the treatment of type 2 diabetes suggests sufficient therapeutic window (90). The mechanisms of the anti-neoplastic action of metformin and other biguanides is still unclear. For instance, it remains unclear whether biguanides act directly on the mitochondria by inhibiting complex I of the ETC because cancer cells deficient in mitochondrial DNA (rho0 cells) are sensitive to metformin (91). Furthermore, tumor cells with complex I mutations are more susceptible to metformin compared to cancer cells without the mutations (92). These reports oppose conclusions of previous studies showing that metformin causes time-dependent inhibition of complex I in isolated mitochondria (93) and that its anticancer effects are attenuated by the expression of *Saccharomyces cerevisiae* NADH dehydrogenase (NDI1) that is biguanide-insensitive (94). In addition, biguanides have been

proposed to exert their antiproliferative effects at clinically relevant concentrations by inducing oxidative stress through the inhibition of mitochondrial glycerol phosphate dehydrogenase (GPD2) (95, 96). At the therapeutically relevant drug concentrations (1-5 µM) the reduced proliferation was not accompanied by suppression of mTOR signaling or diminished mitochondrial complex I activity (95, 96). These studies indicate that further research is required to determine the precise mechanism of the anti-neoplastic effects of biguanides.

Hyperinsulinemia is a risk factor for several cancer types and is associated with adverse prognosis in breast, colon and pancreatic cancer patients (97-99). This is consistent with epidemiological studies demonstrating that type-2 diabetes mellitus and obesity are linked with an increased risk for developing breast, colon, liver, pancreas and kidney cancer (100, 101). Insulin can promote tumorigenesis through its action on insulin/insulin-like growth factor receptors (IR/IGF1R) which activate downstream signaling pathways (commonly implicated in neoplasia) such as PI3K/AKT/mTOR and RAS/RAF/MEK/ERK (102). Hyperinsulinemia can indirectly exert mitogenic effects by elevating the levels of insulin-like growth factors (IGFs), sex hormones (i.e., androgens and estrogens) and increasing the expression of IGF1R (102-104). Mechanistically, metformin acts as an antidiabetic agent by reducing liver gluconeogenesis and increasing glucose uptake in skeletal muscles, thus decreasing blood glucose levels, improving insulin sensitivity and lowering insulin levels in diabetic patients (105). Consequently, the anticancer properties of metformin may be due to its systemic effects on glucose and insulin levels. As such, it is thought that the systemic effects of metformin may underly its anticancer properties especially in cancer patients with hyperinsulinemia. Nonetheless, the results of a large phase III randomized, placebo-controlled, double-blind clinical trial examining the effects of metformin versus placebo in over 3500 non-diabetic women with early-stage breast cancer position biguanides as potential anticancer agents (106). Specifically, the administration of metformin led to weight loss, reduced circulating glucose and insulin levels, increased apoptosis and decreased proliferation of tumor cells (106, 107).

Following the promising results from preclinical studies, there are close to 100 ongoing clinical trials evaluating the anticancer effects of biguanides either as a single agent or in combination with other interventions (108). However, the results of the completed trials have been mostly disappointing due to the incomplete understanding of the molecular mechanism of biguanides. Another plausible reason for the failures in clinical studies evaluating the efficacy of metformin as an antitumor agent may be because many of these studies assume that the commonly prescribed dose of metformin for type-2 diabetes mellitus is sufficient to elicit its anticancer effects. Even though phenformin is more potent and bioavailable due to its hydrophobicity and permeability, metformin is the preferred choice of biguanide in over 90% of the clinical trials (109, 110). The primary reason for the lopsided application in clinical trials is due to phenformin-related toxicities such as lactic acidosis (111). This is in contrast with metformin which is well tolerated and largely nontoxic (112). Despite findings from retrospective epidemiological studies demonstrating that type-2 diabetes mellitus patients treated with metformin had reduced incidence rates of hepatocellular carcinoma, pancreatic cancer, breast cancer or colorectal adenoma, the bioavailability of metformin in treating cancer patients is not robust (113-118). In essence, preventing cancer does not equate to treating cancer. A predominant reason why the anticancer properties of metformin observed in *in vitro* experimental models are not apparent in clinical trials is because of the difference in the effective concentration of biguanides tested (95). In clinical trials, oral intake of biguanides results in plasma levels which are about 10-100 folds less than those used in preclinical studies (95). Preclinical studies employ metformin in the suprapharmacological levels (i.e., millimolar range) (95). Nonetheless, consistent efforts are being made to improve the potency of biguanides (119).

Developing small molecule inhibitors selectively targeting OXPHOS in cancer cells has remained a challenge because most conventional inhibitors of cellular respiration (e.g., rotenone) are also toxic to normal cells, and thus offer do not provide a suitable therapeutic window (120) (115). Novel potent OXPHOS inhibitors such as BAY 87-2243 and its analog IACS-010759 have suitable pharmacokinetic properties (121, 122). They have also been evaluated in clinical studies for acute myeloid leukemia, lymphoma and advanced solid tumors. While the clinical trials administering BAY 87-2243 was discontinued because of toxicity, IACS-010759 was demonstrated to be well-tolerated (123).

4.2.5 Drug combinations with biguanides

Given that cancer cells often undergo metabolic rewiring in response to biguanide-induced energy stress, targeting the compensatory metabolic adaptations through biguanide drug combination treatments is a potential pharmaceutical strategy that has been studied in various preclinical models (24, 124). Moreover, drug combinations that exhibit synergistic antineoplastic effects could mitigate the suboptimal pharmacokinetic issues associated with metformin by reducing its effective concentration.

One of the earliest proposed combinatorial biguanide treatments involved the use of glycolytic inhibitors such as 2-deoxyglucose (2-DG) to block compensatory increase in glycolytic ATP production and NADH oxidation (125, 126). Biguanides have demonstrated synergy with 2-DG to reduce cell viability and proliferation in preclinical models of prostate cancer, breast cancer and chemoresistant lung cancer stem cells (125, 127, 128). However, many clinical trials with 2-DG have been terminated due to lack of clinical efficacy and serious side effects (126).

Kinase inhibitors (KIs) such as erlotinib (EGFR inhibitor), gefitinib (EGFR inhibitor), trastuzumab (HER2 inhibitor), lapatinib (EGFR/HER2 dual inhibitor) and imatinib (BCR-ABL inhibitor) suppress glucose metabolism across various tumor cell models harboring mutations in the corresponding kinases (129-132). However, metabolic flexibility occasionally limits the therapeutic efficacy of these drugs. An example of this is vemurafenib, a BRAF inhibitor commonly used to treat melanoma, which also represses glucose metabolism (24, 133, 134). BRAF inhibitors provide only short-term benefits followed by the development of drug resistance which is accompanied with increased dependence on OXPHOS and glutamine metabolism (133, 135). In one of the studies highlighted in the thesis, we demonstrated that KIs targeting different oncogenic mutations synergize with phenformin across broad spectrum of cancer cell lines (24). Specifically, KIs antagonized the metabolic adaptive pathways activated by phenformin treatments (24). KIs diminished phenformin-induced increases in glycolysis and reductive glutamine metabolism (24). Furthermore, this indicates that the drug combination may be effective against genetic and metabolic heterogenous tumors. In fact, phenformin is currently being tested in a phase I clinical trial to determine the optimal dosage for combination treatments with KIs (Dabrafenib and Trametinib) in patients with metastatic BRAF mutated melanoma (NCT03026517). Nonetheless, we demonstrated that mTORC1- and/or HIF1α-dependent alterations in NEAA biosynthesis and glutamine metabolism, respectively provide cancer cells with metabolic flexibility that allows them to overcome KI and biguanide combinations (24). These data suggest that the applicability of KI/biguanide combinations in the clinic may be limited.

Curiously, preclinical studies have shown that BPTES bolsters the antiproliferative effects of phenformin in LKB1-deficient NSCLC (136). The loss of LKB1 impeded AMPK activation and sensitized tumor cells to the energy stress induced by the phenformin/BPTES drug

combination treatment (136). Abrogation of LKB1 impaired the metabolic flexibility of NSCLC cells and thus, rendered them susceptible to energetic crisis (136). Conceivably, the drug combination treatments impinge on essential metabolic and cellular processes regulated by mTOR signaling. Taken together, there seem to be promise in OXPHOS inhibitors/glutaminase inhibitors drug combination interventions particularly for tumors with limited metabolic flexibility and greatly dependent on glutamine metabolism and OXPHOS. Therefore, further research is required to identify the mechanisms that predict efficacy of combinatorial treatments incorporating small molecule inhibitors of OXPHOS. These studies should provide molecular basis to establish surrogate biomarkers that will facilitate stratification of the patients to identify potential responders to combinatorial approaches using OXPHOS inhibitors and other therapeutics.

4.3 CONCLUSION

Metabolic plasticity is an emerging feature of cancer cells that plays a prominent role in tumor dissemination and therapeutic responses. This thesis highlights previously unappreciated mechanisms underpinning metabolic flexibility of cancer cells in the context of energy stress caused by mitochondrial dysfunction due to abrogation of mitochondrial complex I or IV and/or nutrient deprivation. These findings provide initial insights into cellular networks underlying the metabolic adaptation of cancer cells to energy stress while exposing potential metabolic vulnerabilities. To this end, results reported in this thesis in concert with similar efforts in our laboratory and across the globe are likely to critically improve understanding of the molecular underpinnings of metabolic flexibility of cancer cells. In long-term, these efforts are anticipated to provide molecular bases for more effective approaches to identify and target metabolic vulnerabilities of neoplasia in the clinic.

4.4 LIMITATIONS AND FUTURE PERSPECTIVES

Notably, studies in chapters 2 and 3 were carried out in cell culture models that may not reflect complexity of organismal physiology and its impact on metabolic rewiring of neoplasia. Importantly, cell culture models are thought to insufficiently mimic rapid changes in nutrients, oxygen and hormonal milieu of cancer cells that occur in vivo. Tumor microenvironment affects metabolism of cancer cells. Reciprocally, cancer cells alter the metabolic composition of the extracellular milieu around them which often facilitate their progression (3). Additionally, metabolites produced by the host microbiota may promote or impede tumor initiation and progression (137). Taken together, studying the metabolic alterations of cancer cells warrants the use of in vivo models to fully capture the complexity of cancer metabolism. To this end, future studies using appropriate animal models are required to establish whether phenomena observed in chapters 2 and 3 also occur in vivo. Moreover, in chapter 3, we only monitored steady-state metabolite levels which are not indicative of flux through key metabolic pathways. This limitation will be addressed in future by performing stable isotope tracing analysis, which will allow us to monitor flux through key metabolic pathways upon abrogation of mitochondrial function and/or glutamine deprivation in CRC vs. non-transformed colon epithelial cells. Furthermore, the incorporation of systems biology approaches is required to elucidate the changes to gene expression and signaling pathways which underlie the metabolic adaptability of cancer cells to energy stress. These approaches will help us establish deeper insights into the mechanism underlying metabolic plasticity of cancer cells, which was an overarching objective of this thesis.

4.5 REFERENCES

- 1. Warburg O. The Metabolism of Carcinoma Cells. The Journal of Cancer Research. 1925;9(1):148.
- 2. Hanahan D, Weinberg RA. Hallmarks of cancer: the next generation. Cell. 2011;144(5):646-74.
- 3. Pavlova NN, Thompson CB. The Emerging Hallmarks of Cancer Metabolism. Cell Metab. 2016;23(1):27-47.
- 4. Vander Heiden MG, Cantley LC, Thompson CB. Understanding the Warburg effect: the metabolic requirements of cell proliferation. Science. 2009;324(5930):1029-33.
- 5. Palm W. Metabolic plasticity allows cancer cells to thrive under nutrient starvation. Proceedings of the National Academy of Sciences. 2021;118(14):e2102057118.
- 6. Xiao W, Wang RS, Handy DE, Loscalzo J. NAD(H) and NADP(H) Redox Couples and Cellular Energy Metabolism. Antioxid Redox Signal. 2018;28(3):251-72.
- 7. Lehuede C, Dupuy F, Rabinovitch R, Jones RG, Siegel PM. Metabolic Plasticity as a Determinant of Tumor Growth and Metastasis. Cancer Res. 2016;76(18):5201-8.
- 8. Martínez-Reyes I, Diebold Lauren P, Kong H, Schieber M, Huang H, Hensley Christopher T, et al. TCA Cycle and Mitochondrial Membrane Potential Are Necessary for Diverse Biological Functions. Molecular Cell. 2016;61(2):199-209.
- 9. Fendt SM, Frezza C, Erez A. Targeting Metabolic Plasticity and Flexibility Dynamics for Cancer Therapy. Cancer Discov. 2020;10(12):1797-807.
- 10. Kim J, DeBerardinis RJ. Mechanisms and Implications of Metabolic Heterogeneity in Cancer. Cell Metab. 2019;30(3):434-46.

- 11. Faubert B, Solmonson A, DeBerardinis RJ. Metabolic reprogramming and cancer progression. Science. 2020;368(6487).
- 12. Luo C, Lim JH, Lee Y, Granter SR, Thomas A, Vazquez F, et al. A PGC1α-mediated transcriptional axis suppresses melanoma metastasis. Nature. 2016;537(7620):422-6.
- 13. Mayers JR, Torrence ME, Danai LV, Papagiannakopoulos T, Davidson SM, Bauer MR, et al. Tissue of origin dictates branched-chain amino acid metabolism in mutant Kras-driven cancers. Science. 2016;353(6304):1161-5.
- 14. Bragazzi NL, Sellami M. Chapter Three Cancer bioenergetics as emerging holistic cancer theory: the role of metabolic fluxes and transport proteins involved in metabolic pathways in the pathogenesis of malignancies. State-of-the-art and future prospects. In: Donev R, editor. Advances in Protein Chemistry and Structural Biology. 123: Academic Press; 2021. p. 27-47.
- 15. Martin PL, Yin JJ, Seng V, Casey O, Corey E, Morrissey C, et al. Androgen deprivation leads to increased carbohydrate metabolism and hexokinase 2-mediated survival in Pten/Tp53-deficient prostate cancer. Oncogene. 2017;36(4):525-33.
- 16. Matoba S, Kang JG, Patino WD, Wragg A, Boehm M, Gavrilova O, et al. p53 regulates mitochondrial respiration. Science. 2006;312(5780):1650-3.
- 17. Kimmelman AC. Metabolic Dependencies in RAS-Driven Cancers. Clinical cancer research: an official journal of the American Association for Cancer Research. 2015;21(8):1828-34.
- 18. Satoh K, Yachida S, Sugimoto M, Oshima M, Nakagawa T, Akamoto S, et al. Global metabolic reprogramming of colorectal cancer occurs at adenoma stage and is induced by MYC. Proceedings of the National Academy of Sciences. 2017;114(37):E7697-E706.

- 19. Hao Y, Samuels Y, Li Q, Krokowski D, Guan B-J, Wang C, et al. Oncogenic PIK3CA mutations reprogram glutamine metabolism in colorectal cancer. Nature Communications. 2016;7(1):11971.
- 20. Saxton RA, Sabatini DM. mTOR Signaling in Growth, Metabolism, and Disease. Cell. 2017;168(6):960-76.
- 21. Mossmann D, Park S, Hall MN. mTOR signalling and cellular metabolism are mutual determinants in cancer. Nature Reviews Cancer. 2018;18(12):744-57.
- 22. Szwed A, Kim E, Jacinto E. Regulation and metabolic functions of mTORC1 and mTORC2. Physiological Reviews. 2021;101(3):1371-426.
- 23. Uchenunu O, Pollak M, Topisirovic I, Hulea L. Oncogenic kinases and perturbations in protein synthesis machinery and energetics in neoplasia. J Mol Endocrinol. 2019;62(2):R83-r103.
- 24. Hulea L, Gravel SP, Morita M, Cargnello M, Uchenunu O, Im YK, et al. Translational and HIF-1α-Dependent Metabolic Reprogramming Underpin Metabolic Plasticity and Responses to Kinase Inhibitors and Biguanides. Cell Metab. 2018;28(6):817-32.e8.
- 25. Morita M, Gravel SP, Chénard V, Sikström K, Zheng L, Alain T, et al. mTORC1 controls mitochondrial activity and biogenesis through 4E-BP-dependent translational regulation. Cell Metab. 2013;18(5):698-711.
- 26. Ye J, Kumanova M, Hart LS, Sloane K, Zhang H, De Panis DN, et al. The GCN2-ATF4 pathway is critical for tumour cell survival and proliferation in response to nutrient deprivation. EMBO J. 2010;29(12):2082-96.
- 27. Gold LT, Masson GR. GCN2: roles in tumour development and progression. Biochem Soc Trans. 2022;50(2):737-45.

- 28. Harding HP, Zhang Y, Zeng H, Novoa I, Lu PD, Calfon M, et al. An integrated stress response regulates amino acid metabolism and resistance to oxidative stress. Mol Cell. 2003;11(3):619-33.
- 29. Ben-Sahra I, Hoxhaj G, Ricoult SJH, Asara JM, Manning BD. mTORC1 induces purine synthesis through control of the mitochondrial tetrahydrofolate cycle. Science (New York, NY). 2016;351(6274):728-33.
- 30. Gandin V, Masvidal L, Cargnello M, Gyenis L, McLaughlan S, Cai Y, et al. mTORC1 and CK2 coordinate ternary and eIF4F complex assembly. Nature communications. 2016;7:11127-.
- 31. Mounir Z, Krishnamoorthy JL, Wang S, Papadopoulou B, Campbell S, Muller WJ, et al. Akt determines cell fate through inhibition of the PERK-eIF2α phosphorylation pathway. Science signaling. 2011;4(192):ra62-ra.
- 32. Liu J, Zhang C, Hu W, Feng Z. Tumor suppressor p53 and metabolism. J Mol Cell Biol. 2019;11(4):284-92.
- 33. Stine ZE, Walton ZE, Altman BJ, Hsieh AL, Dang CV. MYC, Metabolism, and Cancer. Cancer Discov. 2015;5(10):1024-39.
- 34. Bouthelier A, Aragonés J. Role of the HIF oxygen sensing pathway in cell defense and proliferation through the control of amino acid metabolism. Biochim Biophys Acta Mol Cell Res. 2020;1867(9):118733.
- 35. Dejure FR, Eilers M. MYC and tumor metabolism: chicken and egg. EMBO J. 2017;36(23):3409-20.
- 36. Dong Y, Tu R, Liu H, Qing G. Regulation of cancer cell metabolism: oncogenic MYC in the driver's seat. Signal Transduct Target Ther. 2020;5(1):124.

- 37. Martínez-Reyes I, Chandel NS. Mitochondrial TCA cycle metabolites control physiology and disease. Nature Communications. 2020;11(1):102.
- 38. Kim SG, Hoffman GR, Poulogiannis G, Buel GR, Jang YJ, Lee KW, et al. Metabolic stress controls mTORC1 lysosomal localization and dimerization by regulating the TTT-RUVBL1/2 complex. Mol Cell. 2013;49(1):172-85.
- 39. Sullivan LB, Gui DY, Hosios AM, Bush LN, Freinkman E, Vander Heiden MG. Supporting aspartate biosynthesis is an essential function of respiration in proliferating cells. Cell. 2015;162(3):552-63.
- 40. Birsoy K, Wang T, Chen WW, Freinkman E, Abu-Remaileh M, Sabatini DM. An essential role of the mitochondrial electron transport chain in cell proliferation is to enable aspartate synthesis. Cell. 2015;162(3):540-51.
- 41. Chen Q, Kirk K, Shurubor YI, Zhao D, Arreguin AJ, Shahi I, et al. Rewiring of Glutamine Metabolism Is a Bioenergetic Adaptation of Human Cells with Mitochondrial DNA Mutations. Cell Metab. 2018;27(5):1007-25.e5.
- 42. Fendt SM, Bell EL, Keibler MA, Davidson SM, Wirth GJ, Fiske B, et al. Metformin decreases glucose oxidation and increases the dependency of prostate cancer cells on reductive glutamine metabolism. Cancer Res. 2013;73(14):4429-38.
- 43. Jiang L, Shestov AA, Swain P, Yang C, Parker SJ, Wang QA, et al. Reductive carboxylation supports redox homeostasis during anchorage-independent growth. Nature. 2016;532(7598):255-8.
- 44. Metallo CM, Gameiro PA, Bell EL, Mattaini KR, Yang J, Hiller K, et al. Reductive glutamine metabolism by IDH1 mediates lipogenesis under hypoxia. Nature. 2012;481(7381):380-

4.

- 45. Sun RC, Denko NC. Hypoxic regulation of glutamine metabolism through HIF1 and SIAH2 supports lipid synthesis that is necessary for tumor growth. Cell Metab. 2014;19(2):285-92.
- 46. Fendt S-M, Bell EL, Keibler MA, Olenchock BA, Mayers JR, Wasylenko TM, et al. Reductive glutamine metabolism is a function of the α -ketoglutarate to citrate ratio in cells. Nature Communications. 2013;4(1):2236.
- 47. Eagle H. Nutrition needs of mammalian cells in tissue culture. Science. 1955;122(3168):501-14.
- 48. Cruzat V, Macedo Rogero M, Noel Keane K, Curi R, Newsholme P. Glutamine: Metabolism and Immune Function, Supplementation and Clinical Translation. Nutrients. 2018;10(11):1564.
- 49. Mohamed A, Deng X, Khuri FR, Owonikoko TK. Altered glutamine metabolism and therapeutic opportunities for lung cancer. Clin Lung Cancer. 2014;15(1):7-15.
- 50. Márquez J, Alonso FJ, Matés JM, Segura JA, Martín-Rufián M, Campos-Sandoval JA. Glutamine Addiction In Gliomas. Neurochemical Research. 2017;42(6):1735-46.
- 51. Lacey JM, Wilmore DW. Is glutamine a conditionally essential amino acid? Nutr Rev. 1990;48(8):297-309.
- 52. Hassanein M, Qian J, Hoeksema MD, Wang J, Jacobovitz M, Ji X, et al. Targeting SLC1a5-mediated glutamine dependence in non-small cell lung cancer. Int J Cancer. 2015;137(7):1587-97.
- 53. van Geldermalsen M, Wang Q, Nagarajah R, Marshall AD, Thoeng A, Gao D, et al. ASCT2/SLC1A5 controls glutamine uptake and tumour growth in triple-negative basal-like breast cancer. Oncogene. 2016;35(24):3201-8.

- 54. Schulte ML, Fu A, Zhao P, Li J, Geng L, Smith ST, et al. Pharmacological blockade of ASCT2-dependent glutamine transport leads to antitumor efficacy in preclinical models. Nature medicine. 2018;24(2):194-202.
- 55. Bröer A, Fairweather S, Bröer S. Disruption of Amino Acid Homeostasis by Novel ASCT2 Inhibitors Involves Multiple Targets. Front Pharmacol. 2018;9:785.
- 56. Chiu M, Sabino C, Taurino G, Bianchi MG, Andreoli R, Giuliani N, et al. GPNA inhibits the sodium-independent transport system L for neutral amino acids. Amino Acids. 2017;49(8):1365-72.
- 57. Bröer A, Rahimi F, Bröer S. Deletion of Amino Acid Transporter ASCT2 (SLC1A5) Reveals an Essential Role for Transporters SNAT1 (SLC38A1) and SNAT2 (SLC38A2) to Sustain Glutaminolysis in Cancer Cells. J Biol Chem. 2016;291(25):13194-205.
- 58. Corti A, Dominici S, Piaggi S, Belcastro E, Chiu M, Taurino G, et al. γ-Glutamyltransferase enzyme activity of cancer cells modulates L-γ-glutamyl-p-nitroanilide (GPNA) cytotoxicity. Sci Rep. 2019;9(1):891.
- 59. Kandasamy P, Gyimesi G, Kanai Y, Hediger MA. Amino acid transporters revisited: New views in health and disease. Trends Biochem Sci. 2018;43(10):752-89.
- 60. Fuchs BC, Bode BP. Amino acid transporters ASCT2 and LAT1 in cancer: partners in crime? Semin Cancer Biol. 2005;15(4):254-66.
- 61. Nicklin P, Bergman P, Zhang B, Triantafellow E, Wang H, Nyfeler B, et al. Bidirectional transport of amino acids regulates mTOR and autophagy. Cell. 2009;136(3):521-34.
- 62. Bröer A, Fairweather S, Bröer S. Disruption of Amino Acid Homeostasis by Novel ASCT2 Inhibitors Involves Multiple Targets. Frontiers in pharmacology. 2018;9:785-.

- 63. Bröer A, Gauthier-Coles G, Rahimi F, van Geldermalsen M, Dorsch D, Wegener A, et al. Ablation of the ASCT2 (SLC1A5) gene encoding a neutral amino acid transporter reveals transporter plasticity and redundancy in cancer cells. J Biol Chem. 2019;294(11):4012-26.
- 64. Bothwell PJ, Kron CD, Wittke EF, Czerniak BN, Bode BP. Targeted Suppression and Knockout of ASCT2 or LAT1 in Epithelial and Mesenchymal Human Liver Cancer Cells Fail to Inhibit Growth. International Journal of Molecular Sciences. 2018;19(7):2093.
- 65. Cormerais Y, Massard PA, Vucetic M, Giuliano S, Tambutté E, Durivault J, et al. The glutamine transporter ASCT2 (SLC1A5) promotes tumor growth independently of the amino acid transporter LAT1 (SLC7A5). J Biol Chem. 2018;293(8):2877-87.
- 66. Matés JM, Campos-Sandoval JA, de los Santos-Jiménez J, Márquez J. Glutaminases regulate glutathione and oxidative stress in cancer. Archives of Toxicology. 2020;94(8):2603-23.
- 67. Yoo HC, Yu YC, Sung Y, Han JM. Glutamine reliance in cell metabolism. Exp Mol Med. 2020;52(9):1496-516.
- 68. Yang L, Venneti S, Nagrath D. Glutaminolysis: A Hallmark of Cancer Metabolism. Annual Review of Biomedical Engineering. 2017;19(1):163-94.
- 69. Shen Y-A, Chen C-L, Huang Y-H, Evans EE, Cheng C-C, Chuang Y-J, et al. Inhibition of glutaminolysis in combination with other therapies to improve cancer treatment. Current Opinion in Chemical Biology. 2021;62:64-81.
- 70. Robinson Mary M, Mcbryant Steven J, Tsukamoto T, Rojas C, Ferraris Dana V, Hamilton Sean K, et al. Novel mechanism of inhibition of rat kidney-type glutaminase by bis-2-(5-phenylacetamido-1,2,4-thiadiazol-2-yl)ethyl sulfide (BPTES). Biochemical Journal. 2007;406(3):407-14.

- 71. Wang J-B, Erickson JW, Fuji R, Ramachandran S, Gao P, Dinavahi R, et al. Targeting Mitochondrial Glutaminase Activity Inhibits Oncogenic Transformation. Cancer Cell. 2010;18(3):207-19.
- 72. Lukey MJ, Cluntun AA, Katt WP, Lin M-cJ, Druso JE, Ramachandran S, et al. Liver-Type Glutaminase GLS2 Is a Druggable Metabolic Node in Luminal-Subtype Breast Cancer. Cell Reports. 2019;29(1):76-88.e7.
- 73. Gross MI, Demo SD, Dennison JB, Chen L, Chernov-Rogan T, Goyal B, et al. Antitumor activity of the glutaminase inhibitor CB-839 in triple-negative breast cancer. Mol Cancer Ther. 2014;13(4):890-901.
- 74. Lampa M, Arlt H, He T, Ospina B, Reeves J, Zhang B, et al. Glutaminase is essential for the growth of triple-negative breast cancer cells with a deregulated glutamine metabolism pathway and its suppression synergizes with mTOR inhibition. PLOS ONE. 2017;12(9):e0185092.
- 75. Hu W, Zhang C, Wu R, Sun Y, Levine A, Feng Z. Glutaminase 2, a novel p53 target gene regulating energy metabolism and antioxidant function. Proc Natl Acad Sci U S A. 2010;107(16):7455-60.
- 76. Matés JM, Campos-Sandoval JA, Márquez J. Glutaminase isoenzymes in the metabolic therapy of cancer. Biochim Biophys Acta Rev Cancer. 2018;1870(2):158-64.
- 77. Xiao D, Ren P, Su H, Yue M, Xiu R, Hu Y, et al. Myc promotes glutaminolysis in human neuroblastoma through direct activation of glutaminase 2. Oncotarget. 2015;6(38):40655-66.
- 78. Duvall B, Zimmermann SC, Gao R-D, Thomas AG, Kalčic F, Veeravalli V, et al. Allosteric kidney-type glutaminase (GLS) inhibitors with a mercaptoethyl linker. Bioorganic & Medicinal Chemistry. 2020;28(20):115698.

- 79. Varghese S, Pramanik S, Williams LJ, Hodges HR, Hudgens CW, Fischer GM, et al. The Glutaminase Inhibitor CB-839 (Telaglenastat) Enhances the Antimelanoma Activity of T-Cell-Mediated Immunotherapies. Mol Cancer Ther. 2021;20(3):500-11.
- 80. Wang Z, Liu F, Fan N, Zhou C, Li D, Macvicar T, et al. Targeting Glutaminolysis: New Perspectives to Understand Cancer Development and Novel Strategies for Potential Target Therapies. Front Oncol. 2020;10:589508.
- 81. Desbats MA, Giacomini I, Prayer-Galetti T, Montopoli M. Metabolic Plasticity in Chemotherapy Resistance. Front Oncol. 2020;10:281.
- 82. Liu P, Cheng H, Roberts TM, Zhao JJ. Targeting the phosphoinositide 3-kinase pathway in cancer. Nature Reviews Drug Discovery. 2009;8(8):627-44.
- 83. Tanaka K, Sasayama T, Irino Y, Takata K, Nagashima H, Satoh N, et al. Compensatory glutamine metabolism promotes glioblastoma resistance to mTOR inhibitor treatment. J Clin Invest. 2015;125(4):1591-602.
- 84. Shen Y-A, Hong J, Asaka R, Asaka S, Hsu F-C, Suryo Rahmanto Y, et al. Inhibition of the MYC-Regulated Glutaminase Metabolic Axis Is an Effective Synthetic Lethal Approach for Treating Chemoresistant Ovarian Cancers. Cancer Research. 2020;80(20):4514-26.
- 85. Zong W-X, Ditsworth D, Bauer DE, Wang Z-Q, Thompson CB. Alkylating DNA damage stimulates a regulated form of necrotic cell death. Genes & development. 2004;18(11):1272-82.
- 86. Affar EB, Shah RG, Dallaire A-K, Castonguay V, Shah GM. Role of poly(ADP-ribose) polymerase in rapid intracellular acidification induced by alkylating DNA damage. Proceedings of the National Academy of Sciences of the United States of America. 2002;99(1):245-50.

- 87. Tan AS, Baty JW, Dong LF, Bezawork-Geleta A, Endaya B, Goodwin J, et al. Mitochondrial genome acquisition restores respiratory function and tumorigenic potential of cancer cells without mitochondrial DNA. Cell Metab. 2015;21(1):81-94.
- 88. Andrzejewski S, Gravel S-P, Pollak M, St-Pierre J. Metformin directly acts on mitochondria to alter cellular bioenergetics. Cancer Metab. 2014;2(1):12.
- 89. Zhao H, Swanson KD, Zheng B. Therapeutic Repurposing of Biguanides in Cancer. Trends Cancer. 2021;7(8):714-30.
- 90. Pollak M. Metformin and other biguanides in oncology: advancing the research agenda. Cancer Prev Res (Phila). 2010;3(9):1060-5.
- 91. Liu X, Chhipa RR, Pooya S, Wortman M, Yachyshin S, Chow LM, et al. Discrete mechanisms of mTOR and cell cycle regulation by AMPK agonists independent of AMPK. Proc Natl Acad Sci U S A. 2014;111(4):E435-44.
- 92. Birsoy K, Possemato R, Lorbeer FK, Bayraktar EC, Thiru P, Yucel B, et al. Metabolic determinants of cancer cell sensitivity to glucose limitation and biguanides. Nature. 2014;508(7494):108-12.
- 93. Owen MR, Doran E, Halestrap AP. Evidence that metformin exerts its anti-diabetic effects through inhibition of complex 1 of the mitochondrial respiratory chain. Biochem J. 2000;348 Pt 3(Pt 3):607-14.
- 94. Wheaton WW, Weinberg SE, Hamanaka RB, Soberanes S, Sullivan LB, Anso E, et al. Metformin inhibits mitochondrial complex I of cancer cells to reduce tumorigenesis. Elife. 2014;3:e02242.
- 95. He L, Wondisford Fredric E. Metformin Action: Concentrations Matter. Cell Metabolism. 2015;21(2):159-62.

- 96. Di Magno L, Manni S, Di Pastena F, Coni S, Macone A, Cairoli S, et al. Phenformin Inhibits Hedgehog-Dependent Tumor Growth through a Complex I-Independent Redox/Corepressor Module. Cell Rep. 2020;30(6):1735-52.e7.
- 97. Goodwin PJ, Ennis M, Pritchard KI, Trudeau ME, Koo J, Madarnas Y, et al. Fasting insulin and outcome in early-stage breast cancer: results of a prospective cohort study. Journal of clinical oncology. 2002;20(1):42-51.
- 98. Giovannucci E. Metabolic syndrome, hyperinsulinemia, and colon cancer: a review. The American journal of clinical nutrition. 2007;86(3):836S-42S.
- 99. Raimondi S, Maisonneuve P, Lowenfels AB. Epidemiology of pancreatic cancer: an overview. Nature reviews Gastroenterology & hepatology. 2009;6(12):699-708.
- 100. Strickler HD, Wylie-Rosett J, Rohan T, Hoover DR, Smoller S, Burk RD, et al. The relation of type 2 diabetes and cancer. Diabetes technology & therapeutics. 2001;3(2):263-74.
- 101. Vigneri P, Frasca F, Sciacca L, Frittitta L, Vigneri R. Obesity and cancer. Nutrition, Metabolism and Cardiovascular Diseases. 2006;16(1):1-7.
- 102. Belfiore A, Frasca F, Pandini G, Sciacca L, Vigneri R. Insulin Receptor Isoforms and Insulin Receptor/Insulin-Like Growth Factor Receptor Hybrids in Physiology and Disease. Endocrine Reviews. 2009;30(6):586-623.
- 103. Wolf I, Sadetzki S, Catane R, Karasik A, Kaufman B. Diabetes mellitus and breast cancer. The Lancet Oncology. 2005;6(2):103-11.
- 104. Pollak MN, Schernhammer ES, Hankinson SE. Insulin-like growth factors and neoplasia. Nature Reviews Cancer. 2004;4(7):505-18.
- 105. Cusi K, DeFronzo R. Metformin: a review of its metabolic effects. Diabetes Reviews. 1998;6(2):89-131.

- 106. Goodwin PJ, Dowling RJO, Ennis M, Chen BE, Parulekar WR, Shepherd LE, et al. Effect of metformin versus placebo on metabolic factors in the MA.32 randomized breast cancer trial. npj Breast Cancer. 2021;7(1):74.
- 107. Niraula S, Dowling RJO, Ennis M, Chang MC, Done SJ, Hood N, et al. Metformin in early breast cancer: a prospective window of opportunity neoadjuvant study. Breast Cancer Research and Treatment. 2012;135(3):821-30.
- 108. Kasznicki J, Sliwinska A, Drzewoski J. Metformin in cancer prevention and therapy. Ann Transl Med. 2014;2(6):57.
- 109. Cetin M, Sahin S. Microparticulate and nanoparticulate drug delivery systems for metformin hydrochloride. Drug Delivery. 2016;23(8):2796-805.
- 110. Rusanov DA, Zou J, Babak MV. Biological Properties of Transition Metal Complexes with Metformin and Its Analogues. Pharmaceuticals. 2022;15(4):453.
- 111. Janzer A, German NJ, Gonzalez-Herrera KN, Asara JM, Haigis MC, Struhl K. Metformin and phenformin deplete tricarboxylic acid cycle and glycolytic intermediates during cell transformation and NTPs in cancer stem cells. Proceedings of the National Academy of Sciences of the United States of America. 2014;111(29):10574-9.
- 112. García Rubiño ME, Carrillo E, Ruiz Alcalá G, Domínguez-Martín A, J AM, Boulaiz H. Phenformin as an Anticancer Agent: Challenges and Prospects. Int J Mol Sci. 2019;20(13).
- 113. Ottaviano LF, Li X, Murray M, Frye JT, Lung BE, Zhang YY, et al. Type 2 diabetes impacts colorectal adenoma detection in screening colonoscopy. Sci Rep. 2020;10(1):7793-.
- 114. Hou Y-C, Hu Q, Huang J, Fang J-Y, Xiong H. Metformin therapy and the risk of colorectal adenoma in patients with type 2 diabetes: A meta-analysis. Oncotarget. 2017;8(5):8843-53.

- 115. Pollak M. Targeting oxidative phosphorylation: why, when, and how. Cancer Cell. 2013;23(3):263-4.
- 116. Wang Z, Lai ST, Xie L, Zhao JD, Ma NY, Zhu J, et al. Metformin is associated with reduced risk of pancreatic cancer in patients with type 2 diabetes mellitus: a systematic review and meta-analysis. Diabetes Res Clin Pract. 2014;106(1):19-26.
- 117. Col NF, Ochs L, Springmann V, Aragaki AK, Chlebowski RT. Metformin and breast cancer risk: a meta-analysis and critical literature review. Breast Cancer Res Treat. 2012;135(3):639-46.
- 118. Zhang H, Gao C, Fang L, Zhao HC, Yao SK. Metformin and reduced risk of hepatocellular carcinoma in diabetic patients: a meta-analysis. Scand J Gastroenterol. 2013;48(1):78-87.
- 119. Sakai T, Matsuo Y, Okuda K, Hirota K, Tsuji M, Hirayama T, et al. Development of antitumor biguanides targeting energy metabolism and stress responses in the tumor microenvironment. Sci Rep. 2021;11(1):4852.
- 120. Sanchez M, Gastaldi L, Remedi M, Cáceres A, Landa C. Rotenone-induced toxicity is mediated by Rho-GTPases in hippocampal neurons. Toxicol Sci. 2008;104(2):352-61.
- 121. Ellinghaus P, Heisler I, Unterschemmann K, Haerter M, Beck H, Greschat S, et al. BAY 87-2243, a highly potent and selective inhibitor of hypoxia-induced gene activation has antitumor activities by inhibition of mitochondrial complex I. Cancer Med. 2013;2(5):611-24.
- 122. Molina JR, Sun Y, Protopopova M, Gera S, Bandi M, Bristow C, et al. An inhibitor of oxidative phosphorylation exploits cancer vulnerability. Nat Med. 2018;24(7):1036-46.
- 123. Yap TA, Rodon Ahnert J, Piha-Paul SA, Fu S, Janku F, Karp DD, et al. Phase I trial of IACS-010759 (IACS), a potent, selective inhibitor of complex I of the mitochondrial electron

- transport chain, in patients (pts) with advanced solid tumors. American Society of Clinical Oncology; 2019.
- 124. Gravel SP, Hulea L, Toban N, Birman E, Blouin MJ, Zakikhani M, et al. Serine deprivation enhances antineoplastic activity of biguanides. Cancer Res. 2014;74(24):7521-33.
- 125. Ben Sahra I, Laurent K, Giuliano S, Larbret F, Ponzio G, Gounon P, et al. Targeting cancer cell metabolism: the combination of metformin and 2-deoxyglucose induces p53-dependent apoptosis in prostate cancer cells. Cancer Res. 2010;70(6):2465-75.
- 126. Pollak M. Potential applications for biguanides in oncology. The Journal of Clinical Investigation. 2013;123(9):3693-700.
- 127. Yakisich JS, Azad N, Kaushik V, Iyer AKV. The Biguanides Metformin and Buformin in Combination with 2-Deoxy-glucose or WZB-117 Inhibit the Viability of Highly Resistant Human Lung Cancer Cells. Stem Cells International. 2019;2019:6254269.
- 128. Bizjak M, Malavašič P, Dolinar K, Pohar J, Pirkmajer S, Pavlin M. Combined treatment with Metformin and 2-deoxy glucose induces detachment of viable MDA-MB-231 breast cancer cells in vitro. Sci Rep. 2017;7(1):1761.
- 129. Makinoshima H, Takita M, Matsumoto S, Yagishita A, Owada S, Esumi H, et al. Epidermal growth factor receptor (EGFR) signaling regulates global metabolic pathways in EGFR-mutated lung adenocarcinoma. J Biol Chem. 2014;289(30):20813-23.
- 130. Zhao Y, Liu H, Liu Z, Ding Y, Ledoux SP, Wilson GL, et al. Overcoming trastuzumab resistance in breast cancer by targeting dysregulated glucose metabolism. Cancer Res. 2011;71(13):4585-97.

- 131. Komurov K, Tseng JT, Muller M, Seviour EG, Moss TJ, Yang L, et al. The glucose-deprivation network counteracts lapatinib-induced toxicity in resistant ErbB2-positive breast cancer cells. Mol Syst Biol. 2012;8:596.
- 132. Gottschalk S, Anderson N, Hainz C, Eckhardt SG, Serkova NJ. Imatinib (STI571)-mediated changes in glucose metabolism in human leukemia BCR-ABL-positive cells. Clin Cancer Res. 2004;10(19):6661-8.
- 133. Haq R, Shoag J, Andreu-Perez P, Yokoyama S, Edelman H, Rowe GC, et al. Oncogenic BRAF regulates oxidative metabolism via PGC1α and MITF. Cancer cell. 2013;23(3):302-15.
- 134. Delgado-Goni T, Miniotis MF, Wantuch S, Parkes HG, Marais R, Workman P, et al. The BRAF Inhibitor Vemurafenib Activates Mitochondrial Metabolism and Inhibits Hyperpolarized Pyruvate-Lactate Exchange in BRAF-Mutant Human Melanoma Cells. Molecular cancer therapeutics. 2016;15(12):2987-99.
- 135. Baenke F, Chaneton B, Smith M, Van Den Broek N, Hogan K, Tang H, et al. Resistance to BRAF inhibitors induces glutamine dependency in melanoma cells. Mol Oncol. 2016;10(1):73-84.
- 136. Parker SJ, Svensson RU, Divakaruni AS, Lefebvre AE, Murphy AN, Shaw RJ, et al. LKB1 promotes metabolic flexibility in response to energy stress. Metabolic Engineering. 2017;43:208-17.
- 137. Garrett WS. Cancer and the microbiota. Science. 2015;348(6230):80-6.

APPENDIX - OTHER WORKS

A.1 Contributions to understanding of the molecular mechanisms of metabolic dysregulation in cancer

In addition to contributing to improving the knowledge of the molecular underpinnings of cancer metabolism through my own projects (Chapters 2 and 3), I was extensively involved in collaborative work aiming to dissect the mechanisms of metabolic reprogramming in both normal and cancer cells. To this end, I provided critical experimental and intellectual inputs in studies wherein we set out to unravel the mechanisms of metabolic plasticity of cancer cells (1-3). Moreover, we exploited potential avenues to target metabolic vulnerabilities of cancer cells and define mechanisms underlying the action of drugs targeting metabolic rewiring in neoplasia (3, 4). Collectively, these studies provide previously unappreciated insights into the mechanisms of metabolic plasticity of neoplasia. As mentioned in the introduction section, metabolic plasticity is a phenomenon whereby cancer cells instead of being addicted to one or few metabolic pathways can utilize a plethora of metabolites and/or nutrients via a variety of metabolic routes, while also being able to direct different metabolites and/or nutrients through the same metabolic pathway (5, 6). Metabolic plasticity thus allows cancer cells to rapidly alternate between metabolic pathways in order to adapt to a variety of stressors including therapeutic insults (5). In addition, our studies provided hitherto unappreciated mechanistic insights into anti-neoplastic action of the combinations of inhibitors of oncogenic kinases and biguanides as well as the sodium-glucose cotransporter-2 (SGLT2) inhibitors (3, 4). In large part, these results were summarized in our review article (7), while the major findings of each of these studies are outlined below.

A.1.1 Identification of hydride ion transfer complex that allows cells to overcome senescence and drives tumorigenesis.

Mitochondrial dysfunction, typically accompanied by decreased ATP levels and NAD+/NADH ratio, and increased reactive oxygen species (ROS) production is thought to play a major role in senescence (8, 9). Senescence constitutes a major tumor suppressive mechanism (10). In addition to its well established function as a transcription factor (11), signal transducer and activator of transcription 3 (STAT3) has also been reported to function in the mitochondria (12). Indeed, it has been shown that the abrogation of STAT3 function results in elevated ROS production and dysfunctional mitochondria in hematopoietic stem cells and hematopoietic progenitor cells (13). This leads to premature aging of blood cells (13). Moreover, it was suggested that oncogenic RAS-induced malignant transformation of primary cells requires STAT3-dependent regulation of mitochondrial functions (14). Altogether, these prior findings suggest a potential role of STAT3 in supporting mitochondrial activity in order to bypass senescence and drive oncogenesis.

My work with Igelmann et al. employed STAT3-deficiency and other models of cellular senescence to highlight the mechanisms that allow cells to reprogram their metabolism and adapt to mitochondrial dysfunction-associated senescence (1). Specifically, mitochondrial dysfunction-associated senescence was induced by depleting STAT3 in normal human fibroblasts (IMR90) (1). As expected, STAT3 depletion resulted in a reduction in cell proliferation and increased senescence-associated- β -galactosidase (SA- β -Gal) activity (1). This was accompanied by dramatic changes in the appearance of mitochondria including the disruption of cristae (1). STAT3 depletion not only disrupted the structural properties of the mitochondria but also suppressed their function (1). This was illustrated by elevated ROS levels, decreased NAD+/NADH ratio and reduced

oxygen consumption relative to control scrambled shRNA infected cells (1). We next observed that abrogating *TP53* or *RB1* tumor suppressors, which enables IMR90 cells to overcome STAT3 depletion-induced senescence resulted in normalization of NAD+/NADH ratio (1). This led us to hypothesize that a decrease in NAD+/NADH ratio may play a major role in metabolic perturbations that are related to induction of senescence. To test this tenet, we restored the NAD+/NADH ratio in STAT3-depleted cells by applying exogenous electron acceptor duroquinone or by expressing *Lactobacillus brevis* (LbNOX) or yeast (NDI1) NADH-oxidases. Strikingly, these interventions allowed STAT3 depleted cells to circumvent senescence (1). Collectively, these findings indicate that decrease in NAD+/NADH ratio plays a major role in the induction of senescence.

Notably, reduced expression of STAT3 increases p53 levels thereby inducing senescence (1, 15). As noted above, we showed that decreasing the expression of p53 in cells depleted of STAT3 circumvented senescence and restored the NAD+/NADH ratio (1). These findings suggest that loss of p53 facilitates senescence bypass by reprogramming redox metabolism to elevate NAD+/NADH ratios in STAT3-depleted cells. To further investigate metabolic perturbations in this model (Fig. A.1.1A), I carried out stable isotope tracer analysis (SITA) using fully labelled ¹³C-glucose in control or *TP53*-deficient STAT3-depleted IMR90 cells [Fig. A.1.1B-D; from Fig. 1J-O in (1)]. This revealed that p53 loss-induced bypass of the senescence in STAT3-depleted IMR90 cells is associated with increased pyruvate carboxylase (PC), malic enzyme 1 (ME1) and malate dehydrogenase 1 (MDH1) activity which was evidenced by the increase in ¹³C-pyruvate, ¹³C-malate and ¹³C-aspartate levels. We next sought to establish the mechanism of increased PC, ME1 and MDH1 activity in response to abrogation of p53 function. To this end, our bioinformatics analysis revealed that *PC*, *ME1* and *MDH1* are transcriptionally repressed by p53 while these

enzymes were downregulated in senescent cells (1). Moreover, we made a surprising observation whereby in cells that bypassed senescence, a proportion of PC was localized in the cytoplasm, which was in stark contrast with almost exclusively mitochondrial localization of this enzyme in senescent or control cells (1). Furthermore, a series of biophysical approaches in conjunction with immunofluorescence, immunoprecipitation and proximity ligation assays revealed that cytoplasmic PC, forms a complex with MDH1 and ME1 (1). Of note, MDH1 and ME1 are cytoplasmic enzymes (16, 17). Thus far, we concluded that the bypass of STAT3-depletion induced senescence is underpinned by formation of PC/ME1/MDH1 complexes. I next employed SITA analysis to further characterize metabolic activity of the latter complex, which revealed that PC supplies MDH1 with oxaloacetate in order to generate malate and oxidize NADH [Fig. A.1.1E-H; from Fig. 4J-K and Fig. S6I-L in (1)]. Malate is then subsequently converted back to pyruvate by ME1 which results in generation of NADPH (Fig. A.1.1A). Based on its ability to transfer hydride ions from NADH to NADP+ we named PC/ME1/MDH1 complexes a hydride ion transfer complex (HTC). Importantly, HTC recycles NAD+ which is a major cofactor in metabolic pathways known to fuel cancer growth [e.g., glycolysis and aspartate synthesis (18, 19)], while producing NADPH that drives lipid synthesis and provides ROS protection via stimulating regeneration of reduced glutathione (1). Indeed, overexpression of HTC enzymes in STAT3depleted IMR90 cells averted senescence while restoring NAD+/NADH ratio, increasing NADPH levels and decreasing ROS (1). Based on this, we predicted that HTC may increase metabolic plasticity and thus play a major role in tumorigenesis. To test this, we overexpressed HTC enzymes in combination with oncogenic RAS and showed that this is sufficient to suppress senescence in mouse embryonic fibroblasts (MEF), drive tumorigenesis and support tumor growth in in mice (1).

These experiments revealed that HTC is not only sufficient to overcome oncogene-induced senescence, but that it can also induce malignant transformation and drive neoplastic growth.

The importance of each enzyme within the HTC is highlighted by the findings that depletion of any of the HTC components leads to senescence. Namely, reducing the expression of PC, MDH1 or ME1 was accompanied by decreased NAD+/NADH in both IMR90 STAT3/p53 depleted fibroblasts or prostate cancer PC-3 cells (1). I performed SITA analysis of PC/STAT3/p53 depleted IMR90 cells supplemented with 3,4-13C-glucose (Fig. A.1.1I-J; from Fig. 1P-Q in (1)). As expected, PC depletion reduced the carbon flux into the HTC cycle as illustrated by the decrease in 13C-malate and 13C-aspartate levels (Fig. A.1.1J). It is also worthwhile to note that in addition to STAT3-depletion and oncogene-induced senescence, overexpression of HTC enzymes in normal human fibroblasts delayed replicative senescence while increasing the NAD+/NADH ratio (1). Altogether, these findings demonstrate that HTC plays a central role in overcoming senescence and driving tumorigenesis and tumor growth.

Importantly, the role of HTC in overcoming mitochondrial dysfunction appears not to be limited only to the senescence. For instance, overexpression of HTC enzymes diminished antiproliferative effects of mitochondrial complex I inhibitor piercidin A in human fibroblast (1). Furthermore, HTC assembly is induced by hypoxia (1). This is consistent with previous observations that hypoxia averts senescence in fibroblasts expressing oncogenic RAS (1, 20). Overall, these findings suggest that HTC plays a major role in adaptation to repression of mitochondrial functions.

In conclusion, these findings highlight the significance of HTC in maintaining cellular redox homeostasis under conditions of mitochondrial dysfunction. Specifically, we identified a cytosolic HTC complex that is formed by PC, ME1 and MDH1 and plays a paramount role in the

rewiring of NAD+ metabolism which allows cells to overcome senescence and become cancerous. (1). Considering that HTC assembly is repressed by the tumor suppressors including TP53, RB1 and PTEN (1), our findings further support the growing body of work that metabolic rewiring plays a major role in tumorigenesis caused by the loss of tumor suppressors (21-26). Accordingly, we observed increased expression and colocalization of HTC enzymes in prostate cancer mouse models and patient specimens. Importantly, by increasing the levels of electron acceptors (i.e., NAD+) while providing reducing equivalents (i.e., NADPH), HTC increases metabolic flexibility of cancer cells. The central role of HTC in metabolic plasticity is further illustrated by its ability to induce rewiring of metabolome thus allowing the cells to adapt to complex I inhibition and hypoxia. Significantly, HTC catalyzes the metabolic cycle with no net-carbon loss. This is important inasmuch as it is thus likely that HTC does not affect cellular pools of pyruvate, oxaloacetate and malate which are important precursors of a number of biosynthetic processes that are crucial for proliferation and survival of cancer cells (27-29). Although this study highlights cytosolic PC, MDH1 and ME1 as key components of the HTC complex, it is plausible that HTC comprises additional interacting partners. Future studies are presently conducted to further confirm the role of HTC in establishing metabolic plasticity of cancer cells in particular in the context of metastatic spread of the disease and drug resistance.

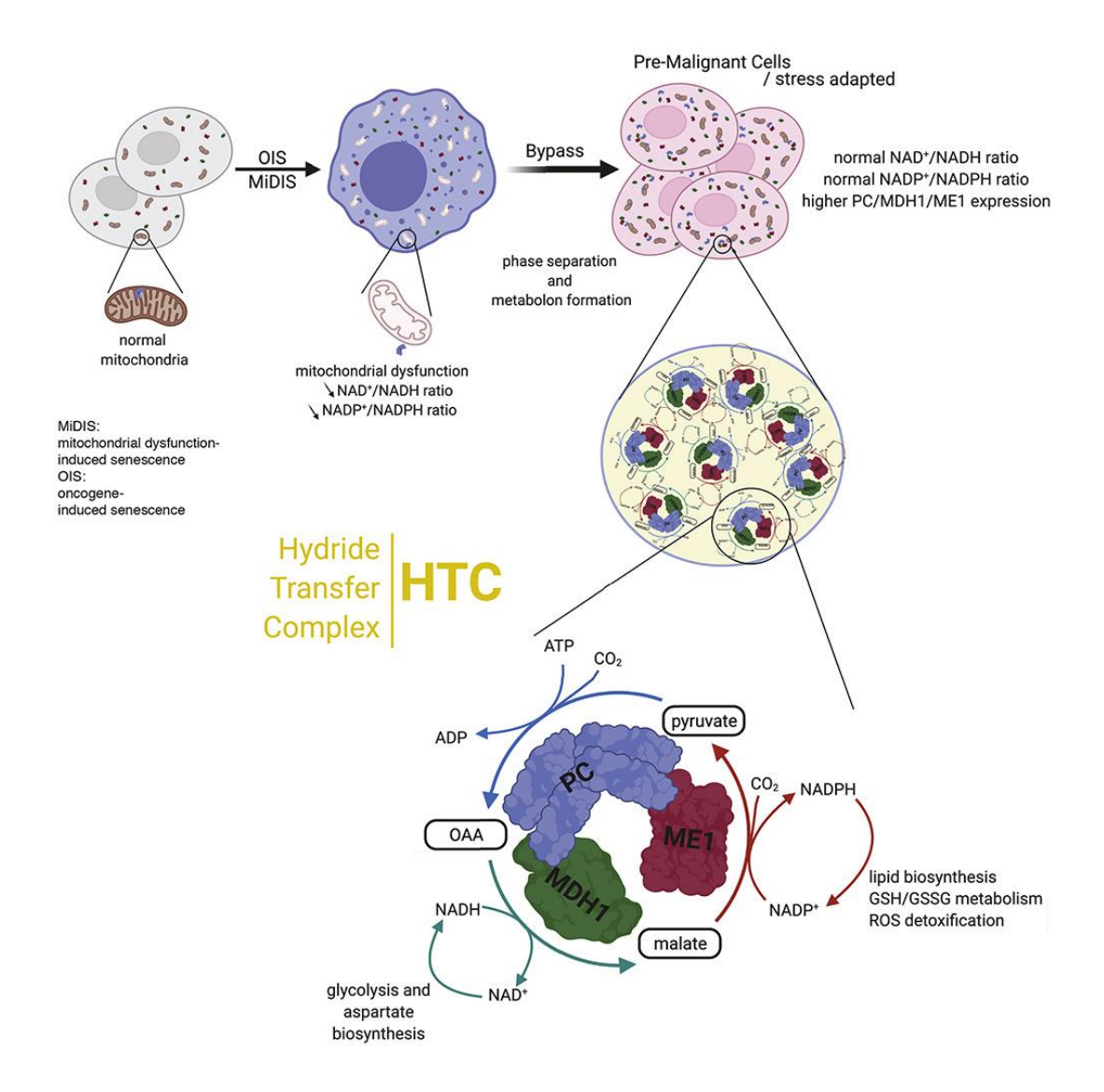


Fig. A.1.1A Schematic of the multi-enzymatic complex (hydride transfer complex) underlying metabolic reprogramming and senescence bypass. To bypass oncogene-induced senescence or mitochondrial dysfunction-induced senescence, the HTC which comprises of PC, MDH1 and ME1, catalyzes a metabolic cycle resulting in the regeneration of NAD+ and NADPH. NAD+ and NADPH are key cofactors for essential metabolic processes including glycolysis and ROS detoxification. Figure is from (1).

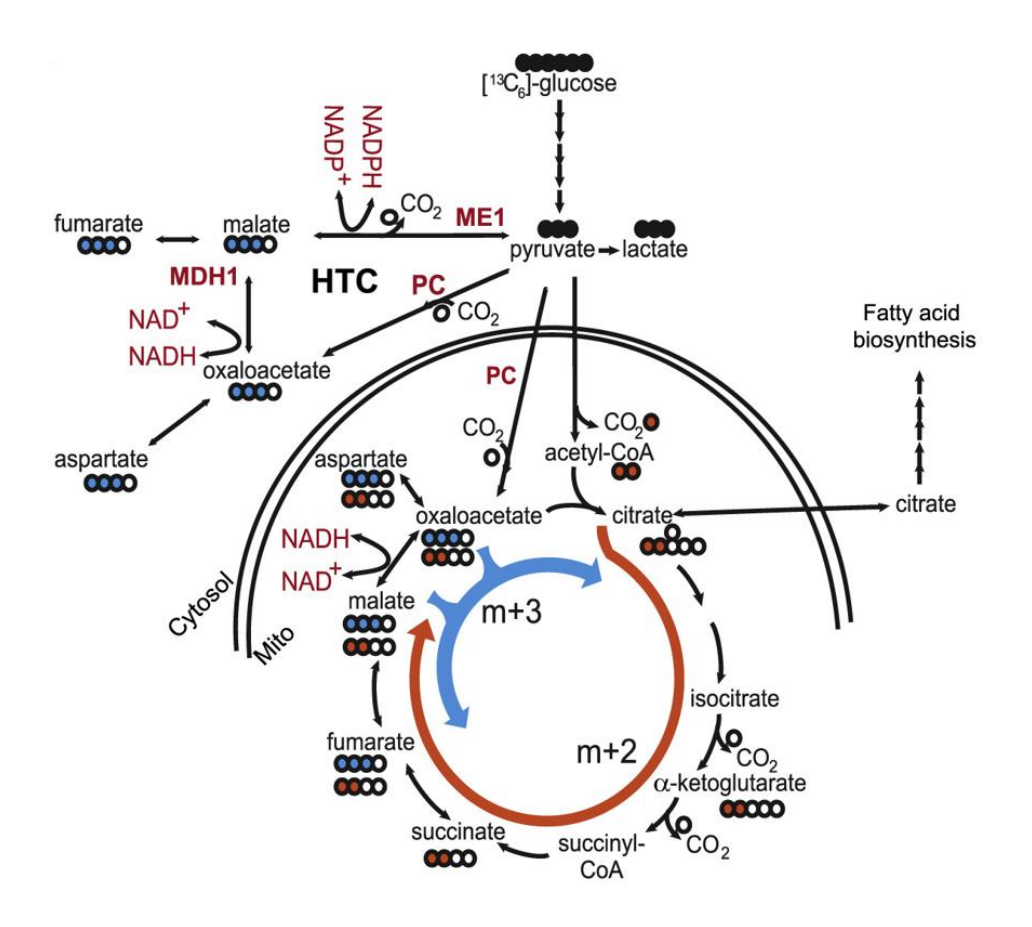


Fig. A.1.1B Model of NAD+ and NADPH regeneration by MDH1, ME1 and PC and schematic of ¹³C metabolite labeling patterns after incubating cells with ¹³C₆-glucose. ¹³C are denoted by filled circles. Red cycle is the forward direction of the citric acid cycle giving (m+2) intermediates (Red-filled circles). Blue cycle begins with pyruvate carboxylase (PC) and is characterized by (m+3) intermediates (Blue-filled circles). HTC, hydride transfer complex; mito, mitochondria. Figure is from (1).

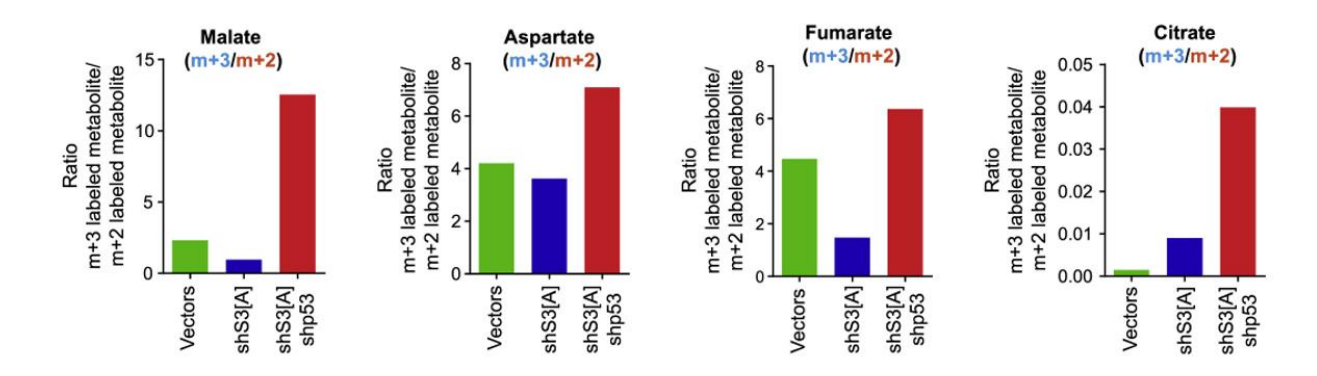


Fig. A.1.1C Reduced expression of p53 reprograms metabolism in STAT3-depleted

IMR90 cells. Ratio of (m+3)/(m+2) isotopomers for the aforementioned metabolites in IMR90 cells expressing control vectors, a shRNA against STAT3 (shS3[A]) alone or in combination with an shRNA against p53 (shp53). The ratios were calculated using SITA data after 10 min of ¹³C₆-glucose flux. Figure is from (1).

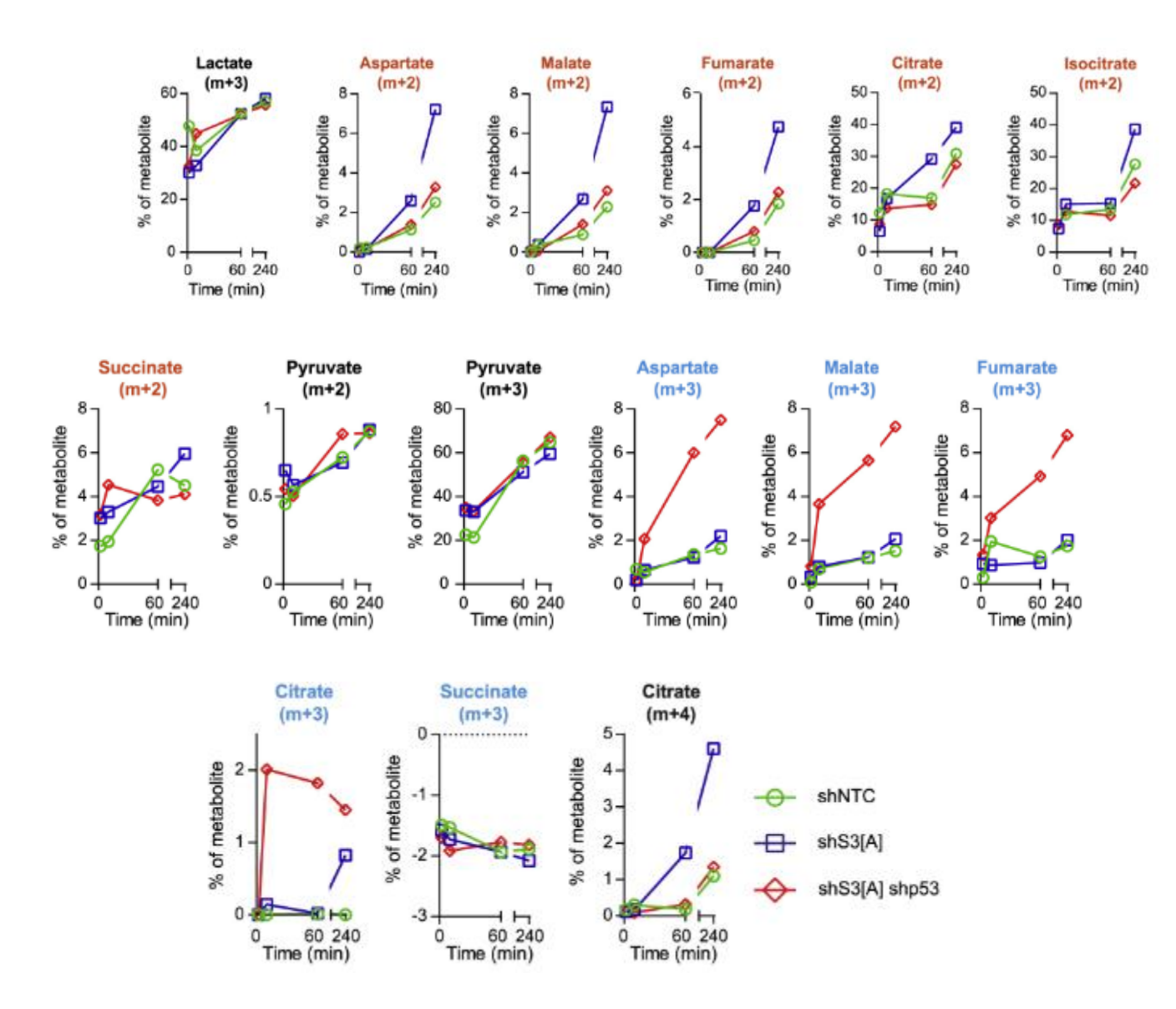


Fig. A.1.1D IMR90 cells depleted of STAT3 and p53 increases CAC anaplerosis via PC while decreasing entry into the CAC through pyruvate dehydrogenase. Mass spectrometry analysis of glucose-derived metabolites (13 C₆-glucose flux) over time in IMR90 cells expressing a control shRNA (shNTC), a shRNA against STAT3 (shS3[A]) alone or in combination with an shRNA against p53 (shp53). Representative plots for the experiments are shown. Figure is from (1).

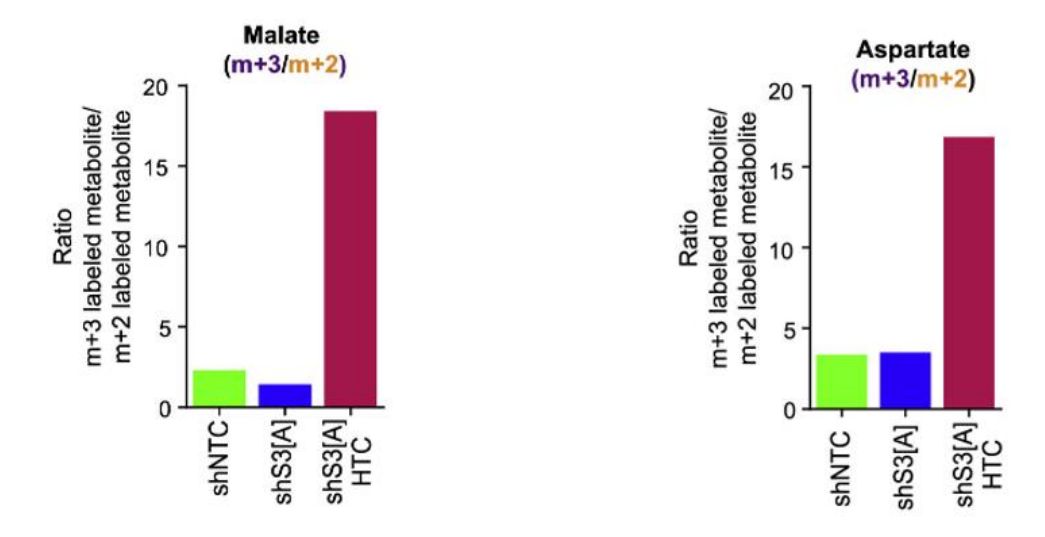


Fig. A.1.1E Expression of the hydride transfer complex enzymes reprograms metabolism in STAT3-depleted IMR90 cells. Ratio of (m+3)/(m+2) isotopomers for the indicated metabolites in IMR90 cells expressing control vectors, a shRNA against STAT3 with either control vectors (shS3[A]) or with vectors expressing HTC enzymes (shS3[A]). The ratios were calculated using SITA data after 10 min of ¹³C6-glucose flux. Figure is from (1).

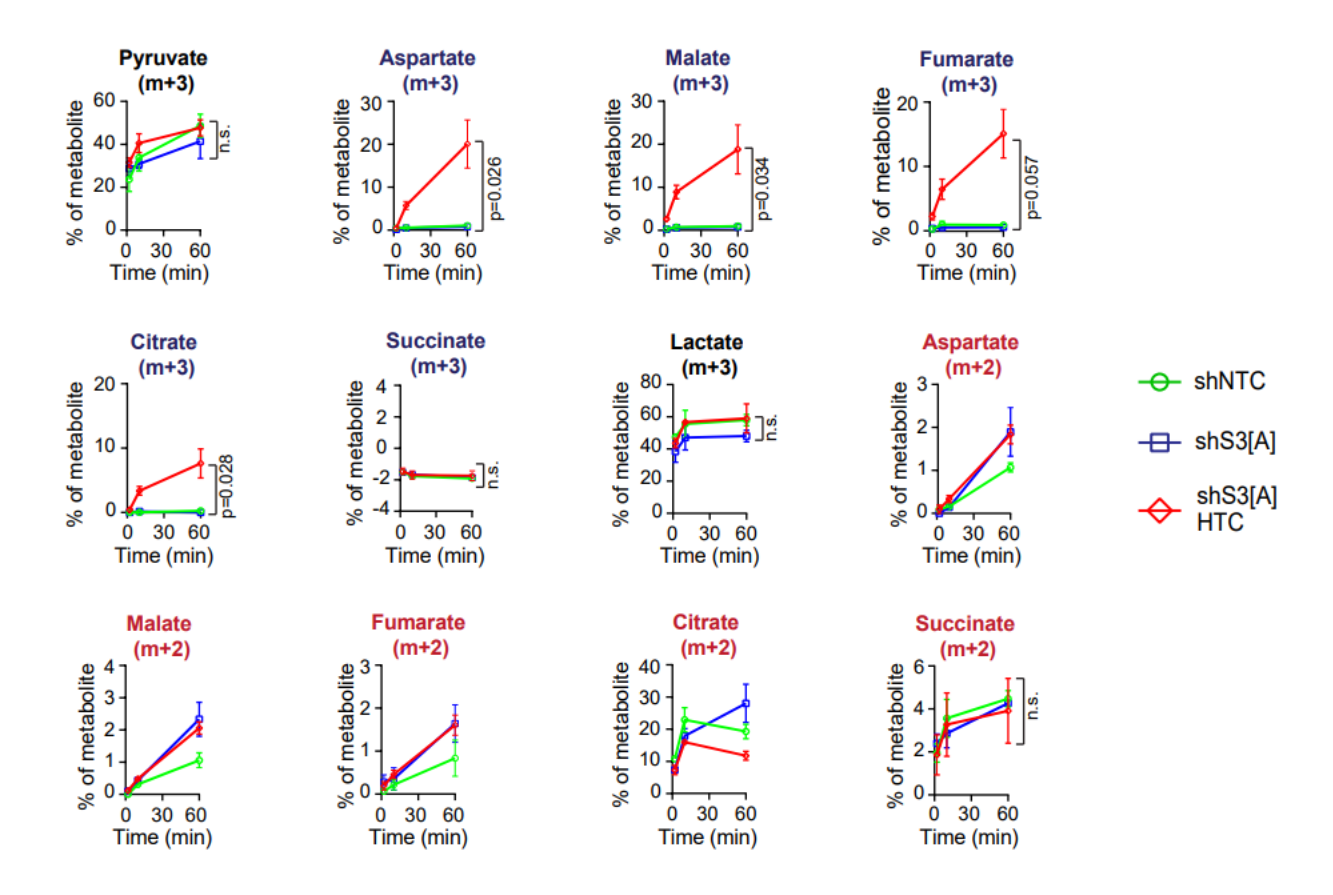


Fig. A.1.1F Expression of the hydride transfer complex enzymes increases CAC anaplerosis via PC in STAT3-depleted IMR90 cells. Mass spectrometry analysis of glucosederived metabolites (¹³C₆-glucose flux) over time in IMR90 cells expressing a control shRNA (shNTC), a shRNA against STAT3 with either control vectors (shS3[A]) or with vectors expressing HTC enzymes (shS3[A]HTC). Mean percent of total labeled metabolites are shown. Figure is from (1).

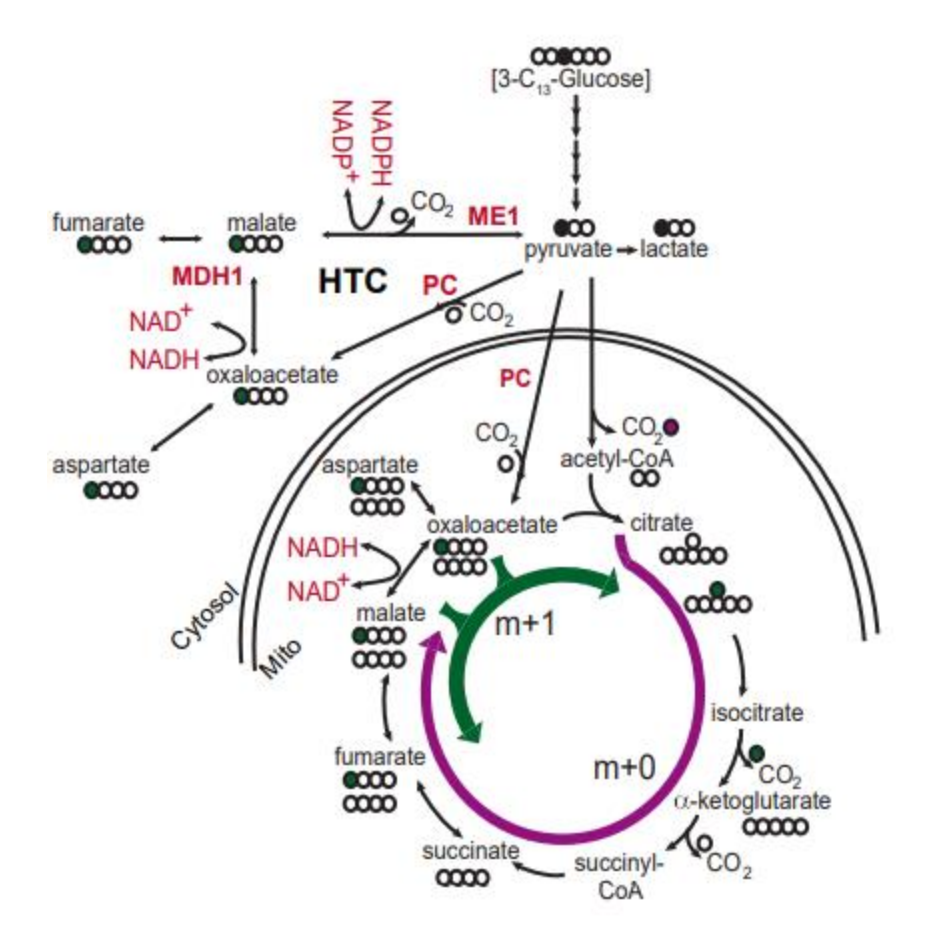


Fig. A.1.1G Schematic model of pyruvate carboxylase (PC) activity labeling pattern after 3-¹³**C-glucose flux.** 3-¹³C-glucose is metabolized into 3-¹³C-pyruvate. During the decarboxylation of 3-¹³C-pyruvate into acetyl-CoA, the labeled carbon is lost as heavy-labeled carbon dioxide and the subsequent citric acid cycle intermediates generated through oxidative decarboxylation are not labeled (magenta cycle). However, carboxylation of 3-¹³C-pyruvate into oxaloacetate by PC retains the labeled carbon and thus, each intermediate further derived from 3-¹³C-oxaloacetate is also labeled [(i.e., m+1 (green cycle)]. The filled circles show labelled carbon. Figure is from (1).

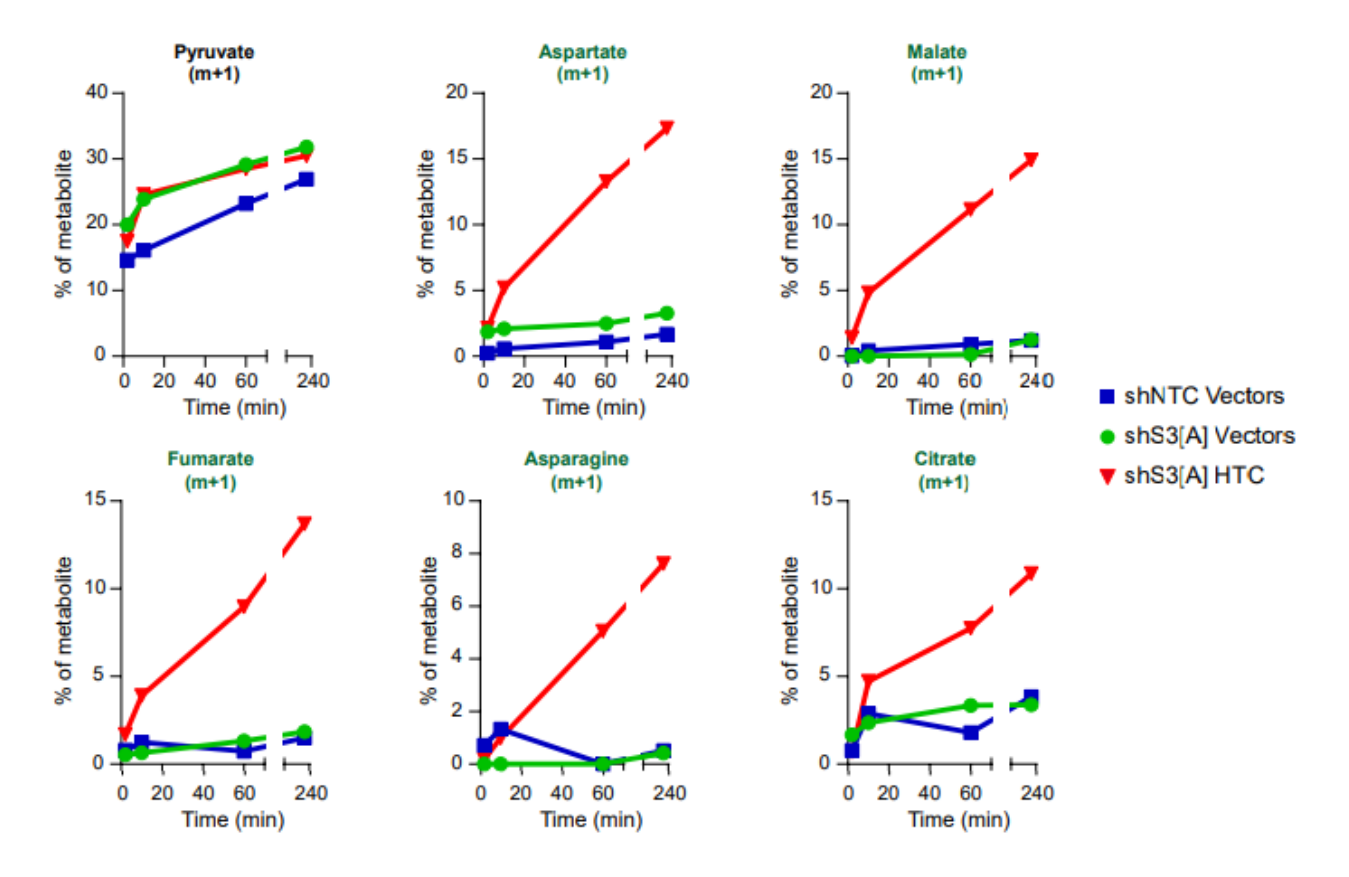


Fig. A.1.1H Expression of the hydride transfer complex enzymes increases CAC anaplerosis via PC in STAT3-depleted IMR90 cells. Mass spectrometry analysis of glucosederived metabolites (3-13C-glucose flux) over time in IMR90 cells expressing a control shRNA (shNTC), a shRNA against STAT3 with either control vectors (shS3[A]) or with vectors expressing HTC enzymes (shS3[A]HTC). Figure is from (1).

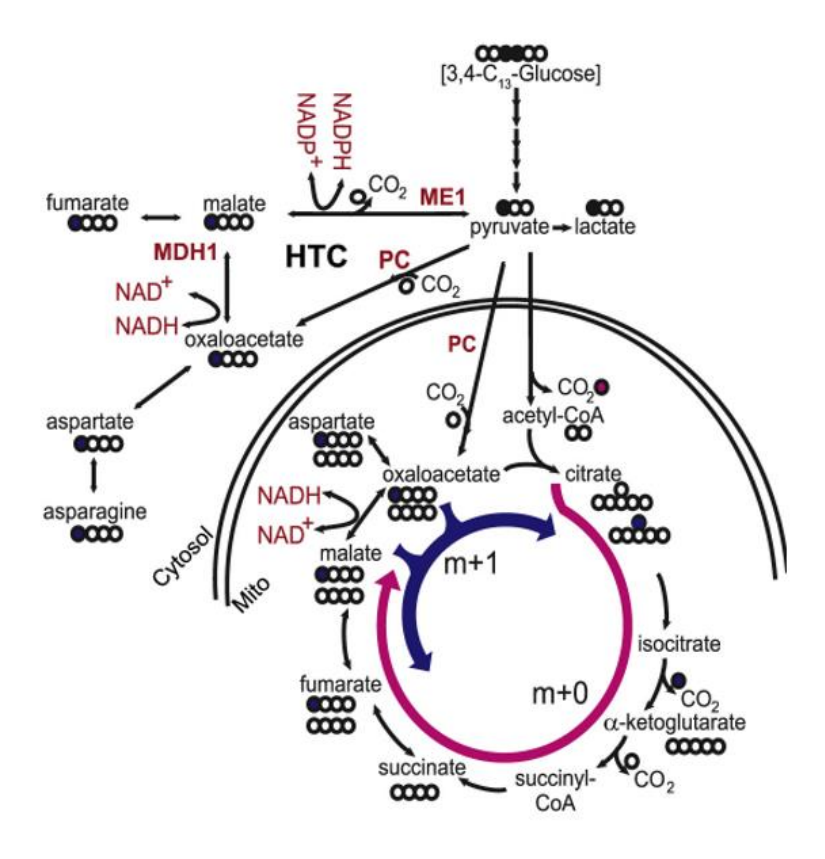


Fig. A.1.1I Schematic model of pyruvate carboxylase (PC) activity labeling pattern after 3,4-¹³C-glucose flux. 3,4-¹³C-glucose is metabolized into 3-¹³C-pyruvate. During the decarboxylation of 3-¹³C-pyruvate into acetyl-CoA, the labeled carbon is lost as heavy-labeled carbon dioxide and the subsequent citric acid cycle intermediates generated through oxidative decarboxylation are not labeled (magenta cycle). However, carboxylation of 3-¹³C-pyruvate into oxaloacetate by PC retains the labeled carbon and thus, each intermediate further derived from 3-¹³C-oxaloacetate is also labeled [(i.e., m+1 (blue cycle)]. The filled circles show labelled carbon. HTC, hydride transfer complex; mito, mitochondria. Figure is from (1).

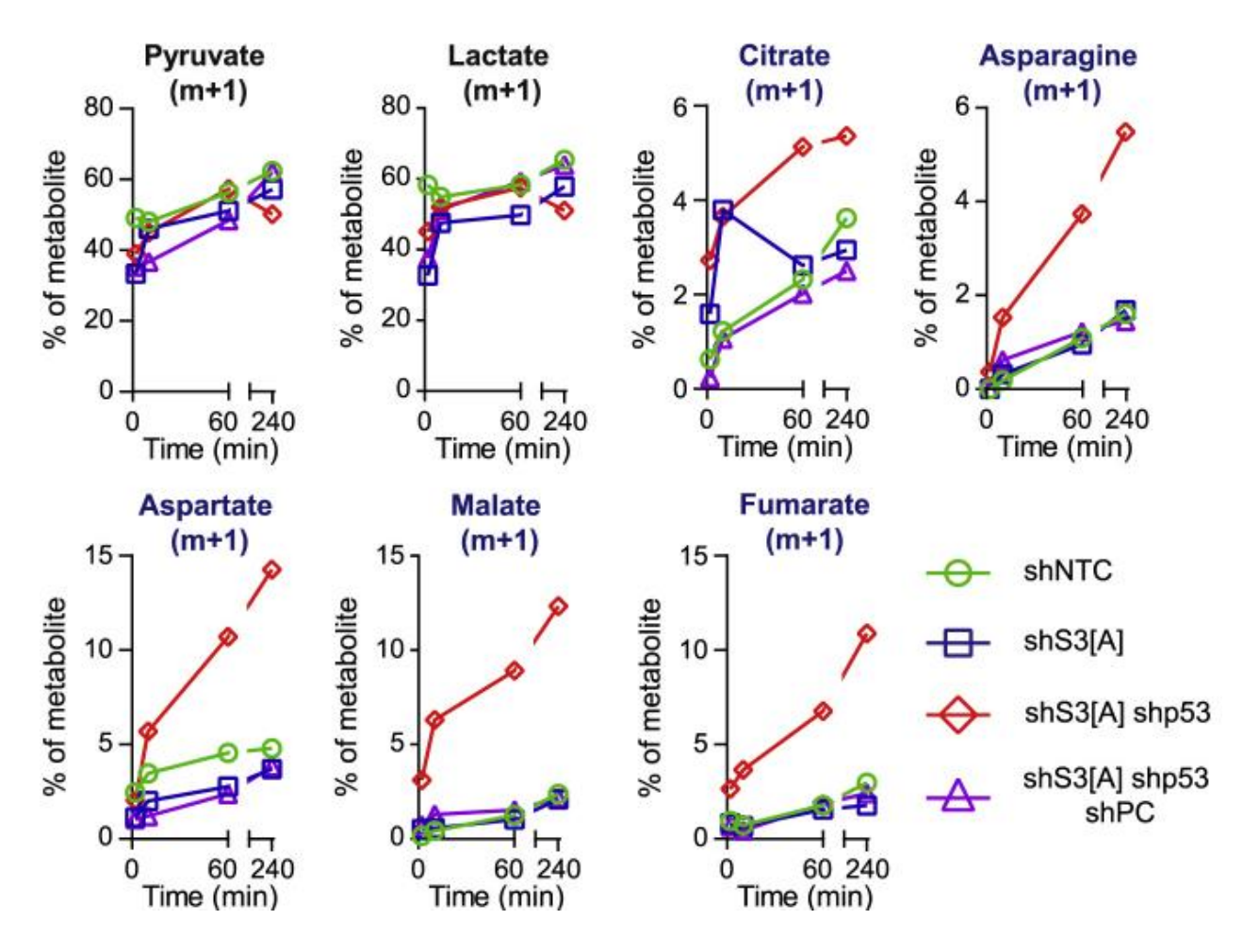


Fig. A.1.1J PC mediates metabolic reprogramming in IMR90 cells depleted of p53 and STAT3. Mass spectrometry analysis of glucose-derived metabolites (3-13C-glucose flux) over time in IMR90 cells expressing a control shRNA (shNTC), a shRNA against STAT3 alone (shS3[A]) or in combination with an shRNA against p53 (shp53), and/or a shRNA against PC (shPC). Figure is from (1).

A.1.2 Elucidating the mechanisms of the anti-neoplastic action of the sodium-glucose cotransporter-2 (SGLT2) inhibitors.

Increase in aerobic glycolysis is arguably one of the most recognized metabolic perturbations commonly observed in proliferating cells and neoplasia (30, 31). Over the last few decades, a panoply of studies have identified genes that are important regulators of glucose metabolism (32). Based on this, a number of lead compounds and/or drugs were developed and/or repurposed to target glucose metabolism in cancer (32). However, most of these efforts did not result in expected outcomes, thus suggesting that further investigation in the role of glucose metabolism in cancer is warranted. To this end, we investigated the mechanisms of antineoplastic action of canagliflozin, which is a sodium glucose cotransporter 2 (SGLT2) inhibitor that is commonly used to treat type 2 diabetes (4). SGLT2 transporters, expressed in the proximal convoluted tubule of the kidneys, are targeted when treating diabetes because they are responsible for roughly 90% of filtered glucose reabsorption (33). Thus, antihyperglycemic agents like canagliflozin inhibit the reabsorption of filtered glucose in the kidney which leads to increased glucose excretion and reduced blood glucose levels (33). The antiproliferative effects of canagliflozin have previously been shown in pancreatic and lung cancer (34, 35). Moreover, SGLT2 expression, which is generally thought to be limited to kidney cells, has been observed in prostate, glioblastoma, and pancreatic cancer (35, 36). However, the mechanism of anti-cancer action of canagliflozin remain obscure.

Supporting previously published studies (37-39), we showed that canagliflozin exhibits the antiproliferative effects in HER2+ (i.e., SKBR3 and BT-474) and luminal A (i.e., MCF7) breast cancer cell lines (4). I generated some of the cell proliferation data which compared the proliferative rates of control murine NT2197 breast cancer cells vs. those treated with

canagliflozin, other antidiabetic drugs like biguanide metformin or the additional SGLT2 inhibitor dapagliflozin [Fig A.1.2A; from Fig. 1C in (4)]. Surprisingly, the anti-proliferative effects of canagliflozin were not dependent on the availability of glucose (4). This suggested that the anti-proliferative effects of canagliflozin are independent of inhibition of glucose transport. In addition, the depletion of SGLT2 transporter neither reduced cell division nor rescued breast cancer cells from the antineoplastic effects of canagliflozin (4). Overall, these findings suggested a potential mechanism of anti-cancer action of canagliflozin that is independent of SGLT2.

Canagliflozin was previously shown to reduce cellular proliferation and decrease survival of prostate and lung cancer cells by inhibiting mitochondrial complex I (39). Also, HER2+ breast cancers have been shown to exhibit increased glutamine anaplerosis, to support neoplastic growth (40). Taking these findings into consideration, we sought to explore the effects of canagliflozin on mitochondrial metabolism in HER2+ breast cancer cells. Herein, we observed that relative to vehicle treated control, canagliflozin reduces oxygen consumption along with decreasing total ATP production in HER2-amplified SKBR3 breast cancer cells (4). In addition, canagliflozin reduced citrate, alpha-ketoglutarate and succinate levels while increasing glutamine levels as compared to vehicle treated control (4). SITA using labelled ¹³C₅-glutamine showed reduced carbon flux into the citric acid cycle (CAC) through the sequential enzymatic activities of glutaminase 1 (GLS1) and glutamate dehydrogenase (GLUD) to produce α-ketoglutarate (4). In conclusion, these experiments demonstrated that canagliflozin alters mitochondrial metabolism of HER2+ breast cancer cells at least in part by inhibiting glutamine anaplerosis with a subsequent decrease in the levels of CAC metabolites.

Considering the observed inhibitory effects of canagliflozin on glutamine metabolism, we set out to further dissect the underlying mechanisms. We first demonstrated that the presence of

glutamine is required for the antineoplastic effects of canagliflozin as oxygen consumption and proliferation were reduced only in the presence of glutamine (4). Moreover, canagliflozin induced glutamine uptake while increasing glutamate excretion which suggests reduced GLUD activity in converting glutamate to alpha-ketoglutarate (4). This was supported by subsequent findings that canagliflozin greatly diminished GLUD activity (4). Altogether, the data suggests that canagliflozin inhibits proliferation of HER2-amplified breast cancer cell lines by interfering with glutamine metabolism via disruption of GLUD function.

Our findings support accruing evidence that glutamine metabolism may represent a valid therapeutic target in cancer. Indeed, recently several inhibitors of glutamine metabolism have been developed (41, 42). To this end, glutamine transporters, such SLC1A5, can be effectively targeted by drugs such as V-9302 (43). Moreover, several inhibitors of GLS1 including CB-839, BPTES and 968 have shown promising results in pre-clinical models (44). Importantly, CB-839 proceeded into clinical trials as a monotherapeutic agent and in combination with chemotherapy or immunotherapy for triple negative breast cancer (TNBC), non-small cell lung cancer (NSCLC) and non-Hodgkin's lymphoma (NHL) patients (ClinicalTrials.gov identifiers: NCT02771626, NCT02071862, NCT02071888). In contrast, fewer clinical trials have been carried out to date investigating the effects of GLUD inhibitors. Nevertheless, epigallocatechin-3-gallate (EGCG) is currently being assessed as an anticancer agent for colorectal cancer patients (NCT:02891538). The use of EGCG as an antineoplastic compound against colorectal cancer provides basis for exploring the effects of canagliflozin beyond HER2+ breast cancer. Collectively, our study provided pioneering evidence that the effects of canagliflozin in HER2-amplified breast cancer are unlikely to be mediated by SGLT2 and are more likely to be the consequence of abrogation of glutamine metabolism.

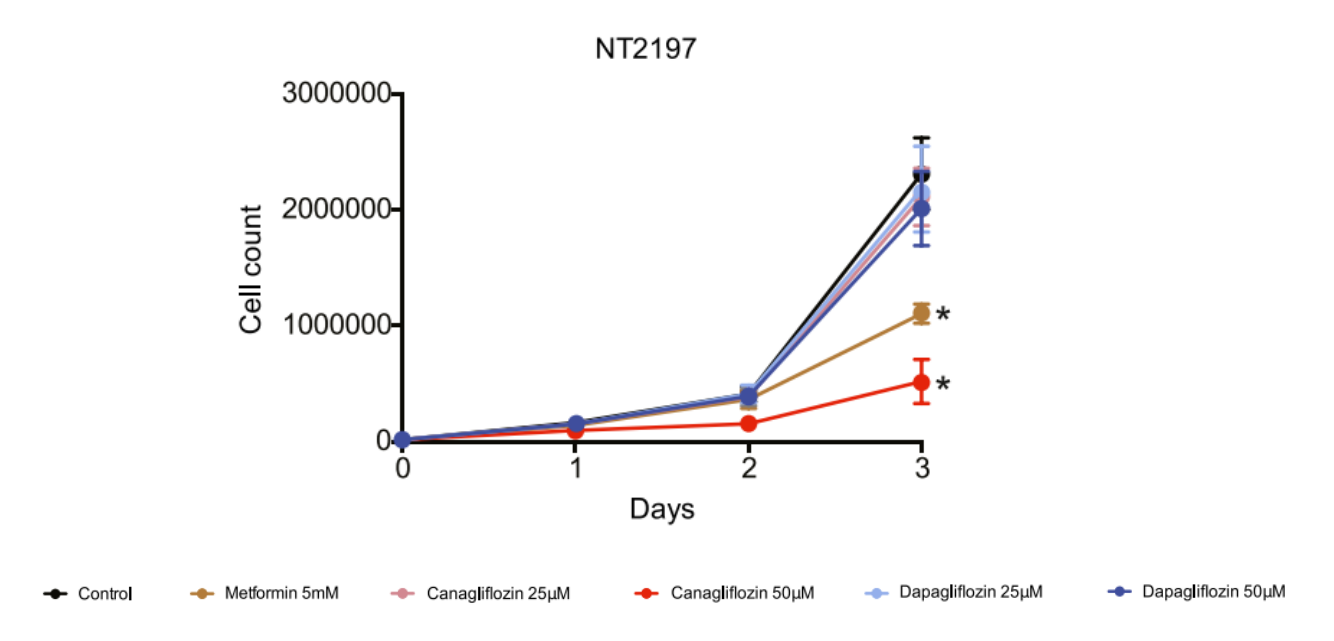


Fig. A.1.2A Canagliflozin reduces the proliferation of NT2197 cells. Number of viable NT2197 cells grown for indicated days was monitored by trypan blue exclusion using automated cell counter. Figure is from (4)

${\bf A.1.3~Establishing~the~role~of~PR/SET~Domain~15~(PRDM15)~in~metabolic~rewiring}$ of B-cell lymphomas.

Transcription factors including c-MYC and HIF1α, act as master regulators of cancer metabolism [summarized in the introduction section and (7)]. Nonetheless, the understanding of how transcriptional programs are integrated with metabolic rewiring in cancer is still incomplete. In collaboration with Mzoughi et al., we identified PRDM15 as transcription factor that is essential for metabolic reprogramming required to support survival and proliferation of B-cell lymphoma cells (2). PRDM15 is generally known to be involved in determination of cell identity during early development (45), but its function in adult tissues was largely unknown. Notwithstanding that we and others observed that PRDM15 is of the most highly overexpressed genes across the spectrum

of different non-Hodgkin's B-cell lymphomas (NBCL) such as follicular lymphoma, diffuse large B-cell lymphoma (DLBCL) and Burkitt's lymphoma (2, 46), its role in the etiopathogenesis and progression of these diseases remained elusive. This motivated us to investigate the role of PRDM15 in NBCL.

We first demonstrated that the abrogation of *PRDM15* using antisense oligonucleotides (AONs) reduces the survival of primary DLBCL cells and various B-cell lymphoma cell lines including P493-6, MC116, OCILY3, Karpas231, PR1, and HT (DLBCL), thus suggesting that PRDM15 plays a major role in B-cell lymphoma biology (2). Interestingly, except for having a slightly longer lifespan, tamoxifen-inducible PRDM15 adult whole-body KO mice (Prdm15 $^{\Delta/\Delta}$;CreER or $^{\Delta/\Delta}$ for short) had no conspicuous phenotypic differences compared to the controls (2). This indicates that PRDM15 is mostly expendable for normal adult murine homeostasis and adult stem cell renewal even though it has been previously described to be essential in embryonic stem cells and during development (2, 47, 48). However, considering that PRDM15 is upregulated in bone marrow B cells obtained from Eµ-Myc mice, we demonstrated that tamoxifen-inducible PRDM15 adult whole-body KO Eμ-Myc (Prdm15Δ/Δ;CreER;Eμ-Myc) mice delayed disease onset whereby Prdm15 $^{\Delta/\Delta}$;CreER;E μ -Myc mice had a median diseasefree survival of 332 days, compared to 107 days in control Eµ-Myc mice (2). Furthermore, the disruption of PRDM15 in primary tumor B-cells derived from tamoxifen-inducible PRDM15 KO Eµ-Myc mouse model decreased proliferation and increased apoptosis (2). In order to illustrate the cell-autonomous role of PRDM15 in tumor maintenance, primary tumors were extracted from PRDM15^{F/F};CreER;Eµ-Myc mice and transplanted into syngeneic recipient mice which were subsequently injected with tamoxifen to deplete PRDM15 in the tumor cells (2). While none of the tamoxifen-injected mice had palpable tumors at the end point of the experiment, all control

mice had tumors and greater disease burden. Collectively, these findings demonstrate that PRDM15 may act as a central factor driving B-cell lymphomagenesis and maintenance of B-cell lymphoma.

To gain further insights in the molecular mechanism(s) that underpin the role of PRDM15 in driving B-cell lymphomagenesis and disease progression, we carried out chromatin immunoprecipitation (ChIP)-sequencing and RNA sequencing experiments in PRDM15proficient and deficient B-cells isolated from Eu-Myc mice to identify promoters that are occupied by PRDM15 in parallel with the changes in mRNA level. These analyses revealed that transcriptional targets of PRDM15 are enriched in metabolic genes including pyruvate kinase (Pkm), insulin receptor (Insr) and insulin like growth factor 1 receptor (IgfIr) (2). Moreover, gene ontology analysis of affected genes highlighted glycolysis and PI3K-AKT-mTOR signaling as two of the most highly affected functions upon Prdm15 loss (2). We confirmed these findings by showing that the loss of *Prdm15* inhibited the activity of PI3K-AKT-mTOR signaling pathway (2). Intriguingly, suppression of mTOR signaling caused by *Prdm15* loss appeared not to be accompanied by the disruption of negative feedbacks that lead to activation of other tumorigenic signaling pathways including MAPK-ERK (2). It is worthwhile to note that the compensatory activation of the latter pathways has been shown to limit the efficacy of clinically used mTOR inhibitors (e.g., everolimus) in oncological indications (49, 50). Considering that mTOR plays a major role in regulation of cellular metabolism, while putative PRDM15 transcriptional targets were also enriched in genes known to regulate glucose metabolism [e.g., glucose transporter 1 (SLC2A1), pyruvate kinase (PKM), hexokinase 3 (HK3) and enolase (ENO)] (2), we next sought to document the effects of PRDM15 loss on the metabolome. I participated in these studies.

Indeed, loss of Prdm15 in B-cell lymphomas derived from mice (i.e., Prdm15^{F/F}; CreER; Eµ-Myc tumors treated with tamoxifen to deplete the expression of Prdm15) was accompanied by decrease in intracellular levels of glucose and glycolytic intermediates including fructose-6-phosphate, glucose-6-phosphate and glucose-1-phosphate (Fig. A.1.3A; from Fig. 6A in (2)). Likewise, the intracellular levels of a pentose phosphate pathway (PPP) intermediate sedoheptulose-7P were reduced when Prdm15 was abrogated as compared to the control (Fig. A.1.3A; from Fig. 6A in (2)). Accordingly, in addition to the downregulation of glycolytic genes, the loss of Prdm15 was also associated with the reduced expression of PPP enzymes (e.g., glucose-6-phophate isomerase) (2). Nucleotides, CAC intermediates (e.g., malate, succinate, fumarate and α-ketoglutarate) and amino acids (asparagine, glutamine, glutamate and proline) were also reduced in B-cell lymphoma cells lacking Prdm15 relative to Prdm15-proficient controls (Fig. A.1.3A; from Fig. 6A in (2)). Furthermore, OXPHOS was greatly diminished by deletion of Prdm15 as compared to control B-cell lymphoma cells (2). Since c-MYC plays a prominent role in regulating glutamine metabolism (51) and our data suggests that c-MYC stimulates PRDM15 transcription (2), I next performed SITA analysis whereby Prdm15-proficient Prdm15^{F/F}; CreER; Eµ-Myc) and tamoxifen-induced Prdm15-deficient B-cell (i.e. Prdm15^{Δ/Δ};CreER;Eμ-Myc) tumor lymphoma cells were labelled with ¹³C₅-glutamine. This analysis revealed that although the total ¹³C-labeled CAC intermediates levels were reduced in association with the loss of PRDM15, the fraction of ¹³C-labeled CAC intermediates is mostly unaffected by PRDM15 status (Fig. A.1.3B-D; from Supplementary Fig. 6D, G-H in (2)). Hence, CAC enzyme activities were unaffected by PRDM15 status in the cell, and that the decrease in the total ¹³C-labeled CAC intermediates levels observed in B-cell lymphomas devoid of PRDM15 is at least partly due to decreased glutamine uptake and/or utilization (2). Taken altogether, these

findings established PRDM15 as a major regulator of metabolic rewiring in B-cell lymphoma, while suggesting that the loss of PRDM15 leads to metabolic catastrophe and subsequent death of B-cell lymphoma cells. These findings thus position PRDM15 as a major factor that underpins metabolic plasticity of B-cell lymphoma cells, whereby PRDM15 appears to be essential for survival and proliferation of B-cell lymphoma cells.

In conclusion, our study pointed out that although PRDM15 is essential for supporting metabolic programs of B-cell lymphoma, but not normal B-cells or other hematopoietic cells. This suggest that PRDM15 may constitute an appealing target for therapeutic intervention. Importantly, in addition to exhibiting low expression in adult tissues, the loss of *Prdm15* in mice did not result in any obvious phenotypic differences in the major examined organs (e.g., spleen, intestines and testes), thereby suggesting a wide therapeutic window for the potential PRDM15-targeted therapies for adults. Although the crystal structure of PRDM15 is yet to be determined and potential inhibitors of PRDM15 may still be in development, antisense oligonucleotides targeting PRDM15 seem to be a plausible approach (2, 52).

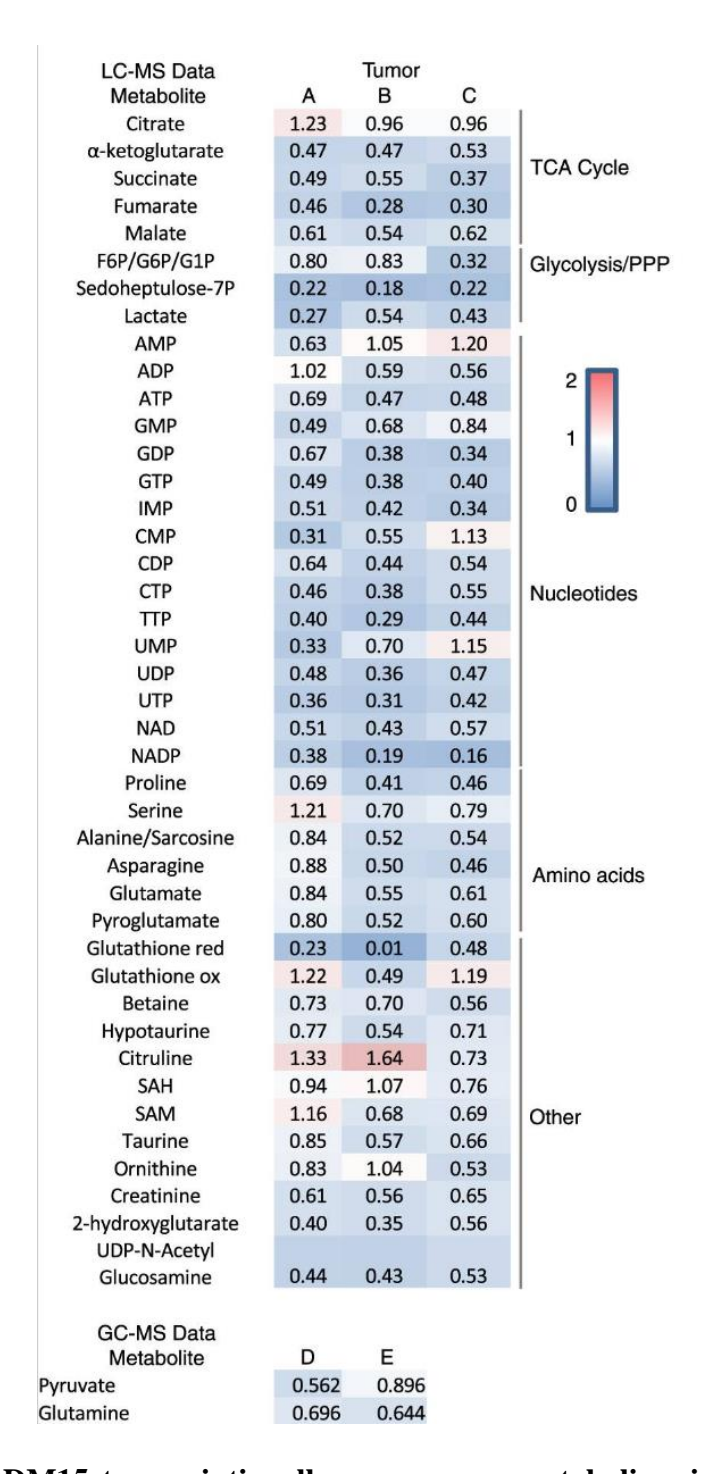


Fig. A.1.3A PRDM15 transcriptionally reprograms metabolism in Eμ-Myc tumor cells. Metabolomics analysis in Prdm15^{F/F}; CreER; Eμ-Myc vs. Prdm15^{Δ/Δ}; CreER; Eμ-Myc cells. The values in the upper panel represent the average intracellular level of each indicated metabolite in Prdm15^{Δ/Δ}; CreER; Eμ-Myc cells relative to the Prdm15^{F/F}; CreER; Eμ-Myc control cells

determined by LC-MS. The data were obtained from three independent tumors (i.e., A, B and C) with each tumor consisting of three technical replicates. The values in the bottom panel are average intracellular levels of pyruvate and glutamate measured in two independent tumors determined by GC-MS. Figure is from (2)

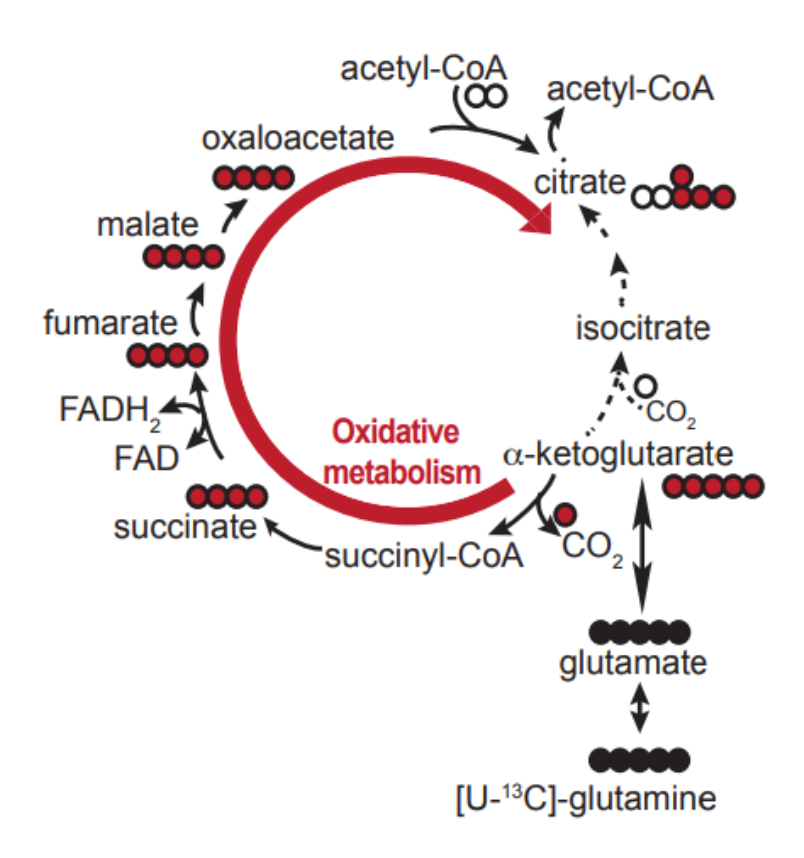


Fig. A.1.3B Schematic model of ¹³C incorporation into CAC intermediates after incubating cells in media containing ¹³C-glutamine. ¹³C-glutamine is metabolized into ¹³C-α-ketoglutarate which undergoes oxidative decarboxylation (red cycle) in the CAC to produce intermediates of the cycle. The filled circles show labelled carbon. Figure is from (2)

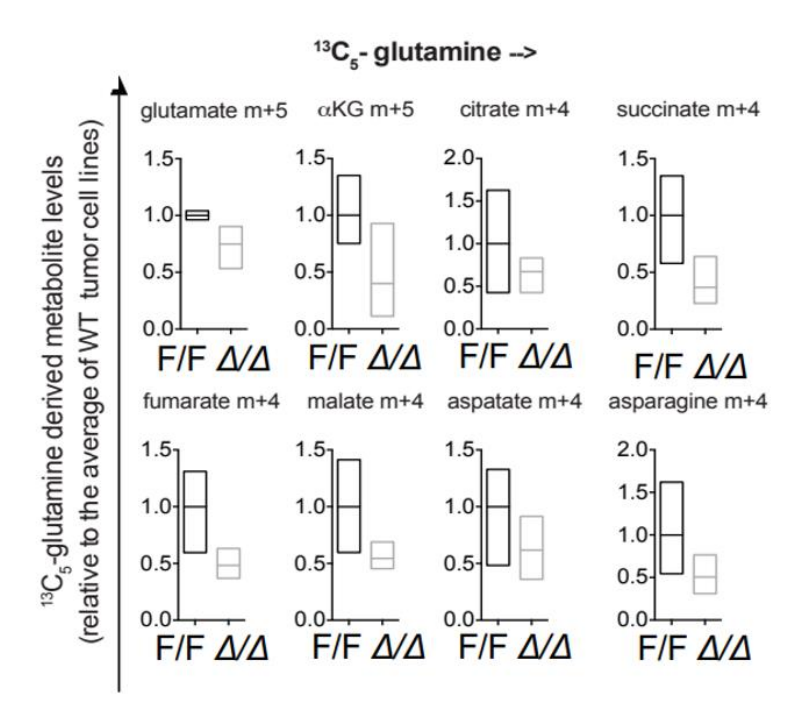


Fig. A.1.3C Loss of PRDM15 in Eμ-Myc tumor cells decreases the intracellular levels of CAC intermediates derived from the oxidative decarboxylation of glutamine-derived α-ketoglutarate. Prdm15^{F/F};CreER;Eμ-Myc and Prdm15^{Δ/Δ};CreER;Eμ-Myc cells were incubated with 13 C5-glutamine for 180 min. SITA were performed and the levels of indicated isotopomer ion amounts are shown as absolute amount and relative to the average of the Prdm15^{F/F};CreER;Eμ-Myc control cells. Figure is from (2).

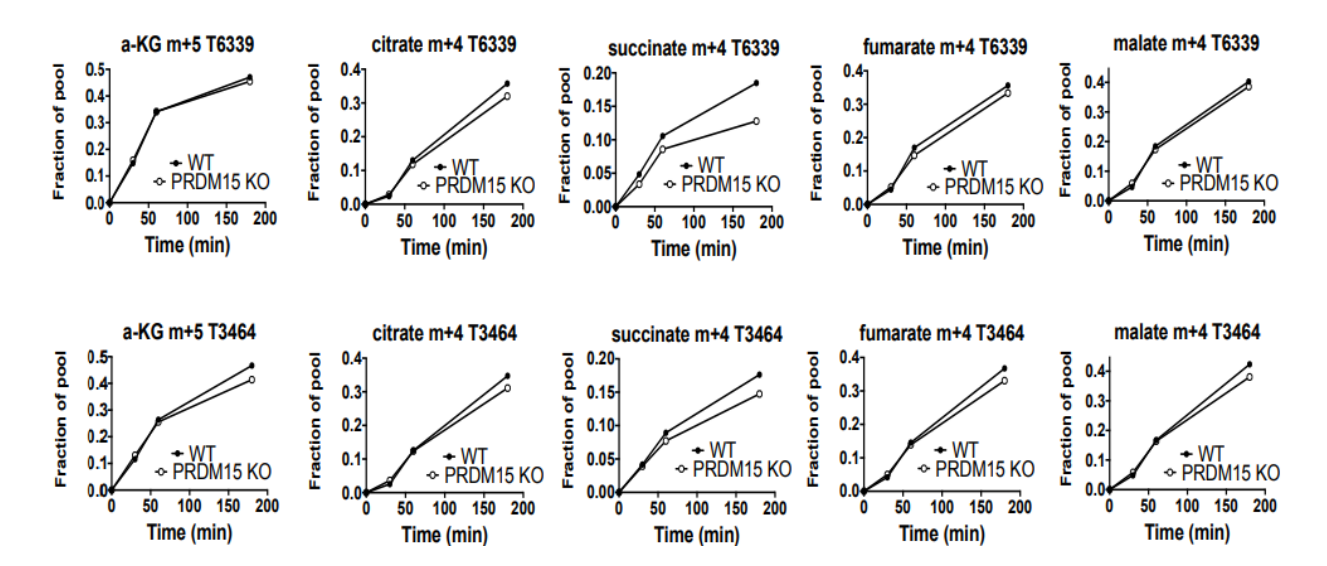


Fig. A.1.3D PRDM15 status has no effect on the activity of CAC enzymes. SITA of $Prdm15^{F/F}$; CreER; E μ -Myc (WT) and $Prdm15^{\Delta/\Delta}$; CreER; E μ -Myc (PRDM15) cells incubated with 13 C₅-glutamine. The fraction of 13 C-CAC intermediates relative to the total pool labelled over time is shown. Data from two independent tumors (i.e., T63339 and T3464) is shown. Figure is from (2).

A.1.4 The role of mTORC1/4E-BP/eIF4E axis and HIF1α in metabolic plasticity of cancer cells and responses to the combinations of inhibitors of oncogenic kinases and biguanides.

To date, attempts to target metabolic vulnerabilities of cancer cells have resulted only in a modest success (53). This is thought to be a consequence of incomplete understanding of the molecular underpinnings of metabolic rewiring in neoplasia (54). More recent evidence points out that when one of the major metabolic pathways is suppressed, cancer cells can compensate by activating alternative metabolic routes (54). For instance, anti-diabetic biguanides (e.g., metformin) exhibit anti-neoplastic effects by suppressing OXPHOS which at least in part is achieved via the inhibition of mitochondrial complex I (55-59). This decrease in OXPHOS is however compensated by increased uptake and utilization of glucose including its reduction to

lactate (59-62). The latter is thought to be required to regenerate NAD+ under conditions wherein the NADH dehydrogenase activity of complex I is reduced (60, 61). In turn, the vast majority of the inhibitors of oncogenic kinases (KIs) including HER2/EGFR inhibitor lapatinib, BRAF inhibitor vemurafenib, or BCR/ABL inhibitor imatinib suppress glucose uptake and glycolysis (63). Therefore, we and others rationalized that combining biguanides and KIs should result in synthetic lethality whereby compensatory increase in glycolysis required for adaptation to energy stress caused by biguanides should be disrupted by KIs (3, 64, 65). To test this hypothesis, we investigated the effects of combination of biguanides and KIs across the range of cancer cell lines whose neoplastic growth is driven by different oncogenic kinases (3). We opted to use phenformin in our experiments motivated by the findings that metformin is a less potent complex I inhibitor compared to phenformin (66), while phenformin has a more favorable pharmacokinetic and pharmacodynamic profile than metformin (67). It is important to note that although phenformin is not in clinical use for the treatment of type 2 diabetes due to relatively higher frequency of lactic acidosis as compared to metformin, its repurposing for oncological indications is well justified considering severity of the side-effects of anti-cancer therapeutics (68).

Using cell line models, we demonstrated that combining phenformin with KIs results in synergistic anti-proliferative effects and induction of apoptosis across a variety of cancer cell lines (3). More specifically, HER2 inhibitor lapatinib, BCR/ABL inhibitor imatinib and BRAF inhibitor vemurafenib synergized with phenformin in HER2+ breast cancer NT2197, BCR-ABL positive K562 myelogenous leukemia and BRAF-mutated A375 melanoma cell lines, respectively (3). Proliferation of HCT116 colon cancer cells is dependent on EGFR activity and is thus sensitive to lapatinib which acts as a dual HER2/EGFR kinase inhibitor (69). Of note, one of my contributions to this study was to carry out experiments showing that lapatinib and phenformin exert synergistic

anti-proliferative effects in HCT116 cells (Fig. A.1.4A; from Fig. 1B and Supplementary Fig. 2F-G of (3)). NT2197 cells were generated by expressing oncogenic Neu/ErbB2 (V664E) (rat orthologue of HER2) in Normal Murine Mammary Gland (NMuMG) cells (70). Importantly, NMuMG cells showed minimal sensitivity to phenformin, lapatinib or combination thereof as compared to NT2197 cells, thus suggesting that this drug combination does not induce major toxicity in normal cells (3). Finally, using xenograft NT2197 model, we showed that *in vivo* effects of a combination of phenformin and lapatinib are significantly stronger than using each drug alone (3).

Thus far, our results showed that phenformin and KIs exert synergistic effects across a variety of cell lines and "driver" oncogenic kinases. Considering the opposing effects of KIs and phenformin on glycolysis (71-75) (60), we next probed the effects of phenformin/KI combinations on metabolome. I actively participated in these studies. As expected, vemurafenib (referred to as PLX4032) and lapatinib inhibited phenformin-induced increase in glucose uptake and lactate production (Fig. A.1.4B; from Fig. 2B and Fig. 2F of (3)). In addition, it was previously shown that biguanides induce reductive glutamine metabolism (62). As described in chapter 2, reductive glutamine metabolism is characterized by the reductive carboxylation of α -ketoglutarate which allows sufficient production of citrate to fuel lipid synthesis under conditions where mitochondrial functions and/or CAC are blocked (76). We observed that vemurafenib and lapatinib largely antagonized phenformin-induced increase in the reductive glutamine metabolism (Fig. A.1.4C; from Fig. 2D and Fig. 2H of (3)). Findings obtained in cell culture were further confirmed in vivo using the NT2197 xenograft model (3). Altogether, these findings indicate that KIs attenuate adaptive metabolic rewiring induced in response to energy stress caused by phenformin treatment. However, the synergy between lapatinib and phenformin could not be explained solely by their opposing effects on glucose metabolism inasmuch as combining phenformin with inhibitors of glycolysis (e.g., phosphofructokinase inhibitor 3PO), resulted only in weak additive effect (3).

Phenformin and KIs impinge on protein synthesis machinery (77) which is one of the most highly energetically demanding processes in the cells that is upregulated in cancer and linked to metabolic reprogramming in neoplasia (78, 79). We therefore investigated whether the effects of KIs and phenformin on protein synthesis may contribute to the observed synergistic effects. Herein, we first focused on two major signaling mechanisms known to regulate protein synthesis: the AMPK-mTORC1 axis and the MAPK-ERK pathway. As expected, phenformin activated AMPK while KIs such as lapatinib, vemurafenib and imatinib inhibited the MAPK-ERK pathway. However, at concentrations used, combining KIs and phenformin resulted in downregulation of mTORC1 signaling to a significantly higher extent than each drug alone (3). Intriguingly, although the active-site mTOR inhibitor, torin1, repressed mTORC1 and global protein synthesis to a higher extent than phenformin/lapatinib combination, the effects of torin1 on apoptosis were dramatically less pronounced that those observed when phenformin and lapatinib were combined (3). This can be explained by the findings that active-site mTOR inhibitors induce metabolic dormancy whereby the reduction in ATP synthesis is offset by the inhibition of energy demanding processes like protein synthesis (79). Hence, it is plausible that residual mTOR signaling in phenformin/lapatinibtreated cells is required to prevent metabolic dormancy and lead to energetic crisis which may explain higher induction of apoptosis in NT2197 cells treated with the latter combination as compared to torin1 treatment.

In addition to regulating global protein synthesis, alterations in mTORC1 signaling have been linked to selective perturbations in the pools of mRNAs that are being translated (80-84). We observed that phenformin/lapatinib combination not only inhibited global protein synthesis, but

also strongly reduced the translation of a number of "eIF4E-sensitve" mRNAs (e.g., MCL1, BCL2 and MYC) (77) to the higher extent than either drug alone (3). We next confirmed that these effects on protein synthesis are mediated via the mTORC1-4E-BP-eIF4E axis by showing that is sufficient to rescue translation of "eIF4E-sensitive" mRNAs in cells treated with phenformin/KI combination to the levels comparable to those observed in control, vehicle treated cells (3). In addition to "classical" "eIF4E-sensitive mRNAs", we observed that the loss of 4E-BPs alleviated the inhibitory effects of phenformin/lapatinib combination on translation of pyruvate carboxylase (PC), phosphoglycerate dehydrogenase (PHGDH), phosphoserine aminotransferase 1 (PSAT1) and asparagine synthetase (ASNS) mRNAs (3). Notably, proteins encoded by the aforementioned mRNAs are implicated in biosynthesis of non-essential amino acid (NEAA) aspartate (PC), asparagine (ASNS) and serine (PHGDH AND PSAT1) (85, 86). It was previously demonstrated that the mTORC1-4E-BP-eIF4E axis regulates translation of mRNAs involved in mitochondrial biogenesis (e.g., TFAM) and functions (e.g., ATP5O) (79), which was also confirmed in the experiments using phenformin/lapatinib combination (3). Collectively, these results suggested that synergistic effects of biguanides and KIs may at least in part be mediated by translational reprograming of NEAA metabolism and bioenergetics via the mTORC1-4E-BP-eIF4E axis.

To test this, I carried out SITA with ¹³C₆-glucose and 3-¹³C-glucose, which revealed that according to alterations in translations, NT2197 cells devoid of 4E-BP1/2 synthesize more serine and aspartate compared to 4E-BP1/2-proficient cells, whereby the flux via these biosynthetic pathways remained significantly elevated after treatment with phenformin and lapatinib combination in 4E-BP1/2 KO cells [Fig. A.1.4D-F; from Fig. 6B and Supplementary Fig. 6B of (3)]. The significance of aspartate and asparagine in determining the sensitivity of cells to phenformin/lapatinib combination was further underscored by the findings that supplementation

of the media with either aspartate or asparagine significantly attenuated the antiproliferative effects of phenformin/lapatinib combination even in 4E-BP1/2-proficient NT2197 cells (3). Conversely, inhibition of serine synthesis by depleting PHGDH potentiated the antiproliferative effect of the drug combination (3). Collectively, these findings show that translational reprogramming of NEAA biosynthesis via the mTORC1-4E-BP-eIF4E axis is a major determinant of the efficacy of combinations of phenformin with KIs.

Notwithstanding that abrogation of 4E-BP1/2 expression attenuated the effects of biguanide/KI combinations in cancer cell lines, it did not rescue proliferation rates to the levels observed in control vehicle-treated cells (3). This suggested that the factors other than the mTORC1-4E-BP-eIF4E axis are implicated in response to combinatorial biguanide/KI treatment. We observed that the HIF-1α levels were more strongly reduced in NT2197 cells treated with phenformin/lapatinib drug combination compared to cells treated with either drug alone (3). Opposite to previous reports showing that in some contexts HIF-1α levels are regulated at the level of translation in a 4E-BP-dependent manner (87), we determined that the changes in HIF-1α levels in response to phenformin/lapatinib combination treatment of NT2197 cells were independent of the 4E-BP status in the cells (3). ¹³C₅-glutamine tracing experiments under conditions where HIF-1α levels were induced by dimethyloxallyl glycine (DMOG), or in renal cancer RCC4 cells devoid or competent for Von Hippel Lindau (VHL) E3 ubiquitin ligase that marks HIF-1α for degradation (88-90) revealed that HIF-1α plays a major role in inducing reductive glutamine metabolism (3). Consistent with previous reports (91), we found that HIF-1 α negatively regulates α -ketoglutarate dehydrogenase (\alpha KGDH) subunit E1 (OGDH) levels which limits oxidative, while bolstering reductive glutamine metabolism (3). Notably, phenformin/lapatinib combination treatment which had no major effect on the levels of HIF-1α and OGDH in VHL-deficient renal cancer RCC4 cells,

reduced the levels of both proteins in their VHL-proficient counterparts (3). As mentioned above, increase in reductive glutamine metabolism limits anti-neoplastic efficacy of biguanides (62). Consistent with this VHL-deficient RCC4 cells exhibited reduced sensitivity to phenformin/lapatinib combination as compared to VHL-proficient RCC4 cells (3). This was accompanied with the inability of the drugs to suppress HIF- 1α levels and reductive glutamine metabolism in the absence of VHL (3).

Altogether, these findings unraveled the previously unappreciated mechanisms that mediate the effects of biguanide and KI combinations. More importantly, these results showed that cancer cells engage alternative metabolic pathways governed by the mTORC1-4E-BP-eIF4E and HIF-1α dependent mechanisms to adapt to biguanide and KI combinations (Fig. A.1.4G; from (3)). These findings therefore suggest that instead of being "addicted" to one or few metabolic pathways, cancer cells exhibit metabolic plasticity whereby they can rewire metabolism using alternative mechanisms and pathways to avoid therapeutic insults and adapt to other types of stress. Considering that the combination of biguanides and KIs are being considered or are already in clinical trials (NCT03026517), these findings suggest that consideration of metabolic plasticity should play a major role in design and interpretation of these trials. Moreover, these and other emerging mechanisms that enhance metabolic flexibility of cancer cells [e.g., PGC1α-dependent metabolic perturbations (92) and PDK1-dependent metabolic reprogramming (93)] are likely to limit the efficacy of targeting metabolic vulnerabilities of neoplasia in the clinic and dictate metastatic spread of the disease (6, 54). Collectively, these findings suggest that future research is warranted to improve understanding of the molecular underpinnings of metabolic reprograming in cancer.

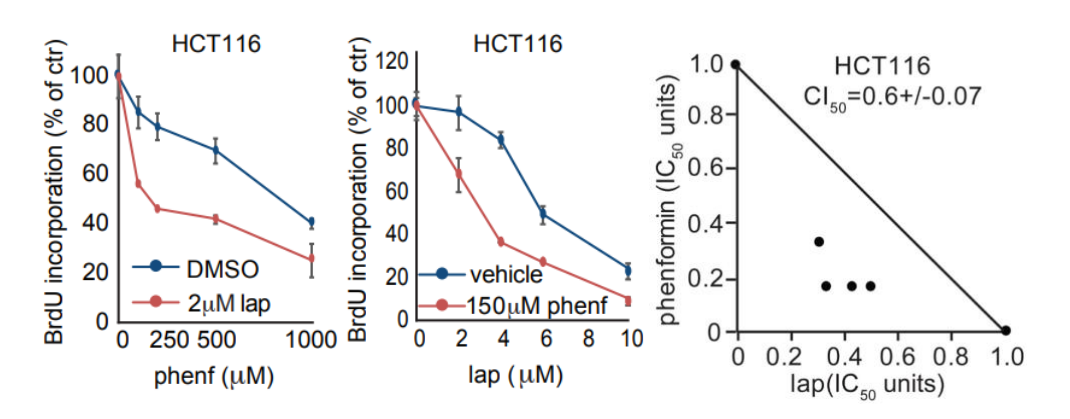


Fig. A.1.4A Lapatinib and phenformin work synergistically to inhibit the proliferation of HCT116 cells. HCT116 cells were treated with phenformin and/or lapatinib, at the indicated concentrations, for three days. Cell proliferation was monitored by BrdU incorporation and expressed as mean values +/- the SD of phenformin untreated (left panel) or lapatinib-untreated cells (middle panel). Combination Index 50 (CI₅₀) for lapatinib and phenformin (right panel) was calculated by isobologram method using the cell proliferation curves (left and middle panels) for HCT116. Data shown are representative of 2 independent experiments, each with 3 technical replicates. Figure is from (3).

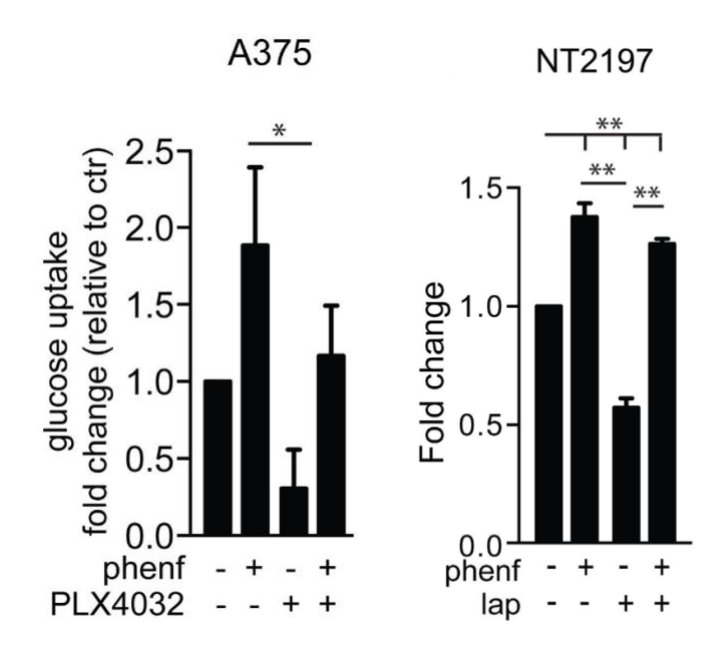


Fig. A.1.4B Kinase inhibitors counters phenformin-induced changes in glucose metabolism. A375 and NT2197 cells were treated with phenformin and/or kinase inhibitors (i.e., A375 cells were treated with PLX4032 while NT2197 cells were treated with lapatinib) for a day. Glucose uptake in drug-treated cells is presented relative to DMSO-treated control cells. Results are presented as mean values +/- the SD. Figure is from (3).

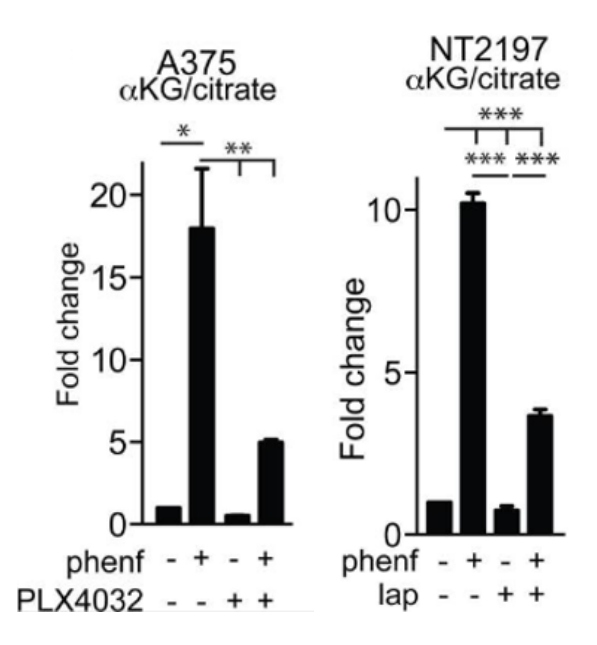


Fig. A.1.4C Kinase inhibitors opposes phenformin-induced changes in reductive glutamine metabolism. A375 and NT2197 cells were treated with phenformin and/or kinase inhibitors (i.e., A375 cells were treated with PLX4032 while NT2197 cells were treated with lapatinib) for a day. Intracellular α-KG/citrate ratios were determined by GC-MS and presented relative to DMSO-treated control cells. Results are presented as mean values +/- the SD. Figure is from (3).

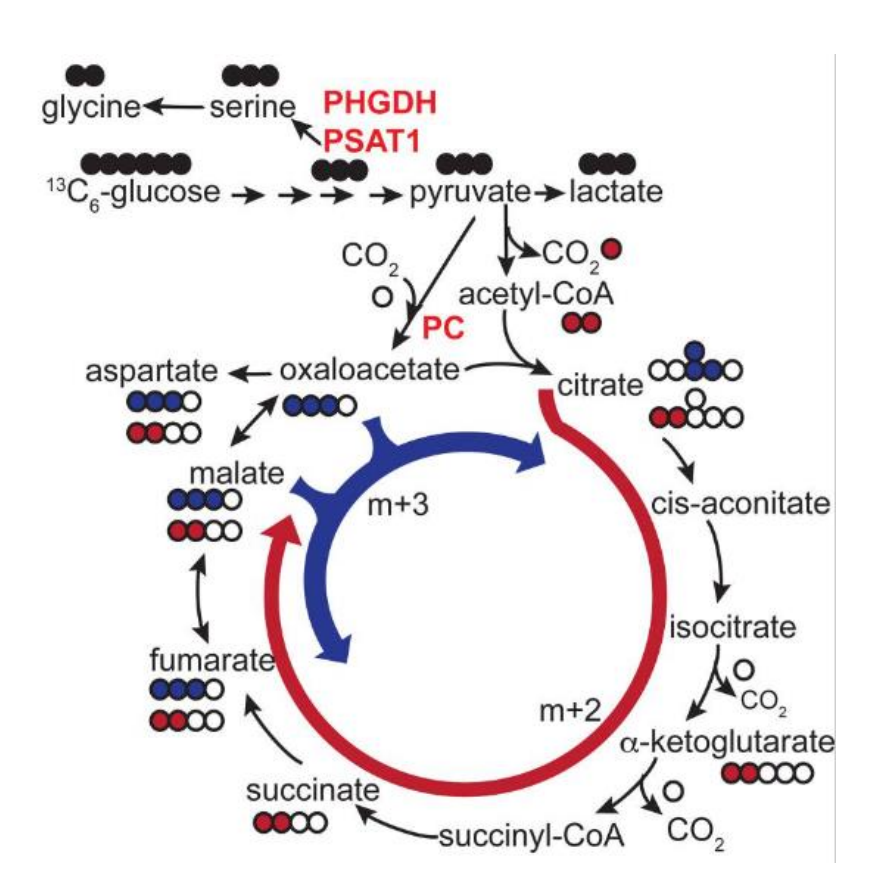


Fig. A.1.4D Schematic of ¹³**C metabolite labeling patterns after incubating cells with** ¹³**C₆-glucose.** ¹³**C** are denoted by filled circles. Red cycle is the forward direction of the CAC giving (m+2) intermediates (Red-filled circles). Blue cycle begins with pyruvate carboxylase (PC) and is characterized by (m+3) intermediates (Blue-filled circles). Figure is from (3).

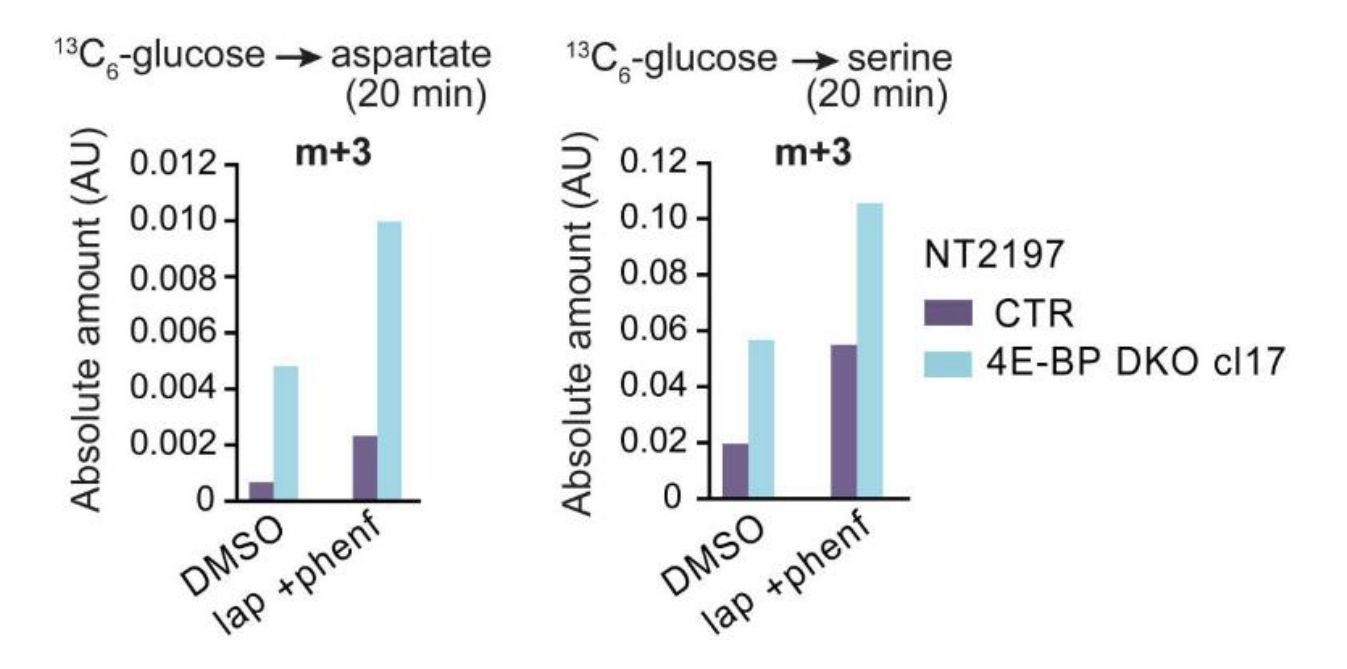


Fig. A.1.4E Deletion of 4E-BP in NT2197 cooperates with lapatinib and phenformin drug-induced increases in the levels of aspartate and serine. Abrogation of 4E-BP NT2197 WT and 4E-BP KO cells were incubated with ¹³C₆-glucose for 20 min. SITA were performed and the absolute levels of aspartate (m+3) and serine (m+3) ions are shown. Data are representative of 2 independent experiments. AU: arbitrary units. Figure is from (3).

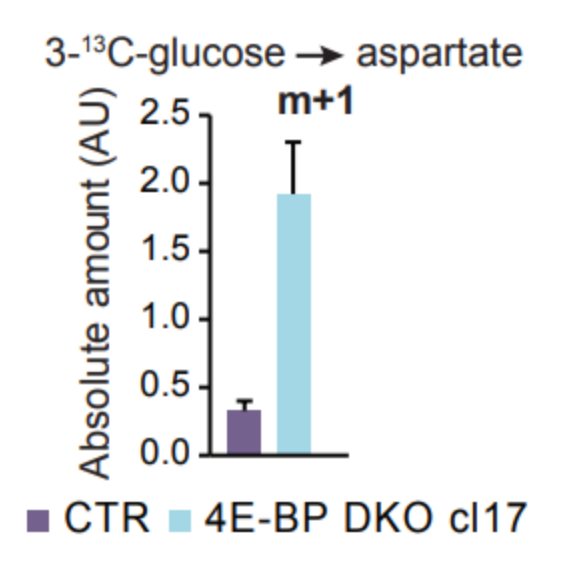


Fig. A.1.4F Loss of 4E-BP increases the activity of PC in NT2197 cells. NT2197 WT and 4E-BP KO cells were incubated with 3-¹³C-glucose for 10 min. SITA were performed and the absolute levels of (m+1) ions of aspartate are shown. Data represents the average of 3 independent experiments +/- SD. AU: arbitrary units. Figure is from (3).

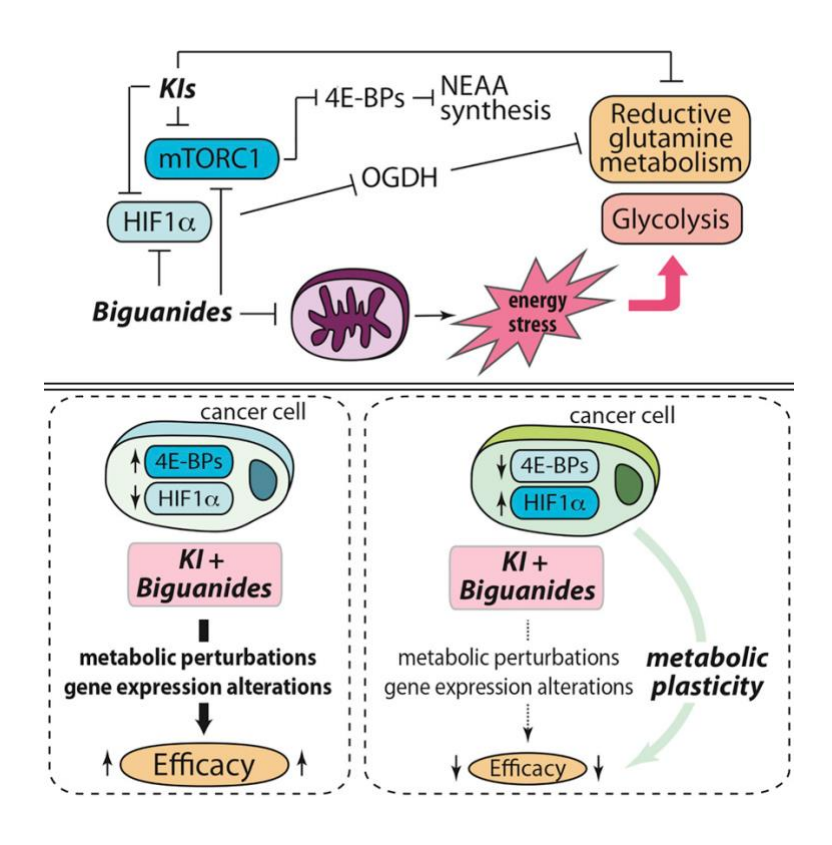


Fig. A.1.4G Schematic of the molecular mechanisms underlying the synergic efficacy of kinase inhibitors (KI) and biguanides in treating cancer cells. Cancer cells exhibit metabolic plasticity mediated by mTORC1/4E-BP1 and HIF-1α. Drug combination treatments with KIs and biguanides can limit such metabolic plasticity. However, cancer cells can activate non-redundant adaptive mechanisms which allows them to survive the drug combinations. Figure is from (3).

A.2 CONCLUSION:

In this chapter, I described a number of collaborative studies in which I participated both experimentally and conceptually. Altogether, these studies provided hitherto unappreciated insights into mechanisms of metabolic reprogramming required to fuel neoplastic growth that also provide cancer cells with flexibility to adapt to fluctuations in nutrient and oxygen availability as well as to overcome therapeutic insults. Moreover, these findings highlighted previously unknown mechanisms of action of drugs targeting cancer metabolism and associated signaling pathways. Finally, these results in conjunction with a bevy of other recent studies highlighted the central role of metabolic plasticity in cancer maintenance, progression and therapeutic responses (54). Notwithstanding these advances in the field, there is still much to learn about the mechanisms governing metabolomes of cancer cells. Future research efforts addressing gaps in knowledge pertinent to the metabolic plasticity of neoplasia are thus required to provide the molecular basis for more efficient therapeutic strategies that take advantage of metabolic differences between normal and malignant cells.

A.3 REFERENCES

- 1. Igelmann S, Lessard F, Uchenunu O, Bouchard J, Fernandez-Ruiz A, Rowell MC, et al. A hydride transfer complex reprograms NAD metabolism and bypasses senescence. Mol Cell. 2021;81(18):3848-65.e19.
- 2. Mzoughi S, Fong JY, Papadopoli D, Koh CM, Hulea L, Pigini P, et al. PRDM15 is a key regulator of metabolism critical to sustain B-cell lymphomagenesis. Nat Commun. 2020;11(1):3520.
- 3. Hulea L, Gravel SP, Morita M, Cargnello M, Uchenunu O, Im YK, et al. Translational and HIF-1α-Dependent Metabolic Reprogramming Underpin Metabolic Plasticity and Responses to Kinase Inhibitors and Biguanides. Cell Metab. 2018;28(6):817-32.e8.
- 4. Papadopoli D, Uchenunu O, Palia R, Chekkal N, Hulea L, Topisirovic I, et al. Perturbations of cancer cell metabolism by the antidiabetic drug canagliflozin. Neoplasia. 2021;23(4):391-9.
- 5. Lehuede C, Dupuy F, Rabinovitch R, Jones RG, Siegel PM. Metabolic Plasticity as a Determinant of Tumor Growth and Metastasis. Cancer Res. 2016;76(18):5201-8.
- 6. Bergers G, Fendt SM. The metabolism of cancer cells during metastasis. Nat Rev Cancer. 2021;21(3):162-80.
- 7. Uchenunu O, Pollak M, Topisirovic I, Hulea L. Oncogenic kinases and perturbations in protein synthesis machinery and energetics in neoplasia. J Mol Endocrinol. 2019;62(2):R83-r103.
- 8. Wiley CD, Velarde MC, Lecot P, Liu S, Sarnoski EA, Freund A, et al. Mitochondrial Dysfunction Induces Senescence with a Distinct Secretory Phenotype. Cell Metab. 2016;23(2):303-14.
- 9. Moiseeva O, Bourdeau V, Roux A, Deschênes-Simard X, Ferbeyre G. Mitochondrial dysfunction contributes to oncogene-induced senescence. Mol Cell Biol. 2009;29(16):4495-507.

- 10. Campisi J. Cellular senescence as a tumor-suppressor mechanism. Trends Cell Biol. 2001;11(11):S27-31.
- 11. Bromberg J, Darnell JE, Jr. The role of STATs in transcriptional control and their impact on cellular function. Oncogene. 2000;19(21):2468-73.
- 12. Wegrzyn J, Potla R, Chwae YJ, Sepuri NB, Zhang Q, Koeck T, et al. Function of mitochondrial Stat3 in cellular respiration. Science. 2009;323(5915):793-7.
- 13. Mantel C, Messina-Graham S, Moh A, Cooper S, Hangoc G, Fu XY, et al. Mouse hematopoietic cell-targeted STAT3 deletion: stem/progenitor cell defects, mitochondrial dysfunction, ROS overproduction, and a rapid aging-like phenotype. Blood. 2012;120(13):2589-99.
- 14. Gough DJ, Corlett A, Schlessinger K, Wegrzyn J, Larner AC, Levy DE. Mitochondrial STAT3 supports Ras-dependent oncogenic transformation. Science. 2009;324(5935):1713-6.
- 15. Mallette FA, Gaumont-Leclerc MF, Ferbeyre G. The DNA damage signaling pathway is a critical mediator of oncogene-induced senescence. Genes Dev. 2007;21(1):43-8.
- 16. Lo AS, Liew CT, Ngai SM, Tsui SK, Fung KP, Lee CY, et al. Developmental regulation and cellular distribution of human cytosolic malate dehydrogenase (MDH1). J Cell Biochem. 2005;94(4):763-73.
- 17. Pongratz RL, Kibbey RG, Shulman GI, Cline GW. Cytosolic and mitochondrial malic enzyme isoforms differentially control insulin secretion. J Biol Chem. 2007;282(1):200-7.
- 18. Birsoy K, Wang T, Chen WW, Freinkman E, Abu-Remaileh M, Sabatini DM. An essential role of the mitochondrial electron transport chain in cell proliferation is to enable aspartate synthesis. Cell. 2015;162(3):540-51.

- 19. Sullivan LB, Gui DY, Hosios AM, Bush LN, Freinkman E, Vander Heiden MG. Supporting aspartate biosynthesis is an essential function of respiration in proliferating cells. Cell. 2015;162(3):552-63.
- 20. Kilic Eren M, Tabor V. The role of hypoxia inducible factor-1 alpha in bypassing oncogene-induced senescence. PLoS One. 2014;9(7):e101064.
- 21. Bensaad K, Tsuruta A, Selak MA, Vidal MN, Nakano K, Bartrons R, et al. TIGAR, a p53-inducible regulator of glycolysis and apoptosis. Cell. 2006;126(1):107-20.
- 22. Matoba S, Kang JG, Patino WD, Wragg A, Boehm M, Gavrilova O, et al. p53 regulates mitochondrial respiration. Science. 2006;312(5780):1650-3.
- 23. Dias PL, Shanmuganathan SS, Rajaratnam M. Lactic dehydrogenase activity of aqueous humour in retinoblastoma. Br J Ophthalmol. 1971;55(2):130-2.
- 24. Hsieh MCF, Das D, Sambandam N, Zhang MQ, Nahlé Z. Regulation of the PDK4 isozyme by the Rb-E2F1 complex. J Biol Chem. 2008;283(41):27410-7.
- 25. Martin PL, Yin JJ, Seng V, Casey O, Corey E, Morrissey C, et al. Androgen deprivation leads to increased carbohydrate metabolism and hexokinase 2-mediated survival in Pten/Tp53-deficient prostate cancer. Oncogene. 2017;36(4):525-33.
- 26. Garcia-Cao I, Song MS, Hobbs RM, Laurent G, Giorgi C, de Boer VC, et al. Systemic elevation of PTEN induces a tumor-suppressive metabolic state. Cell. 2012;149(1):49-62.
- 27. Park JH, Lee SY. Metabolic pathways and fermentative production of L-aspartate family amino acids. Biotechnol J. 2010;5(6):560-77.
- 28. Gray LR, Tompkins SC, Taylor EB. Regulation of pyruvate metabolism and human disease. Cellular and molecular life sciences: CMLS. 2014;71(14):2577-604.

- 29. Inigo M, Deja S, Burgess SC. Ins and Outs of the TCA Cycle: The Central Role of Anaplerosis. Annual Review of Nutrition. 2021;41(1):19-47.
- 30. Warburg O. On the origin of cancer cells. Science. 1956;123(3191):309-14.
- 31. Warburg O. The Metabolism of Carcinoma Cells. The Journal of Cancer Research. 1925;9(1):148.
- 32. Hay N. Reprogramming glucose metabolism in cancer: can it be exploited for cancer therapy? Nat Rev Cancer. 2016;16(10):635-49.
- 33. Hsia DS, Grove O, Cefalu WT. An update on sodium-glucose co-transporter-2 inhibitors for the treatment of diabetes mellitus. Curr Opin Endocrinol Diabetes Obes. 2017;24(1):73-9.
- 34. Scafoglio CR, Villegas B, Abdelhady G, Bailey ST, Liu J, Shirali AS, et al. Sodium-glucose transporter 2 is a diagnostic and therapeutic target for early-stage lung adenocarcinoma. Sci Transl Med. 2018;10(467).
- 35. Scafoglio C, Hirayama BA, Kepe V, Liu J, Ghezzi C, Satyamurthy N, et al. Functional expression of sodium-glucose transporters in cancer. Proc Natl Acad Sci U S A. 2015;112(30):E4111-9.
- 36. Kepe V, Scafoglio C, Liu J, Yong WH, Bergsneider M, Huang SC, et al. Positron emission tomography of sodium glucose cotransport activity in high grade astrocytomas. J Neurooncol. 2018;138(3):557-69.
- 37. Komatsu S, Nomiyama T, Numata T, Kawanami T, Hamaguchi Y, Iwaya C, et al. SGLT2 inhibitor ipragliflozin attenuates breast cancer cell proliferation. Endocr J. 2020;67(1):99-106.
- 38. Kaji K, Nishimura N, Seki K, Sato S, Saikawa S, Nakanishi K, et al. Sodium glucose cotransporter 2 inhibitor canagliflozin attenuates liver cancer cell growth and angiogenic activity by inhibiting glucose uptake. Int J Cancer. 2018;142(8):1712-22.

- 39. Villani LA, Smith BK, Marcinko K, Ford RJ, Broadfield LA, Green AE, et al. The diabetes medication Canagliflozin reduces cancer cell proliferation by inhibiting mitochondrial complex-I supported respiration. Molecular metabolism. 2016;5(10):1048-56.
- 40. McGuirk S, Gravel SP, Deblois G, Papadopoli DJ, Faubert B, Wegner A, et al. PGC-1α supports glutamine metabolism in breast cancer. Cancer Metab. 2013;1(1):22.
- 41. Cluntun AA, Lukey MJ, Cerione RA, Locasale JW. Glutamine Metabolism in Cancer: Understanding the Heterogeneity. Trends Cancer. 2017;3(3):169-80.
- 42. Yang WH, Qiu Y, Stamatatos O, Janowitz T, Lukey MJ. Enhancing the Efficacy of Glutamine Metabolism Inhibitors in Cancer Therapy. Trends Cancer. 2021;7(8):790-804.
- 43. Schulte ML, Fu A, Zhao P, Li J, Geng L, Smith ST, et al. Pharmacological blockade of ASCT2-dependent glutamine transport leads to antitumor efficacy in preclinical models. Nature medicine. 2018;24(2):194-202.
- 44. Yoo HC, Yu YC, Sung Y, Han JM. Glutamine reliance in cell metabolism. Exp Mol Med. 2020;52(9):1496-516.
- 45. Fumasoni I, Meani N, Rambaldi D, Scafetta G, Alcalay M, Ciccarelli FD. Family expansion and gene rearrangements contributed to the functional specialization of PRDM genes in vertebrates. BMC Evol Biol. 2007;7:187.
- 46. Giallourakis CC, Benita Y, Molinie B, Cao Z, Despo O, Pratt HE, et al. Genome-wide analysis of immune system genes by expressed sequence Tag profiling. J Immunol. 2013;190(11):5578-87.
- 47. Mzoughi S, Zhang J, Hequet D, Teo SX, Fang H, Xing QR, et al. PRDM15 safeguards naive pluripotency by transcriptionally regulating WNT and MAPK-ERK signaling. Nat Genet. 2017;49(9):1354-63.

- 48. Mzoughi S, Di Tullio F, Low DHP, Motofeanu CM, Ong SLM, Wollmann H, et al. PRDM15 loss of function links NOTCH and WNT/PCP signaling to patterning defects in holoprosencephaly. Sci Adv. 2020;6(2):eaax9852.
- 49. Mendoza MC, Er EE, Blenis J. The Ras-ERK and PI3K-mTOR pathways: cross-talk and compensation. Trends Biochem Sci. 2011;36(6):320-8.
- 50. Di Nicolantonio F, Arena S, Tabernero J, Grosso S, Molinari F, Macarulla T, et al. Deregulation of the PI3K and KRAS signaling pathways in human cancer cells determines their response to everolimus. J Clin Invest. 2010;120(8):2858-66.
- 51. Wise DR, Thompson CB. Glutamine addiction: a new therapeutic target in cancer. Trends in biochemical sciences. 2010;35(8):427-33.
- 52. Di Tullio F, Schwarz M, Zorgati H, Mzoughi S, Guccione E. The duality of PRDM proteins: epigenetic and structural perspectives. Febs j. 2022;289(5):1256-75.
- 53. Stine ZE, Schug ZT, Salvino JM, Dang CV. Targeting cancer metabolism in the era of precision oncology. Nature Reviews Drug Discovery. 2022;21(2):141-62.
- 54. Fendt SM, Frezza C, Erez A. Targeting Metabolic Plasticity and Flexibility Dynamics for Cancer Therapy. Cancer Discov. 2020;10(12):1797-807.
- 55. Wheaton WW, Weinberg SE, Hamanaka RB, Soberanes S, Sullivan LB, Anso E, et al. Metformin inhibits mitochondrial complex I of cancer cells to reduce tumorigenesis. Elife. 2014;3:e02242.
- 56. Di Magno L, Di Pastena F, Bordone R, Coni S, Canettieri G. The Mechanism of Action of Biguanides: New Answers to a Complex Question. Cancers (Basel). 2022;14(13).

- 57. El-Mir MY, Nogueira V, Fontaine E, Avéret N, Rigoulet M, Leverve X. Dimethylbiguanide inhibits cell respiration via an indirect effect targeted on the respiratory chain complex I. J Biol Chem. 2000;275(1):223-8.
- 58. Owen MR, Doran E, Halestrap AP. Evidence that metformin exerts its anti-diabetic effects through inhibition of complex 1 of the mitochondrial respiratory chain. Biochem J. 2000;348 Pt 3(Pt 3):607-14.
- 59. LaMoia TE, Shulman GI. Cellular and Molecular Mechanisms of Metformin Action. Endocrine Reviews. 2020;42(1):77-96.
- 60. Javeshghani S, Zakikhani M, Austin S, Bazile M, Blouin MJ, Topisirovic I, et al. Carbon source and myc expression influence the antiproliferative actions of metformin. Cancer Res. 2012;72(23):6257-67.
- 61. Gravel SP, Hulea L, Toban N, Birman E, Blouin MJ, Zakikhani M, et al. Serine deprivation enhances antineoplastic activity of biguanides. Cancer Res. 2014;74(24):7521-33.
- 62. Fendt SM, Bell EL, Keibler MA, Davidson SM, Wirth GJ, Fiske B, et al. Metformin decreases glucose oxidation and increases the dependency of prostate cancer cells on reductive glutamine metabolism. Cancer Res. 2013;73(14):4429-38.
- 63. Paech F, Bouitbir J, Krähenbühl S. Hepatocellular Toxicity Associated with Tyrosine Kinase Inhibitors: Mitochondrial Damage and Inhibition of Glycolysis. Front Pharmacol. 2017;8:367.
- 64. Yuan P, Ito K, Perez-Lorenzo R, Del Guzzo C, Lee JH, Shen CH, et al. Phenformin enhances the therapeutic benefit of BRAF(V600E) inhibition in melanoma. Proc Natl Acad Sci U S A. 2013;110(45):18226-31.

- 65. Trousil S, Chen S, Mu C, Shaw FM, Yao Z, Ran Y, et al. Phenformin Enhances the Efficacy of ERK Inhibition in NF1-Mutant Melanoma. J Invest Dermatol. 2017;137(5):1135-43.
- 66. Bridges HR, Jones AJ, Pollak MN, Hirst J. Effects of metformin and other biguanides on oxidative phosphorylation in mitochondria. Biochem J. 2014;462(3):475-87.
- 67. Yendapally R, Sikazwe D, Kim SS, Ramsinghani S, Fraser-Spears R, Witte AP, et al. A review of phenformin, metformin, and imeglimin. Drug Development Research. 2020;81(4):390-401.
- 68. García Rubiño ME, Carrillo E, Ruiz Alcalá G, Domínguez-Martín A, J AM, Boulaiz H. Phenformin as an Anticancer Agent: Challenges and Prospects. Int J Mol Sci. 2019;20(13).
- 69. Baba I, Shirasawa S, Iwamoto R, Okumura K, Tsunoda T, Nishioka M, et al. Involvement of deregulated epiregulin expression in tumorigenesis in vivo through activated Ki-Ras signaling pathway in human colon cancer cells. Cancer Res. 2000;60(24):6886-9.
- 70. Ursini-Siegel J, Hardy WR, Zuo D, Lam SH, Sanguin-Gendreau V, Cardiff RD, et al. ShcA signalling is essential for tumour progression in mouse models of human breast cancer. EMBO J. 2008;27(6):910-20.
- 71. Haq R, Shoag J, Andreu-Perez P, Yokoyama S, Edelman H, Rowe GC, et al. Oncogenic BRAF regulates oxidative metabolism via PGC1α and MITF. Cancer cell. 2013;23(3):302-15.
- 72. Abildgaard C, Rizza S, Christiansen H, Schmidt S, Dahl C, Abdul-Al A, et al. Screening of metabolic modulators identifies new strategies to target metabolic reprogramming in melanoma. Sci Rep. 2021;11(1):4390.
- 73. Komurov K, Tseng JT, Muller M, Seviour EG, Moss TJ, Yang L, et al. The glucose-deprivation network counteracts lapatinib-induced toxicity in resistant ErbB2-positive breast cancer cells. Mol Syst Biol. 2012;8:596.

- 74. Deblois G, Smith HW, Tam IS, Gravel SP, Caron M, Savage P, et al. ERRα mediates metabolic adaptations driving lapatinib resistance in breast cancer. Nat Commun. 2016;7:12156.
- 75. Khan H, Anshu A, Prasad A, Roy S, Jeffery J, Kittipongdaja W, et al. Metabolic Rewiring in Response to Biguanides Is Mediated by mROS/HIF-1a in Malignant Lymphocytes. Cell Rep. 2019;29(10):3009-18.e4.
- 76. Fendt S-M, Bell EL, Keibler MA, Olenchock BA, Mayers JR, Wasylenko TM, et al. Reductive glutamine metabolism is a function of the α -ketoglutarate to citrate ratio in cells. Nature Communications. 2013;4(1):2236.
- 77. Bhat M, Robichaud N, Hulea L, Sonenberg N, Pelletier J, Topisirovic I. Targeting the translation machinery in cancer. Nature Reviews Drug Discovery. 2015;14(4):261-78.
- 78. Buttgereit F, Brand MD. A hierarchy of ATP-consuming processes in mammalian cells. Biochem J. 1995;312 (Pt 1)(Pt 1):163-7.
- 79. Morita M, Gravel SP, Chénard V, Sikström K, Zheng L, Alain T, et al. mTORC1 controls mitochondrial activity and biogenesis through 4E-BP-dependent translational regulation. Cell Metab. 2013;18(5):698-711.
- 80. Larsson O, Morita M, Topisirovic I, Alain T, Blouin MJ, Pollak M, et al. Distinct perturbation of the translatome by the antidiabetic drug metformin. Proc Natl Acad Sci U S A. 2012;109(23):8977-82.
- 81. Hsieh AC, Costa M, Zollo O, Davis C, Feldman ME, Testa JR, et al. Genetic dissection of the oncogenic mTOR pathway reveals druggable addiction to translational control via 4EBP-eIF4E. Cancer Cell. 2010;17(3):249-61.

- 82. Hsieh AC, Liu Y, Edlind MP, Ingolia NT, Janes MR, Sher A, et al. The translational landscape of mTOR signalling steers cancer initiation and metastasis. Nature. 2012;485(7396):55-61.
- 83. Thoreen CC, Chantranupong L, Keys HR, Wang T, Gray NS, Sabatini DM. A unifying model for mTORC1-mediated regulation of mRNA translation. Nature. 2012;485(7396):109-13.
- 84. Meyuhas O, Dreazen A. Ribosomal protein S6 kinase from TOP mRNAs to cell size. Prog Mol Biol Transl Sci. 2009;90:109-53.
- 85. Zhang J, Pavlova NN, Thompson CB. Cancer cell metabolism: the essential role of the nonessential amino acid, glutamine. EMBO J. 2017;36(10):1302-15.
- 86. Lieu EL, Nguyen T, Rhyne S, Kim J. Amino acids in cancer. Experimental & Molecular Medicine. 2020;52(1):15-30.
- 87. Dodd KM, Yang J, Shen MH, Sampson JR, Tee AR. mTORC1 drives HIF-1α and VEGF-A signalling via multiple mechanisms involving 4E-BP1, S6K1 and STAT3. Oncogene. 2015;34(17):2239-50.
- 88. Haase VH. The VHL tumor suppressor: master regulator of HIF. Curr Pharm Des. 2009;15(33):3895-903.
- 89. Maxwell PH, Wiesener MS, Chang GW, Clifford SC, Vaux EC, Cockman ME, et al. The tumour suppressor protein VHL targets hypoxia-inducible factors for oxygen-dependent proteolysis. Nature. 1999;399(6733):271-5.
- 90. Semenza GL. Hypoxia-inducible factor 1 (HIF-1) pathway. Sci STKE. 2007;2007(407):cm8.

- 91. Sun RC, Denko NC. Hypoxic regulation of glutamine metabolism through HIF1 and SIAH2 supports lipid synthesis that is necessary for tumor growth. Cell Metab. 2014;19(2):285-92.
- 92. Andrzejewski S, Klimcakova E, Johnson RM, Tabariès S, Annis MG, McGuirk S, et al. PGC-1α Promotes Breast Cancer Metastasis and Confers Bioenergetic Flexibility against Metabolic Drugs. Cell Metab. 2017;26(5):778-87.e5.
- 93. Dupuy F, Tabariès S, Andrzejewski S, Dong Z, Blagih J, Annis MG, et al. PDK1-Dependent Metabolic Reprogramming Dictates Metastatic Potential in Breast Cancer. Cell Metab. 2015;22(4):577-89.